ERRATUM

p118 para 2, 1st line: "**61**" for "**37**"

ADDENDA

p109, 8th line: delete "unprotected phenol is required to assist in the electrophilic aromatic substitution" and read "*ortho* acetate group deactivates electrophilic aromatic substitution, while the combined steric bulk of the acetate and methyl groups may hinder reaction with bromine"

p131 para 1, last line: after "(20.5 g, 36%; recovered yield: 60%)" insert "as a brown solid"

MOLECULAR APPROACHES TO THE TREATMENT OF MOTOR NEURON DEGENERATION

Laura K. Wood

BSc (Hons), Monash University

A thesis submitted for the degree of Doctor of Philosophy

School of Chemistry, Monash University

July 2012

Failure is the condiment that gives success its flavour

- Truman Capote

GENERAL DECLARATION

I hereby declare that this thesis contains no material that has been accepted for the award of any other degree or diploma at any university or equivalent institution and that, to the best of my knowledge, this thesis contains no material previously published or written by another person, except where due reference is made in the text of this thesis.

Signed: _____ Date: _____

Laura K. Wood

TABLE OF CONTENTS

ABSTRACT

This thesis describes methods towards the synthesis and evaluation of potential small molecule agents for the treatment of motor neuron degeneration. Several factors are known to contribute to the mechanisms of neurodegeneration, including cellular degradation caused by the production of radical oxygen species and dysfunction of glutamate transporters and receptors leading to the disruption of Ca^{2+} homeostasis in neurons. The work undertaken in this thesis attempted to target these factors by incorporating antioxidant and Ca^{2+}-chelating function within the same structure, thus simultaneously combating known pathways towards apoptosis.

Chapter One provides a background to the pathogenesis of neurodegenerative disease and specifically amyotrophic lateral sclerosis (ALS). This chapter gives an overview of the many pathways, both genetically inheritable and sporadic, that may lead to the premature activation of apoptotic pathways in neurons, as well as current and proposed approaches towards interrupting these pathways.

Chapter Two describes the synthesis of compounds based on the structure of 1,2-bis(*o*-aminophenoxy)ethane-*N*,*N*,*N*',*N*'-tetraacetic acid (BAPTA), an effective Ca^{2+} chelator. As studies have indicated that BAPTA acts as an effective treatment against neurodegeneration but has difficulty crossing the blood brain barrier, modification of BAPTA by the introduction of hydrophilic groups was pursued in this chapter. A number of tetraethyl ester derivatives of BAPTA were synthesised, including bis-phenol acid **20** and tetraethyl ester **19**, which underwent reaction with 2-(2-chloroethoxy)ethanol to produce the polyethylene glycol derivative **21** and glycosylation to give the protected glucose derivative **23**. The target compounds were evaluated for antioxidant potency using a linoleic acid protocol, with results indicating that a number of hydrophilic BAPTA derivatives had moderate to high antioxidant efficiency, particularly phenolic analogues **19** and **20**, which exhibited efficiencies comparable to vitamin E.

A number of methods towards the formation and functionalisation of chroman cores are investigated in Chapter Three. For the purposes of this project, installation of functionalised chains was required at chroman positions C2 and C8, in order to incorporate Ca^{2+}-chelating arms similar to BAPTA. From mono-protected tri- and dimethylhydroquinone (**34** and **39**, respectively), reaction with paraformaldehyde and selected alkenes formed C2-functionalised chromans in one step, however it was discovered that a slight increase in the overall yield of 2,5,7-trimethyl chromans was achieved when two-step syntheses *via* a butoxymethyl intermediate was performed. In an effort to further increase the yields of functionalised

2,5,7-trimethyl chromans, synthesis using mono-acetylated bromo dimethylhydroquinone **61** produced C8-bromo chromans **65** and **66** in high yield, which could be successfully debrominated under reductive conditions to give C8-unsubstituted chromans. Phthalimide **72** was formed from the derivatisation of bromo chroman **66**, as means of installing a nitrogen on the C2 chain in a effort towards the synthesis of target compound **A**. As part of an alternative pathway, several failed attempts were made to form phthalamidyl-functionalised C2 chains *via* etherification with chromans, thus instead installation of the desired functionality was achieved by reacting acetamide alkene **89** with bromo intermediate **61** to form chroman **90**, which contained the desired backbone for future formation of target **B** (**91**).

Synthetic pathways towards an alternative dual-action target **112** are detailed in Chapter Four. Two different synthetic routes were pursued, the first of which involved chroman core formation by reaction of 2,6-dimethylhydroquinone with methyl vinyl ketone and trimethyl orthoformate, followed by a series of transformations of the C2 chain to give the benzyl-protected alcohol **101**. Further C2 chain derivatisation and C8 functionalisation yielded the protected target **107** with a total yield of 4% after eleven steps. Alternatively, as a more efficient approach towards the final target, a similar sequence of functionalisation reactions were undertaken with previously synthesised acetate-protected alcohol **41**, yielding the deprotected target compound **112**, which exhibited antioxidant efficiency higher than vitamin E and significantly higher than BAPTA.

ACKNOWLEDGEMENTS

First and foremost, I wish to express my gratitude to the "Boss", Prof. Steven Langford, for his ongoing guidance and patience, for always having the right answer, and for giving me the freedom to follow my instincts and interests throughout my candidature. I always walked away from my meetings with Steve with a renewed sense of clarity and direction, and I will be eternally grateful for the opportunities and support he's given me these last few years.

Huge thanks must go to the many members of the Langford group who've come and gone over the years – we've been a through a lot together, challenged each other and we've worked well as a team. I'd like to give special thanks to Corrine for being so helpful as my go-to person towards the end of my project, to Brad, Elisse and Shadi for being great listeners and to Manny for his procrastination techniques and bursts of spontaneous singing.

To all the friends I've made along the way, I'd like to express my appreciation for the amazing experiences, laughs and fond memories. Special mention must go to Bianca, who constantly reminded me to "just keep swimming", and particularly Jacinta, who always made time for me, provided sound advice and kept me grounded when things got a little crazy – thank you for being a great friend and confidante. Thanks also to the members of the Junk-Deacon group, who made me feel like one of their own and provided great conversations and fun-filled experiences. A massive thank you also goes to all my supportive friends and colleagues at Biota, for the pep talks and the welcome distractions, whichever I needed more at the time.

Many thanks to the School of Chemistry staff who have helped me throughout my degree: the ever-helpful Peter Nichols for his assistance with NMR spectroscopy; Sally Duck & Phil Holt for mass spectrometry; Victor de Guzman for HPLC; Craig Forsyth and Kristina Konstas for collecting X-ray crystal data and Sue for her guidance with deciphering it; and Bruce Dobney, for being probably the most patient and universally helpful person in the School.

I gratefully acknowledge the Australian Government for financial support in the form of an Australian Postgraduate Award, and Monash University for generously providing me with a travel grant to allow me to present my work overseas.

To Dad, Mum, Neil, Kathy, John, Penny and all the O'Dea and Wood family members – thank you for your ongoing enthusiasm, encouragement and constant reminders that I should have finished by now! (Now you can stop asking...)

Finally, to my husband Steve – thank you for believing in me when I didn't believe in myself, and for helping me find the strength I didn't know I had. I couldn't have achieved this without you.

ABBREVIATIONS AND ACRONYMS

AAPH	2,2'-azobis(2-amidinopropane) dihydrochloride
AATA	1-(2-aminophenoxy)-2-(2-aminoethoxy)ethane-*N*,*N*,*N*',*N*'-tetraacetic acid
Aβ	β-amyloid
AcOH	acetic acid
ALS	amyotrophic lateral sclerosis
AMPA	α-amino-3-hydroxy-5-methyl-4-isoxazolepropionic acid
Ar	aromatic
ATP	adenosine triphosphate
BAPTA	1,2-bis(*o*-aminophenoxy)ethane-*N*,*N*,*N*',*N*'-tetraacetic acid
BAPTA-AM	BAPTA acetoxymethyl ester
BHT	butylated hydroxytoluene
BnCl	benzyl chloride
t-BuOH	*tert*-butanol
CNS	central nervous system
CSF	cerebrospinal fluid
DABCO	1,4-diazabicyclo[2.2.2]octane
DBU	1,8-diazabicycloundec-7-ene
DIPEA	*N*,*N*-diisopropylethylamine
DMAP	4-dimethylaminopyridine
DMF	dimethylformamide
DMSO	dimethyl sulfoxide
DNA	deoxyribonucleic acid
EAAT	excitatory amino acid transporter
EGTA	ethylene glycol bis(*β*-aminoethyl ether)-*N*,*N*,*N*',*N*'-tetraacetic acid
EI	electron impact
ESI	electrospray ionisation
Et	ethyl
fALS	familial ALS
FRS	free radical scavenger
GluA1-4	AMPA receptor subunits, previously referred to as GluR1-4
GSH	glutathione
HRMS	high resolution mass spectrometry

IMS	intermembrane space
KA	kainate
LMWA	low molecular weight antioxidant
Me	methyl
MND	motor neuron disease
MP	melting point
mRNA	messenger RNA
MS	mass spectrometry
mtDNA	mitochondrial DNA
m/z	mass-to-charge ratio
NAD^+	nicotinamide adenine dinucleotide
NADH	reduced form of nicotinamide adenine dinucleotide
NMDA	*N*-methyl-D-aspartate
NMR	nuclear magnetic resonance
NO	nitric oxide
PBS	Pharmaceutical Benefits Scheme
Ph	phenyl
Phth	phthalimide
PNA	peptide nucleic acid
RBF	round-bottom flask
RNA	ribonucleic acid
RNS	reactive nitrogen species
ROS	reactive oxygen species
ppm	parts per million
sALS	sporadic ALS
siRNA	small interfering RNA
SOD1	copper/zinc superoxide dismutase
SOD1	gene that encodes for the SOD1 enzyme
$SOD1^{G93A}$	*SOD1* mutation that exhibits a 93rd codon substitution from glycine to alanine
TFA	trifluoroacetic acid
THF	tetrahydrofuran
TLC	thin layer chromatography
TsCl	*p*-toluenesulfonyl chloride

CHAPTER ONE

INTRODUCTION

1.1 An introduction to neurodegenerative disease

Neurodegeneration is a condition that involves the progressive loss of neurological function, caused by the degeneration of neurons. Many different types of diseases are neurodegenerative, for example amyotrophic lateral sclerosis, Alzheimer's disease, Huntington's disease and Parkinson's disease.[1,2] Both the production of reactive oxygen species (ROS) from the electron transport chain in mitochondria and glutamate-induced calcium ion (Ca^{2+}) excitotoxicity have been implicated in the onset and progression of neurodegenerative diseases, among other hypotheses, such as the accumulation of β-amyloid plaques and dysfunction of glutamate transporters and receptors.[1-8]

1.1.1 Amyotrophic lateral sclerosis

The most common form of motor neuron disease in humans is amyotrophic lateral sclerosis (ALS), also known generically as motor neuron disease (MND), or Lou Gehrig's disease in the United States. MND is a neurodegenerative disorder that leads to the death of both the upper and lower motor neurons found in the brain and spinal cord.[1,6-8] Discovered by French neurologist Jean-Martin Charcot in 1869,[3] incidence of the disease occurs at roughly 1-3 per 100,000 people, with a prevalence of about 4-6 per 100,000.[6,7] It is estimated that currently about 1200 Australians are living with the disease, with roughly 370 new patients diagnosed every year.[9] ALS is typically an age-dependent condition, and most sufferers are afflicted in middle-adult life, leading to motor weakness in the extremities, spasticity, paralysis and eventually death, typically within 3 to 5 years of the onset of symptoms with current therapies.[1,3,6-8,10]. The disease has claimed the life of a number of famous people, including baseballer Lou Gehrig, former Chinese leader Mao Zedong and Australian artist Pro Hart. Renowned physicist Stephen Hawking suffers from an extremely rare, slowly progressing form of ALS, having been diagnosed nearly five decades ago.

Characteristic of ALS is the selective targeting of motor neurons, particularly in the brain stem, cerebral cortex and spinal cord, leaving cognitive function intact in a majority of cases, while muscle function associated with limb movement and breathing are greatly debilitated.[1,6-8] Progression of the disease is usually accompanied with trouble swallowing (dysphagia), talking and difficulty breathing, and death is usually associated with respiratory failure.[8]

Cases of spontaneous recovery or improvement have been reported,[11,12] however they are exceptionally rare. Currently there is no cure or effective preventative treatment for ALS.

Riluzole, a glutamate antagonist (Figure 1.1), is the only currently approved treatment for ALS and only extends survival by 2 to 3 months,[13-15] usually with side effects.[9,13-18] Thus, there is a need to examine alternative potential treatments for this debilitating and terminal condition.

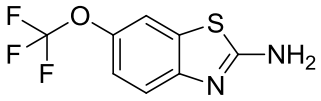

Figure 1.1 Structure of riluzole, a substituted benzothiazole.

One of the problems with developing a treatment for ALS is that the exact cause of the condition is often varied and difficult to determine. Several hypotheses concerning the mechanisms that contribute to the disease have been developed. ALS can be classified into two major types: familial ALS (fALS), which is an inheritable form of ALS, and sporadic ALS (sALS), which appears to occur spontaneously, without familial history of ALS. Whilst most cases of ALS are sporadic, fALS accounts for 5-10% of all ALS cases,[1,3,6-8,10] the vast majority of which occur by autosomal dominant transmission,[3,6,19] and is pathologically and clinically indistinguishable from sALS.[7] Studies have shown links between about 20% of cases of the fALS form of neurodegeneration and the mutation of *SOD1*,[3,7,20] the gene that encodes the cytoplasmic human antioxidant enzyme copper/zinc superoxide dismutase (SOD1). It has been found that mutant SOD1 enzymes exhibit a toxic gain-of-function, which catalyse the oxidation of cellular substrates present in motor neurons, leading to neuron death.[3,7,8,10]

Various studies of ALS patients throughout the years have exposed a few notable differences between sALS and fALS, in particular the gender ratio of sufferers, age of symptom onset and expected survival of patients after onset of the disease. While the onset of ALS may occur anywhere from childhood to late 80s, the disease is considerably more common later in life. sALS is largely an age-dependent condition, with an average age of onset of 58-63 years,[8] while the onset of fALS generally occurs a lower age, with mean onset at 47-52 years,[8] although juvenile cases are known.[6,10] Mean age of onset is generally earlier in ALS arising from SOD1 mutations compared to non-SOD fALS cases[21] and onset age is generally a predictor of survival, with younger patients of both sALS and fALS surviving significantly longer than those who develop the disease at a later age.[19,22,23] It has been suggested that the reason for longer survival in younger patients is due to greater neuronal reserves.[22] In rare cases, patients have been known to live longer than 20 years with the disease,[24] although the reasons for why some patients live much longer than others are largely unknown, likely to be due to the multifactorial nature of the disease. Overall, ALS is more common in men than in women, with an average

male to female ratio between 2:1 and 1.5:1,[22,23] which has been reported to be over 3:1 under the age of 40 and decreases with increasing age of onset, approaching 1:1 over the age of 70.[22,23]

1.2 Genetics and ALS

While little is known about the mechanisms of sporadic ALS, population studies of fALS patients have provided some insight into the inheritance of the familial form of the disease.[19-21,25,26] Familial ALS can be inherited as an autosomal recessive or autosomal dominant trait, although transmission of fALS is nearly always autosomal dominant,[19] while it is clinically and pathologically indistinguishable from sALS.[7] Recessive forms of ALS, however, usually have juvenile onset.[6] While roughly 10% of all ALS patients are referred to as fALS cases, this figure generally refers to only a dominant mode of inheritance with high penetrance, where a high proportion of individuals who carry the mutant gene express the disease phenotype.[27] In reality, cases with dominant inheritance and low penetrance, recessive inheritance, or oligogenic inheritance may be misdiagnosed as sALS, as the complicated familial pattern of inheritance is not always understood.[27]

1.2.1 Mutant SOD1 and fALS

In roughly 15-20% of cases of fALS, studies originating with Rosen *et al*.[20] in 1993 have shown a relation between a mutation of the gene that encodes the human antioxidant enzyme copper/zinc superoxide dismutase (SOD1), and the onset of the disease, caused by the production of ROS.[3,7,20,28,29] Normally, SOD1 in humans converts superoxide anions ($^{\bullet}O_2^-$), formed as an undesirable byproduct of phosphorylation in mitochondria,[30-32] to oxygen and hydrogen peroxide (H_2O_2) (Scheme 1.1),[29,33] which is further converted to water by enzymes such as catalase and glutathione peroxidase.[2] Thus, SOD1 converts harmful free radicals into innocuous molecules in the process.

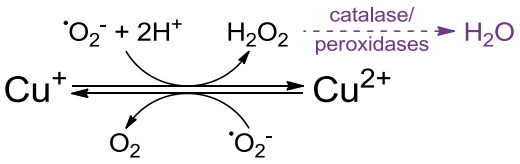

Scheme 1.1 Mechanism for normal SOD1 conversion of superoxide (O_2^-) to hydrogen peroxide (H_2O_2) and molecular oxygen (O_2).

SOD1 exists as a homodimeric enzyme, present in virtually every cell type, though it is particularly abundant in motor neurons, particularly in the spinal cord.[2920,33] Within cells, the SOD1 enzyme is found largely in the cytoplasm, although it may localise in mitochondria or the nucleus.[29,34-36] Each monomer within the homodimeric structure binds one zinc ion, generally accepted to have a structural function, and one copper ion, which provides catalytic activity for the dismutation of superoxide.[37]

The gene *SOD1*, which encodes for the enzyme SOD1, was the first gene conclusively associated with fALS, and this form of the disease is often specifically referred to as ALS1.[3,38] Several other loci have been linked to fALS in recent years, but few have been attributed to specific genes, which code for a variety of difference cellular processes, including oxidation, DNA repair, axonal transport and RNA processing; examples of ALS-linked genes include *ALS2*, *TARDBP*, *VAPB*, *SETX* and *ANG*.[1,3,6,8,10,38,39] Over 160 different mutations of *SOD1* are currently known,[38] a vast majority of which are dominantly inheritable.[3,6,19] Located on chromosome 21,[20] the majority of *SOD1* mutations are point mutations, although mutations due to deletions, insertions and truncations are also known.[38] Some *SOD1* mutations have specific geographic distribution; for instance, the A4V mutation (which codes for a 4th codon substitution from alanine to valine, also referred to as *SOD1*^{A4V}) is the most common mutation in the United States,[21,26,28] while D90A is a common adult-onset recessively inherited mutation in Europe.[25] Mutations may present a wide variety of phenotypes, including varied onset age, duration and clinical severity;[19,21,40] for example, fALS patients with the A4V mutation, one of the most clinically severe *SOD1* mutations,[26] have a mean disease duration of around 1.2 to 1.4 years,[21,26] compared to 2.5 years in other fALS patients,[26] and much shorter than the average duration of 10.1 years in patients with the G93C mutation.[21] It is important to note that some *SOD1* mutations may have diminished penetrance and therefore may be recorded as apparent cases of sALS.[27] The study of *SOD1* mutants has uncovered interesting insights into the pathogenic pathways of neurodegeneration. As sALS and fALS patients are clinically indistinguishable,[7] studies on the *SOD1*-linked form of the disease may have the potential for revealing common mechanisms of the disease.

1.2.2 SOD1 mouse models

Knowledge of the link between SOD1 and ALS has led to the development of novel experimental methods involving transgenic species,[3,10] in particular transgenic mice expressing the mutant gene *SOD1*^{G93A},[41] the most widely used mouse model for ALS.[7,10] These mice develop symptoms and pathology that mimic human ALS patients,[41] and have led to the generation of a series of other transgenic rodents that express a wide variety of SOD1 enzyme mutants and

develop neurodegenerative pathophysiology similar to human ALS,[41-44] used to extensively study the pathogenic mechanisms of neurodegeneration.

Figure 1.2 shows some fALS physical symptoms in a transgenic *SOD1* mouse model. Mutant *SOD1* transgenic mice have proven to be a useful tool in the study of motor neuron degeneration, as shown with the discovery of riluzole as a treatment for ALS, as it is effective in improving the survival of both *SOD1* transgenic mice and sALS patients.[15,45] Efforts towards finding an effective treatment for ALS have resulted in the study of numerous other different therapies in transgenic mice.[46]

a)

b)

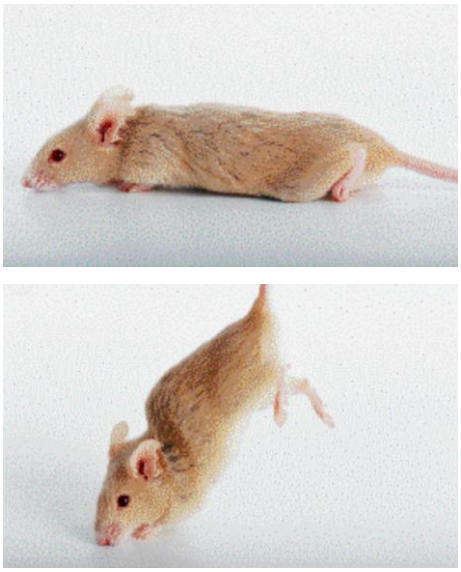

Figure 1.2 A *SOD1*^{G93A} transgenic mouse, displaying hind-limb muscle atrophy and paralysis: a) at rest; and b) under dorsal flex testing conditions.

While transgenic mice have proven useful in the study of future treatments of motor neuron degeneration, some success in transgenic mouse models has not always correlated with success in human trials.[46] For example, creatine has been shown to have neuroprotective properties in *SOD1*^{G93A} mice, with a significant extension in survival and improvement of motor function, protecting the neurons from oxidative damage.[47] The neuroprotective effect of creatine has shown promise in human clinical trials for Parkinson's disease and Huntington's disease,[48] however human ALS clinical trials have shown limited beneficial effect.[49] There are obvious advantages in studying disease mechanisms in rodents, given their short life span and high breeding rates, however despite the wealth of information provided about ALS mechanisms by transgenic rodent models, there are a number of problems that may arise in the comparison of such models with human ALS patients. Rodents and humans metabolise drugs differently and have different genetic and physiological backgrounds, and not all features of human ALS are

reproduced in mutant *SOD1* rodents, while mouse/rat models and human ALS patients often practicably experience different modes of delivery in drug administration, which may exacerbate special metabolism differences.[37,46,50] Moreover, differences in the apparent efficacy in rodent models and human clinical trials may arise due to the timing of drug administration – as drug candidates tend to be administered to transgenic rodents prior to clinical onset, efficacy results may appear to be different across species as human ALS patients are only treated well into disease progression.[46,50] This is highlighted by the fact that the efficacy of riluzole is greatest when administered to *SOD1* transgenic mice early in disease progression, compared to human ALS patients, where a "probable" or "definite" ALS diagnosis is required before administration.[45] Also, in transgenic rodent models, a higher level of gene expression (~10-30 fold increase) is necessary to induce pathogenic phenotype compared to ALS patients, where only a single copy of the mutant gene is required to develop fALS.[50] Furthermore, *SOD1* transgenic models may not fully represent the entire ALS population, given that only 1-2% of ALS patients experience motor neuron death due to mutant SOD1 enzymes, and even less due to the popular G93A mutation.[46,50] While it is possible that some therapies may target possible downstream pathways common to sALS, SOD1-fALS and non-SOD1-fALS patients, it is also possible that limited understanding of sporadic cases of ALS may be gained from fALS models, since the pathophysiology of both forms of the disease is largely unknown.[46] Despite the aforementioned differences, *SOD1* transgenic mouse and rat models have been highly valuable in conducting pharmacokinetic studies and testing efficacy of therapeutics, which is possibly due to the likely common pathways between the various forms of motor neuron degeneration.[37,50]

1.2.3 The gain-of-function model of SOD1

Studies have suggested that the pathogenic mechanism of ALS develops *via* SOD1 enzyme mutations through a gain-of-function mechanism independent of SOD1 activity, not a loss of function as originally proposed – meaning that the absence of the *SOD1* gene does not lead to development of ALS, and that progression of the disease does not correlate to the enzyme's activity, rather the novel toxic properties acquired by mutation.[3,7,8,10] This is supported by the autosomal dominant mode of transmission and the lack of correlation between clinical severity in ALS patients and enzyme activity levels,[40] as well as evidence that mutant *SOD1* transgenic mice develop severe and progressive motor neuron degeneration,[41] while mice overexpressing or lacking wild type SOD1 do not.[51,52] There are currently two hypothesised SOD1 gain-of-function mechanisms by which neurodegeneration may progress: by the aggregation or oligomerisation of misfolded SOD1 proteins; or by oxidative damage caused by

aberrant oxidative reactions[1,3,7,8,10]. It is likely that the true pathological mode of action of mutant SOD1 is a mixture of both oxidative damage and protein aggregation.

The SOD1 oxidative damage theory suggests that mutant SOD1 enzymes catalyse aberrant oxidative reactions that damage substrates essential for cell function and viability or may promote the oxidative damage of the enzyme itself. This is supported by evidence that mutant *SOD1* genes increase cellular markers of oxidative damage compared to wild type *SOD1*, resulting in mitochondrial dysfunction and motor neuron death in cell cultures and transgenic mice.[53-57] The gain-of-function hypothesis is supported by evidence that a normal level of SOD1 activity is observed in *SOD1* transgenic mice that display neurodegeneration.[43,44] Furthermore, it has been observed that $^{\bullet}O_2^-$ levels are significantly lower in mutant *SOD1* transgenic mice compared to controls, while H_2O_2 and $^{\bullet}OH$ levels are increased, indicating that increased reactive oxygen species (ROS) levels in transgenic mice are not due to decreased dismutase activity.[56] Evidence suggests that an increased rate of the oxidation of substrates by hydrogen peroxide associated with A4V- and G93A-encoded mutant SOD1 enzymes may account for gain-of-function toxic property, and the effect is reduced *in vitro* by treatment with copper chelators.[58] Further studies have suggested that the same mutant SOD1 enzymes exhibit enhanced free radical-generating function relative to the wild type enzyme, due to a small decrease in the K_m for H_2O_2, as mutant and wild type SOD1 enzymes have the same H_2O_2 dismutation activity.[59,60] It should be noted that some SOD1 mutations affect the metal-binding capacity of the enzyme,[61] putting the copper-mediated oxidative stress hypothesis into question. Further evidence that other mechanisms must play a part in the gain-of-function action of mutant SOD1 is that copper knockout in *SOD1* transgenic mice does not change the onset or progression of neurodegeneration.[62]

Intracellular protein aggregates are frequently associated with neurodegenerative disorders and are present in all forms of ALS, particularly in spinal cord motor neurons.[1,3,6,7,10] While the association between these aggregates and onset of the disease is unclear, several hypotheses have been put forward to explain their formation and function. Protein misfolding may occur as a consequence of products of oxidative stress, namely from the carbonylation, nitration and other forms of modification of common proteins.[37] Aggregate formation is a common, and possibly toxic, property of several investigated mutant SOD1 enzymes; insoluble SOD1 aggregates have been shown to form from mutant SOD1 enzymes *in vitro*, *in vivo* and in human ALS patients, arising from abnormal folding.[51,61,63,64] In addition to the misfolding of mutant SOD1 species, evidence suggests that even wild type SOD1 (as well as mutant SOD1) can misfold and form aggregates,[3] thereby providing a possible cell death pathway between sALS and fALS. The link between cell death pathways and formation of these intracellular aggregates is not yet fully understood, however various theories involve the mechanical interference of

such aggregates with intercellular and axonal transport, and the sequestration of proteins critical for cell viability – for example the anti-apoptotic protein Bcl-2.[34,37]

1.2.4 Mitochondrial dysfunction, apoptosis and neurodegenerative disease

A common feature of a number of neurodegenerative diseases is mitochondrial dysfunction that can inevitably lead to cell death.[30,31,65-67] Mitochondria are eukaryote organelles responsible for cell metabolism, with vital cellular functions including ATP production, regulating apoptosis, participating in calcium signalling and maintaining calcium homeostasis in cells.[30,66,67] Because of the potential for disruption of the electron transport chain, mitochondria are a major source of ROS.[30,67] While it is established that mitochondrial dysfunction leads to a flux of cytoplasmic ROS by disruption of the mitochondrial respiratory chain,[30,31,67] there is also considerable evidence to suggest that mitochondrial damage can be attributed to oxidative stress in both sALS and fALS cases, as mitochondria themselves are targets of ROS.[30,54,65,68,69] This suggests a possible common oxidative mechanism of neuronal death between sALS and fALS. Furthermore, markers of oxidative damage to mitochondrial DNA (mtDNA) have been demonstrated in SOD1 transgenic mice,[70] while significantly higher levels of mutant mtDNA have been observed in the spinal cord of ALS patients compared to controls,[71] supporting an established correlation between mtDNA mutation and neurodegeneration.[67]

Because mitochondria can be a large source of ROS and regulate apoptotic processes, mitochondrial dysfunction can lead to cell death either by energy failure or apoptosis.[30,31,65-67] Apoptosis is a process by which a cell undergoes programmed cell death, either as a means of shaping tissues and organs within a developing organism, or to kill unfavourable cells for the sake of the organism.[72,73] It involves a cascade of the activation of proteins that destroy molecules necessary for cell viability,[73] plays an important role in a number of diseases – including cancer, where proliferation of unwanted cells occurs – and is a common cause of neuronal death in neurodegenerative disorders such as Alzheimer's disease, Parkinson's disease, and stroke, often involving an increased susceptibility of neurons to apoptosis.[66,72-74] Although the mechanisms of motor neurodegeneration are mostly unclear, evidence suggests that mitochondrial-dependent apoptosis may play a part in motor neuron death in ALS.[66,72,73,75]

Apoptosis is initiated by a number of apoptogenic factors. Members of the Bcl-2 family may be either pro- or anti-apoptotic, and may initiate the release of cytochrome *c* from mitochondria, which plays a key part in the activation of cell-death pathways.[72-77] Cytochrome *c* is an important part of the mitochondrial electron-transport chain, which is required for the generation of ATP, and it has been shown to display an antioxidant effect on ROS produced in the cell.[73] When released from the mitochondria into the cytoplasm, it forms a cytoplasmic

molecular complex called an apoptosome, which in turn activates members of the caspase family, a set of intracellular cysteine proteases capable of degrading vital cell proteins and activating the enzymatic degradation of other cellular constituents such as lipids and DNA.[72-79] Caspases have been shown to play a role in the pathogenesis of neurodegenerative disease, as supported by mutant SOD1 transgenic mouse models and cell culture studies.[79-81]

1.2.5 The localisation of mutant SOD1 in mitochondria

The SOD1 protein is mainly localised in the cytosol, however it also found in a number of organelles, including the mitochondria.[20,66,67] Both the wild type and fALS-related human mutant SOD1 enzymes are found in brain and spinal cord mitochondria, localised in the matrix, inner/outer membranes and particularly in the intermembrane space (IMS) of mitochondria.[31,66,67] Mutant SOD1 enzymes appear to have a much greater association with motor neuron mitochondria than wild type SOD1 enzymes do,[35,82] and it has been shown that their presence has a tendency to shift the redox potential of mitochondria and disrupt respiration, due to mitochondrial membrane damage.[42,66,82] This can lead to downstream consequences such as disrupted redox processes,[82] impaired respiration and ATP production,[82] as well as the disruption of calcium homeostasis[54,66] and the activation of the apoptotic cascade, as observed in numerous *SOD1* transgenic *in vitro* and *in vivo* models.[34,55,75,79,80,83] Evidence of SOD1-induced damage to mitochondria has been found in transgenic mouse models of fALS,[31,42,65,66,75] and death due to SOD1-induced mitochondrial dysfunction can be prevented by antioxidant administration *in vitro* and *in vivo*,[55,57] as well as apoptosis inhibitors.[55,80] Cell death is not observed when mutant SOD1 accumulates in the cytoplasm or other organelles,[83] indicating that localisation of mutant SOD1 within mitochondria is important in the pathogenesis of SOD1-related fALS.

1.2.6 Non-*SOD1* fALS

Although the *SOD1* gene has provided the strongest link with motor neuron degeneration, due to the low prevalence of ALS it has been difficult to determine other genes linked to the disease. To date, roughly 20 genes linked to ALS have been identified.[1,6,8,10,38,39] One such gene is *ALS2*, located on chromosome 2, which codes for the protein alsin, mutants of which have been linked with ALS2, an autosomal recessive form of juvenile ALS.[84,85] Other genes include *SETX*, which codes for the protein senataxin, associated with ALS4, a rare dominant juvenile onset disease with slow progression,[86] and *VAPB*, which codes for the vesicle associated membrane protein, linked with ALS8, a dominantly inherited adult onset form of the disease.[87]

Additionally, recent research has found a link between ALS and the gene *TARDBP*, which codes for the TAR DNA-binding protein (TDP-43).[1,3,6,10,39,88] Under normal conditions, TDP-43 regulates gene expression process including transcription and splicing, however the protein has been identified as a major component of ubiquitinated protein aggregates (intraneuronal inclusions) in ALS and dominant mutations of the gene have been linked to 3-4% of fALS cases and 1-2% of sALS cases.[1,3,6,10,39,88-91]

1.2.7 Genetics and sALS

While a vast majority of ALS patients acquire the disease sporadically, still very little is understood about the causes of this form of the disease. Despite evidence to suggest the involvement of genetics with an increased risk of developing sALS, including data from twin studies of apparently sporadic forms of the disease,[92] no gene has been conclusively linked to the disease.[6] Candidate gene analysis of sALS patients have identified a number of polymorphisms in genes as potential risk factors for sALS,[39,93] however these findings have not been conclusively replicable.[6] Additionally, several studies have shown a link between sALS and polymorphisms on chromosome 9p21, which has also been linked with fALS.[6] It must be noted that mutant alleles with low penetrance may be misdiagnosed as sALS cases.[27,94] In particular, the common *SOD1* mutation I113T has frequently been found in patients diagnosed with sALS,[94] although cases of families with high penetrance of the mutation have also been reported.[21]

1.2.8 Proposed modes of action of neurodegeneration

Studies have also shown that the production of radical species through excitotoxicity is a major factor in the degeneration of neurons, not only in the case of ALS, but also for a number of other neurodegenerative disorders.[1,6,8,95,96] Glutamate receptor stimulation and an influx of intracellular Ca^{2+} increases the production of free radicals, by activating enzymes that produce free radical molecules, leading to cytotoxicity and oxidative stress, a condition that describes exposure to oxygen radicals beyond the threshold of natural antioxidant defence mechanisms (Figure 1.3).[1,6,8,95,96]

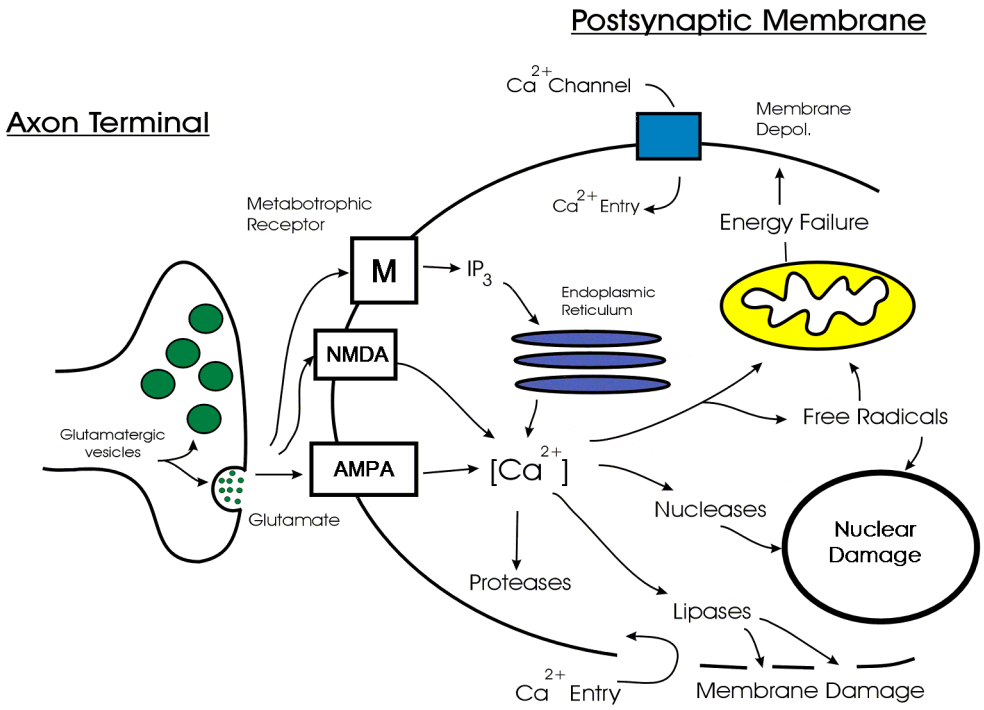

Figure 1.3 Glutamate-induced Ca^{2+} excitotoxicity. Excess glutamate leads to an influx of intracellular Ca^{2+}, which can result in an over-production of toxic species (*e.g.* free radicals) and the initiation of cellular death pathways.

1.3 Oxidative stress and the human body

In aerobic organisms, there is a fine balance between the production of reactive oxygen species during processes of oxidative metabolism in mitochondria and the ability of a biological system to protect itself by antioxidative processes from oxidative damage by reactive species. The disruption of this balance favouring the production of reactive oxygen species leads to a condition of oxidative stress and can result in cellular injury.[1,2,6,95,96] Several common neurological disorders are associated with oxidative stress, although it is not always established whether oxidative damage is a cause or consequence of neurodegeneration.[1,2,6,95,96]

1.3.1 Reactive oxygen species

Reactive oxygen species (ROS) refer to a group of reactive, oxygen-containing molecules and ions that can have a large impact on cellular processes. These can include oxygen ions, peroxides and free radicals. Examples of ROS include hydroxyl ($^{\bullet}OH$), superoxide ($^{\bullet}O_2^-$) and nitric oxide ($NO^{\bullet}$) free radicals, as well as hydrogen peroxide (H_2O_2), singlet oxygen ($^1O_2$), hypochlorous acid (HOCl) and ozone (O_3).[95,96] They can be formed in the human body by both

deliberate pathways and by chemical side reactions, and can be removed by naturally occurring enzymatic and non-enzymatic antioxidants.[1,2,96] Molecular oxygen itself is a notable ROS, and in its ground (triplet) state is a diradical with parallel spins of two lone electrons.[95] Spin restriction does not allow acceptance of a pair of electrons of opposite spin, so O_2 reacts slowly with non-radicals, however it can react quickly with radical species.[95]

1.3.2 The cellular impact of ROS

ROS can have a disastrous effect on biological tissue, causing a free radical chain reaction (Scheme 1.2, Scheme 1.3), which leads to autoxidation, or "lipid peroxidation", when the reactant is a lipid, resulting in a decrease in the integrity of the cell.[95,96] The first step of the reaction involves the production of lipid radicals from radical species, represented as R• in Scheme 1.2 and Scheme 1.3. Radical species may arise from the homolytic cleavage of molecular precursors, for example the cleavage of hydrogen peroxide to form hydroxyl radicals (•OH), which are extremely reactive towards biological molecules and prone to initiating free radical chain reactions.[95,96] Initiation of lipid peroxidation may occur by addition of the radical species R• to a double bond, or more likely hydrogen abstraction, to form the lipid radical (L•), which may react very rapidly with oxygen in an aerobic environment to form a peroxyl radical (LOO•), which may then abstract hydrogen from other cellular components (LH) to form a lipid hydroperoxide (LOOH) and further carbon-centred radicals (L•).[95] Thus, the free radical chain reaction propagates until termination to give molecular products occurs. Due to the nature of the propagation step, many lipid molecules can be autoxidated from the product of a single free radical.[95]

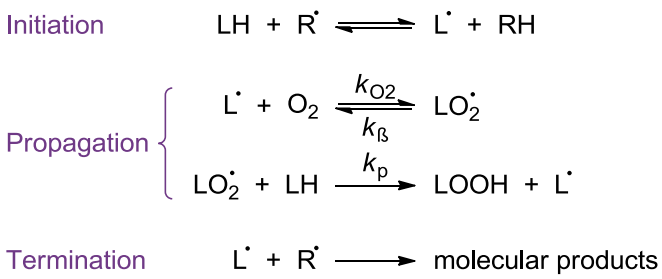

Scheme 1.2 The Free Radical Chain Reaction.[95] "LH" represents a general lipid molecule, typical of those found in cell membranes. NB: not exhaustive with respect to reactions possible at each step.

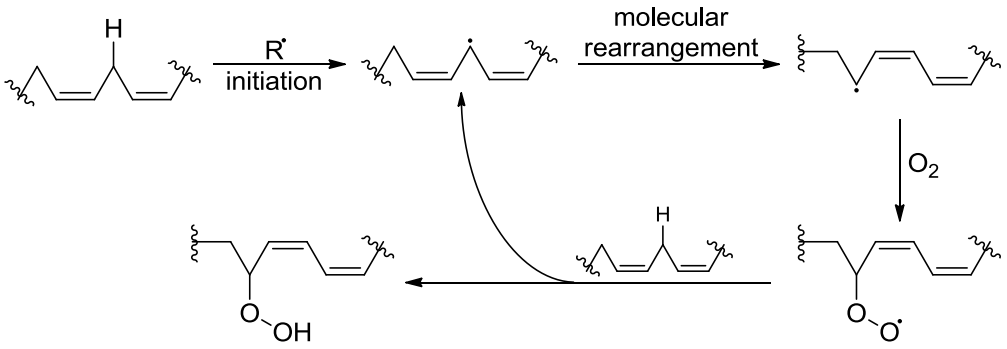

Scheme 1.3 A molecular representation of typical lipid peroxidation pathways.[95]

Allylic hydrogens are susceptible to hydrogen abstraction by a radical species due to the weakened C-H bond energy arising from the adjacent carbon-carbon double bond.[95] Bis-allylic hydrogens, where there is a double bond located on either side of the C-H bond, are particularly susceptible to hydrogen abstraction, and are therefore a likely site of lipid radical formation. Carbon-centred radicals formed from the abstraction of a bis-allylic hydrogen often undergo molecular rearrangement to form stable conjugated dienes, as shown in Scheme 1.3.[95]

Principal targets of chain-carrying peroxyl radicals are polyunsaturated fatty acids and esters located within the cellular membranes, and thus as the purpose of these biomembranes is to separate the various biochemical environments into specific regions of the cell, degradation of these membranes has a drastic effect on the protection and function of biological cells.[95] Lipid peroxidation has been observed in fALS mouse models, supporting the hypothesis of the role of oxidative stress in fALS.[97] The central nervous system (CNS) is more susceptible to oxidative stress than other tissues, as neurons contain a high proportion of easily oxidised substituents, including polyunsaturated lipids in the membrane, have a high oxygen consumption rate and flux of ROS from respiratory processes, and are lacking in efficient endogenous antioxidant defences.[1,6,96] As motor neurons rely heavily on membrane integrity and energy supply, disruption of the mitochondrial function and damage to cell membranes can have dire consequences on the survival of the cell. This is believed to be the cause of numerous debilitating disorders, including many neurodegenerative diseases.[1,6,95,96]

Evidence of ROS and oxidative damage has been reported for years in both sALS and fALS patients, indicating oxidative stress plays a role in the pathogenesis of ALS.[95,98-102] Cellular markers of oxidative stress that have been observed in human ALS patients and mouse models include: nitrotyrosine, a stable oxidation product of peroxynitrite,[99,100,102] lipid peroxidation byproducts malondialdehyde[97,98,100] and 4-hydroxynonenal[101] (found also in Alzheimer's disease cases[103]), as well as protein carbonyls and oxidised DNA.[98]

1.3.3 ROS production

During the normal process of the reduction of oxygen in mitochondria, low levels of potentially toxic ROS are produced. Respiratory complexes can leak electrons, which lead to the generation of superoxide ($^{\bullet}O_2^-$), an anionic radical, from the one-electron reduction of molecular oxygen (Scheme 1.4).[2,73,95,96] It has been suggested that around 2-3% of O_2 reduced in mitochondria *via* the electron transport chain forms $^{\bullet}O_2^-$.[95] Superoxide itself is not a very reactive radical, however it does react rapidly with other radical species, such as nitric oxide ($NO^{\bullet}$).[72,95] Superoxide is converted to H_2O_2 and O_2 by superoxide dismutases SOD1 (in cytoplasm) and SOD2 (in mitochondria).[2,37]

$$O_2 + e^- \longrightarrow {}^{\bullet}O_2^-$$
$$^{\bullet}O_2^- + 2H^+ + e^- \longrightarrow H_2O_2$$
$$H_2O_2 + e^- \longrightarrow OH^- + {}^{\bullet}OH$$
$$^{\bullet}OH + H^+ + e^- \longrightarrow H_2O$$

Scheme 1.4 The reduction of O_2 to H_2O occurs *via* sequential one-electron reductions, forming several ROS in the process.[73]

In addition to superoxide, other ROS such as hydrogen peroxide and hydroxyl radicals can be formed during normal respiratory processes (Scheme 1.4), as well as from the abnormal leakage of electrons from mitochondria.[73] Like superoxide, H_2O_2 has limited chemical reactivity, although they both have the ability to generate more reactive species *in vivo*.[7,95] Hydrogen peroxide may cross cell membranes and react with iron or even copper ions to form more damaging ROS such as $^{\bullet}OH$.[7,95] The hydroxyl radical itself may be produced by a number of processes, such as the homolytic fission of H_2O_2 by UV light or reaction of H_2O_2 with metal ions.[7,95] It reacts very rapidly with many biological substrates, including DNA, proteins and lipids, and can initiate lipid peroxidation, leading to a loss of membrane integrity, which can lead to other subsequent deleterious pathways.[95]

Redox-active transition metals, in particular copper and iron, can play a significant role in the production of ROS.[7,95] Transition metals can undergo "redox cycling", a process by which metals are alternately oxidised and reduced, which may lead to the generation of toxic ROS.[1,37] Metals are usually stringently managed in living organisms, sequestered within complexes or bound to enzymes or metal carriers.[37] Unbound transition metal ions have the ability to reduce H_2O_2 to generate highly reactive hydroxyl radicals,[95] as shown in Scheme 1.5. In the case where a ferrous ion (Fe^{2+}) acts as the reductant, the reaction is commonly known as the Fenton reaction.[104-106]

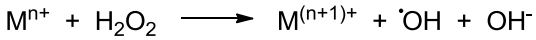

Scheme 1.5[37,95]

Iron, whilst playing an important role in many biochemical processes, also has the potential for toxicity in most organisms. The disproportionation of hydrogen peroxide by iron, as shown in Scheme 1.6, is often loosely referred to as "Fenton chemistry", named after Henry Fenton's work on the oxidative action of iron in the 1890s,[104] or "Haber-Weiss chemistry", based on findings of Fritz Haber and Joseph Weiss in the 1930s.[105,106] It involves a catalytic process by which ferrous and ferric ions are alternately oxidised and reduced respectively by hydrogen peroxide, forming hydroxyl radicals, hydroxyl anions, peroxyl radicals and protons in the process.[95]

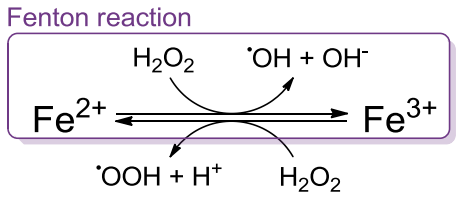

Scheme 1.6 The disproportionation of hydrogen peroxide by iron.[95]

A similar iron-mediated redox process known as the Haber-Weiss reaction generates hydroxyl radicals (and hydroxide ions) from the reaction of superoxide and hydrogen peroxide, as shown in Scheme 1.7.[105,106]

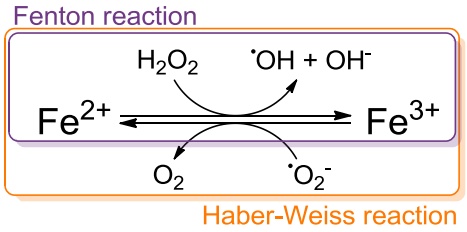

Scheme 1.7 The Haber-Weiss reaction.[105,106]

Evidence suggests that iron may play a part in the pathogenesis of sALS;[107,108] an increase in iron levels in the spinal cord has been observed in sALS patients.[108] Studies have also shown an increased incidence of mutations in the Hfe gene (associated with the iron-overload disease haemochromatosis) in patients with sALS, indicating some involvement of iron handling in the

pathogenesis of the disease.[109,110] Furthermore, an upregulation of ferritin in end-stage *SOD1* transgenic mice indicates an excessive accumulation of iron.[111]

The involvement of copper in the mechanisms of SOD1-fALS motor neuron degeneration has been supported by various studies, both *in vitro* and *in vivo*.[55,112] Copper chelators have been shown to delay disease onset and increase survival in *SOD1* transgenic mice[112] and prevent cell death in SOD1-fALS cell models,[55,113] supporting the toxic gain-of-function hypothesis of SOD1 mutations. Furthermore, *SOD1* transgenic mice genetically bred for a spinal cord copper deficiency had a significant delay in motor neuron degeneration and prolonged survival.[114] It is known that many mutant SOD1 proteins do not bind copper effectively,[115] and the inadequate buffering of Cu can lead to aberrant oxidative chemistry, inducing oxidative stress and subsequent cell death.[116,117]

Free iron and copper ions in cells can also react with lipid peroxides, in a similar manner to the Fenton reaction, to form alkoxyl radicals (Scheme 1.8), which may then propagate lipid peroxidation.[95]

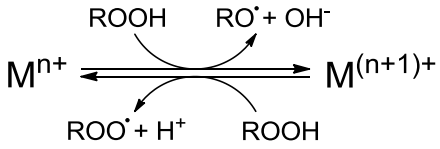

Scheme 1.8

While ROS make up the majority of oxidising species in aerobic organisms, oxidative stress may also arise from the presence of reactive nitrogen species (RNS), as well as reactive chlorine and bromine species.[95] Stress conditions can lead to nitric oxide synthase upregulation,[118,119] which can elevate levels of nitric oxide (NO•), a secondary messenger in signalling and neurotransmission. Nitric oxide can react with superoxide to give peroxynitrite (ONOO-), which is classified as both an ROS and an RNS.[95,96] Peroxynitrite and other RNS can oxidise and nitrate amino acid aromatic side chains and other substrates, leading to a condition called "nitrosative stress".[37,120] Oxidation and nitration of lipids and nitration of amino acids (for example the nitration of tyrosine to from 3-nitrotyrosine) can lead to enzyme inactivation.[95] Peroxynitrite has been shown to participate in lipid peroxidation and inhibit mitochondrial respiration, thus contributing to neurodegenerative disorders that occur *via* oxidative and nitrosative processes.[121]

1.3.4 Natural defences against oxidative damage

It is well established that free radicals and ROS are continuously formed in aerobic organisms during normal respiratory processes.[1,2,95,96] As a result, aerobic organisms have evolved to develop elaborate antioxidant protection in order to deal with oxygen management and the potential for oxidative stress.[95] Intracellular antioxidant defence in the CNS can be attributed to antioxidant proteins and enzymes and low molecular weight antioxidant (LMWA) species.[122] A number of enzymes act as antioxidants by reducing or dismutating ROS to innocuous molecules. In human cells, superoxide dismutases protect cellular substrates from oxidative stress by converting superoxide to hydrogen peroxide and water, while superoxide reductases reduce O_2^- to H_2O_2.[2,73,95,122] Hydrogen peroxide formed by these and other processes can be converted to harmless species by catalase and peroxidases.[2,73,95,122] In particular, glutathione peroxidases are a family of enzymes that use the thiol-containing tripeptide glutathione (GSH) to reduce hydrogen peroxide and organic hydroperoxides to water and alcohols, respectively, subsequently forming glutathione disulfide (GSSG), which is reduced back to GSH by glutathione reductase.[95] While enzyme activity plays a large part in the human body's defence against oxidative stress, a number of non-enzymatic proteins may also act as endogenous antioxidants. The proteins transferrin and ferritin, which transport and store iron, respectively, can be considered as endogenous antioxidants as they sequester iron, a metal responsible for many oxidative processes in organisms.[95] Of the LWMA species, a majority of the small molecule antioxidants are obtained from dietary sources, while only a few are synthesised endogenously. Reduced GSH is a major intracellular antioxidant,[74,95,122] while other LWMA species include plant phenols and polyphenols, retinoic acid (vitamin A), tocopherols (vitamin E), ascorbic acid (vitamin C), uric acid, lipoic acid, melatonin and coenzyme Q_{10}.[95,122-126]

1.4 Calcium influx and excitotoxicity

1.4.1 Excitotoxic mechanisms and neurodegeneration

Glutamate (Figure 1.4) is the primary excitatory neurotransmitter in the central nervous system,[8,127,128] responsible for a number of neurologic functions such as learning, memory and movement.[128] Excitotoxicity, a pathological process by which neurons die from over-activation of glutamate receptors at the synaptic cleft caused by an excess of glutamate, is strongly implicated as a major contributing factor in the pathogenesis of neuronal death.[7,8,127-129] The link between glutamate-mediated excitotoxicity and ALS is well established, with early

studies indicating that many ALS patients exhibit a significant increase in glutamate in cerebrospinal fluid (CSF).[130]

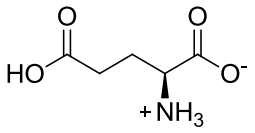

Figure 1.4 Glutamate, the major neurotransmitter in the CNS.

One of the causes of neuronal death appears to be the disruption of calcium homeostasis *via* activation of Ca^{2+} channels, release of Ca^{2+} from intracellular stores and production of free radicals by Ca^{2+}-dependent enzymes.[127-129] Excess Ca^{2+} influx in neurons can result from an overstimulation of glutamate receptors, such as the *N*-methyl-D-aspartate (NMDA) receptor and α-amino-3-hydroxy-5-methyl-4-isoxazolepropionic acid (AMPA) receptor, leading to cytotoxic effects, especially in mitochondria (Figure 1.3).[54,127-129,131-134]

Calcium is an important secondary messenger in the CNS, important in signalling pathways vital for cell survival,[66,128] however an excess of intracellular Ca^{2+} can have disastrous effects, as studies have demonstrated a correlation between the disruption of Ca^{2+} homeostasis and neurodegeneration.[66,127-129] Evidence has shown that high levels of cytosolic free Ca^{2+} are not necessarily toxic to neurons,[134] however potential-driven uptake of Ca^{2+} into mitochondria triggers glutamate-induced neuronal death.[134,135]

Numerous toxic pathways may be activated by glutamate-induced Ca^{2+} influx. In a number of neurodegenerative disorders, the increase in Ca^{2+} levels in the neuron results in activation of Ca^{2+}-dependent proteins and enzymes (Figure 1.3),[128] which can lead to nuclear and membrane damage, and as well as an increase of ROS.[54,131-133,136] In particular, Ca^{2+} uptake from glutamate receptor stimulation results in increased ROS production from mitochondrial electron transport chain processes.[132,133,136] It is though that the process of neuronal death due to oxidative stress may be self-sustaining, since hydroxyl radicals may be released from mitochondria as the organelle wall integrity is compromised, electron transport chain may be altered, mtDNA may be oxidised and membrane degradation may lead to the disruption of Ca^{2+} homeostasis.[2,30,37,67]

There may be a number of mechanisms by which the over-stimulation of glutamate receptors is initiated: increased synaptic glutamate due to uncontrolled release of glutamate from presynaptic neurons; increased synaptic glutamate due to deficient glutamate transport function; or altered expression or sensitivity of glutamate receptors, leading to increased Ca^{2+} influx in neurons at normal glutamate levels.[127-129,137] In the case of motor neuron disease, there

is significant evidence to suggest that the dysfunction of both glutamate transporters and Ca^{2+}-permeable receptors influence the pathogenic pathways of neuronal death.[127-129,137]

1.4.2 Glutamate transporters and excitotoxicity

Glutamate exists almost entirely intracellularly due to the activity of high-affinity glutamate transporters. It is usually found at low concentrations (≤1 μM) in extracellular fluid,[138] significantly lower than in cells, where glutamate concentration is approximately 10 mM.[139] Extracellular glutamate levels are regulated by the rapid uptake of the amino acid by glutamate transporters,[5,128] preventing overstimulation of excitatory amino acid receptors and resulting excitotoxic neuronal damage that readily occurs at concentrations of above 10 μM.[140] Five different subtypes of high-affinity glutamate or excitatory amino acid transporters (EAATs), located in the plasma membranes of both neurons and astrocytes, have been identified.[5,128,141,142] Immunocytochemistry has shown that glutamate transporter subtypes are distributed differently within cell types and across regions of the brain and the CNS; EAAT1 (GLAST in rodents) and EAAT2 (GLT-1 in rodents) are located primarily in astrocytes, while EAAT3 (EAAC1 in rodents), EAAT4 and EAAT5 are expressed by neurons in the brain.[5,128,141,142]

Antisense knockdown experiments and biochemical studies have indicated that astrocyte transporter EAAT2/GLT-1, located within the brain and spinal cord,[5,141,142] is the predominant glutamate transporter subtype in buffering extracellular glutamate at an appropriate level in the CNS and protecting neurons from excitotoxicity.[143-147] In 1992, Rothstein *et al.*[148] first demonstrated that ALS patients present reduced glutamate transport function in the spinal cord and regions of the brain, compared to healthy subjects and patients with Alzheimer's disease and Huntington's disease. Studies have since shown that the decreased transport function is primarily due to a significant decrease of EAAT2 levels in ALS patients.[149-152] The loss of functional glutamate transport could account for significantly increased levels of glutamate in the CSF of some ALS patients compared to controls.[130,140]

Several *in vitro* and *in vivo* studies have supported the involvement of impaired glutamate transport function in motor neuron degeneration, however the extent to which transporter dysfunction contributes to neurodegeneration has been difficult to assess.[5,128] A decrease of EAAT2/GLT-1 has been observed in the spinal cord of *SOD1* transgenic rats at the onset of neuron degeneration[144] and in *SOD1*^{G93A} mice at advanced stages of the disease.[153] It has been demonstrated that decreases in transporter levels are specifically localised to regions of neuron loss in the CNS, such as the motor cortex and spinal cord, and do not occur in areas of no neuronal degeneration.[151,153] *In vitro* inhibition of glutamate transporters has been shown to lead to an increase in extracellular glutamate and the slow degeneration of motor neurons;

toxicity was prevented by non-NMDA receptor antagonists (although not NMDA receptor antagonists), supporting the hypothesis that progressive motor neuron degeneration in ALS may be due in part to defective glutamate transport.[154] In *SOD1*^{G93A} mice, a lack of change in GLT-1 levels at the pre-symptomatic stage of the disease indicates that the loss of transport function is not a primary event in the neurodegenerative cascade; rather changes in transporter and glutamate levels merely contribute to the disease progression.[153] This hypothesis is supported by observations in *SOD1*^{G93A} mice bred to overexpress GLT-1, where increase in the transporter did not delay disease onset or increase survival, but did delay motor neuron loss and grip-strength decline.[155] While a lot of data suggests at least some involvement of glutamate transport deficiency in motor neuron degeneration, one study demonstrated that *in vivo* administration of glutamate transport blockers significantly elevated extracellular glutamate in rats, however despite this no motor neuron degeneration, gliosis or motor activity deficits were observed.[156]

Evidence has shown that glutamate transporters can be rendered inactive due to oxidative stress.[120,157-160] Of the glutamate transporters found in humans and rodents, GLT-1/EAAT2 is particularly susceptible to oxidative damage.[101,145,161] GLT-1/EAAT2 function has been demonstrated to be reduced by mutant (but not wild type) SOD1 *in vitro*[161] and in mice[44,153] and rats.[144] A mechanism of inhibition by oxidation is supported by a similar pattern of GLT-1 inactivation observed when the transporter was exposed to peroxidation by H_2O_2 under Fenton conditions,[161] and the restoration of transport function after treatment with the antioxidant Mn^{III}TBAP.[161] This supports the hypothesis that SOD1-linked fALS occurs *via* an excitotoxic mechanism caused by the toxic properties of SOD1 mutants.

1.4.3 Glutamate receptors and excitotoxicity

Glutamate secreted from glutamatergic vesicles stimulates ionotropic (ligand-gated) glutamate receptors such as the NMDA receptor, AMPA receptor and kainite (KA) receptor, and metabotropic receptors (Figure 1.3), all of which regulate the influx of ions such as K^+, Na^+ and Ca^{2+} into the neuron.[127,128,162-166] Overstimulation of these receptors can lead to an increase in cytosolic free Ca^{2+} levels.[127,128,162,163] *In vitro* studies have shown that motor neurons are particularly sensitive to glutamate excitotoxicity resulting from AMPA receptor activation.[128,154,164,166]

AMPA receptors are predominantly heteromeric, tetrameric, ligand-gated channels, consisting of four subunits, GluA1-4 (previously referred to as GluR1-4), of which the subunit GluA2 is functionally dominant in determining Ca^{2+} permeability.[128,163,165-167] Calcium permeability of AMPA receptors depends on their GluA subunit composition; AMPA receptors

lacking the GluA2 subunit are permeable to Ca^{2+} (Figure 1.5), an influx of which can lead to excitotoxicity.[166] The functional dominance of the GluA2 subunit results from post-transcriptional messenger RNA (mRNA) editing, which involves the replacement of a neutral glutamine (Q) residue – found in GluA1, 3 and 4 – with a positively charged arginine (R) residue at what is known as the "Q/R site" in the second transmembrane region of GluA2.[128,165,168] In the non-diseased state, virtually all GluA2 subunits are impermeable to Ca^{2+} due to editing of effectively 100% of *GRIA2*, the gene that encodes GluA2.[168,169] Evidence has suggested that the increased Ca^{2+} permeability of AMPA receptors in ALS patients may be due to either a significant decrease in post-transcriptional editing of *GRIA2*,[168,170] reduced *GRIA2* expression,[171] or combination of both factors.[169]

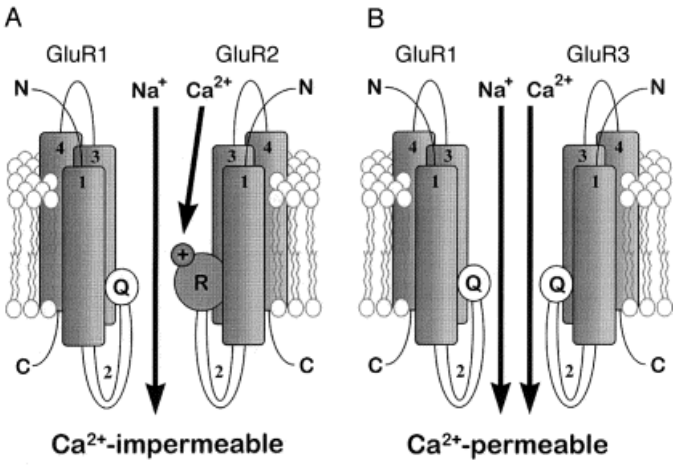

Figure 1.5[171] The presence or absence of an edited GluA2 (GluR2) subunit determines the Ca^{2+} permeability of AMPA receptors.

Various *in vivo* studies support the theory that a high proportion of Ca^{2+}-permeable AMPA receptors in motor neurons may cause the cells to be highly susceptible to excitotoxicity from Ca^{2+} influx.[163] In *SOD1* transgenic mice, deficiency or overexpression of GluA2 can either accelerate or ameliorate motor neuron degeneration, respectively,[172,173] which supports evidence that the *SOD1*^{G93A} mutation causes changes in the expression and function of AMPA receptors, increasing vulnerability of motor neurons to excitotoxicity.[174] Treatment with AMPA receptor antagonists has also been shown to slow disease progression and extend survival of *SOD1* transgenic mice.[175-177]

While a decrease in permeability-regulating GluA2 has been observed in spinal cords of fALS *SOD1*^{G93A} mice before the onset of neurodegenerative symptoms, a modest upregulation of Ca^{2+}-permeable GluA3 has been shown to occur concomitantly,[175] indicating a possible deleterious involvement of GluA3 in the excitotoxic mechanisms of ALS. Supporting these

observations, treatment of *SOD1*^{G93A} mice with peptide nucleic acids antisense to GluA3 mRNA has been shown to significantly extend disease onset and mouse survival.[178,179] This evidence suggests that GluA3 may act as ideal candidate as a therapeutic target for the treatment of neurodegeneration. There is also promise in the development of specific AMPA receptor antagonists for treatment of glutamate-induced neurodegenerative disorders.

1.4.4 Beta-amyloid

Numerous studies on the causes of Alzheimer's disease have suggested that fragments of the protein β-amyloid (Aβ) may accumulate in cell membranes, producing ROS by catalytic processes,[4,96,180-182] which in turn may impair the function of glial glutamate transporters,[183,184] subsequently disrupting Ca^{2+} homeostasis and contributing to neuronal degeneration from excitotoxicity.[182] Oxidative stress caused by Aβ has been shown to be ameliorated by number of antioxidants, including catalase, vitamin E and Trolox™.[181,182,184] In addition to the oxidative processes that arise from the presence of Aβ, studies have shown that the oligomer has the ability form Ca^{2+}-conducting pores in neuronal membranes, leading to influx of Ca^{2+} and subsequent neurotoxic cascades.[185,186]

1.5 Small molecule approaches to treating ALS

1.5.1 Riluzole

The only currently approved treatment for ALS is the glutamate antagonist riluzole (Figure 1.1). Marketed as Rilutek®, it has been available in Australia since 2002, and has been covered under the Pharmaceutical Benefits Scheme (PBS) since June 2003.[9,16] The drug is often administered in 50 mg doses, usually twice a day,[27,187] and although it can increase life expectancy by an average of 2 to 3 months,[13-15] there are a number of common side-effects of the drug, include nausea, vomiting, asthenia, anorexia, diarrhoea, dizziness, gastrointestinal disorders, and liver dysfunction.[9,13-18]

The action of riluzole has not yet been extensively determined; however it is proposed that riluzole interrupts glutamatergic neurotransmission, both though the blockage of voltage-gated sodium channels, which inhibits glutamate release, and the indirect antagonism of glutamate receptors.[128,129,188-190] Trials in the 1990s indicated the efficacy of riluzole as a treatment for ALS, with increased tracheotomy-free survival by a matter of 2 to 3 months,[13-15] however there is limited evidence of a beneficial effect of riluzole in patients over 75 years.[18] A

survival benefit of greater than 6 months has been suggested, however an increase in the quality of care of ALS patients may affect this figure.[191]

The recommended orally administered dosage of riluzole is 100 mg a day,[14,27,187] which has been determined by clinical trials and efficacy studies to have the optimum benefit-to-risk ratio,[14,15] and the drug has been found to be well tolerated by patients for up to 7 years.[192] While riluzole is by no means a cure for ALS, if the drug is administered as early as possible it can slow disease progression, thus possibly allowing ALS sufferers a higher quality of life for a longer period of time.[9] The benefit of riluzole has been shown to be more significant in patients with bulbar onset, compared to limb onset.[13,193] Despite the benefit of increased lifespan, and the increase survival and preservation of motor function in *SOD1*^{G93A} mice early in disease progression,[45,194] riluzole does not appear to improve quality of life or motor function of ALS patients.[14,15] Due to riluzole's limited efficacy, concern over adverse side-effects and the prohibitive cost of the drug, there is a requirement for alternative treatments of ALS on the market.

1.5.2 Antioxidants

Antioxidants are molecules that prevent oxidative degradation, either by reducing the rate of initiation of radicals (*preventative* antioxidants) or interfering with one or more of the oxidative steps (*chain-breaking* antioxidants).[195] Chain-breaking antioxidants such as vitamin E, vitamin C, and food additive butylated hydroxytoluene (BHT) quench the propagating chain by "trapping" peroxyl radicals, typically forming radicals themselves (Scheme 1.9), which can be stabilised *via* resonance.[195,196]

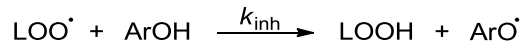

Scheme 1.9 An example of the action of chain-breaking antioxidants.

In order for an antioxidant to be an effective free radical scavenger, the rate of inhibition (k_{inh}) must be larger than the rate of propagation of lipid peroxidation (k_p, Scheme 1.2). Vitamin E is an efficient antioxidant, as it scavenges peroxyl radicals around 10^4 times faster than the rate of lipid peroxidation.[195,197]

Vitamin E is a commonly known chain-breaking antioxidant, and the term "vitamin E" can generally refer to any of four structurally related compounds called tocopherols (Figure 1.6), of which α-tocopherol is most potent and most commonly found in nature,[95,195,198] while the natural (2*R*,4'*R*,8'*R*) diastereoisomer offers the best antioxidative protection.[95,199] Studies have

shown that vitamin E is the major – and possibly only – lipid soluble, chain-breaking antioxidant in human blood.[200,201] As labelled in Figure 1.6, the general structure of vitamin E consists of a reactive chromanol "head" group and a hydrophobic phytyl "tail" side chain.[195,202] It is generally accepted that the tocopherols orientate within biomembranes with the chromanol head towards the surface and the hydrophobic phytyl side chain incorporated within the hydrophobic bilayer.[195,202]

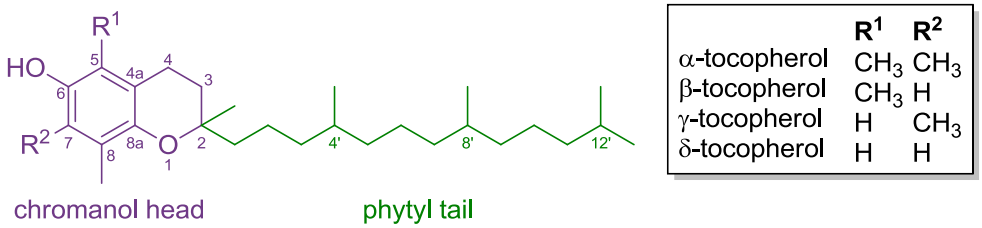

Figure 1.6 The general structure of vitamin E. "Natural" vitamin E, 2*R*,4'*R*,8'*R*-α-tocopherol, is the most common and most biologically potent form of vitamin E.

The chromanol core is effective as a free radical scavenger, due to its ability to react with radical species to form a phenoxyl radical stabilised *via* resonance structures as shown in Figure 1.7.

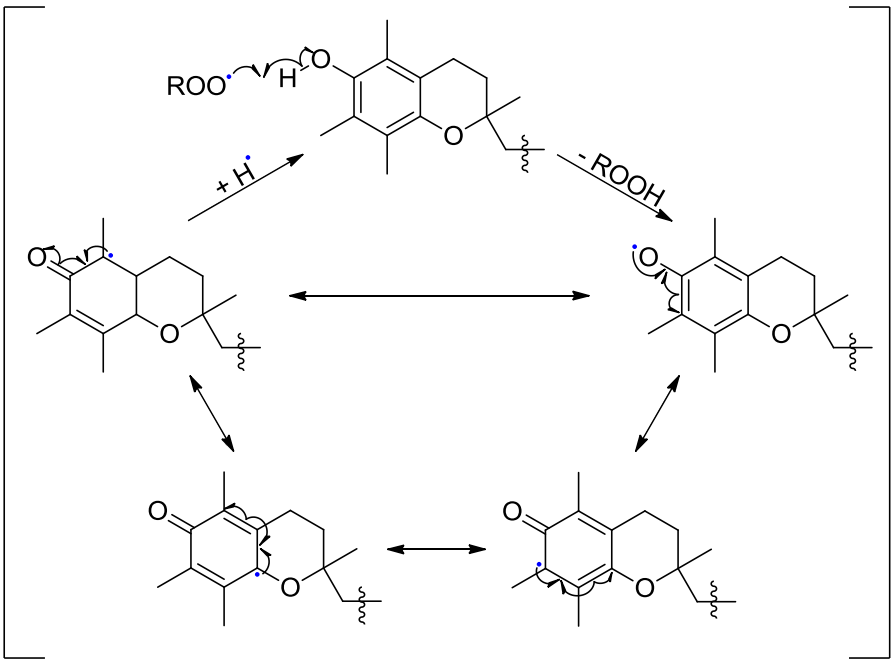

Figure 1.7 Radical capture is stabilised through resonance structures of α-tocopherol.

Effective hydrogen donation of vitamin E is also due to low bond dissociation enthalpy of the phenolic hydroxyl bond, resulting from the electron-donating oxygen situated *para* to the

phenolic hydroxyl group.[203] Vitamin E may transfer its phenolic hydrogen atom to an incoming lipid peroxyl radical, forming a phenoxyl radical itself, in the process converting the peroxyl radical to a hydroperoxide, which is consumed by other pathways.[195,202]

In certain cases, vitamin E may be regenerated from the phenoxyl radical by vitamin C, a water soluble reducing agent. Vitamin E and vitamin C have been shown to act synergistically *in vitro*, with vitamin E acting as the primary antioxidant, of which the resulting phenoxyl radical is regenerated to vitamin E on reaction with vitamin C.[195,204,205] This interaction is believed to occur at the membrane interface, thus effectively transporting the potentially damaging radical from the membrane to the aqueous phase,[195,205] as vitamin E acts as the better antioxidant in the lipid phase, whereas vitamin C is an excellent inhibitor of peroxidation in the aqueous phase.[195,205,206] The resulting vitamin C radical may then be enzymatically reduced back to vitamin C by endogenous antioxidants, for example NADH (Figure 1.8).[204]

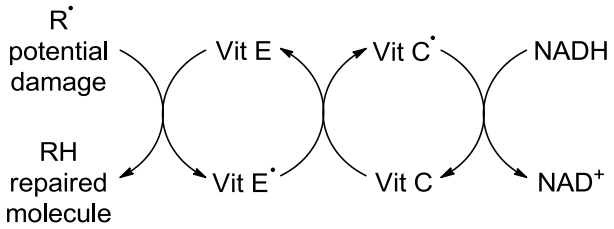

Figure 1.8[204] The antioxidant action of vitamin E and subsequent regeneration by vitamin C and NADH.

While treatment with vitamin E has been shown to have a beneficial effect in *SOD1* transgenic mice,[194] to date there has been limited success in human ALS patients,[7,207,208] however long-term regular users of vitamin E supplements have less than half the risk of dying of ALS than non-users.[209]

Many antioxidants have been synthesised based on the structure of vitamin E.[210-218] Extensive efforts have been made to synthesise an antioxidant even more potent than α-tocopherol, and some success has been found with the development of benzofuran derivatives of vitamin E,[210-213] due to the favourable dihedral orbital angle of the furanyl oxygen to the aromatic plane.[195,219] Another consideration when designing a vitamin E derivative is solubility. Vitamin E is a highly lipophilic molecule and although it intercalates easily within lipid membranes, it is not water soluble due to its long hydrophobic side chain, which can cause problems biologically. Studies on vitamin E analogues with hydrophilic side chains have shown increased bioavailability, and the ability to target specific organs,[213,214] or organelles such as mitochondria,[215] with retention of antioxidant activity. In particular, Trolox™ (Figure 1.9), a water soluble derivative of vitamin E, has been demonstrated to display potent antioxidant

activity.[217,218] Structure-activity relationship studies have indicated that the potent antioxidant activity is due not only to the phenolic group of the necessary chromanol core, but also the carboxylic acid, in any of the 2*R*, 2*S*, or racemic compounds.[218]

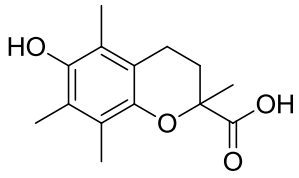

Figure 1.9 Trolox™, a water soluble vitamin E (α-tocopherol) derivative.

Treatment of ALS patients with other antioxidants has been met with limited success. Despite evidence that antioxidants such as *Gingko biloba* extract,[220] spin-trapping molecule DMPO[57] and antioxidant porphyrins AEOL10150[221] and FeTCPP[222] protect against oxidative damage, delay paralysis and extend survival in *SOD1* transgenic mice, there is little evidence of their efficacy in human ALS patients. Overall, clinical trials of antioxidant therapies have shown little therapeutic effect on patients to date.[1,7,207,223]

1.5.3 Calcium chelators

Since intracellular free Ca^{2+} is an important secondary messenger in biological systems, and an excess of intracellular Ca^{2+} can have a large effect on the function of neurons,[66,128] it is important to examine various means of measuring and regulating the amount of intracellular Ca^{2+}, especially since neurons have low levels of natural Ca^{2+} buffers.[128] One example of an effective Ca^{2+}-chelating agent is 1,2-bis(*o*-aminophenoxy)ethane-*N*,*N*,*N*',*N*'-tetraacetic acid (BAPTA), shown in Figure 1.10. First synthesised by Tsien,[224] the compound was designed with two features in mind: aromatic chromophores to allow for monitoring of Ca^{2+} chelation by spectroscopy; and low nitrogen pK_a values for pH insensitivity and Ca^{2+}-chelating speed. At physiological pH, BAPTA exists in its deprotonated form ($BAPTA^{4-}$), and exhibits high selectivity ($>10^5$) for Ca^{2+} over Mg^{2+}, but with low anilinium nitrogen pK_a values of 6.36 and 5.47, which result in pH insensitivity and a high rate of uptake and release of Ca^{2+}, due to the low probability of protonation.[224] The reason for the selectivity for Ca^{2+} over Mg^{2+} is believed to be due to the binding cavity, which is an appropriate size to be able to encapsulate Ca^{2+}, however the carboxylic acid groups of the molecule prevent encapsulation of the smaller ion Mg^{2+}, due to steric considerations.[224]

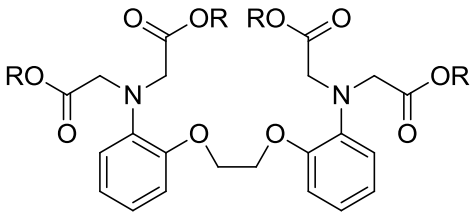

Figure 1.10 Ca^{2+}-binding agent 1,2-bis(*o*-aminophenoxy)ethane-*N*,*N*,*N*',*N*'-tetraacetic acid (BAPTA, R=H) and its tetraethyl ester (R=Et).

Work in collaboration with our research group has found that BAPTA also exhibits antioxidant properties, which are possible due to the captodative nature of the chelating side chains.[225,226] These studies have determined that BAPTA exhibits antioxidant function, regardless of whether or not it is bound to Ca^{2+}. Thus, it appears that BAPTA and BAPTA derivatives may be useful when devising a treatment against both an influx of Ca^{2+} and oxidative stress. The efficacy of BAPTA has led to the synthesis of a number of BAPTA derivatives as possible candidates to reduce the effect of oxidative stress on neurons due to Ca^{2+} influx.[226-231] Deprotonated BAPTA is negatively charged, with four carboxylate groups, and is unable to cross biomembranes and therefore unable to permeate into cells. Esters of BAPTA, however, may provide lipophilicity required for crossing cell membranes, as well as the potential to be hydrolysed to the tetracarboxylate parent species within cells. One such compound, the acetoxymethyl ester of BAPTA (BAPTA-AM), has been shown to exhibit cell permeability and undergo hydrolysis *in vitro*,[231] and protect against excitotoxic cell injury *in vitro* and *in vivo*.[232,233] Studies conducted in our research group have shown that intraperitoneal injections of the tetraethyl ester derivative of BAPTA (Figure 1.10) can significantly increase survival in transgenic ALS mice. Importantly, survival is increased further in transgenic rats when BAPTA tetraethyl ester is infused intrathecally.[234,235] This indicates issues with the prodrug crossing the blood brain barrier to reach the desired region of action, likely due to the largely hydrophobic structure.

1.5.4 Other therapeutic approaches

A number of other pharmacological treatments for motor neuron degeneration have been examined.[7,37,46,50,236] Administration of minocycline, an antibiotic agent, delays disease onset and extends survival in *SOD1*^{G93A} mice by inhibiting cytochrome *c* release from mitochondria,[237,238] however phase III clinical trials of minocycline failed in human patients.[239] Various therapeutic agents targeting excitotoxic pathways have also been studied. Ceftriaxone, a β-lactam antibiotic that stimulates the transcription of glutamate transporter GLT-1/EAAT2, has

been shown to delay neurodegeneration and increase survival in *SOD1* transgenic mice,[5,240] although early clinical trials have shown limited evidence of clinical efficacy.[241] Despite this, phase III clinical studies are ongoing in the United States and Canada.[242-244] AMPA receptor antagonists have also shown to have a beneficial effect in transgenic mice,[175,176] while a phase II clinical trial of Talampanel[245] has been terminated due to conclusively negative results in humans.[242]

As well as pharmacological approaches, therapies that target gene translation and transcription are possible candidates in the treatment of motor neuron degeneration. RNA silencing may be achieved using small interfering RNAs (siRNAs), double-stranded RNA duplexes of 21 to 23 nucleotides, which promote degradation of selected target mRNAs, thus decreasing protein expression levels of a single gene.[246] While siRNA designed to selectively target mutant alleles have been shown to be effective in the treatment of *SOD1*-linked fALS models *in vitro* and *in vivo*,[247] targeting individual point mutations would not be a feasible strategy in the treatment of such a multifactorial disease such as ALS, where a number of point mutations have been linked to the disease. Interfering RNA broadly targeting all alleles of the *SOD1* gene has been shown to reduce gene expression in *SOD1*^{G93A} transgenic mice, resulting in improved motor performance, significant delay in disease onset and increase of survival.[248,249]

Administration of antisense oligonucleotides to SOD1 mRNA has been shown to reduce both SOD1 protein and mRNA levels in the brain and spinal cord of transgenic rats, slowing disease progression significantly.[250] Similarly, treatment with antisense peptide nucleic acid (PNA) oligomers directed against GluA3 showed neuroprotection against an AMPA agonist *in vitro* and extended survival in a *SOD1*^{G93A} transgenic mouse model.[179] Likewise, treatment of *SOD1*^{G93A} mice with antisense PNA oligomers targeting p75^{NTR}, a neurotrophin receptor implicated in the pathogenesis of mutant SOD1-mediated neuronal death, has been demonstrated to delay motor impairment and increase mouse survival.[251]

1.5.5 A multi-functional approach to treating neurodegeneration

Therapeutic trials of antioxidants such as vitamin E and vitamin C on patients with ALS and other diseases such as Alzheimer's disease and Parkinson's disease have shown no significant benefit.[1,7,207,208,223] The reason for this appears to be that antioxidants alone are not enough to combat the large amount of oxidative stress that motor neurons must endure. Thus, a multi-factorial approach to the prevention and treatment of neurodegenerative disorders may prove to be advantageous. Ideally, a candidate for the treatment of neurodegeneration would perform multiple specific functions. Studies have indicated that if a drug candidate could simultaneously target multiple specific factors that lead to neuron death, the efficacy of the drug

in combating neurodegeneration could be increased.[7,37,50,128] Combinatorial therapies that incorporate drugs that target multiple pathways or cell types may play a role in neurodegeneration and have been of recent interest.[7,37,50,128] However, the large expense of such trials means that they are not readily approved by regulatory agencies and thus are rarely attempted.[252]

A number of combinatorial therapies have shown promising results in transgenic models, and even exhibited synergistic effects.[7,37,50,128] Of particular interest is the combination of creatine, an endogenous amino acid (shown to exhibit antioxidant properties[253]), and minocycline, an apoptosis inhibitor.[254] When administered separately, both agents have been shown to improve motor performance and extend survival in transgenic mice, although when administered together they exhibit an additive neuroprotective effect in delaying disease onset and increasing survival in the ALS model.[254] Other combinatorial treatments shown to exhibit an additive effect on motor function and survival in ALS mouse models include the combination of minocycline, riluzole and nimodipine, a voltage-gated calcium channel antagonist,[255] as well as the concurrent administration of Neu2000, a potent antioxidant, and lithium carbonate, a mood stabiliser that prevent apoptosis.[256]

1.6 Project aims and experimental plan

One well known problem of combinatorial therapies is the possibility of unfavourable interactions between therapeutic agents or mode of action at different places.[37] It is anticipated that this effect can be overcome with the design of multifunctional drug candidates that incorporate two or more desired modes of action. In the case of treating motor neuron degeneration, it is envisaged that incorporating both antioxidant function and Ca^{2+}-buffering capability in the one molecule by prove favourable in targeting known cell death pathways.

The aims of the project are as follows:

- To synthesise a series of potential drug candidates that incorporate both a free radical scavenger and a Ca^{2+} chelator (Figure 1.11). The target molecule has a multi-functional approach: the free radical scavenger part of the molecule may reduce oxidative stress on neurons by converting free radicals into innocuous molecules, while the Ca^{2+}-buffering component could regulate the amount of free Ca^{2+} in the neuron, thus preventing activation of enzymes that initiate cell death pathways (Figure 1.3). Thus, a

synergistic approach to the treatment and prevention of neurodegeneration can be applied.

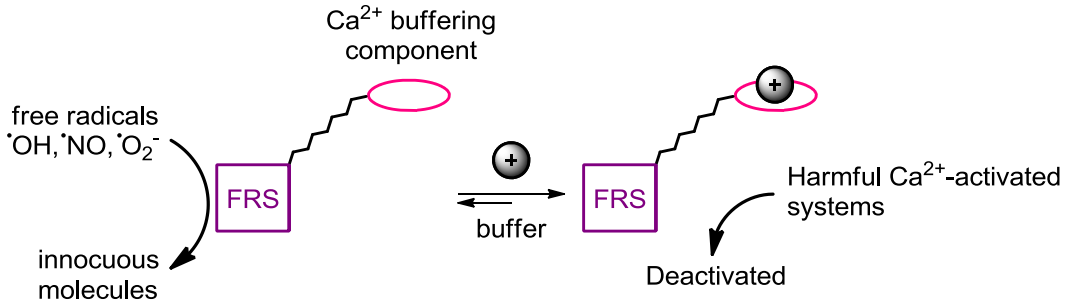

Figure 1.11 Proposed structure and function of the potential drug candidate, incorporating both a free radical scavenger (FRS) and Ca^{2+}-buffering component.

- To conduct antioxidant efficiency testing and binding studies on the dual-action compounds.

With the general function of the dual-action candidates (Figure 1.11) in mind, two series of targets were designed for synthesis throughout this project. For both series, it is envisaged that the tetraethyl ester targets will be able to cross cell membranes and be hydrolysed to form free acetates *in situ*, thus allowing for binding to Ca^{2+} ions in cells. Synthesis of the free carboxylic acids, however, may also allow for eventual testing of Ca^{2+}-binding capability and antioxidant activity while complexed with Ca^{2+}.

1.6.1 Soluble BAPTA derivatives

Previous work on both BAPTA and its tetraethyl ester have indicated that BAPTA itself acts as an effective treatment in ALS transgenic mice and rats, however it appeared that there were problems both with the water solubility of the prodrug for administration and the ability of the compound to cross the blood brain barrier to reach the desired area of action. A series of slightly hydrophilic BAPTA derivatives, depicted generally in Figure 1.12, will be synthesised. It has been hypothesised that variation of the R-group may allow for greater water solubility, thus the target should act as a more effective treatment than BAPTA against neurodegeneration.

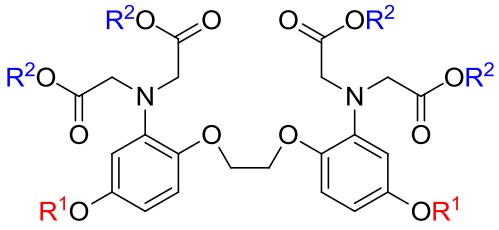

Figure 1.12 Soluble BAPTA derivative targets. R-groups may include, but are not limited to, amines, polyethers, alcohols and protons.

1.6.2 Vitamin E/BAPTA hybrids

The second series of targets, shown generally in Figure 1.13, combine the antioxidant chromanol of vitamin E and the Ca^{2+}-binding cavity of BAPTA in one compound, hopefully leading to dual-action properties. Since the antioxidant function of the chromanol lies in the placement of the pyran oxygen *para* to the phenolic O-H, it will be interesting to determine how placement of an anilinic nitrogen atom or phenolic oxygen at the *meta* position may affect the ability of the compound to donate a hydrogen atom, and thus how the antioxidant properties are affected. It is, however, expected that the installation of the chromanol will increase water solubility compared to BAPTA itself. It is anticipated that throughout the project, various techniques for the synthesis of chroman cores will be explored, allowing for installation of varied functional groups on chroman formation.

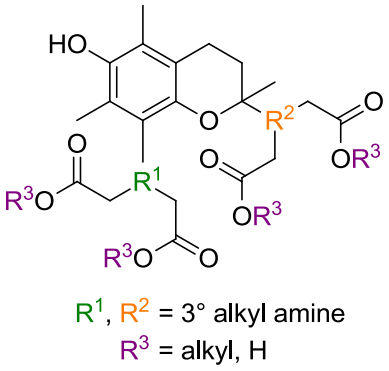

Figure 1.13 Vitamin E/BAPTA hybrid targets. R^1 and R^2 represent tertiary alkyl amines, while R^3 groups may include, but are not limited to, amines, polyethers, alcohols and protons.

1.7 References

1. Shukla, V.; Mishra, S. K.; Pant, H. C., *Adv. Phar. Sc.* **2011**, 1-13.

2. Cui, H.; Kong, Y.; Zhang, H., *J. Signal Transduct.* **2012**, 1-13.

3. Joyce, P.; Fratta, P.; Fisher, E.; Acevedo-Arozena, A., *Mamm. Genome* **2011**, *22*, 420-448.

4. Ma, T.; Klann, E., *J. Neurochem.* **2012**, *120*, 140-148.

5. Kim, K.; Lee, S.-G.; Kegelman, T. P.; Su, Z.-Z.; Das, S. K.; Dash, R.; Dasgupta, S.; Barral, P. M.; Hedvat, M.; Diaz, P.; Reed, J. C.; Stebbins, J. L.; Pellecchia, M.; Sarkar, D.; Fisher, P. B., *J. Cell. Physiol.* **2011**, *226*, 2484-2493.

6. Ferraiuolo, L.; Kirby, J.; Grierson, A. J.; Sendtner, M.; Shaw, P. J., *Nat. Rev. Neurol.* **2011**, *7*, 616-630.

7. Contestabile, A., *Curr. Med. Chem.* **2011**, *18*, 5655-5665.

8. Kiernan, M. C.; Vucic, S.; Cheah, B. C.; Turner, M. R.; Eisen, A.; Hardiman, O.; Burrell, J. R.; Zoing, M. C., *Lancet* **2011**, *377*, 942-955.

9. Kiernan, M. C., *Med. J. Aust.* **2005**, *182*, 319-320.

10. Swarup, V.; Julien, J.-P., *Prog. Neuropsychopharmacol. Biol. Psychiatry* **2011**, *35*, 363-369.

11. Tucker, T.; Layzer, R. B.; Miller, R. G.; Chad, D., *Neurology* **1991**, *41*, 1541-1544.

12. Tsai, C. P.; Ho, H. H.; Yen, D. J.; Wang, V.; Lin, K. P.; Liao, K. K.; Wu, Z. A., *Eur. Neurol.* **1993**, *33*, 387-389.

13. Bensimon, G.; Lacomblez, L.; Meininger, V., *N. Engl. J. Med.* **1994**, *330*, 585-591.

14. Lacomblez, L.; Bensimon, G.; Meininger, V.; Leigh, P. N.; Guillet, P., *Lancet* **1996**, *347*, 1425-1431.

15. Miller, R. G.; Mitchell, J. D.; Lyon, M.; Moore, D. H., *Amyotroph. Lateral Sc.* **2003**, *4*, 191-206.

16. Schedule of Pharmaceutical Benefits. www.pbs.gov.au (accessed 27 February 2012).

17. Bensimon, G.; Doble, A., *Expert Opin. Drug Saf.* **2004**, *3*, 525-534.

18. Bensimon, G.; Lacomblez, L.; Delumeau, J. C.; Bejuit, R.; Truffinet, P.; Meininger, V., *J. Neurol.* **2002**, *249*, 609-615.

19. Strong, M. J.; Hudson, A. J.; Alvord, W. G., *Can. J. Neurol. Sci.* **1991**, *18*, 45-58.

20. Rosen, D. R.; Siddique, T.; D., P.; Figlewicz, D. A.; Sapp, P.; Hentati, A.; Donaldson, D.; Goto, J.; O'Regan, J. P.; Deng, H. X., *Nature* **1993**, *362*, 59-62.

21. Cudkowicz, M. E.; McKenna-Yasek, D.; Sapp, P. E.; Chin, W.; Geller, B.; Hayden, D. L.; Schoenfeld, D. A.; Hosler, B. A.; Horvitz, H. R.; Brown, R. H., *Ann. Neurol.* **1997**, *41*, 210-221.

22. Eisen, A.; Schulzer, M.; MacNeil, M.; Pant, B.; Mak, E., *Muscle & Nerve* **1993**, *16*, 27-32.

23. Haverkamp, L. J.; Appel, V.; Appel, S. H., *Brain* **1995**, *118*, 707-719.

24. Grohme, K.; v. Maravic, M.; Gasser, T.; Borasio, G. D., *Neuromuscular Disord.* **2001**, *11*, 414-416.

25. Andersen, P. M.; Forsgren, L.; Binzer, M.; Nilsson, P.; Ala-Hurula, V.; Keranen, M.-L.; Bergmark, L.; Saarinen, A.; Haltia, T.; Tarvainen, I.; Kinnunen, E.; Udd, B.; Marklund, S. L., *Brain* **1996**, *119*, 1153-1172.

26. Rosen, D. R.; Bowling, A. C.; Patterson, D.; Usdin, T. B.; Sapp, P.; Mezey, E.; McKenna-Yasek, D.; O'Regan, J.; Rahmani, Z.; Ferrante, R. J.; Brownstein, M. J.; Kowall, N. W.; Beal, M. F.; Horvitz, H. R.; Brown, R. H., *Hum. Mol. Genet.* **1994**, *3*, 981-987.

27. Andersen, P. M.; Borasio, G. D.; Dengler, R.; Hardiman, O.; Kollewe, K.; Leigh, P. N.; Pradat, P.-F.; Silani, V.; Tomik, B., *Eur. J. Neurol.* **2005**, *12*, 921-938.

28. Deng, H.-X.; Hentati, A.; Tainer, J. A.; Iqbal, Z.; Cayabyab, A.; Hung, W.-Y.; Getzoff, E. D.; Hu, P.; Herzfeldt, B.; Roos, R. P.; Warner, C.; Deng, G.; Soriano, E.; Smyth, C.; Parge, H. E.; Ahmed, A.; Roses, A. D.; Hallewell, R. A.; Pericak-Vance, M. A.; Siddique, T., *Science* **1993**, *261*, 1047-1051.

29. Milani, P.; Gagliardi, S.; Cova, E.; Cereda, C., *Neurol. Res. Int.* **2011**, 1-9.

30. Duffy, L. M.; Chapman, A. L.; Shaw, P. J.; Grierson, A. J., *Neuropathol. Appl. Neurobiol.* **2011**, *37*, 336-352.

31. Faes, L.; Callewaert, G., *J. Bioenerg. Biomembr.* **2011**, *43*, 587-592.

32. Reddy, P. H.; Reddy, T. P., *Curr. Alzheimer Res.* **2011**, *8*, 393-409.

33. McCord, J. M.; Fridovich, I., *J. Biol. Chem.* **1969**, *244*, 6049-6055.

34. Pasinelli, P.; Belford, M. E.; Lennon, N.; Bacskai, B. J.; Hyman, B. T.; Trotti, D.; Brown Jr, R. H., *Neuron* **2004**, *43*, 19-30.

35. Liu, J.; Lillo, C.; Jonsson, P. A.; Velde, C. V.; Ward, C. M.; Miller, T. M.; Subramaniam, J. R.; Rothstein, J. D.; Marklund, S.; Andersen, P. M.; Brännström, T.; Gredal, O.; Wong, P. C.; Williams, D. S.; Cleveland, D. W., *Neuron* **2004**, *43*, 5-17.

36. Sau, D.; De Biasi, S.; Vitellaro-Zuccarello, L.; Riso, P.; Guarnieri, S.; Porrini, M.; Simeoni, S.; Crippa, V.; Onesto, E.; Palazzolo, I.; Rusmini, P.; Bolzoni, E.; Bendotti, C.; Poletti, A., *Hum. Mol. Genet.* **2007**, *16*, 1604-1618.

37. Cozzolino, M.; Ferri, A.; Carrì, M. T., *Antioxid. Redox Sign.* **2008**, *10*, 405-444.

38. ALS Online Genetics Database. http://alsod.iop.kcl.ac.uk/ (accessed 27 February 2012).

39. Sreedharan, J., *CNS Neurol. Disord. Drug Targets* **2010**, *9*, 259-267.

40. Shibata, N., *Neuropathology* **2001**, *21*, 82-92.

41. Gurney, M. E.; Pu, H.; Chiu, A. Y.; Canto, M. C. D.; Polchow, C. Y.; Alexander, D. D.; Caliendo, J.; Hentati, A.; Kwon, Y. W.; Deng, H.-X.; Chen, W.; Zhai, P.; Sufit, R. L.; Siddique, T., *Science* **1994**, *264*, 1772-1775.

42. Wong, P. C.; Pardo, C. A.; Borchelt, D. R.; Lee, M. K.; Copeland, N. G.; Jenkins, N. A.; Sisodia, S. S.; Cleveland, D. W.; Price, D. L., *Neuron* **1995**, *14*, 1105-1116.

43. Ripps, M. E.; Huntley, G. W.; Hof, P. R.; Morrison, J. H.; Gordon, J. W., *Proc. Natl. Acad. Sci. USA* **1995**, *92*, 689-693.

44. Bruijn, L. I.; Becher, M. W.; Lee, M. K.; Anderson, K. L.; Jenkins, N. A.; Copeland, N. G.; Sisodia, S. S.; Rothstein, J. D.; Borchelt, D. R.; Price, D. L.; Cleveland, D. W., *Neuron* **1997**, *18*, 327-338.

45. Gurney, M. E.; Fleck, T. J.; Himes, C. S.; Hall, E. D., *Neurology* **1998**, *50*, 62-66.

46. Benatar, M., *Neurobiol. Dis.* **2007**, *26*, 1-13.

47. Klivenyi, P.; Ferrante, R. J.; Matthews, R. T.; Bogdanov, M. B.; Klein, A. M.; Andreassen, O. A.; Mueller, G.; Wermer, M.; Kaddurah-Daouk, R.; Beal, M. F., *Nat. Med.* **1999**, *5*, 347-350.

48. Beal, M., *Amino Acids* **2011**, *40*, 1305-1313.

49. Groeneveld, G. J.; Veldink, J. H.; Tweel, I. v. d.; Kalmijn, S.; Beijer, C.; Visser, M. d.; Wokke, J. H. J.; Franssen, H.; Berg, L. H. v. d., *Ann. Neurol.* **2003**, *53*, 437-445.

50. Carrì, M. T.; Grignaschi, G.; Bendotti, C., *Trends Pharmacol. Sci.* **2006**, *27*, 267-273.

51. Bruijn, L. I.; Houseweart, M. K.; Kato, S.; Anderson, K. L.; Anderson, S. D.; Ohama, E.; Reaume, A. G.; Scott, R. W.; Cleveland, D. W., *Science* **1998**, *281*, 1851-1854.

52. Reaume, A. G.; Elliott, J. L.; Hoffman, E. K.; Kowall, N. W.; Ferrante, R. J.; Siwek, D. R.; Wilcox, H. M.; Flood, D. G.; Beal, M. F.; Brown, R. H.; Scott, R. W.; Snider, W. D., *Nat. Genet.* **1996**, *13*, 43-47.

53. Liu, R.; Althaus, J. S.; Ellerbrock, B. R.; Becker, D. A.; Gurney, M. E., *Ann. Neurol.* **1998**, *44*, 763-770.

54. Kruman, I. I.; Pedersen, W. A.; Springer, J. E.; Mattson, M. P., *Exp. Neurol.* **1999**, *160*, 28-39.

55. Ghadge, G. D.; Lee, J. P.; Bindokas, V. P.; Jordan, J.; Ma, L.; Miller, R. J.; Roos, R. P., *J. Neurosci.* **1997**, *17*, 8756-8766.

56. Liu, D.; Wen, J.; Liu, J.; Li, L., *FASEB J.* **1999**, *13*, 2318-2328.

57. Liu, R.; Li, B.; Flanagan, S. W.; Oberley, L. W.; Gozal, D.; Qiu, M., *J. Neurochem.* **2002**, *80*, 488-500.

58. Wiedau-Pazos, M.; Goto, J. J.; Rabizadeh, S.; Gralla, E. B.; Roe, J. A.; Lee, M. K.; Valentine, J. S.; Bredesen, D. E., *Science* **1996**, *271*, 515-518.

59. Yim, H.-S.; Kang, J.-H.; Chock, P. B.; Stadtman, E. R.; Yim, M. B., *J. Biol. Chem.* **1997**, *272*, 8861-8863.

60. Yim, M. B.; Kang, J. H.; Yim, H. S.; Kwak, H. S.; Chock, P. B.; Stadtman, E. R., *Proc. Natl. Acad. Sci. USA* **1996**, *93*, 5709-5714.

61. Wang, J.; Slunt, H.; Gonzales, V.; Fromholt, D.; Coonfield, M.; Copeland, N. G.; Jenkins, N. A.; Borchelt, D. R., *Hum. Mol. Genet.* **2003**, *12*, 2753-2764.

62. Subramaniam, J. R.; Lyons, W. E.; Liu, J.; Bartnikas, T. B.; Rothstein, J.; Price, D. L.; Cleveland, D. W.; Gitlin, J. D.; Wong, P. C., *Nat. Neurosci.* **2002**, *5*, 301-307.

63. Johnston, J. A.; Dalton, M. J.; Gurney, M. E.; Ron, R. K., *Proc. Natl. Acad. Sci. USA* **2000**, *97*, 12571-12576.

64. Rakhit, R.; Cunningham, P.; Furtos-Matei, A.; Dahan, S.; Qi, X.-F.; Crow, J. P.; Cashman, N. R.; Kondejewski, L. H.; Chakrabartty, A., *J. Biol. Chem.* **2002**, *277*, 47551-47556.

65. Carrì, M.; Cozzolino, M., *J. Bioenerg. Biomembr.* **2011**, *43*, 593-599.

66. Shi, P.; Gal, J.; Kwinter, D. M.; Liu, X.; Zhu, H., *Biochim. Biophys. Acta* **2010**, *1802*, 45-51.

67. Filosto, M.; Scarpelli, M.; Cotelli, M.; Vielmi, V.; Todeschini, A.; Gregorelli, V.; Tonin, P.; Tomelleri, G.; Padovani, A., *J. Neurol.* **2011**, *258*, 1763-1774.

68. Kirkinezos, I. G.; Bacman, S. R.; Hernandez, D.; Oca-Cossio, J.; Arias, L. J.; Perez-Pinzon, M. A.; Bradley, W. G.; Moraes, C. T., *J. Neurosci.* **2005**, *25*, 164-172.

69. Mattiazzi, M.; D'Aurelio, M.; Gajewski, C. D.; Martushova, K.; Kiaei, M.; Beal, M. F.; Manfredi, G., *J. Biol. Chem.* **2002**, *277*, 29626-29633.

70. Warita, H.; Hayashi, T.; Murakami, T.; Manabe, Y.; Abe, K., *Mol. Brain Res.* **2001**, *89*, 147-152.

71. Wiedemann, F. R.; Manfredi, G.; Mawrin, C.; Beal, M. F.; Schon, E. A., *J. Neurochem.* **2002**, *80*, 616-625.

72. Holcik, M.; LaCasse, E.; MacKenzie, A.; Korneluk, R., Eds. *Apoptosis in Health and Disease: Clinical and Therapeutic Aspects*. 1st ed.; Cambridge University Press: Cambridge, 2005.

73. Caroppi, P.; Sinibaldi, F.; Fiorucci, L.; Santucci, R., *Curr. Med. Chem.* **2009**, *16*, 4058-4065.

74. Naoi, M.; Maruyama, W.; Yi, H.; Inaba, K.; Akao, Y.; Shamoto-Nagai, M., *J. Neural. Transm.* **2009**, *116*, 1371-1381.

75. Guégan, C.; Vila, M.; Rosoklija, G.; Hays, A. P.; Przedborski, S., *J. Neurosci.* **2001**, *21*, 6569-6576.

76. Ribe, E. M.; Serrano-saiz, E.; Akpan, N.; Troy, C. M., *Biochem. J.* **2008**, *415*, 165-182.

77. Manfredi, G.; Xu, Z., *Mitochondrion* **2005**, *5*, 77-87.

78. Bossy-Wetzel, E.; Newmeyer, D. D.; Green, D. R., *EMBO J.* **1998**, *17*, 37-49.

79. Pasinelli, P.; Houseweart, M. K.; Brown, R. H., Jr.; Don, W. C., *Proc. Natl. Acad. Sci. USA* **2000**, *97*, 13901-13906.

80. Li, M.; Ona, V. O.; Guégan, C.; Chen, M.; Jackson-Lewis, V.; Andrews, L. J.; Olszewski, A. J.; Stieg, P. E.; Lee, J.-P.; Przedborski, S.; Friedlander, R. M., *Science* **2000**, *288*, 335-339.

81. Friedlander, R. M.; Brown, R. H.; Gagliardini, V.; Wang, J.; Yuan, J., *Nature* **1997**, *388*, 31-32.

82. Ferri, A.; Cozzolino, M.; Crosio, C.; Nencini, M.; Casciati, A.; Gralla, E. B.; Rotilio, G.; Valentine, J. S.; Carrì, M. T., *Proc. Natl. Acad. Sci. USA* **2006**, *103*, 13860-13865.

83. Takeuchi, H.; Kobayashi, Y.; Ishigaki, S.; Doyu, M.; Sobue, G., *J. Biol. Chem.* **2002**, *277*, 50966-50972.

84. Yang, Y.; Hentati, A.; Deng, H.-X.; Dabbagh, O.; Sasaki, T.; Hirano, M.; Hung, W.-Y.; Ouahchi, K.; Yan, J.; Azim, A. C.; Cole, N.; Gascon, G.; Yagmour, A.; Ben-Hamida, M.; Pericak-Vance, M.; Hentati, F., *Nat. Genet.* **2001**, *29*, 160-165.

85. Hadano, S.; Hand, C. K.; Osuga, H.; Yanagisawa, Y.; Otomo, A.; Devon, R. S.; Miyamoto, N.; Showguchi-Miyata, J.; Okada, Y.; Singaraja, R.; Figlewicz, D. A.; Kwiatkowski, T.; Hosler, B. A.; Sagie, T., *Nat. Genet.* **2001**, *29*, 166-173.

86. Chen, Y.-Z.; Bennett, C. L.; Huynh, H. M.; Blair, I. P.; Puls, I.; Irobi, J.; Dierick, I.; Abel, A.; Kennerson, M. L.; Rabin, B. A.; Nicholson, G. A.; Auer-Grumbach, M.; Wagner, K.; De Jonghe, P.; Griffin, J. W.; Fischbeck, K. H.; Timmerman, V.; Cornblath, D. R.; Chance, P. F., *Am. J. Hum. Genet.* **2004**, *74*, 1128-1135.

87. Nishimura, A. L.; Mitne-Neto, M.; Silva, H. C. A.; Richieri-Costa, A.; Middleton, S.; Cascio, D.; Kok, F.; Oliveira, J. R. M.; Gillingwater, T.; Webb, J.; Skehel, P.; Zatz, M., *Am. J. Hum. Genet.* **2004**, *75*, 822-831.

88. Neumann, M.; Sampathu, D. M.; Kwong, L. K.; Truax, A. C.; Micsenyi, M. C.; Chou, T. T.; Bruce, J.; Schuck, T.; Grossman, M.; Clark, C. M.; McCluskey, L. F.; Miller, B. L.; Masliah, E.; Mackenzie, I. R.; Feldman, H.; Feiden, W.; Kretzschmar, H. A.; Trojanowski, J. Q.; Lee, V. M.-Y., *Science* **2006**, *314*, 130-133.

89. Mackenzie, I. R. A.; Bigio, E. H.; Ince, P. G.; Geser, F.; Neumann, M.; Cairns, N. J.; Kwong, L. K.; Forman, M. S.; Ravits, J.; Stewart, H.; Eisen, A.; McClusky, L.; Kretzschmar, H. A.; Monoranu, C. M.; Highley, J. R.; Kirby, J.; Siddique, T.; Shaw, P. J.; Lee, V. M. Y.; Trojanowski, J. Q., *Ann. Neurol.* **2007**, *61*, 427-434.

90. Sreedharan, J.; Blair, I. P.; Tripathi, V. B.; Hu, X.; Vance, C.; Rogelj, B.; Ackerley, S.; Durnall, J. C.; Williams, K. L.; Buratti, E.; Baralle, F.; de Belleroche, J.; Mitchell, J. D.; Leigh, P. N.; Al-Chalabi, A.; Miller, C. C.; Nicholson, G.; Shaw, C. E., *Science* **2008**, *319*, 1668-1672.

91. Tan, C.-F.; Eguchi, H.; Tagawa, A.; Onodera, O.; Iwasaki, T.; Tsujino, A.; Nishizawa, M.; Kakita, A.; Takahashi, H., *Acta Neuropathol.* **2007**, *113*, 535-542.

92. Graham, A. J.; Macdonald, A. M.; Hawkes, C. H., *J. Neurol. Neurosurg. Psychiatry* **1997**, *62*, 562-569.

93. Schymick, J. C.; Talbot, K.; Traynor, B. J., *Hum. Mol. Genet.* **2007**, *16*, R233-R242.

94. Andersen, P., *Curr. Neurol. Neurosci. Rep.* **2006**, *6*, 37-46.

95. Halliwell, B.; Gutteridge, J. M. C. *Free Radicals in Biology and Medicine*, 4th ed.; Oxford University Press: Oxford, 2007.

96. Adibhatla, R. M.; Hatcher, J. F., *Antioxid. Redox Sign.* **2010**, *12*, 125-169.

97. Hall, E. D.; Andrus, P. K.; Oostveen, J. A.; Fleck, T. J.; Gurney, M. E., *J. Neurosci. Res.* **1998**, *53*, 66-77.

98. Ferrante, R. J.; Browne, S. E.; Shinobu, L. A.; Bowling, A. C.; Baik, M. J.; MacGarvey, U.; Kowall, N. W.; Jr., R. H. B., *J. Neurochem.* **1997**, *69*, 2064-2074.

99. Beal, M. F.; Ferrante, R. J.; Browne, S. E.; Matthews, R. T.; Kowall, N. W.; Jr, R. H. B., *Ann. Neurol.* **1997**, *42*, 644-654.

100. Ferrante, R. J.; Shinobu, L. A.; Schulz, J. B.; Matthews, R. T.; Thomas, C. E.; Kowall, N. W.; Gurney, M. E.; Beal, M. F., *Ann. Neurol.* **1997**, *42*, 326-334.

101. Pedersen, W. A.; Fu, W.; Keller, J. N.; Markesbery, W. R.; Appel, S.; Smith, R. G.; Kasarskis, E.; Mattson, M. P., *Ann. Neurol.* **1998**, *44*, 819-824.

102. Tohgi, H.; Abe, T.; Yamazaki, K.; Murata, T.; Ishizaki, E.; Isobe, C., *Ann. Neurol.* **1999**, *46*, 129-131.

103. Markesbery, W. R.; Lovell, M. A., *Neurobiol. Aging* **1998**, *19*, 33-36.

104. Fenton, H. J. H., *J. Chem. Soc.* **1894**, *65*, 899-903.

105. Haber, F.; Weiss, J., *Naturwissenschaften* **1932**, *20*, 948-950.

106. Haber, F.; Weiss, J., *Proc. R. Soc. Lond. A* **1934**, *147*, 332-351.

107. Leveugle, B.; Spik, G.; Perl, D. P.; Bouras, C.; Fillit, H. M.; Hof, P. R., *Brain Res.* **1994**, *650*, 20-31.

108. Kasarskis, E. J.; Tandon, L.; Lovell, M. A.; Ehmann, W. D., *J. Neurol. Sci.* **1995**, *130*, 203-208.

109. Wang, X.-S.; Lee, S.; Simmons, Z.; Boyer, P.; Scott, K.; Liu, W.; Connor, J., *J. Neurol. Sci.* **2004**, *227*, 27-33.

110. Goodall, E. F.; Greenway, M. J.; van Marion, I.; Carroll, C. B.; Hardiman, O.; Morrison, K. E., *Neurology* **2005**, *65*, 934-937.

111. Olsen, M. K.; Roberds, S. L.; Ellerbrock, B. R.; Fleck, T. J.; McKinley, D. K.; Gurney, M. E., *Ann. Neurol.* **2001**, *50*, 730-740.

112. Hottinger, A. F.; Fine, E. G.; Gurney, M. E.; Zurn, A. D.; Aebischer, P., *Eur. J. Neurosci.* **1997**, *9*, 1548-1551.

113. Azzouz, M.; Poindron, P.; Guettier, S.; Leclerc, N.; Andres, C.; Warter, J.-M.; Borg, J., *J. Neurobiol.* **2000**, *42*, 49-55.

114. Kiaei, M.; Bush, A. I.; Morrison, B. M.; Morrison, J. H.; Cherny, R. A.; Volitakis, I.; Beal, M. F.; Gordon, J. W., *J. Neurosci.* **2004**, *24*, 7945-7950.

115. Hayward, L. J.; Rodriguez, J. A.; Kim, J. W.; Tiwari, A.; Goto, J. J.; Cabelli, D. E.; Valentine, J. S.; Brown, R. H., *J. Biol. Chem.* **2002**, *277*, 15923-15931.

116. Gabbianelli, R.; Ferri, A.; Rotilio, G.; Carrì, M. T., *J. Neurochem.* **1999**, *73*, 1175-1180.

117. Corson, L. B.; Strain, J. J.; Culotta, V. C.; Cleveland, D. W., *Proc. Natl. Acad. Sci. USA* **1998**, *95*, 6361-6366.

118. Catania, M. V.; Aronica, E.; Yankaya, B.; Troost, D., *J. Neurosci.* **2001**, *21*, RC148.

119. Almer, G.; Vukosavic, S.; Romero, N.; Przedborski, S., *J. Neurochem.* **1999**, *72*, 2415-2425.

120. Trotti, D.; Rossi, D.; Gjesdal, O.; Levy, L. M.; Racagni, G.; Danbolt, N. C.; Volterra, A., *J. Biol. Chem.* **1996**, *271*, 5976-5979.

121. Brookes, P. S.; Land, J. M.; Clark, J. B.; Heales, S. J. R., *J. Neurochem.* **1998**, *70*, 2195-2202.

122. Gilgun-Sherki, Y.; Melamed, E.; Offen, D., *Neuropharmacology* **2001**, *40*, 959-975.

123. Packer, L.; Fuchs, J., Eds. *Vitamin E in Health and Disease*. 1st ed.; Marcel Dekker, Inc.: New York, 1993.

124. Pieri, C.; Marra, M.; Moroni, F.; Recchioni, R.; Marcheselli, F., *Life Sci.* **1994**, *55*, PL271-PL276.

125. Obrenovich, M. E.; Li, Y.; Parvathaneni, K.; Yendluri, B. B.; Palacios, H. H.; Leszek, J.; Aliev, G., *CNS Neurol. Disord. Drug Targets* **2011**, *10*, 192-207.

126. Quideau, S.; Deffieux, D.; Douat-Casassus, C.; Pouységu, L., *Angew. Chem. Int. Ed.* **2011**, *50*, 586-621.

127. Lau, A.; Tymianski, M., *Pflüg. Arch. Eur. J. Phys.* **2010**, *460*, 525-542.

128. Le Verche, V.; Ikiz, B.; Jacquier, A., *J. Receptor Ligand Channel Res.* **2011**, *4*, 1-22.

129. Grosskreutz, J.; Van Den Bosch, L.; Keller, B. U., *Cell Calcium* **2010**, *47*, 165-174.

130. Rothstein, J. D.; Tsai, G.; Kuncl, R. W.; Clawson, L.; Cornblath, D. R.; Drachman, D. B.; Pestronk, A.; Stauch, B. L.; Coyle, J. T., *Ann. Neurol.* **1990**, *28*, 18-25.

131. Lafon-Cazal, M.; Pietri, S.; Culcasi, M.; Bockaert, J., *Nature* **1993**, *364*, 535-537.

132. Reynolds, I.; Hastings, T., *J. Neurosci.* **1995**, *15*, 3318-3327.

133. Dugan, L.; Sensi, S.; Canzoniero, L.; Handran, S.; Rothman, S.; Lin, T.; Goldberg, M.; Choi, D., *J. Neurosci.* **1995**, *15*, 6377-6388.

134. Stout, A. K.; Raphael, H. M.; Kanterewicz, B. I.; Klann, E.; Reynolds, I. J., *Nat. Neurosci.* **1998**, *1*, 366-373.

135. Zhu, L. P.; Yu, X. D.; Ling, S.; Brown, R. A.; Kuo, T. H., *Cell Calcium* **2000**, *28*, 107-117.

136. Dykens, J. A., *J. Neurochem.* **1994**, *63*, 584-591.

137. Rattray, M.; Bendotti, C., *Exp. Neurol.* **2006**, *201*, 15-23.

138. Bouvier, M.; Szatkowski, M.; Amato, A.; Attwell, D., *Nature* **1992**, *360*, 471-474.

139. Kvamme, E.; Schousboe, A.; Hertz, L.; Torgner, I. A.; Svenneby, G., *Neurochem. Res.* **1985**, *10*, 993-1008.

140. Shaw, P. J.; Forrest, V.; Ince, P. G.; Richardson, J. P.; Wastell, H. J., *Neurodegeneration* **1995**, *4*, 209-216.

141. Rothstein, J. D.; Martin, L.; Levey, A. I.; Dykes-Hoberg, M.; Jin, L.; Wu, D.; Nash, N.; Kuncl, R. W., *Neuron* **1994**, *13*, 713-725.

142. Lehre, K.; Levy, L.; Ottersen, O.; Storm-Mathisen, J.; Danbolt, N., *J. Neurosci.* **1995**, *15*, 1835-1853.

143. Tanaka, K.; Watase, K.; Manabe, T.; Yamada, K.; Watanabe, M.; Takahashi, K.; Iwama, H.; Nishikawa, T.; Ichihara, N.; Kikuchi, T.; Okuyama, S.; Kawashima, N.; Hori, S.; Takimoto, M.; Wada, K., *Science* **1997**, *276*, 1699-1702.

144. Howland, D. S.; Liu, J.; She, Y.; Goad, B.; Maragakis, N. J.; Kim, B.; Erickson, J.; Kulik, J.; DeVito, L.; Psaltis, G.; DeGennaro, L. J.; Cleveland, D. W.; Rothstein, J. D., *Proc. Natl. Acad. Sci. USA* **2002**, *99*, 1604-1609.

145. Haugeto, Ø.; Ullensvang, K.; Levy, L. M.; Chaudhry, F. A.; Honoré, T.; Nielsen, M.; Lehre, K. P.; Danbolt, N. C., *J. Biol. Chem.* **1996**, *271*, 27715-27722.

146. Lehre, K. P.; Danbolt, N. C., *J. Neurosci.* **1998**, *18*, 8751-8757.

147. Rothstein, J. D.; Dykes-Hoberg, M.; Pardo, C. A.; Bristol, L. A.; Jin, L.; Kuncl, R. W.; Kanai, Y.; Hediger, M. A.; Wang, Y.; Schielke, J. P.; Welty, D. F., *Neuron* **1996**, *16*, 675-686.

148. Rothstein, J. D.; Martin, L. J.; Kuncl, R. W., *N. Engl. J. Med.* **1992**, *326*, 1464-1468.

149. Maragakis, N. J.; Dykes-Hoberg, M.; Rothstein, J. D., *Ann. Neurol.* **2004**, *55*, 469-477.

150. Lin, C.-L. G.; Bristol, L. A.; Jin, L.; Dykes-Hoberg, M.; Crawford, T.; Clawson, L.; Rothstein, J. D., *Neuron* **1998**, *20*, 589-602.

151. Rothstein, J. D.; Kammen, M. V.; Levey, A. I.; Martin, L. J.; Kuncl, R. W., *Ann. Neurol.* **1995**, *38*, 73-84.

152. Bristol, L. A.; Rothstein, J. D., *Ann. Neurol.* **1996**, *39*, 676-679.

153. Bendotti, C.; Tortarolo, M.; Suchak, S. K.; Calvaresi, N.; Carvelli, L.; Bastone, A.; Rizzi, M.; Rattray, M.; Mennini, T., *J. Neurochem.* **2001**, *79*, 737-746.

154. Rothstein, J. D.; Jin, L.; Dykes-Hoberg, M.; Kuncl, R. W., *Proc. Natl. Acad. Sci. USA* **1993**, *90*, 6591-6595.

155. Guo, H.; Lai, L.; Butchbach, M. E. R.; Stockinger, M. P.; Shan, X.; Bishop, G. A.; Lin, C.-l. G., *Hum. Mol. Genet.* **2003**, *12*, 2519-2532.

156. Tovar-y-Romo, L. B.; Santa-Cruz, L. D.; Zepeda, A.; Tapia, R., *Neurochem. Int.* **2009**, *54*, 186-191.

157. Volterra, A.; Trotti, D.; Tromba, C.; Floridi, S.; Racagni, G., *J. Neurosci.* **1994**, *14*, 2924-2932.

158. Volterra, A.; Trotti, D.; Racagni, G., *Mol. Pharmacol.* **1994**, *46*, 986-992.

159. Trotti, D.; Nussberger, S.; Volterra, A.; Hedger, M. A., *Eur. J. Neurosci.* **1997**, *9*, 2207-2212.

160. Trotti, D.; Rizzini, B. L.; Rossi, D.; Haugeto, O.; Racagni, G.; Danbolt, N. C.; Volterra, A., *Eur. J. Neurosci.* **1997**, *9*, 1236-1243.

161. Trotti, D.; Rolfs, A.; Danbolt, N. C.; Brown, R. H.; Hediger, M. A., *Nat. Neurosci.* **1999**, *2*, 427-433.

162. MacDermott, A. B.; Mayer, M. L.; Westbrook, G. L.; Smith, S. J.; Barker, J. L., *Nature* **1986**, *321*, 519-522.

163. Weiss, J. H., *Front. Mol. Neurosci.* **2011**, *4*, 1-7.

164. Carriedo, S. G.; Yin, H. Z.; Weiss, J. H., *J. Neurosci.* **1996**, *16*, 4069-4079.

165. Greger, I. H.; Ziff, E. B.; Penn, A. C., *Trends Neurosci.* **2007**, *30*, 407-416.

166. Hollmann, M.; Hartley, M.; Heinemann, S., *Science* **1991**, *252*, 851-853.

167. Mayer, M. L., *Curr. Opin. Neurobiol.* **2005**, *15*, 282-288.

168. Kawahara, Y.; Ito, K.; Sun, H.; Aizawa, H.; Kanazawa, I.; Kwak, S., *Nature* **2004**, *427*, 801.

169. Burnashev, N.; Monyer, H.; Seeburg, P. H.; Sakmann, B., *Neuron* **1992**, *8*, 189-198.

170. Kawahara, Y.; Kwak, S.; Sun, H.; Ito, K.; Hashida, H.; Aizawa, H.; Jeong, S.-Y.; Kanazawa, I., *J. Neurochem.* **2003**, *85*, 680-689.

171. Pellegrini-Giampietro, D. E.; Gorter, J. A.; Bennett, M. V. L.; Zukin, R. S., *Trends Neurosci.* **1997**, *20*, 464-470.

172. Van Damme, P.; Braeken, D.; Callewaert, G.; Robberecht, W.; Van Den Bosch, L., *J. Neuropathol. Exp. Neurol.* **2005**, *64*, 605-612.

173. Tateno, M.; Sadakata, H.; Tanaka, M.; Itohara, S.; Shin, R.-M.; Miura, M.; Masuda, M.; Aosaki, T.; Urushitani, M.; Misawa, H.; Takahashi, R., *Hum. Mol. Genet.* **2004**, *13*, 2183-2196.

174. Spalloni, A.; Albo, F.; Ferrari, F.; Mercuri, N.; Bernardi, G.; Zona, C.; Longone, P., *Neurobiol. Dis.* **2004**, *15*, 340-350.

175. Tortarolo, M.; Grignaschi, G.; Calvaresi, N.; Zennaro, E.; Spaltro, G.; Colovic, M.; Fracasso, C.; Guiso, G.; Elger, B.; Schneider, H.; Seilheimer, B.; Caccia, S.; Bendotti, C., *J. Neurosci. Res.* **2006**, *83*, 134-146.

176. Van Damme, P.; Leyssen, M.; Callewaert, G.; Robberecht, W.; Van Den Bosch, L., *Neurosci. Lett.* **2003**, *343*, 81-84.

177. Canton, T.; Böhme, G. A.; Boireau, A.; Bordier, F.; Mignani, S.; Jimonet, P.; Jahn, G.; Alavijeh, M.; Stygall, J.; Roberts, S.; Brealey, C.; Vuilhorgne, M.; Debono, M.-W.; Le Guern, S.; Laville, M.; Briet, D.; Roux, M.; Stutzmann, J.-M.; Pratt, J., *J. Pharmacol. Exp. Ther.* **2001**, *299*, 314-322.

178. Cheema, S. S.; Langford, S. J.; Bruce, S.; Turner, B.; Scott, R.; Cheung, N. S.; Beart, P. M. Agents and Methods for the Treatment of Disorders Associated with Motor Neuron Degeneration. International Patent Application WO2003/099299 A1, December 4, 2003.

179. Rembach, A.; Turner, B. J.; Bruce, S.; Cheah, I. K.; Scott, R. L.; Lopes, E. C.; Zagami, C. J.; Beart, P. M.; Cheung, N. S.; Langford, S. J.; Cheema, S. S., *J. Neurosci. Res.* **2004**, *77*, 573-582.

180. Pappolla, M. A.; Chyan, Y.-J.; Omar, R. A.; Hsiao, K.; Perry, G.; Smith, M. A.; Bozner, P., *Am. J. Pathol.* **1998**, *152*, 871-877.

181. Behl, C.; Davis, J. B.; Lesley, R.; Schubert, D., *Cell* **1994**, *77*, 817-827.

182. Ueda, K.; Shinohara, S.; Yagami, T.; Asakura, K., *J. Neurochem.* **1997**, *68*, 265-271.

183. Masliah, E.; Hansen, L.; Alford, M.; Deteresa, R.; Mallory, M., *Ann. Neurol.* **1996**, *40*, 759-766.

184. Harris, M. E.; Wang, Y.; Pedigo, N. W.; Hensley, K.; Butterfield, D. A.; Carney, J. M., *J. Neurochem.* **1996**, *67*, 277-286.

185. Kawahara, M.; Kuroda, Y., *Brain Res. Bull.* **2000**, *53*, 389-397.

186. Lockhart, B. P.; Benicourt, C.; Junien, J.-L.; Privat, A., *J. Neurosci. Res.* **1994**, *39*, 494-505.

187. Francis, K.; Bach, J. R.; DeLisa, J. A., *Arch. Phys. Med. Rehabil.* **1999**, *80*, 951-963.

188. Cheah, B. C.; Vucic, S.; Krishnan, A. V.; Kiernan, M. C., *Curr. Med. Chem.* **2010**, *17*, 1942-1959.

189. Bellingham, M. C., *CNS Neurosci. Ther.* **2011**, *17*, 4-31.

190. Doble, A., *Neurology* **1996**, *47*, 233S-241S.

191. Traynor, B. J.; Alexander, M.; Corr, B.; Frost, E.; Hardiman, O., *J. Neurol. Neurosurg. Psychiatry* **2003**, *74*, 1258-1261.

192. Lacomblez, L.; Bensimon, G.; Leigh, P.; Debove, C.; Bejuit, R.; Truffinet, P.; Meininger, V., *Amyotroph. Lateral Sc.* **2002**, *3*, 23-29.

193. Traynor, B. J.; Alexander, M.; Corr, B.; Frost, E.; Hardiman, O., *J. Neurol.* **2003**, *250*, 473-479.

194. Gurney, M. E.; Cutting, F. B.; Zhai, P.; Doble, A.; Taylor, C. P.; Andrus, P. K.; Hall, E. D., *Ann. Neurol.* **1996**, *39*, 147-157.

195. Burton, G. W.; Ingold, K. U., *Acc. Chem. Res.* **1986**, *19*, 194-201.

196. Fujisawa, S.; Kadoma, Y.; Yokoe, I., *Chem. Phys. Lipids* **2004**, *130*, 189-195.

197. Niki, E.; Saito, T.; Kawakami, A.; Kamiya, Y., *J. Biol. Chem.* **1984**, *259*, 4177-4182.

198. Scott, J. W.; Bizzarro, F. T.; Parrish, D. R.; Saucy, G., *Helv. Chim. Acta* **1976**, *59*, 290-306.

199. Ingold, K.; Burton, G.; Foster, D.; Hughes, L.; Lindsay, D.; Webb, A., *Lipids* **1987**, *22*, 163-172.

200. Burton, G. W.; Joyce, A.; Ingold, K. U., *Arch. Biochem. Biophys.* **1983**, *221*, 281-290.

201. Ingold, K. U.; Webb, A. C.; Witter, D.; Burton, G. W.; Metcalfe, T. A.; Muller, D. P. R., *Arch. Biochem. Biophys.* **1987**, *259*, 224-225.

202. Niki, E.; Kawakami, A.; Saito, M.; Yamamoto, Y.; Tsuchiya, J.; Kamiya, Y., *J. Biol. Chem.* **1985**, *260*, 2191-2196.

203. Lucarini, M.; Pedulli, G. F.; Cipollone, M., *J. Org. Chem.* **1994**, *59*, 5063-5070.

204. Packer, J. E.; Slater, T. F.; Willson, R. L., *Nature* **1979**, *278*, 737-738.

205. Doba, T.; Burton, G. W.; Ingold, K. U., *Biochim. Biophys. Acta* **1985**, *835*, 298-303.

206. Frei, B.; England, L.; Ames, B. N., *Proc. Natl. Acad. Sci. USA* **1989**, *86*, 6377-6381.

207. Orrell, R. W.; Lane, R. J. M.; Ross, M., *Cochrane Database Syst. Rev.* **2007**, 1-30.

208. Galbussera, A.; Tremolizzo, L.; Brighina, L.; Testa, D.; Lovati, R.; Ferrarese, C.; Cavaletti, G.; Filippin, G., *Neurol. Sci.* **2006**, *27*, 190-193.

209. Ascherio, A.; Weisskopf, M. G.; O'Reilly, E. J.; Jacobs, E. J.; McCullough, M. L.; Calle, E. E.; Cudkowicz, M.; Thun, M. J., *Ann. Neurol.* **2005**, *57*, 104-110.

210. Ingold, K. U.; Burton, G. W.; Foster, D. O.; Hughes, L., *FEBS Lett.* **1990**, *267*, 63-65.

211. Campo, G. M.; Squadrito, F.; Campo, S.; Altavilla, D.; Quartarone, C.; Ceccarelli, S.; Ferlito, M.; Avenoso, A.; Squadrito, G.; Saitta, A.; Caputi, A. P., *J. Mol. Cell. Cardiol.* **1998**, *30*, 1493-1503.

212. Iuliano, L.; Pedersen, J. Z.; Camastra, C.; Bello, V.; Ceccarelli, S.; Violi, F., *Free Radic. Biol. Med.* **1999**, *26*, 858-868.

213. Grisar, J. M.; Bolkenius, F. N.; Petty, M. A.; Verne, J., *J. Med. Chem.* **1995**, *38*, 453-458.

214. Grisar, J. M.; Petty, M. A.; Bolkenius, F. N.; Dow, J.; Wagner, J.; Wagner, E. R.; Haegele, K. D.; De Jong, W., *J. Med. Chem.* **1991**, *34*, 257-260.

215. Smith, R. A. J.; Porteous, C. M.; Coulter, C. V.; Murphy, M. P., *Eur. J. Biochem.* **1999**, *263*, 709-716.

216. Cohen, N.; Schaer, B.; Saucy, G.; Borer, R.; Todaro, L.; Chiu, A.-M., *J. Org. Chem.* **1989**, *54*, 3282-3292.

217. Cort, W.; Scott, J.; Araujo, M.; Mergens, W.; Cannalonga, M.; Osadca, M.; Harley, H.; Parrish, D.; Pool, W., *J. Am. Oil Chem. Soc.* **1975**, *52*, 174-178.

218. Scott, J.; Cort, W.; Harley, H.; Parrish, D.; Saucy, G., *J. Am. Oil Chem. Soc.* **1974**, *51*, 200-203.

219. Shanks, D.; Frisell, H.; Ottosson, H.; Engman, L., *Org. Biomol. Chem.* **2006**, *4*, 846-852.

220. Ferrante, R.; Klein, A.; Dedeoglu, A.; Flint Beal, M., *J. Mol. Neurosci.* **2001**, *17*, 89-96.

221. Crow, J. P.; Calingasan, N. Y.; Chen, J.; Hill, J. L.; Beal, M. F., *Ann. Neurol.* **2005**, *58*, 258-265.

222. Wu, A. S.; Kiaei, M.; Aguirre, N.; Crow, J. P.; Calingasan, N. Y.; Browne, S. E.; Beal, M. F., *J. Neurochem.* **2003**, *85*, 142-150.

223. Barber, S. C.; Mead, R. J.; Shaw, P. J., *Biochim. Biophys. Acta* **2006**, *1762*, 1051-1067.

224. Tsien, R. Y., *Biochemistry* **1980**, *19*, 2396-2404.

225. Macfarlane, K. J. Small Molecules & Peptide Nucleic Acids for the Treatment and Prevention of Neurodegeneration. PhD Thesis, Monash University, Melbourne, 2004.

226. Cheema, S. S.; Langford, S.; Cheung, N. S.; Beart, P. M.; Macfarlane, K. J.; Mulcair, M. Agents and Methods for the Treatment of Disorders Associated with Oxidative Stress. U.S. Patent Application US2005/0288359 A1, December 29, 2005.

227. Robitaille, P.-M. L.; Jiang, Z., *Biochemistry* **1992**, *31*, 12585-12591.

228. Grynkiewicz, G.; Poenie, M.; Tsien, R. Y., *J. Biol. Chem.* **1985**, *260*, 3440-3450.

229. Spigelman, I.; Tymianski, M.; Wallace, C. M.; Carlen, P. L.; Velumian, A. A., *Neuroscience* **1996**, *75*, 559-572.

230. Gressel, J.; Michaeli, D.; Kampel, V.; Amsellem, Z.; Warshawsky, A., *J. Agric. Food Chem.* **2002**, *50*, 6353-6360.

231. Tsien, R. Y., *Nature* **1981**, *290*, 527-528.

232. Wie, M. B.; Koh, J. Y.; Won, M. H.; Lee, J. C.; Shin, T. K.; Moon, C. J.; Ha, H. J.; Park, S. M.; Kim, H. C., *Prog. Neuropsychopharmacol. Biol. Psychiatry* **2001**, *25*, 1641-1659.

233. Tymianski, M.; Wallace, M. C.; Spigelman, I.; Uno, M.; Carlen, P. L.; Tator, C. H.; Charlton, M. P., *Neuron* **1993**, *11*, 221-235.

234. Unthank, J. K. Novel 'Dual-Action' Agents for the Treatment and Prevention of Neurodegenerative Disorders. PhD Thesis, Monash University, Melbourne, 2006.

235. Turner, B. J. Toxic Mechanisms and Therapeutic Strategies in a Transgenic Mouse Model of Human Familial Amyotrophic Lateral Sclerosis. PhD Thesis, Howard Florey Institute of Experimental Physiology & Medicine, Melbourne, 2005.

236. Traynor, B. J.; Bruijn, L.; Conwit, R.; Beal, F.; O'Neill, G.; Fagan, S. C.; Cudkowicz, M. E., *Neurology* **2006**, *67*, 20-27.

237. Kriz, J.; Nguyen, M. D.; Julien, J.-P., *Neurobiol. Dis.* **2002**, *10*, 268-278.

238. Zhu, S.; Stavrovskaya, I. G.; Drozda, M.; Kim, B. Y. S.; Ona, V.; Li, M.; Sarang, S.; Liu, A. S.; Hartley, D. M.; Wu, D. C.; Gullans, S.; Ferrante, R. J.; Przedborski, S.; Kristal, B. S.; Friedlander, R. M., *Nature* **2002**, *417*, 74-78.

239. Gordon, P. H.; Moore, D. H.; Miller, R. G.; Florence, J. M.; Verheijde, J. L.; Doorish, C.; Hilton, J. F.; Spitalny, G. M.; MacArthur, R. B.; Mitsumoto, H.; Neville, H. E.; Boylan, K.; Mozaffar, T.; Belsh, J. M.; Ravits, J.; Bedlack, R. S.; Graves, M. C.; McCluskey, L. F.; Barohn, R. J.; Tandan, R., *Lancet Neurol.* **2007**, *6*, 1045-1053.

240. Rothstein, J. D.; Patel, S.; Regan, M. R.; Haenggeli, C.; Huang, Y. H.; Bergles, D. E.; Jin, L.; Dykes Hoberg, M.; Vidensky, S.; Chung, D. S.; Toan, S. V.; Bruijn, L. I.; Su, Z.-z.; Gupta, P.; Fisher, P. B., *Nature* **2005**, *433*, 73-77.

241. Beghi, E.; Bendotti, C.; Mennini, T.; Miller, T.; Cleveland, D., *Science* **2005**, *308*, 632b-633.

242. ALS Therapy Development Institute. www.als.net (accessed 27 February 2012).

243. The ALS Association. www.alsa.org (accessed 27 February 2012).

244. The ALS Society of Canada. www.als.ca (accessed 27 February 2012).

245. Pascuzzi, R. M.; Shefner, J.; Chappell, A. S.; Bjerke, J. S.; Tamura, R.; Chaudhry, V.; Clawson, L.; Haas, L.; Rothstein, J. D., *Amyotroph. Lateral Sc.* **2010**, *11*, 266-271.

246. Dykxhoorn, D. M.; Novina, C. D.; Sharp, P. A., *Nat. Rev. Mol. Cell Biol.* **2003**, *4*, 457-467.

247. Ding, H.; Schwarz, D. S.; Keene, A.; Affar, E. B.; Fenton, L.; Xia, X.; Shi, Y.; Zamore, P. D.; Xu, Z., *Aging Cell* **2003**, *2*, 209-217.

248. Raoul, C.; Abbas-Terki, T.; Bensadoun, J.-C.; Guillot, S.; Haase, G.; Szulc, J.; Henderson, C. E.; Aebischer, P., *Nat. Med.* **2005**, *11*, 423-428.

249. Ralph, G. S.; Radcliffe, P. A.; Day, D. M.; Carthy, J. M.; Leroux, M. A.; Lee, D. C. P.; Wong, L.-F.; Bilsland, L. G.; Greensmith, L.; Kingsman, S. M.; Mitrophanous, K. A.; Mazarakis, N. D.; Azzouz, M., *Nat. Med.* **2005**, *11*, 429-433.

250. Smith, R. A.; Miller, T. M.; Yamanaka, K.; Monia, B. P.; Condon, T. P.; Hung, G.; Lobsiger, C. S.; Ward, C. M.; McAlonis-Downes, M.; Wei, H.; Wancewicz, E. V.; Bennett, C. F.; Cleveland, D. W., *J. Clin. Invest.* **2006**, *116*, 2290-2296.

251. Turner, B. J.; Cheah, I. K.; Macfarlane, K. J.; Lopes, E. C.; Petratos, S.; Langford, S. J.; Cheema, S. S., *J. Neurochem.* **2003**, *87*, 752-763.

252. McGeer, E. G.; McGeer, P. L., *Biodrugs* **2005**, *19*, 31-37.

253. Lawler, J. M.; Barnes, W. S.; Wu, G.; Song, W.; Demaree, S., *Biochem. Biophys. Res. Commun.* **2002**, *290*, 47-52.

254. Zhang, W.; Narayanan, M.; Friedlander, R. M., *Ann. Neurol.* **2003**, *53*, 267-270.

255. Kriz, J.; Gowing, G.; Julien, J.-P., *Ann. Neurol.* **2003**, *53*, 429-436.

256. Shin, J. H.; Cho, S. I.; Lim, H. R.; Lee, J. K.; Lee, Y. A.; Noh, J. S.; Joo, I. S.; Kim, K.-W.; Gwag, B. J., *Mol. Pharmacol.* **2007**, *71*, 965-975.

CHAPTER TWO

MODIFICATION OF THE BAPTA CORE FOR BIO- AND CHELATING-ABILITY

2.1 Introduction

Calcium is an important secondary messenger in the central nervous system, crucial in regulating pathways vital for normal cell function; however disruption of calcium homeostasis may activate apoptotic cascades, leading to potentially premature cell death.[1,2] Glutamate-induced Ca^{2+} excitotoxicity may activate numerous cytotoxic pathways. Excess cytosolic free Ca^{2+} in neurons can result from an overstimulation of ionotropic glutamate receptors, as summarised in Figure 1.3, leading to cytotoxic effects, especially in mitochondria, or resulting in activation of Ca^{2+}-dependent enzymes and proteins, which can lead to nuclear and membrane damage as well as an increase in production of ROS from mitochondrial electron transport chain processes.[1-19]

One well-known Ca^{2+} chelator is ethylene glycol bis(*β*-aminoethyl ether)-*N*,*N*,*N*',*N*'-tetraacetic acid (EGTA) (Figure 2.1a) which selectively binds Ca^{2+} over magnesium ions (Mg^{2+}) in its fully deprotonated form, and thus may have many useful biological applications.[20] The reason for this selectivity is due to the flexible binding cavity of EGTA, which is an appropriate size to be able to encapsulate Ca^{2+} optimally, however in an induced-fit state, encapsulation of the smaller ion Mg^{2+} is sub-optimal, due to steric considerations.[21] At physiological pH, the Ca^{2+}-buffering ability of EGTA is strongly dependent on slight variations in pH.[22] This is due to the relatively high nitrogen pK_a values of the molecule (pK_a = 8.96, 9.58), as the speed of uptake of Ca^{2+} is significantly decreased when the nitrogens are protonated.[22]

a)

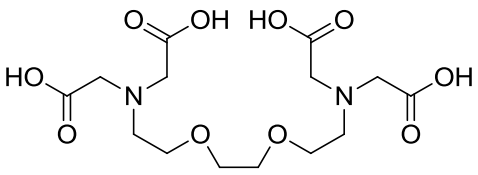

b)

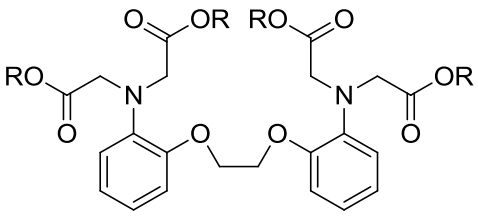

Figure 2.1 a) Ethylene glycol bis(*β*-aminoethyl ether)-*N*,*N*,*N*',*N*'-tetraacetic acid (EGTA). **b)** Ca^{2+}-binding agent BAPTA (R=H) and its tetraethyl ester (R=Et).

While EGTA is effective in selectively binding Ca^{2+} over Mg^{2+}, it is not readily detected within cells using spectroscopic methods and the rate of chelation is highly dependent on pH. Recognising this, Tsien[21] developed 1,2-bis(*o*-aminophenoxy)ethane-*N*,*N*,*N*',*N*'-tetraacetic acid (BAPTA, Figure 2.1b), an effective UV-detectable Ca^{2+}-specific molecular probe. Developed in the 1980s, BAPTA effectively buffers Ca^{2+} at physiological pH, with a dissociation constant of 10^{-7} M.[21] Compared to EGTA, BAPTA benefits from faster buffering times and pH insensitivity[23]

due to very low anilinic pK_a values (pK_a = 6.36, 5.47).[21] BAPTA still exhibits high selectivity (>10^5) for binding Ca^{2+} over Mg^{2+},[21] is shown to be non-toxic to cells *in vitro* and *in vivo*,[21,24-32] and may be administered as the cell-permeant acetoxymethyl ester (BAPTA-AM), which can undergo intracellular hydrolysis to form the active tetraacetate protecting against excitotoxic cell injury *in vitro* and *in vivo*.[27-33]

In addition to Ca^{2+} binding, previous work within our research group has shown that BAPTA can exhibit antioxidant properties, in both the presence and absence of Ca^{2+}.[34,35] This is likely to be due to the captodative radical stabilisation effect, where a carbon-centred radical may be stabilised by the combined effect of captor (electron-withdrawing) and dative (electron-donating) substituents attached to the radical carbon (Scheme 2.1).[36,37]

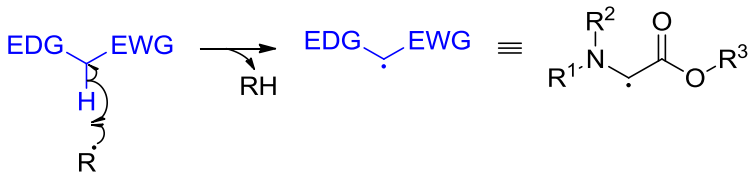

Scheme 2.1 The captodative effect – radical stabilisation is aided by the positioning of electron-withdrawing groups (EWG) and electron-donating groups (EDG).

In the case of BAPTA and its derivatives, the presence of both an electron-donating tertiary amine and an electron-withdrawing carboxylate group allow for radical stabilisation due to multiple possible resonance forms of the radical (Scheme 2.2). This donor-acceptor combination of carboxyl and amino substituents is known to be effective in stabilising carbon-centred radicals in this fashion.[38]

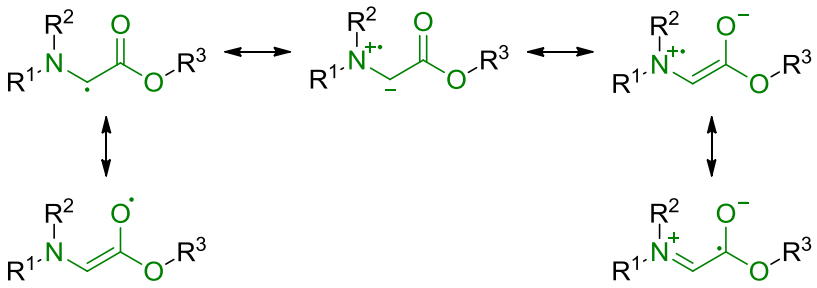

Scheme 2.2 Radical stabilisation *via* multiple resonance structures.

The combination of antioxidant function and Ca^{2+}-chelating efficiency makes BAPTA and its derivatives promising candidates for treatment against both an influx of intracellular Ca^{2+} and oxidative stress. Unpublished studies conducted in our research group on the tetraethyl ester

derivative of BAPTA (Figure 2.1b) have shown that 5 mg/kg thrice-weekly intraperitoneal injections in female mice can significantly increase survival in transgenic ALS mice (Figure 2.2).[39]

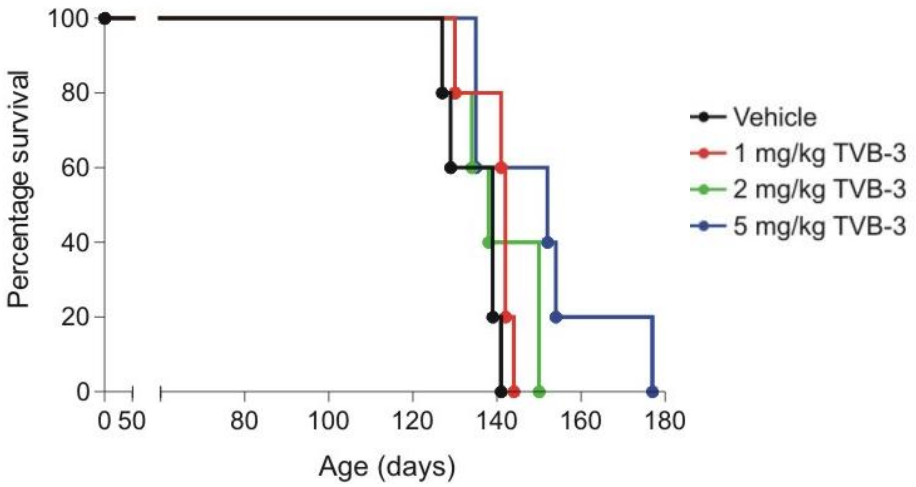

Figure 2.2[39] Kaplan-Meier plot showing survival of female transgenic ALS mice, treated with intraperitoneal injections of the tetraethyl ester derivative of BAPTA (TVB-3). (Average endpoint of vehicle: 135.0 ± 2.9 days; treated: 150.6 ± 7.7 days.)

Intrathecal infusion of the tetraethyl ester BAPTA derivative has shown an even greater increase in the survival of transgenic ALS rats (Figure 2.3),[24,39] indicating that although the BAPTA derivative is effective in increasing the survival of ALS-affected mice and rats on hydrolysis to form BAPTA in the body, problems with solubility may prevent the prodrug from reaching the desired area of action, most likely due to problems crossing the blood brain barrier.

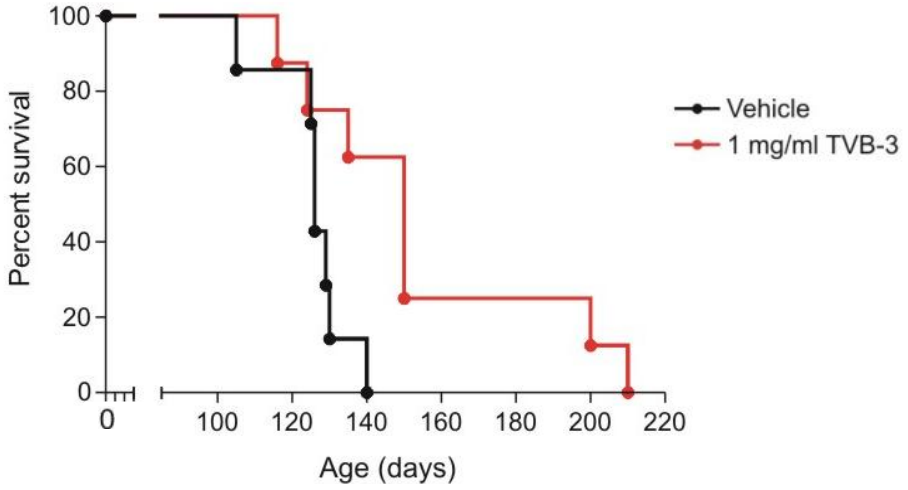

Figure 2.3[24,39] Kaplan-Meier plot showing survival of female transgenic ALS rats, treated with intrathecal infusion of the tetraethyl ester derivative of BAPTA (TVB-3). (Average endpoint of vehicle: 125.9 ± 4.0 days; treated: 154.4 ± 12.0 days.)

Additionally, the tetraester is not very soluble in HEPES buffer or sodium chloride solution & requires 10% dimethyl sulfoxide solution to invoke solubility. This suggests that a more water soluble derivative of BAPTA may be a more effective candidate for treatment of ALS. This may also enable greater solubility of the prodrug for administration.

Given the solubility problems associated with BAPTA and its tetraethyl ester, it is proposed that a series of derivatives, depicted generally in Figure 2.4, may offer the benefits of Ca^{2+}-chelating ability and antioxidant action, with increased hydrophilicity to allow improved bioavailability. It is anticipated that while tetraethyl ester derivatives of each analogue would act as appropriate targets for medicinal administration, hydrolysed carboxylic acid and carboxylate salt derivatives may provide suitable models for *in vitro* antioxidant and Ca^{2+} binding studies, as the administered targets are expected to be hydrolysed *in vitro*.

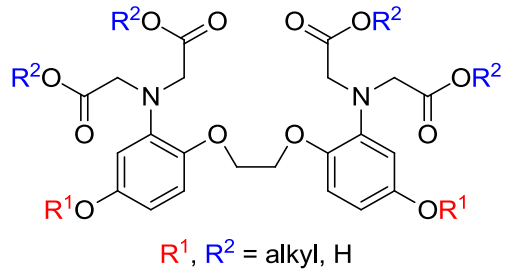

Figure 2.4 Soluble BAPTA derivative targets. R-groups may include, but are not limited to: amines, polyethers, alcohols and protons.

2.2 Synthesis of the calcium chelator 1,2-bis(*o*-aminophenoxy)ethane-*N*,*N*,*N*',*N*'-tetraacetic acid (BAPTA)

The tetraethyl ester of BAPTA (**3**) was synthesised in two steps, based on the work of Tsien and minor modifications made within our group, with an additional step performed to hydrolyse the ester to BAPTA acid **4** (Scheme 2.3).[21,24,34] Commercially available 1,2-bis(2-nitrophenoxy)ethane **1** was reduced by the slow addition of hydrazine hydrate in the presence of palladium on charcoal, yielding two crops of the bis-anilino compound **2**, at a total yield of 93%.

With compound **2** in hand, alkylation *via* Finkelstein conditions with ethyl bromoacetate in the presence of sodium iodide and *N*,*N*-diisopropylethylamine (DIPEA) produced tetraethyl ester **3**, in 87% yield (Scheme 2.3).[21] Proton NMR spectroscopy indicated product formation, with resonances attributable to ethyl ester protons at 4.05 and 1.14 ppm, integrating to eight and twelve protons, respectively, as well an eight-proton signal at 4.15 ppm

corresponding to the methylene protons adjacent to the aniline nitrogens. Tetra-alkylation was also indicated by electrospray ionisation (ESI) mass spectrometry peaks at m/z 589.3 and 611.3, representative of $[M+H]^+$ and $[M+Na]^+$ ions, respectively. In this step, *N*,*N*-diisopropylethylamine (also known as Hünig's base) was used as the strong base to deprotonate the anilinic nitrogens, compared to 1,8-bis(dimethylamino)naphthalene, used commonly in the literature.[21] Both agents are strongly basic and act as weak nucleophiles due to their steric bulk, however *N*,*N*-diisopropylethylamine is inexpensive, making it an appropriate reagent for large-scale synthesis. The base can also be regenerated from the resulting ammonium salt by alkalinisation with concentrated sodium hydroxide solution, making it readily reusable. Saponification of tetraethyl ester **3**, followed by an acidic workup afforded BAPTA (**4**) in high yield.[34]

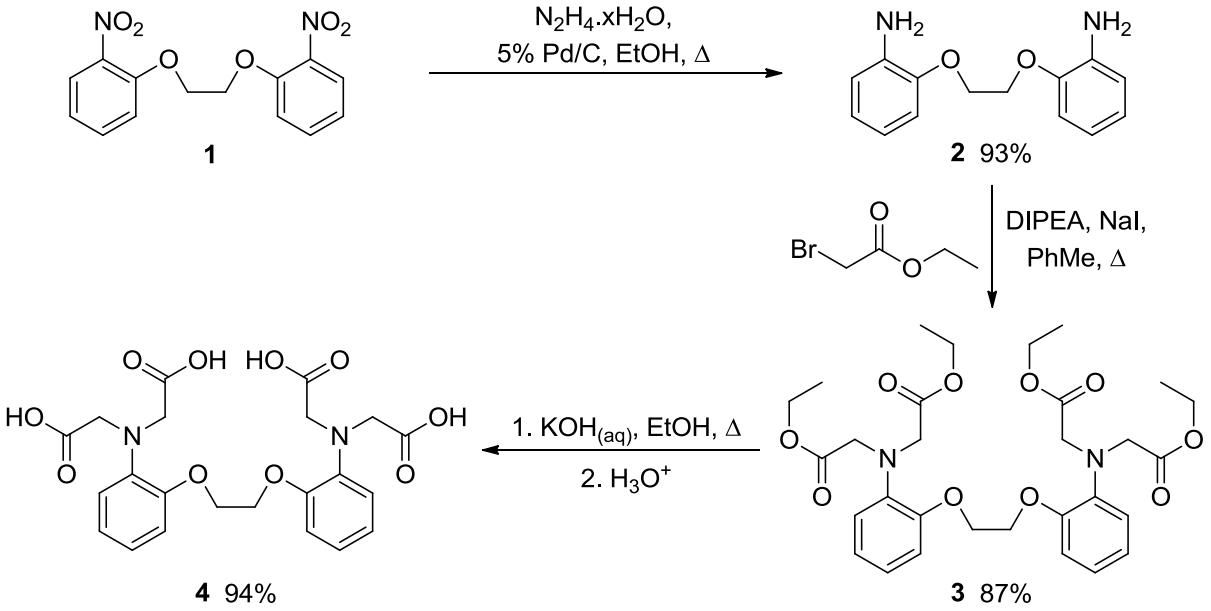

Scheme 2.3

2.3 Synthesis of nitrated derivatives of BAPTA

Various methods for the functionalisation of BAPTA have been employed in the literature, which have the ability to modulate Ca^{2+} binding constants and alter properties such as fluorescence or absorption wavelength.[21,40-47] One such method involves the electrophilic aromatic substitution of the parent compound to form 5,5'-dinitro BAPTA (**6**), a compound with a Ca^{2+} dissociation constant of approximately 10^{-2} M,[40] which is at least five orders of magnitude

higher than BAPTA. This is due to the electron-withdrawing *para* substituted nitro groups, which weaken binding, increasing the dissociation constant.

Dinitro BAPTA tetraethyl ester **5** was synthesised by addition of nitric acid to a suspension of BAPTA ester **3** in glacial acetic acid (Scheme 2.4), in excellent yield.[40] High resolution ESI mass spectrometry indicated product formation, with a $[M+Na]^+$ signal at m/z 701.2269. Proton NMR spectroscopy also supported full conversion of starting material to **5**, with three resonances attributable to two aromatic protons each at 7.84, 7.72, and 6.71 ppm, with an ABX splitting pattern, in stark contrast to the multiplet at 6.86 ppm, representative of eight aromatic protons of the starting material.

Base-catalysed hydrolysis of **5** and subsequent acidic workup yielded the tetraacetic acid **6** (Scheme 2.4). It is anticipated that nitro compounds **5** and **6** may be further functionalised to form a variety of derivatives, potentially *via* the reduction and alkylation of the nitro groups.

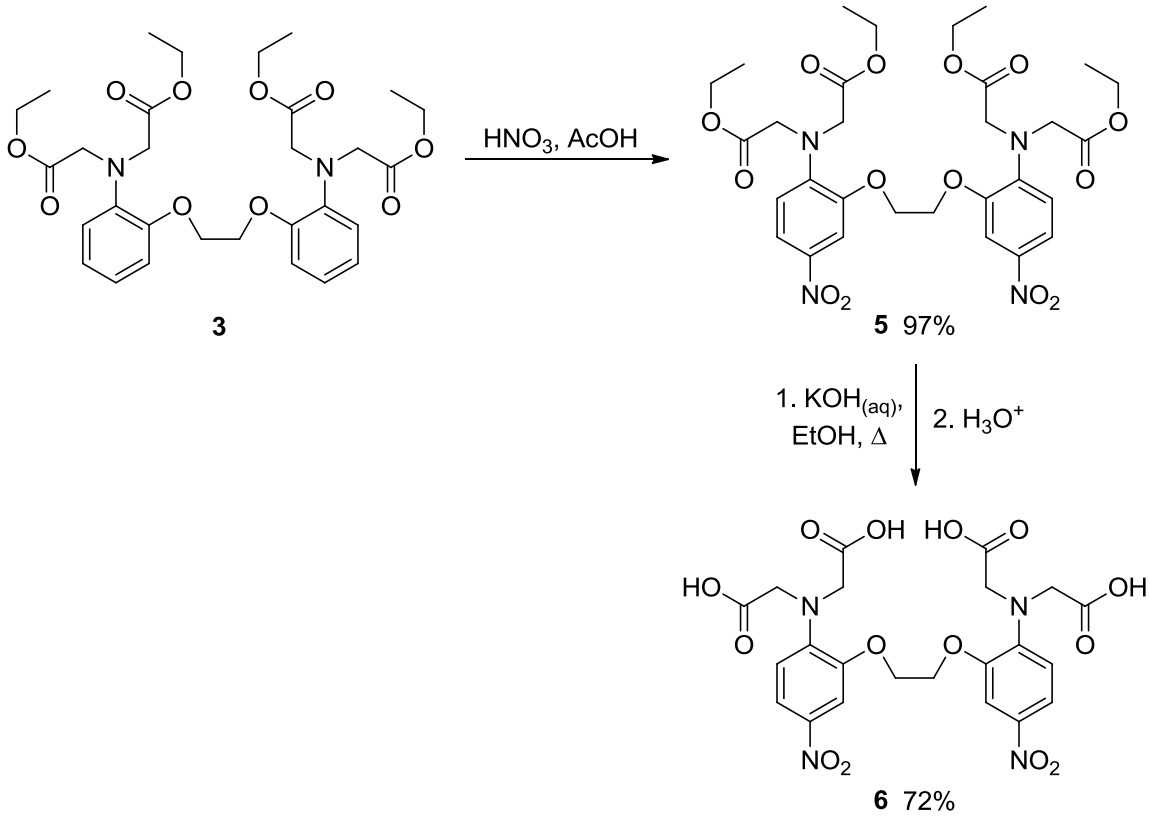

Scheme 2.4

2.4 Synthesis of the BAPTA/EGTA hybrid AATA

In an effort to design a spectroscopically active intracellular Ca^{2+} probe, Robitaille and Jiang[48] synthesised ^{13}C-enriched 1-(2-aminophenoxy)-2-(2-aminoethoxy)ethane-*N*,*N*,*N*',*N*'-tetraacetic acid (AATA) (Figure 2.5). A hybrid of BAPTA and EGTA, AATA exhibits Ca^{2+} binding constants and exchange rates intermediate between those of EGTA and BAPTA, as well as amine pK_a values of 5.94 and 9.03.[48] Importantly, AATA still exhibits the high selectivity for Ca^{2+} over Mg^{2+} found with both EGTA and BAPTA. However, since the rates at which AATA binds and releases Ca^{2+} is less than those observed for BAPTA, this may have an effect on the buffering capability of AATA in a physiological environment.[48] One advantage of use of AATA in biological studies, however, is that it is expected that the molecule will exhibit water solubility greater than BAPTA, due to its more aliphilic nature and hence solve a problem encountered with *in vitro* studies.

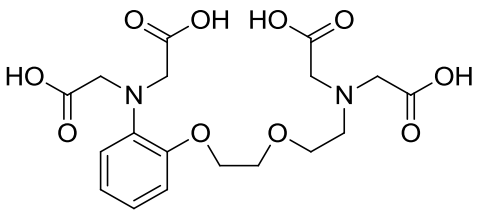

Figure 2.5 BAPTA/EGTA hybrid, 1-(2-aminophenoxy)-2-(2-aminoethoxy)ethane-*N*,*N*,*N*',*N*'-tetraacetic acid (AATA).

The tetraethyl ester of AATA (**12**) was synthesised in six steps, based on the work of Robitaille and Jiang (Scheme 2.5).[48] Firstly, etherification between 2-nitrophenol and 2-(2-chloroethoxy)ethanol was performed in dimethylformamide in the presence of potassium carbonate. As the reaction progressed, a colour change of the mixture from red to yellow could be observed, indicating consumption of the potassium nitrophenolate that had been formed *in situ*. Subsequent workup gave the product **7** in excellent yield.

From the alcohol **7**, esterification using *p*-toluenesulfonyl chloride in the presence of triethylamine and 4-dimethylaminopyridine (DMAP) gave the ester **8**, with product formation indicated by low resolution mass spectrometry, with a peak at *m*/*z* 404.2, attributable to the $[M+Na]^+$ ion. From the ester, a substitution reaction with potassium phthalimide produced the corresponding phthalimide product **9** in good yield, indicated by the absence of the methyl peak at 2.43 ppm in the ^1H NMR spectrum, as well as new aromatic proton resonances attributable to the phthalimide group.

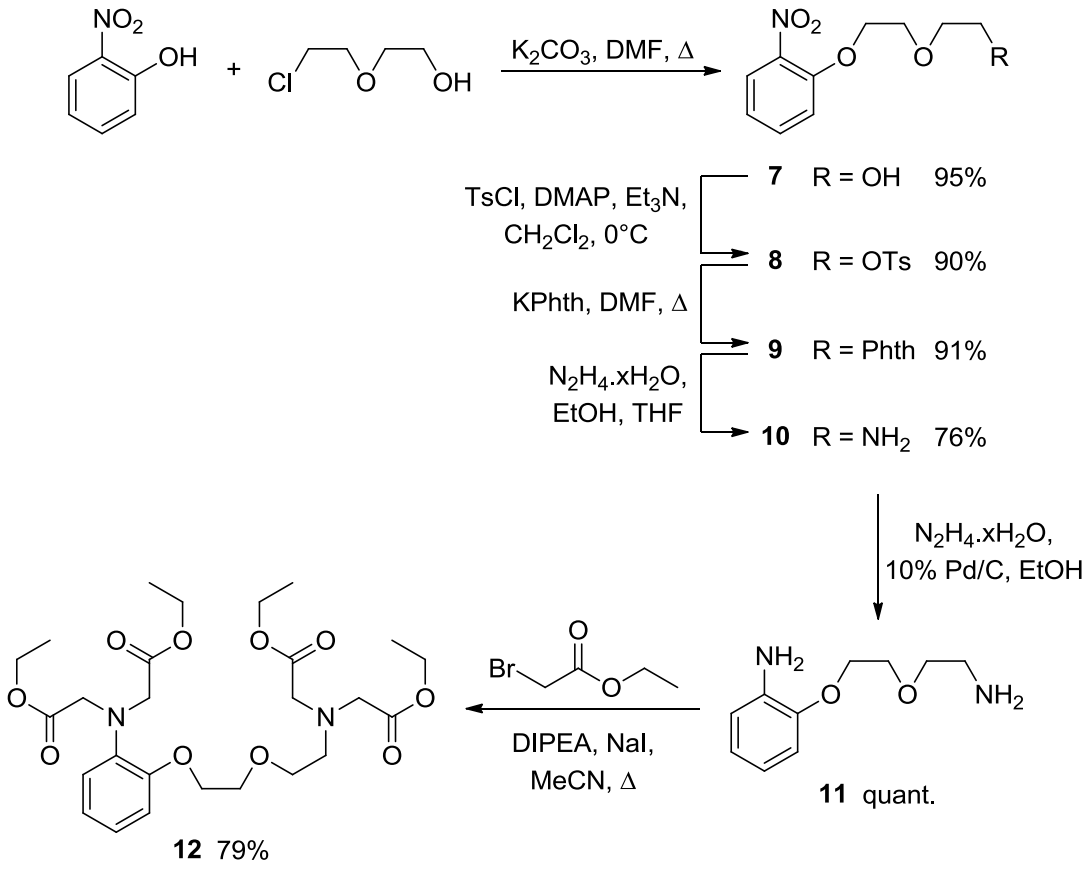

Scheme 2.5

From phthalimide **9**, reaction with hydrazine hydrate in an ethanol/tetrahydrofuran mixture gave the nitro amine compound **10** in good yield, which was subsequently reduced to the bis-amino compound **11** on further reaction with hydrazine hydrate, this time in the presence of palladium on charcoal (Scheme 2.5). Alkylation of **11** under Finkelstein conditions using ethyl bromoacetate and *N*,*N*-diisopropylethylamine as base gave the AATA tetraethyl ester **12** in good yield after purification by column chromatography.[48] With **12** in hand, antioxidant testing and Ca^{2+} binding studies may be undertaken for comparison with BAPTA and other derivatives.

2.5 Synthesis of hydrophilic BAPTA derivatives

Given the solubility problems associated with *in vivo* administration BAPTA and its tetraethyl ester, it was proposed that a series of derivatives, depicted generally in Figure 2.4, would increase hydrophilicity for improved bioavailability, while retaining the benefits of Ca^{2+}-chelating ability and antioxidant action.

1,4-Bis(benzyloxy)benzene **13** was synthesised from hydroquinone by the addition of benzyl chloride, as shown in Scheme 2.6.[45] The product **13** was formed with a yield of 84% after recrystallisation. The bis-protected hydroquinone was then nitrated by the addition of a dilute mixture of nitric acid in glacial acetic acid, with heating (Scheme 2.6).[45] The resulting brilliant yellow solid **14** was obtained in 93% after precipitation with water. Proton NMR spectroscopy supported mono-nitration with the presence of two distinct signals at 5.18 and 5.05 ppm, integrating to two protons each and attributed to the two benzyl CH_2 groups, as well as an ABX splitting pattern attributed to the three inequivalent protons on the nitrated benzene ring, at 7.48, 7.12 and 7.04 ppm. Nitration was also supported by low resolution mass spectrometry (ESI), with a peak at m/z 358.0, representing the $[M+Na]^+$ ion, with no peaks corresponding to either the starting material or products of further nitration.

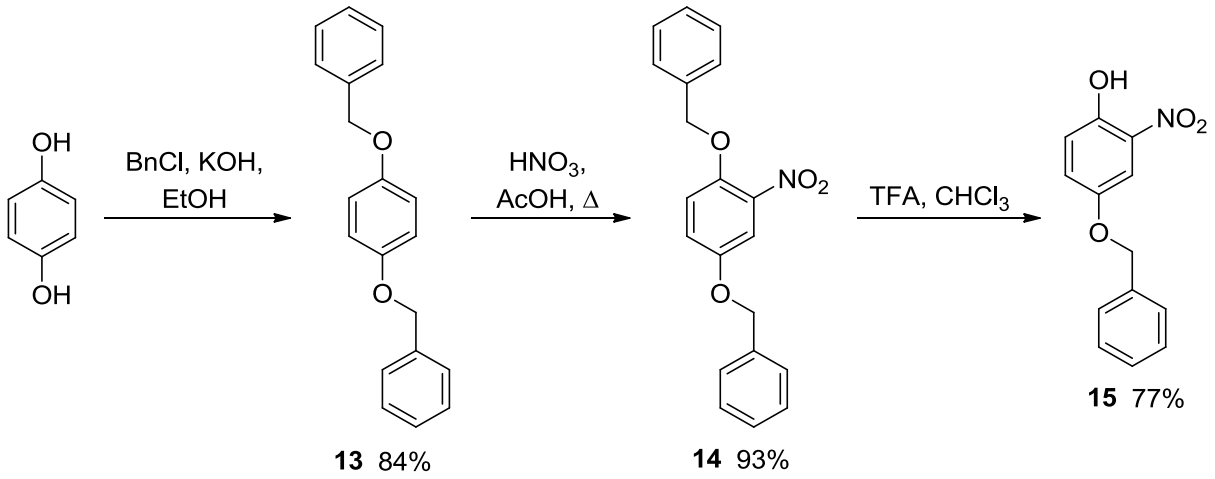

Scheme 2.6

The nitrated compound **14** was regioselectively deprotected by the addition of trifluoroacetic acid in ethanol-free chloroform (Scheme 2.6).[45] After the reaction mixture was neutralised, the product was isolated by extraction with chloroform, followed by basification, filtration of the resulting red phenolate salt, acidification of the precipitate and further extraction with diethyl ether. Following recrystallisation from methanol, the mono-protected compound **15** was obtained in 77% yield. Selective deprotection was supported by the absence of one benzyl -CH_2- peak at 5.18 ppm in the ^{1}H NMR spectrum, and electron impact mass spectrometry, which gave a peak at m/z 245, corresponding to the molecular ion.

With the mono-protected nitro compound **15** in hand, reaction with 1,2-dichloroethane in a heated pressure vessel gave the beige coloured 1,2-bis(4-benzyloxy-2-nitrophenoxy)ethane **16** in quantitative yield (Scheme 2.7).[46] The two-to-one stoichiometry of the starting materials

was found to be optimal for product formation, as a higher proportion of 1,2-dichloroethane resulted in some of the mono-reacted product. Formation of the bis compound was supported by low resolution mass spectrometry (ESI), with a peak at *m/z* 538.9, corresponding to $[M+Na]^+$, and ^1H NMR spectroscopy, with a resonance at 4.44 ppm, attributed to the newly installed ethylene protons, integrating to four protons. Carbon NMR spectroscopy also supported formation of **16** with a new resonance at 70.2 ppm, due to the ethylene carbons, as well as slight shifts of both tertiary and quaternary aromatic carbon resonances, supporting the ether formation.

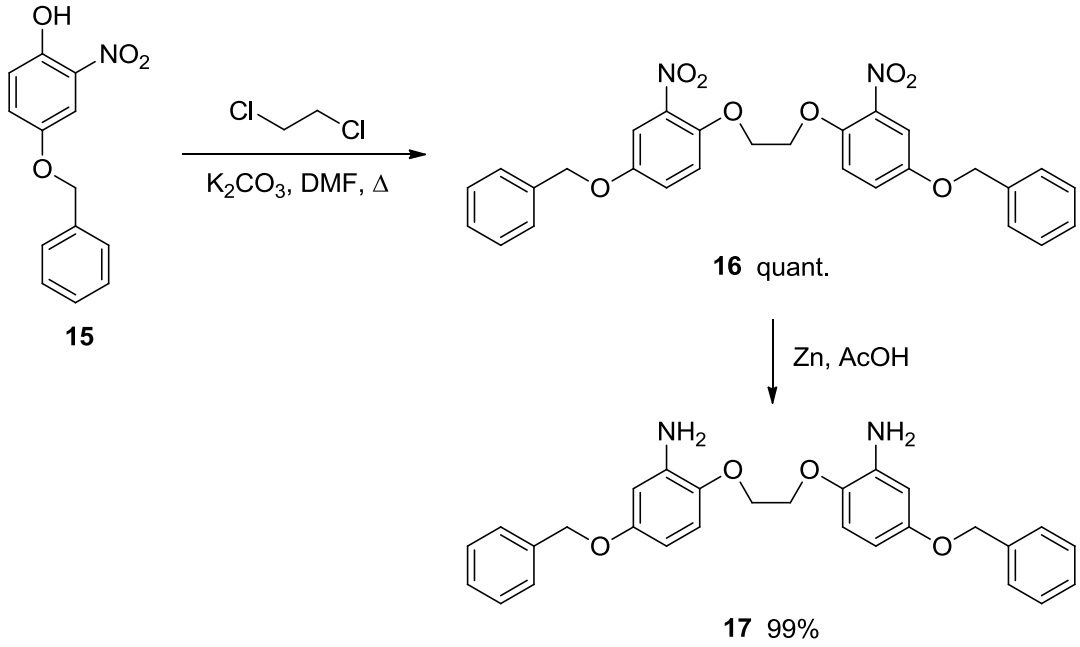

Scheme 2.7

From this point, it was necessary to employ a method that would enable reduction of the aromatic nitro groups to anilines. Similar work by Tsien[21] towards the synthesis of BAPTA used a palladium-catalysed hydrogenation to achieve the reduction, however this would be inadequate due to the need to preserve the benzyl protect groups. Thus, a widely used zinc-based reduction of the nitro groups was utilised. Since the bis-nitro compound **16** was insoluble in methanol, a common solvent for such a reaction – to which an acid is added and vigorously stirred – the starting material was dissolved in glacial acetic acid, thus ensuring both that the material was in solution and that the necessary proton source was *in situ*. Once **16** was dissolved, reduction with zinc powder and subsequent workup gave the bis-aniline compound **17** in excellent yield (Scheme 2.7).

At this point, the next proposed step was to alkylate the free aniline groups of **17** in order to form the Ca^{2+}-chelating BAPTA arms of the compound, with a view to removing the protecting groups and functionalising the resulting phenols at a later time. Examples in the literature of similar reactions with electrophiles indicated that inadvertent further alkylation of the tertiary amines may not be a problem during phenol functionalisation,[41,45,46] most likely due to the reduced nucleophilic character of the anilinic nitrogens, compared to aliphatic amines.

The bis-aniline compound **17** was dissolved in toluene and alkylated by the addition of an excess of ethyl bromoacetate in the presence of sodium iodide and *N*,*N*-diisopropylethylamine and the resulting crude mixture was purified by passing through a silica plug, using 40% ethyl acetate/hexane, to give the tetraethyl ester compound **18** in 74% yield, shown in Scheme 2.8.

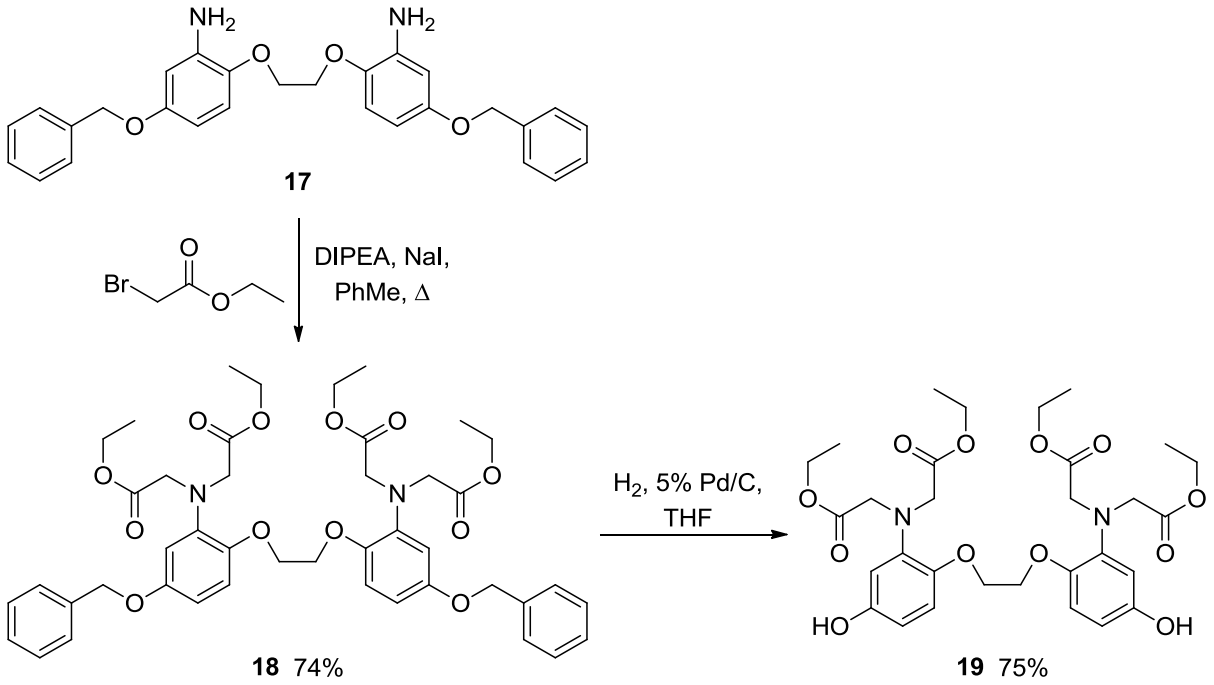

Scheme 2.8

Proton NMR spectroscopy supported tetra-alkylation, with new resonances at 4.14, 4.07 and 1.17 ppm, integrating to 8 protons, 8 protons and 12 protons, respectively. Carbon NMR spectroscopy also supported alkylation, with new peaks resulting from the addition of the alkyl arms, in particular the carbonyl signal at 171.4 ppm. High resolution mass spectrometry (ESI) supported product formation with peaks at m/z 801.3605 and m/z 823.3427, corresponding to the $[M+H]^+$ and $[M+Na]^+$ ions. From the tetraethyl ester **18**, hydrogenation in tetrahydrofuran in the presence of palladium on charcoal resulted in the deprotected compound **19**, in good yield (Scheme 2.8), after purification by column chromatography.

X-ray crystallography of **19**$(H_2O)_{1.5}$ (Figure 2.6 and Figure 2.7) shows the polydentate binding cavity of the structure, which exists in a triclinic crystal system with space group P-1. One of the N(2) substituent arms is disordered over two positions, one of which is associated with a water molecule. Single crystals of **19**$(H_2O)_{1.5}$ suitable for analysis were grown by vapor diffusion from methanol and hexane.

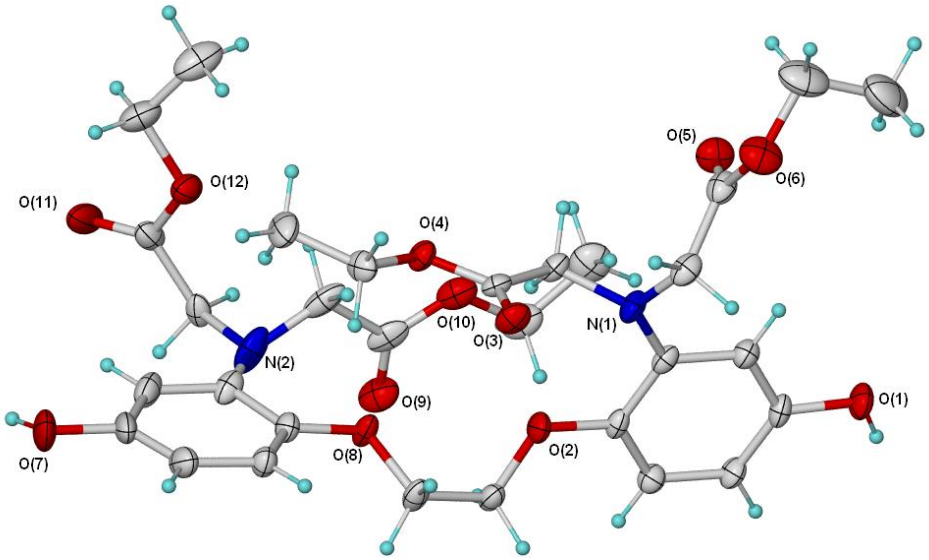

Figure 2.6 Molecular diagram of **19** as shown with 50% thermal ellipsoids and hydrogen atoms as spheres of arbitrary size. Only one component of the disordered acetate ester arm is shown. Lattice water molecules have been omitted for clarity.

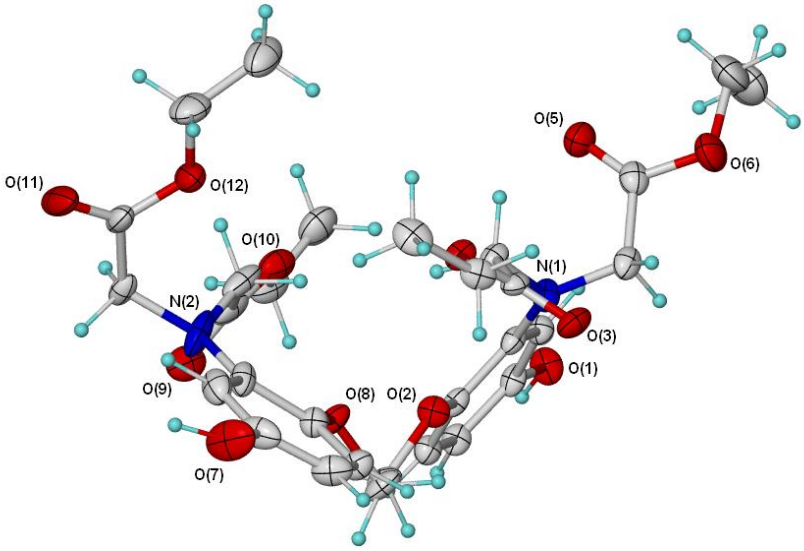

Figure 2.7 Side view of **19**, showing how the ester arms and backbone might encapsulate the Ca^{2+} ion, due to the available coordination sites.

It is envisaged that phenolic compound **19** could act as a suitable dual-action target, due to possible increased solubility in water and resulting bioavailability compared to BAPTA. It is also envisaged that the target could display antioxidant effects due to the phenolic groups and the methylenic hydrogens that were believed to exhibit antioxidant activity in BAPTA.

From **19**, saponification and subsequent treatment with acid afforded the tetraacetic acid **20** in 55% yield (Scheme 2.9). It was important that the acid workup was used to form the acid instead of halting at the potassium salt, as the protonated phenols may be important for improved antioxidant activity.

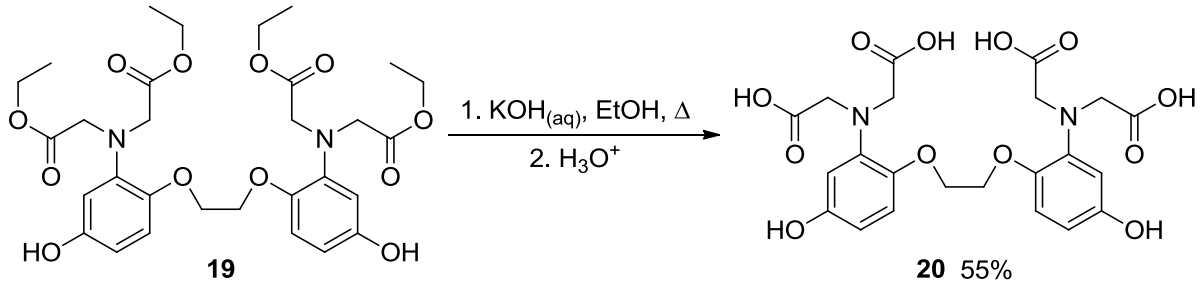

Scheme 2.9

Further functionalisation of **19** by etherification of the phenols with sugar or polyethylene glycol derivatives could be expected to vary water solubility, provide targeting to specific regions, and could provide a method for the formation of a wide range of targets. One such target that was synthesised was **21**, a polyethylene glycol obtained from a Williamson etherification of the precursor **19** and 2-(2-chloroethoxy)ethanol (Scheme 2.10), with an unoptimised yield of 30% after purification. Issues with the yield appeared to be largely due to difficulty isolating the product from the starting material and mono-alkylated intermediate.

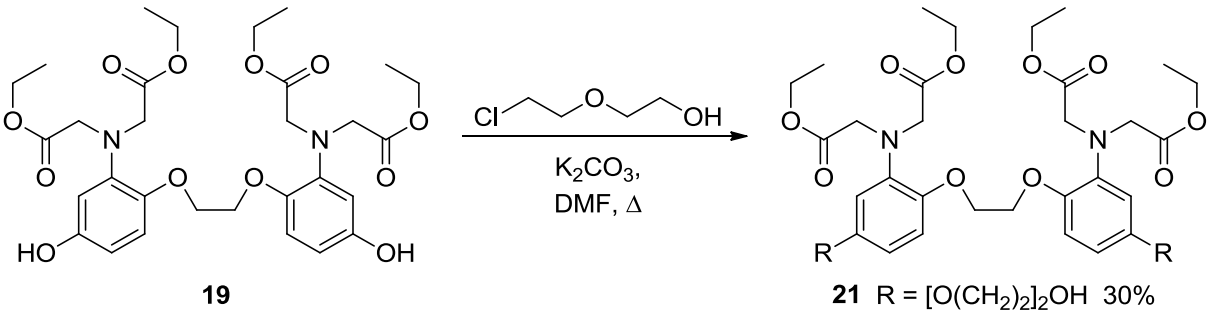

Scheme 2.10

Product formation was supported by high resolution mass spectrometry, with $[M+H]^+$ and $[M+Na]^+$ peaks at m/z 621.2652 and m/z 643.2474, respectively. Also indicative were four new resonances in the ^{1}H NMR spectrum at 4.06, 3.82, 3.76 and 3.65 ppm, integrating to four protons each, attributable to the newly installed methylene protons, as well as four new secondary carbons signals in the ^{13}C NMR spectrum. Figure 2.8 shows the proton NMR spectrum of **21**.

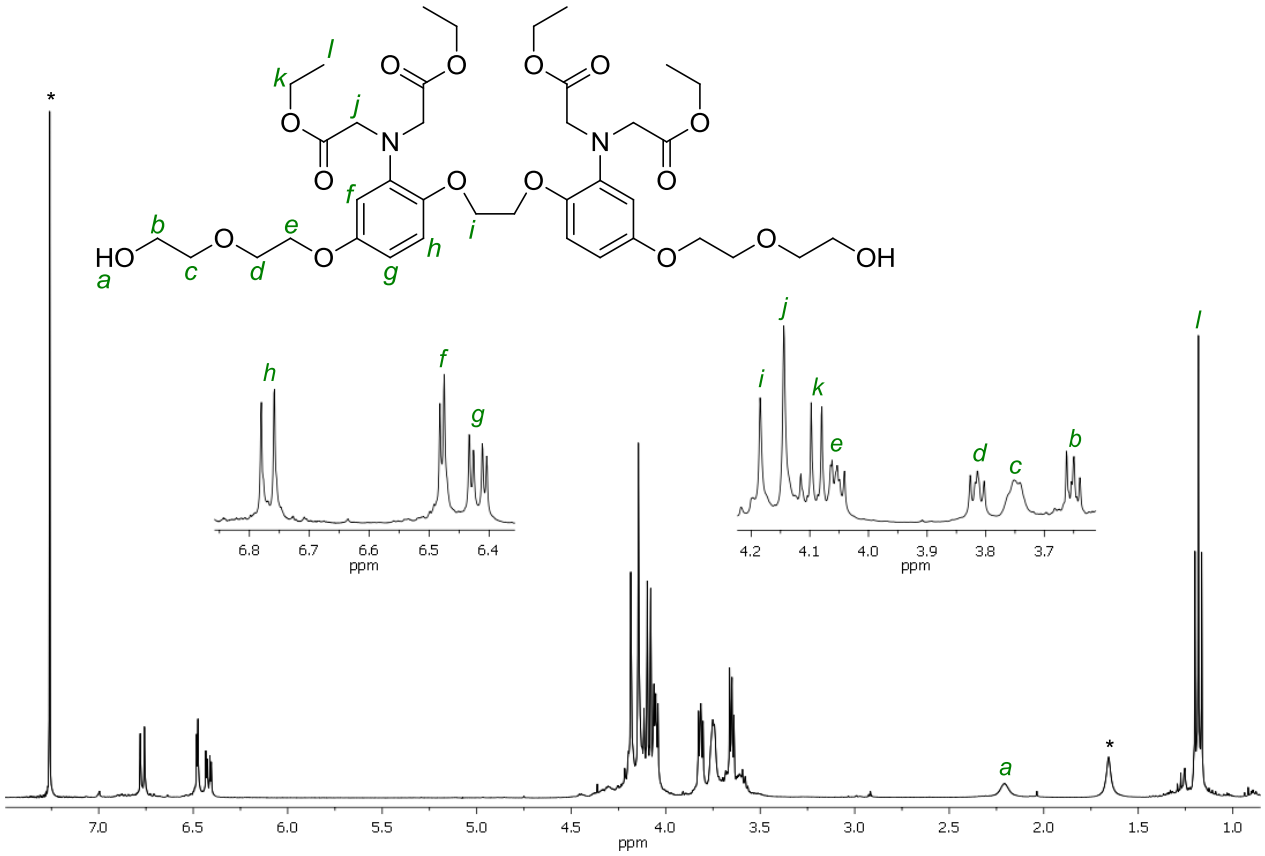

Figure 2.8 400 MHz ^{1}H NMR spectrum of **21** in $CDCl_3$ at 303K. * Denotes residual solvent peaks.

As an alternative to PEGylated target **21**, glycosylation is another pathway that has the potential to increase water solubility. Due to increased polarity as well as preserved solubility in organic solvents, it is anticipated that a glycosylated target would have the desired amphiphilic nature for crossing the blood brain barrier, potentially using the glucose transporter GLUT-1.[49-52] Firstly, acetylation of α-D-glucose was achieved by reaction with acetic anhydride in the presence of sodium acetate under reflux, forming 1,2,3,4,6-penta-*O*-acetyl-β-D-glucose (**22**) in 51% yield after recrystallisation from methanol (Scheme 2.11).[53] The inversion of stereochemistry at the anomeric carbon is supported in the ^{1}H NMR spectrum by the coupling constant of 8.3 Hz for the H1 proton resonance at 5.71 ppm, indicating axial-axial coupling.

From protected sugar **22**, reaction with **19** in the presence of boron trifluoride diethyl etherate produced glycoside **23** in moderate yield (Scheme 2.11).[54] The Lewis acid-promoted reaction conserved the sugar stereochemistry, as described in the literature,[54,55] supported by the coupling constant of 7.6 Hz for the H1 proton resonance in the ^{1}H NMR spectrum.

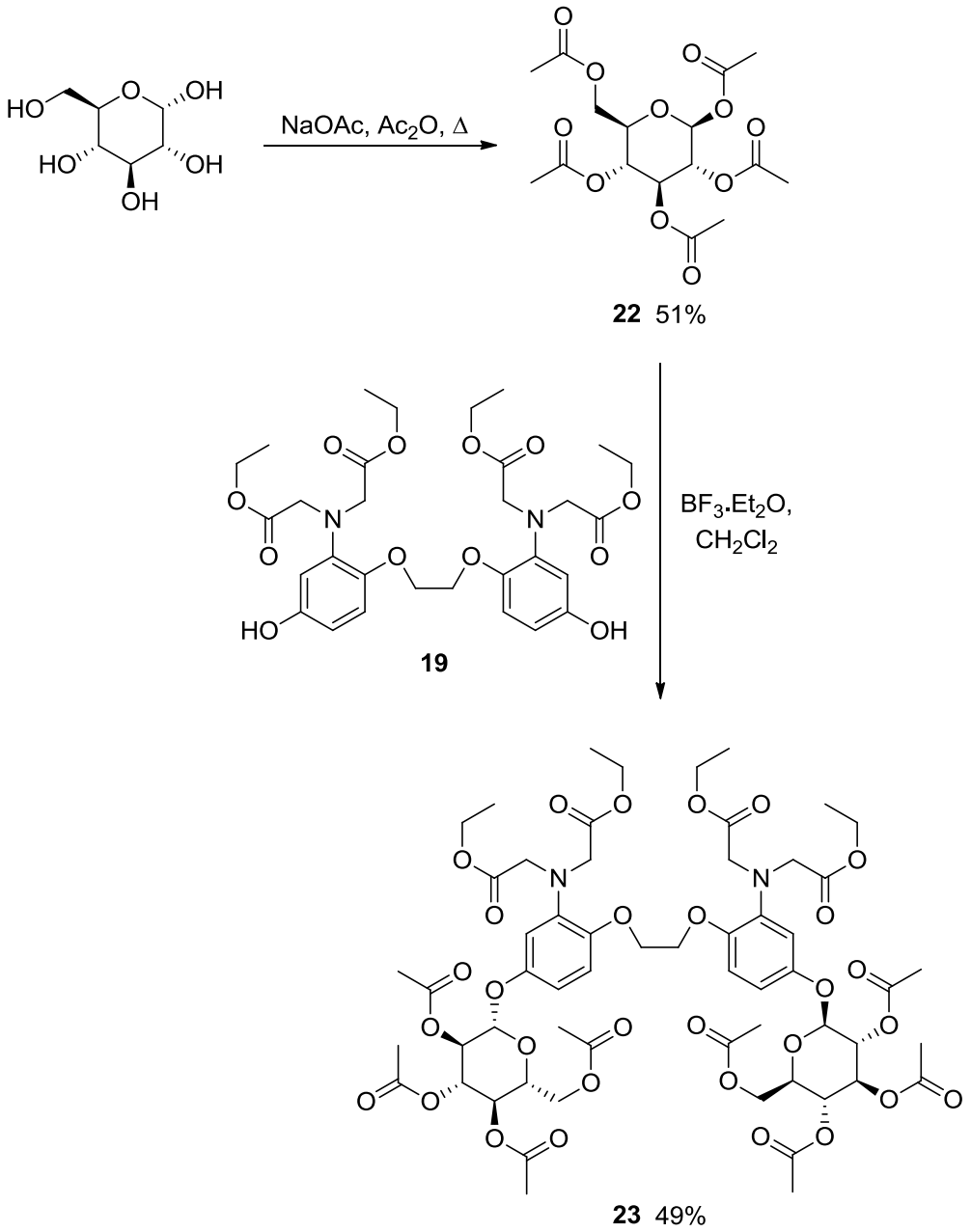

Scheme 2.11

From this point, **23** itself may be considered as a dual-action target for motor neuron degeneration, particularly as a pro-drug. Alternatively, it is envisaged that **23** may be selectively cleaved with dibutyltin oxide[56] to produce the deacetylated compound **24** (Scheme 2.12), which

is expected to be considerably more hydrophilic than targets **19**, **21** and **23**, as well as BAPTA tetraethyl ester **3**, due to the numerous alcohol groups. Unfortunately, this reaction was not attempted in the course of this study.

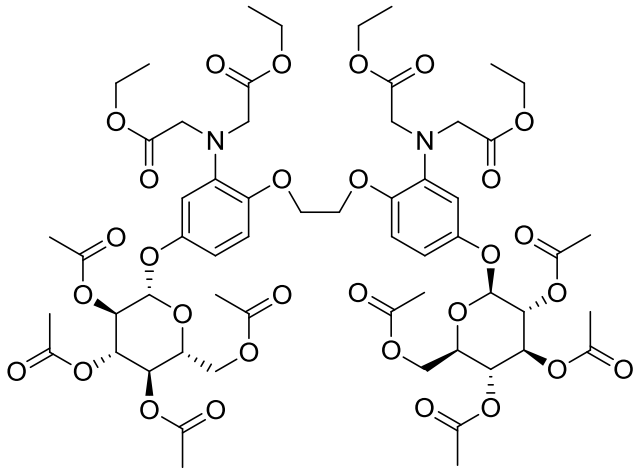

23

Bu_2SnO

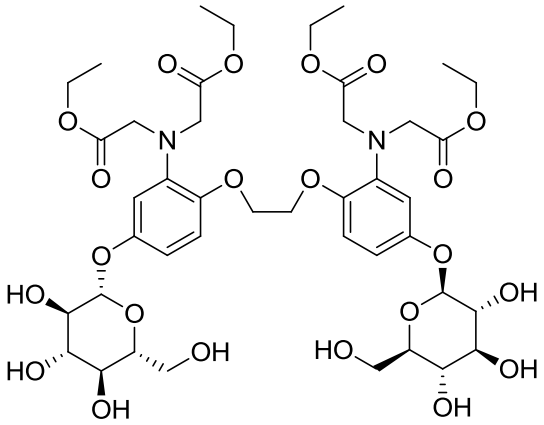

24

Scheme 2.12

2.6 Aqueous antioxidant testing of candidates

In order to evaluate the antioxidant activity of our target compounds against lipid peroxidation, a test involving the radical-initiated oxidation of linoleic acid was employed.[57] Thermal decomposition of the water soluble radical generator 2,2'-azobis(2-amidinopropane) dihydrochloride (AAPH) at a temperature-controlled rate initiates radical formation, producing

a peroxyl radical species that propagates the free radical chain reaction, leading to the oxidation of linoleic acid (Scheme 2.13). The resulting linoleic acid radical undergoes molecular rearrangement and reaction with dissolved oxygen to ultimately form a conjugated diene hydroperoxide species that is observable by UV-visible spectroscopy at 234 nm.[58]

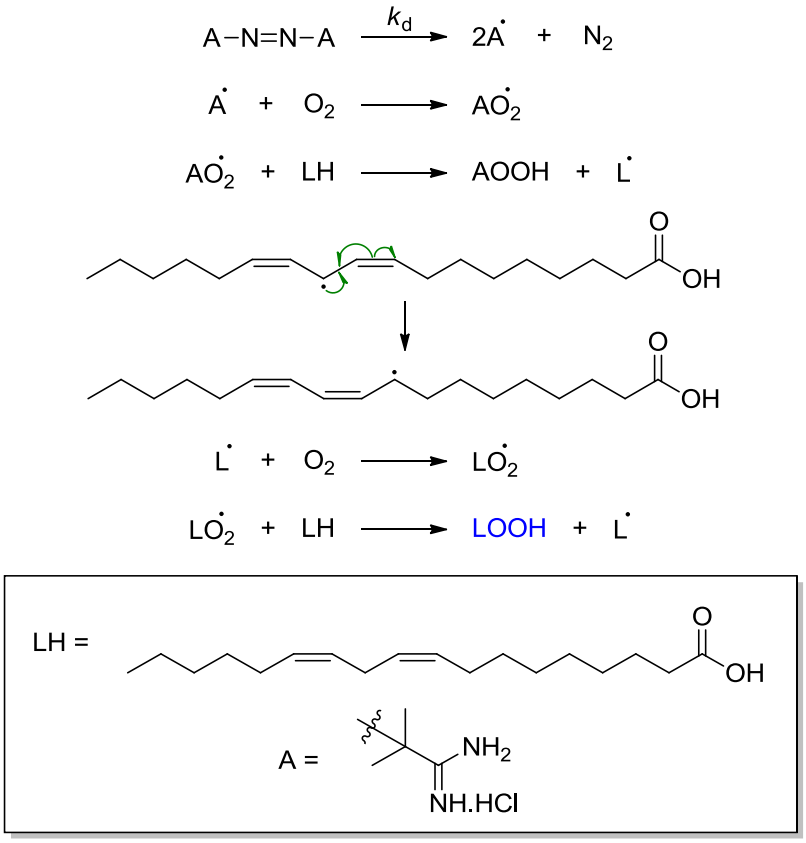

Scheme 2.13 Production of conjugated diene hydroperoxide (blue) from the AAPH-initiated oxidation of linoleic acid.

This process mimics the biological mechanisms involved in lipid peroxidation arising from cellular oxidative stress, and so antioxidants may be evaluated by their ability to inhibit such oxidative processes. Antioxidant efficiency was measured by ability of the tested molecules to quench free radicals, thus slowing the rate of oxidation of linoleic acid, as demonstrated by a reduction in absorbance by UV-visible spectroscopy at 234 nm that results from the diminished production of conjugated diene linoleic acid moieties.

Antioxidant efficiency was calculated using the following equation:

$$\textbf{Efficiency (\%)} = [1-(K_2/K_1)] \times 100$$

where: K_1 = rate of oxidation of standard (no antioxidant)
= [difference in absorbance]/[time (s)]
K_2 = rate of oxidation in presence of antioxidant
= [difference in absorbance]/[time (s)]

The well-known potent antioxidant vitamin E was tested prior to the target compounds to provide a benchmark for antioxidant efficiency (Table 2.1); the result obtained was comparable to efficiency described in the literature.[57]

Table 2.1 Antioxidant efficiencies calculated from the oxidation of linoleic acid.

Compound[a]	Efficiency (±5%)
Vitamin E[b]	91
3 (BAPTA ester)[c]	35
4 (BAPTA)[d]	79
5[c]	33
6[d]	96
12[c]	16
18[c]	88
19[b]	92
20[d]	93
21[b]	56
23[b]	24

[a] Final concentration of compounds was 33 μM
[b] Solubilised in methanol 33% (v/v)
[c] Solubilised in methanol 100% (v/v)
[d] Solubilised in dimethyl sulfoxide 33% (v/v)

Antioxidant testing of BAPTA tetraethyl ester **3**, acid **4**, and dinitro compounds **5** and **6** indicated that all these compounds act well as antioxidants, however the free carboxylic acid exhibited higher efficiency in each case, likely to be due to enhanced radical stabilisation from the carboxylate group. This result is acceptable as we anticipate that target esters will hydrolyse *in vivo* to form the more active acid/carboxylate, as described in Chapter One. Interestingly, 5,5'-dinitro BAPTA (**6**) exhibited a very high antioxidant efficiency compared to BAPTA, apparently due to the electron-withdrawing properties that would lead to decreased electron density around the anilinic nitrogens, which may further enhance radical stabilisation. This hypothesis is further supported by a contrasting result, the very low antioxidant efficiency demonstrated by AATA tetraethyl ester **12**, which indicates that the aliphatic derivative does not stabilise radicals as effectively as its aromatic counterparts, possibly due to increased electron density around the aliphatic nitrogen. It must be noted, however, that the aromatic derivatives exhibited lower solubility in the aqueous buffer solution, an issue that we have sought to overcome in designing a series of soluble BAPTA derivatives.

All of our novel targets exhibited some antioxidant activity, however **19** and **20** provided the most promising results, with efficiency comparable to vitamin E. This is likely to be due to the combination of the presence of Ca^{2+}-chelating groups and the phenols, which may also display antioxidant function. Polyphenols such as flavonoids are known to be efficient antioxidants;[59-62] devising a series of polyphenol BAPTA derivatives may prove useful in further improving antioxidant efficiency and water solubility in the future. While our preliminary results are promising, further derivatisation, ester hydrolysis, *in vitro* and *in vivo* testing of compounds would be required in order to determine the suitability of this series of compounds in the prevention and treatment of neurodegeneration.

2.7 Conclusion

In review, we have synthesised a number of BAPTA derivative targets and precursors, in an effort towards finding suitable candidates for the prevention of motor neuron degeneration. The tetraethyl ester of BAPTA was synthesised in two steps from 1,2-bis(2-nitrophenoxy)ethane, with a further step to produce the acid BAPTA. 5,5'-Dinitro BAPTA compounds were synthesised from BAPTA tetraethyl ester, while aliphatic derivative AATA tetraethyl ester was formed in six steps from 2-nitrophenol and 2-(2-chloroethoxy)ethanol *via* esterification and Gabriel synthesis steps.

The pathway towards the synthesis of hydrophilic BAPTA derivatives yielded the bis-phenol target **19**, which was hydrolysed to give the acid **20**. Reaction of the target **19** with

2-(2-chloroethoxy)ethanol produced the polyethylene glycol tetraethyl ester **21**, expected to have considerably greater water solubility than BAPTA. Protected glucose derivative **23** was also prepared by the glycosylation of **19**. It is expected that these targets and precursors may be further functionalised and hydrolysed to form additional targets that may be tested for antioxidant efficiency and Ca^{2+}-binding capacity.

Aqueous antioxidant testing achieved promising results for number of hydrophilic BAPTA derivative targets, particularly the phenolic analogues **19** and **20**, which exhibited efficiencies comparable to vitamin E. It is hypothesised that the high antioxidant potency may potentially be due to combined antioxidant activity of the phenols and the Ca^{2+}-chelating groups. While initial results are promising, additional *in vitro* and *in vivo* testing of compounds will be required in order to determine the suitability of this series of compounds in the prevention and treatment of neurodegenerative disease.

2.8 Experimental details

2.8.1 General experimental methods for all chapters

Analytical thin layer chromatography (TLC) was performed on plastic plates coated in silica gel (Silica 60 F_{254}). Column chromatography was conducted using Merck silica gel 60, with a pore size between 0.063 and 0.200 mm. The eluent conditions are expressed as volume (v/v) ratios. Components were detected by fluorescence under 254 mm ultraviolet irradiation.

Proton (^{1}H) and carbon (^{13}C) nuclear magnetic resonance (NMR) spectra were recorded using a Bruker AV 200 MHz spectrometer (at 50 MHz for ^{13}C spectra), a Bruker DPX 300 MHz spectrometer (at 75 MHz for ^{13}C spectra), a Bruker DRX 400 MHz spectrometer (at 100 MHz for ^{13}C spectra) or a Bruker Avance 400 MHz spectrometer (at 100 MHz for ^{13}C spectra). All NMR spectra were obtained as solutions in deuterated chloroform ($CDCl_3$) stored over Na_2CO_3 or in deuterated dimethyl sulfoxide (d_6-DMSO). Unless otherwise stated, all NMR spectra were obtained at 303 K. Chemical shifts (δ) were calibrated against the residual solvent resonance. Each proton resonance is assigned according to the following format: (operating frequency of spectrometer, solvent): chemical shift measured in parts per million (ppm), multiplicity (denoted as s (singlet), d (doublet), t (triplet), q (quartet), or m (multiplet)), observed coupling constants (*J*, Hz), number of protons and assignment. Broad resonances are denoted as br. ^{13}C NMR spectra were recorded using the proton decoupled pulse sequence or JMOD and are assigned as follows: (operating frequency of spectrometer, solvent): chemical shift (ppm).

Mass spectrometry (MS) results were obtained by Sally Duck, Finlay Shanks and Phillip Holt, School of Chemistry, Monash University. Low resolution ESI spectra were recorded on a

Micromass Platform (QMS – quadrupole mass electrospray) or a Micromass ZMD mass spectrometer. Electron impact (EI) mass spectrometry was recorded on a Shimadzu QP505A GCMS system with a solids probe. High resolution ESI mass spectrometry (HRMS) measurements were obtained using a Bruker BioApex 4.7T ultrahigh resolution FT-ICR mass spectrometer or Agilent Technologies 6220 Accurate-Mass TOF LC/MS spectrometer. The predominant ion peaks (m/z) were recorded. $[M]^+$ denotes the molecular ion. Spectra were recorded using ESI mode unless otherwise stated.

UV-visible spectra were recorded using a Varian Cary 100 Bio UV-Visible Spectrophotometer.

Melting points (MP) were determined using a Stuart Scientific melting point apparatus (SMP3).

X-ray crystal diffraction patterns were determined using a Bruker X8 Apex CCD diffractometer or a Bruker Apex II KAPPA CCD diffractometer using graphite monochromated MoKα X-ray radiation λ = 0.71073 Å at 123(2) K. The crystal data was solved and refined using SHELXS-97[63] and SHLEXL-97[64] suite of programs with the graphical interface X-Seed.[65] Crystal structure determinations were performed by Dr Craig Forsyth and Dr Kristina Konstas, School of Chemistry, Monash University, Clayton.

2.8.2 Reagents and solvents

All solvents used were AR grade or HPLC grade. All experiments were conducted under nitrogen or argon unless otherwise stated. Acetonitrile was dried by storage over 4Å molecular sieves before use. Dry tetrahydrofuran and diethyl ether were obtained by distillation from sodium and benzophenone, under nitrogen. Dry methanol was obtained by distillation over calcium sulfate under nitrogen. Dry dichloromethane was obtained from distillation over calcium hydride. Ethanol-free chloroform was obtained by washing with water, drying over CaH_2 and passing through a column of activated alumina.

2.8.3 Aqueous linoleic acid antioxidant testing

Antioxidant testing was used to determine the efficiency of antioxidants in aqueous systems. Adapting a method described in the literature,[57] and within our research group,[24,34,35] 2,2'-azobis(2-amidinopropane)dihydrochloride (AAPH) was employed as a free radical initiator. Formation of the conjugated diene linoleic acid hydroperoxide through the oxidation of linoleic acid at 37°C was monitored at 234 nm for 15 min using UV-visible absorption spectroscopy. Optimal reagent quantities employed for testing were:

2.78 mL of 0.05 M phosphate buffer (pH 7.4)
60 µL of linoleic acid dispersion stock
10 µL of 0.01 M antioxidant stock
150 µL of 40 mM AAPH stock

The linoleic acid dispersion was prepared as follows: To 5 mL of 0.05 M borate buffer (pH 9), containing 250 µL of Tween 20, 250 µL of linoleic acid was added dropwise with continuous stirring. The resulting dispersion was clarified by the addition of 1 mL of 1 M NaOH solution. The solution was diluted to 50 mL with additional borate buffer. The solution was stored under argon in the dark below 0°C until required.

2.8.4 Synthesis of BAPTA and soluble BAPTA derivatives

Synthesis of 1,2-bis(2-aminophenoxy)ethane – 2:

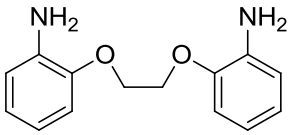

1,2-Bis(2-nitrophenoxy)ethane **1** (55.0 g, 181 mmol), EtOH (275 mL) and 5% Pd/C (5.50 g) were stirred together in a round bottom flask. The reaction mixture was cooled in an ice bath, and a condenser and thermometer were attached before dropwise addition of hydrazine hydrate (44 mL, 0.905 mol) (approx. 0.5 mL/min) by dropping funnel, taking care to not let the reaction heat above 30°C. After the addition, the reaction was allowed to warm slowly to room temperature. After stirring overnight, the reaction mixture was heated at reflux for a further 24 h, then underwent a hot filtration through celite and was washed with hot EtOH. Product precipitated out of the filtrate, which was cooled on ice. The precipitate was filtered and washed with a minimal amount of cold EtOH to give a 1st crop of product **2** (18.0 g, 41%), as a fluffy white solid. Further product was washed from the celite with hot $CHCl_3$, which was then removed *in vacuo* to give a 2nd crop of product **2** (22.9 g, 52%), obtaining a total product yield of 40.9 g (93%), as white fluffy crystals.

^{1}H NMR (300 MHz, $CDCl_3$) δ: 6.86, m, 4H, Ar-*H*; 6.75, m, 4H, Ar-*H*; 4.37, s, 4H, -O-CH_2CH_2-O-; 3.85, br s, 4H, -NH_2. **^{13}C NMR (75 MHz, $CDCl_3$) δ:** 146.3, 137.0, 122.0, 118.4, 115.4, 112.7, 67.6. **MS (ESI, +ve):** *m*/*z* 245.1 $[M+H]^+$. **MP:** 130.6-132.0°C (Literature[66]: 132°C).

Synthesis of tetraethyl 1,2-bis(o-aminophenoxy)ethane-N,N,N',N'-tetraacetate (BAPTA tetraethyl ester) – 3:

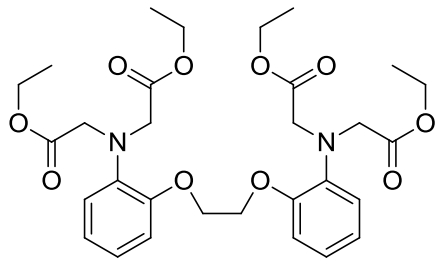

Adapted from Tsien.[21] Bis-anilino compound **2** (65.2 g, 267 mmol), ethyl bromoacetate (134 mL, 1.21 mol), DIPEA (223 mL, 1.28 mol), NaI (8.01 g, 53.4 mmol) and toluene (220 mL) were all combined in a round bottom flask, and were stirred at reflux overnight. On completion, the reaction mixture was allowed to cool slightly, then filtered to remove the diisopropylethylammonium salt, which could be converted back to the free amine on treatment with concentrated NaOH solution. The salt precipitate was washed further with hot toluene to extract the desired product, and the filtrate was removed by rotary evaporation to give a pale brown solid. The precipitate was stirred in EtOH overnight to remove impurities, then filtered, and washed with EtOH, and dried over a water aspirator, to give pure tetraethyl ester product **3** (136.6 g, 87%), as a cream powder.

^{1}H NMR (400 MHz, $CDCl_3$) δ: 6.86, m, 8H, Ar-H; 4.28, s, 4H, -O-C*H*$_2$C*H*$_2$-O-; 4.15, s, 8H, -N-C*H*$_2$-CO_2-; 4.05, q, ^3J 7.1 Hz, 8H, -C*H*$_2$$CH_3$; 1.14, t, ^3J 7.1 Hz, 12H, -CH_2C*H*$_3$. **^{13}C NMR (100 MHz, $CDCl_3$) δ:** 171.7 (*C*=O), 150.5, 139.6, 122.3, 121.7, 119.2, 113.5, 67.3, 60.8, 53.7, 14.2. **MS (ESI, +ve):** *m*/*z* 589.3 $[M+H]^+$; 611.3 $[M+Na]^+$. **MP:** 95.5-96.8°C (Literature[21]: 95-97°C).

Synthesis of 1,2-bis(*o*-aminophenoxy)ethane-*N,N,N'*,*N'*-tetraacetic acid (BAPTA) – 4:

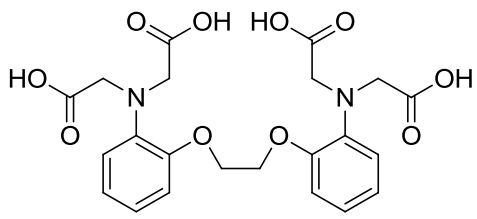

Adapted from Tsien.[21] BAPTA ester **3** (507 mg, 0.861 mmol) was dissolved in a minimal amount of warm EtOH (18 mL) and the solution was treated with a concentrated solution of KOH (253 mg, 4.51 mmol) in H_2O (1.5 mL). The reaction was heated at 60°C for 15 min, after which time the solvent was removed by rotary evaporation to give a cream solid. The residue was dissolved in a minimal amount of H_2O, cooled in an ice bath, and concentrated HCl was added to pH 2, forming a white precipitate. The product was extracted with EtOAc (100 mL) and dried over $NaSO_4$, filtered and the solvent removed *in vacuo* to give BAPTA acid **4** (387 mg, 94%), as a white solid.

^{1}H NMR (400 MHz, d_6-DMSO) δ: 6.97, m, 2H, Ar-*H*; 6.85, m, 4H, Ar-*H*; 6.75, m, 2H, Ar-*H*; 4.24, s, 4H, -O-C*H*$_2$C*H*$_2$-O-; 4.04, s, 8H, -N-C*H*$_2$-CO$_2$-. **^{13}C NMR (100 MHz, d_6-DMSO) δ:** 172.5 (*C*=O), 149.5, 139.3, 121.4, 121.1, 118.2, 114.7, 67.2, 53.5. **MS (ESI, +ve):** *m*/*z* 499.2 [M+Na]$^+$. **MS (ESI, -ve):** *m*/*z* 475.0 [M-H]$^-$. **MP:** 178.4-178.9°C.

Synthesis of tetraethyl 5,5'-dinitro-1,2-bis(*o*-aminophenoxy)ethane-*N*,*N*,*N*',*N*'-tetraacetate (dinitro BAPTA tetraethyl ester) – 5:

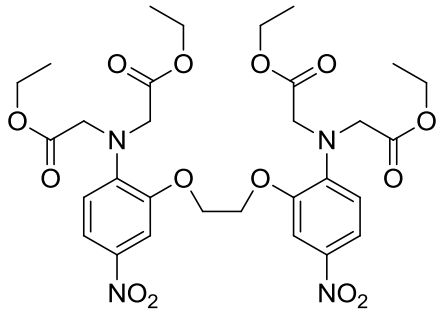

Adapted from Pethig *et al.*[40] BAPTA ester **3** (501 mg, 0.851 mmol) was stirred as a suspension in glacial AcOH (2.5 mL). Concentrated HNO_3 (114 µL) was added dropwise, turning the solution from colourless to black, and after 15 min of stirring the reaction mixture had turned into a bright yellow slurry. After 25 min, saturated $NaHCO_3$ solution (5 mL) was added to the slurry, and the resulting precipitate was filtered, washed with H_2O and dried to give **5** (560 mg, 97%), a bright yellow solid.

^{1}H NMR (300 MHz, $CDCl_3$) δ: 7.84/7.72/6.71, ABX system, $^3J_{AX}$ 8.9 Hz, $^4J_{AB}$ 2.5 Hz, 6H, Ar-*H*; 4.34, s, 4H, -O-C*H*$_2$C*H*$_2$-O-; 4.21, s, 8H, -N-C*H*$_2$-CO$_2$-; 4.10, q, ^3J 7.1 Hz, 8H, -C*H*$_2$CH$_3$; 1.18, t, ^3J 7.1 Hz, 12H, -CH$_2$C*H*$_3$. **^{13}C NMR (75 MHz, $CDCl_3$) δ:** 170.5 (*C*=O), 148.5, 145.6, 141.1, 118.8, 116.3, 108.5, 67.5, 61.5, 54.0, 14.2. **MS (ESI, +ve):** *m*/*z* 701.1 [M+Na]$^+$. **HRMS (ESI, +ve):** *m*/*z* 701.2269 [M+Na]$^+$, $C_{30}H_{38}N_4O_{14}$ required *m*/*z* 701.2277. **MP:** 150.5-152.9°C.

Synthesis of 5,5'-dinitro-1,2-bis(*o*-aminophenoxy)ethane-*N*,*N*,*N*',*N*'-tetraacetic acid (dinitro BAPTA acid) – 6:

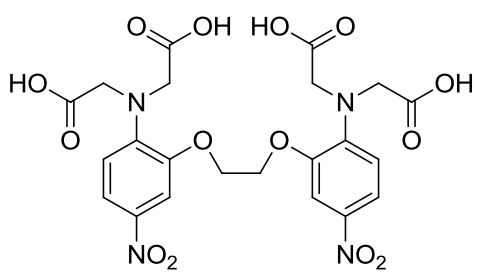

Adapted from Tsien.[21] Ester **5** (100 mg, 0.147 mmol) was dissolved in hot MeOH (20 mL) and the solution was treated with a concentrated solution of KOH (90 mg, 1.6 mmol) in H_2O (0.5 mL). The reaction was heated at 60°C for 45 min, after which time the solvent was removed by rotary evaporation, to give a dark

orange oil. The residue was dissolved in a minimal amount of H_2O (15 mL) and the solution was acidified to pH 2 with concentrated HCl, forming a brown precipitate. The product was extracted with EtOAc (100 mL), dried ($MgSO_4$), filtered and the solvent removed *in vacuo* to give acid **6** (60 mg, 72%), as a dark yellow powder.

^{1}H NMR (400 MHz, $CDCl_3$) δ: 7.81/7.67/6.66, ABX system, $^3J_{AX}$ 9.1 Hz, $^4J_{AB}$ 2.4 Hz, 6H, Ar-*H*; 4.32, s, 4H, -O-C*H*$_2$C*H*$_2$-O-; 4.18, s, 8H, -N-C*H*$_2$-CO_2-. **^{13}C NMR (100 MHz, $CDCl_3$) δ:** 171.6, 147.3, 145.6, 138.8, 118.4, 114.6, 108.1, 67.3, 54.0. **MP:** 125.8-126.9°C (decomp.).

Synthesis of 2-(2-(2-nitrophenoxy)ethoxy)ethanol – 7:

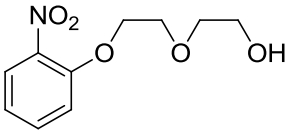

To a solution of 2-nitrophenol (1.00 g, 7.19 mmol) in 2 mL of DMF, 2-(2-chloroethoxy)ethanol (1.14 mL, 10.8 mmol) and K_2CO_3 (2.00 g, 14.5 mmol) were added. The reagents were stirred in a sealed pressure tube at 100°C for 5 d. Reaction progress was monitored by a gradual colour change from red to yellow. On completion, water (10 mL) was added, to yield a yellow precipitate. The product was extracted with EtOAc (2 × 20 mL) washed with H_2O (50 mL), dried over $MgSO_4$, filtered and the solvent concentrated *in vacuo* to give pure **7** (1.55 g, 95%), as a clear pale yellow oil.

^{1}H NMR (300 MHz, $CDCl_3$) δ: 7.65, dd, ^3J 8.1 Hz, ^4J 1.7 Hz, 1H, Ar-*H*; 7.39, ddd, ^3J 8.5, 7.4 Hz, ^4J 1.7 Hz, 1H, Ar-*H*; 7.00, dd, ^3J 8.5 Hz, ^4J 1.0 Hz, 1H, Ar-*H*; 6.89, ddd, ^3J 8.2, 7.3 Hz, ^4J 1.0 Hz, 1H, Ar-*H*; 4.13, t, ^3J 4.7 Hz, 2H, -O-C*H*$_2$CH$_2$-O-; 3.75, t, ^3J 4.7 Hz, 2H, -O-CH$_2$C*H*$_2$-O-; 3.57, m, 2H, -C*H*$_2$CH$_2$OH; 3.53, m, 2H, -CH$_2$C*H*$_2$OH; 2.96, br s, 1H, -O*H*. **^{13}C NMR (75 MHz, $CDCl_3$) δ:** 151.9, 139.7, 134.0, 125.1, 120.4, 114.8, 72.5, 69.1, 68.8, 61.3. **MS (ESI, +ve):** *m*/*z* 250.1 $[M+Na]^+$.

Synthesis of 2-(2-(2-nitrophenoxy)ethoxy)ethyl 4-methylbenzenesulfonate – 8:

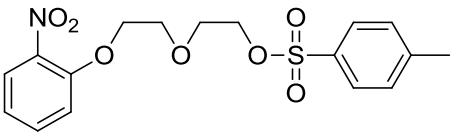

Alcohol **7** (1.15 g, 5.06 mmol), DMAP (130 mg, 1.06 mmol) and Et_3N (1.41 mL, 10.1 mmol) were dissolved in CH_2Cl_2 (10 mL) before the solution was stirred and cooled to 0°C. *p*-Toluenesulfonyl chloride (1.93 g, 10.1 mmol) was added slowly in portions and the reaction was allowed to warm to room temperature and stirred overnight. The reaction was monitored

by TLC. On completion, the solvent was removed under reduced pressure and the product extracted into EtOAc, washed with NH_4Cl, brine and water, dried over $MgSO_4$, filtered and the solvent removed *in vacuo* to give **8** (1.73 g, 90%) as a yellow oil.

^{1}H NMR (300 MHz, $CDCl_3$) δ: 7.81, dd, ^3J 8.1 Hz, ^4J 1.7 Hz, 1H, Ar-*H*; 7.79/7.34, AA'XX' system, $^3J_{AX/A'X'}$ 8.2 Hz, 4H, Ts-*H*; 7.54, ddd, ^3J 8.5, 7.4 Hz, ^4J 1.6 Hz, 1H, Ar-*H*; 7.12, dd, ^3J 8.5 Hz, ^4J 0.9 Hz, 1H, Ar-*H*; 7.05, ddd, ^3J 8.1, 7.3 Hz, ^4J 1.1 Hz, 1H, Ar-*H*; 4.20, t, ^3J 4.6 Hz, 2H, -CH_2-; 4.20, t, ^3J 4.6 Hz, 2H, -CH_2-; 3.84, t, ^3J 4.6 Hz, 2H, -CH_2-; 3.80, t, ^3J 4.6 Hz, 2H, -CH_2-; 2.43, s, 3H, -CH_3. **^{13}C NMR (75 MHz, $CDCl_3$) δ:** 152.0, 144.8, 139.9, 134.1, 132.9, 129.8, 127.8, 125.3, 120.6, 115.0, 69.6, 69.4, 69.3, 69.0, 21.4. **MS (ESI, +ve):** *m/z* 404.2 $[M+Na]^+$.

Synthesis of *N*-(2-(2-(2-nitrophenoxy)ethoxy)ethyl)phthalimide – 9:

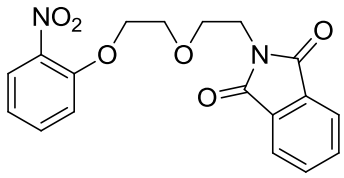

Ester **8** (1.71 g, 4.49 mmol) was dissolved in DMF (12 mL), and potassium phthalimide (4.16 g, 22.5 mmol) was added slowly. The reaction was stirred and heated at 100°C overnight, after which time the reaction mixture underwent hot filtration. On cooling, CH_2Cl_2 (20 mL) was added to the filtrate, and the organic solution was washed with saturated aqueous $NaHCO_3$ (2 × 30 mL) and H_2O (30 mL). The organic phase was dried ($MgSO_4$), filtered and the solvent removed under reduced pressure. Water (2 mL) was added to precipitate the product from residual DMF, and the solid was filtered, washed with H_2O and dried over an aspirator to give the phthalimide **9** (1.46 g, 91%), as a cream powder.

^{1}H NMR (400 MHz, $CDCl_3$) δ: 7.82, m, 2H, Phth-*H*; 7.77, dd, ^3J 8.3 Hz, ^4J 1.7 Hz, 1H, Ar-*H*; 7.69, m, 2H, Phth-*H*; 7.47, ddd, ^3J 8.6, 7.3 Hz, ^4J 1.7 Hz, 1H, Ar-*H*; 7.08, dd, ^3J 8.4 Hz, ^4J 0.8 Hz, 1H, Ar-*H*; 6.99, ddd, ^3J 8.3, 7.2 Hz, ^4J 1.1 Hz, 1H, Ar-*H*; 4.22, t, ^3J 4.7 Hz, 2H, -CH_2-; 3.93-3.82, m, 6H, -CH_2-. **^{13}C NMR (100 MHz, $CDCl_3$) δ:** 168.4 (*C*=O), 152.4, 140.2, 134.2, 134.0, 132.2, 125.7, 123.4, 120.7, 115.4, 69.8, 69.0, 68.6, 37.5. **MS (ESI, +ve):** *m/z* 357.1 $[M+H]^+$, 379.1 $[M+Na]^+$. **HRMS (ESI, +ve):** *m/z* 379.0903 $[M+Na]^+$; $C_{18}H_{16}N_2O_6$ required *m/z* 379.0901. **MP:** 147.5-149.9°C.

Synthesis of 2-(2-(2-nitrophenoxy)ethoxy)ethanamine – 10:

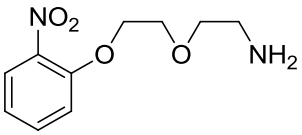

Phthalimide **9** (7.14 g, 20.0 mmol) was dissolved in a mixture of THF (55 mL) and EtOH (35 mL). Hydrazine hydrate (9.75 mL, 200 mmol) was added dropwise and the reaction mixture was stirred at room temperature overnight, after which time the mixture thickened. The slurry was filtered and washed with EtOH to remove the byproduct precipitate. The filtrate was concentrated *in vacuo* to give a yellow oil and white solid. The crude product was dissolved in $CHCl_3$ and filtered to remove further impurities. The filtrate was concentrated by rotary evaporation to give pure **10** (3.43 g, 76%), as a yellow oil.

^{1}H NMR (300 MHz, $CDCl_3$) δ: 7.79, dd, ^3J 8.1 Hz, ^4J 1.6 Hz, 1H, Ar-*H*; 7.49, ddd, ^3J 8.8, 7.1 Hz, ^4J 1.6 Hz, 1H, Ar-*H*; 7.09, d, ^3J 8.5 Hz, 1H, Ar-*H*; 7.01, ddd, ^3J 8.2, 7.3 Hz, ^4J 0.9 Hz, 1H, Ar-*H*; 4.24, t, ^3J 4.7 Hz, 2H, -C*H*$_2$-; 3.84, t, ^3J 4.7 Hz, 2H, -C*H*$_2$-; 3.57, t, ^3J 5.2 Hz, 2H, -C*H*$_2$-; 2.84, t, ^3J 5.2 Hz, 2H, -C*H*$_2$-; 2.27, br s, 2H, -N*H*$_2$. **^{13}C NMR (100 MHz, $CDCl_3$) δ:** 152.0, 139.8, 134.0, 125.2, 120.5, 114.9, 72.8, 69.2, 68.7, 41.1. **MS (ESI, +ve):** *m*/*z* 227.1 $[M+H]^+$.

Synthesis of 2-(2-(2-aminoethoxy)ethoxy)aniline – 11:

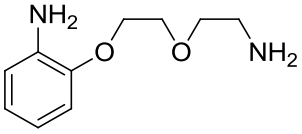

Nitro amine compound **10** (492 mg, 2.17 mmol) was dissolved in absolute EtOH (10 mL), and 10% Pd/C (49 mg) was added to the stirred solution. Hydrazine hydrate (900 μL, 18.5 mmol) was added slowly, with gas evolution, and the reaction was heated at reflux for 21 h. Reaction progress was monitored by TLC. When all starting material had been consumed, the reaction was filtered through celite while hot to remove the catalyst, and the solvent was removed *in vacuo* to give **11** (425 mg, quant.) as a pale brown oil. The product was used in subsequent reactions without purification.

^{1}H NMR (300 MHz, $CDCl_3$) δ: 6.66, m, 2H, Ar-*H*; 6.55, m, 2H, Ar-*H*; 3.94, t, ^3J 4.7 Hz, 2H, -C*H*$_2$-; 3.60, t, ^3J 4.7 Hz, 2H, -C*H*$_2$-; 3.34, t, ^3J 5.3 Hz, 2H, -C*H*$_2$-; 2.67, t, ^3J 5.2 Hz, 2H, -C*H*$_2$-. **^{13}C NMR (75 MHz, $CDCl_3$) δ:** 145.6, 136.7, 121.1, 117.2, 114.5, 112.2, 72.7, 68.8, 67.6, 41.1. **MS (ESI, +ve):** *m*/*z* 197.0 $[M+H]^+$. **HRMS (ESI, +ve):** *m*/*z* 197.1285 $[M+H]^+$; $C_{10}H_{16}N_2O_2$ required *m*/*z* 197.1285.

Synthesis of tetraethyl 1-(2-aminophenoxy)-2-(2-aminoethoxy)ethane-*N*,*N*,*N*',*N*'-tetraacetate (AATA tetraethyl ester) – 12:

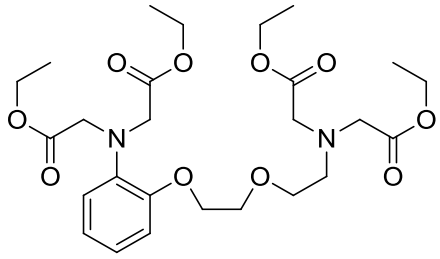

Adapted from Robitaille and Jiang.[48] Bis-amino compound **11** (1.69 g, 8.61 mmol) was dissolved in MeCN (45 mL), to which NaI (645 mg, 4.30 mmol), DIPEA (16.5 mL, 94.7 mmol) and ethyl bromoacetate (9.59 mL, 86.1 mmol) were added. The reaction mixture was heated at reflux overnight and then cooled to room temperature, after which time toluene (100 mL) was added. The reaction mixture was filtered and the filtrate was washed with 0.1 M HCl solution and H_2O, and the organic phase was dried ($NaSO_4$), filtered and the solvent removed *in vacuo* to give a brown oil (8.4 g). Purification by column chromatography (50% EtOAc/hexane) gave the tetraethyl ester **12** (3.70 g, 79%), as a yellow oil.

^{1}H NMR (400 MHz, $CDCl_3$) δ: 6.75, m, 4H, Ar-*H*; 4.1-3.9, m, 14H, -C*H*$_2$CH$_3$/-C*H*$_2$CH$_3$ /-OC*H*$_2$CH$_2$O-/Ar-N-C*H*$_2$-CO$_2$-; 3.62, t, ^3J 5.0 Hz, 2H, -O-CH$_2$C*H*$_2$-O-; 3.54, t, ^3J 5.5 Hz, 2H, -O-C*H*$_2$CH$_2$-N-; 3.49, s, 4H, -N-C*H*$_2$-CO$_2$-; 2.87, t, ^3J 5.4 Hz, 2H, -O-CH$_2$C*H*$_2$-N-; 1.21, t, ^3J 7.1 Hz, 6H, -CH$_2$C*H*$_3$; 1.11, t, ^3J 7.2 Hz, 6H, -CH$_2$C*H*$_3$. **^{13}C NMR (100 MHz, $CDCl_3$) δ:** 171.1 (*C*=O), 171.0 (*C*=O), 150.3, 139.1, 122.0, 121.2, 119.2, 114.0, 70.1, 69.1, 67.8, 60.2, 60.0, 55.6, 53.5, 53.3, 14.0, 13.9. **MS (ESI, +ve):** *m/z* 541.4 $[M+H]^+$, 563.3 $[M+Na]^+$. **HRMS (ESI, +ve):** *m/z* 541.2755 $[M+H]^+$, $C_{26}H_{40}N_2O_{10}$ required *m/z* 541.2756; *m/z* 563.2577 $[M+H]^+$, $C_{26}H_{40}N_2O_{10}$ required *m/z* 563.2575.

Synthesis of 1,4-bis(benzyloxy)benzene – 13:

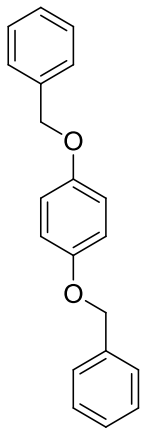

From Grynkiewicz *et al.*[45] To a stirred suspension of hydroquinone (30.0 g, 0.272 mol) and benzyl chloride (69.1 mL, 0.599 mol) in EtOH (55 mL), was added a solution of KOH (33.65 g, 0.600 mol) in EtOH (150 mL). After 30 min, the reaction mixture was poured into cold water and stirred overnight. The resulting precipitate was filtered over a water aspirator, and recrystallised from boiling EtOH to yield **13** as brilliant white fluffy crystals (66.3 g, 84%).

^{1}H NMR (300 MHz, $CDCl_3$) δ: 7.38, m, 10H, Bn-*H*; 6.91, s, 4H, Ar-*H*; 5.02, s, 4H, Ar-C*H*$_2$-O-. **^{13}C NMR (75 MHz, $CDCl_3$) δ:** 153.4, 137.5, 128.7, 128.0, 127.6, 116.0, 70.9. **MS (EI):** *m/z* 290 $[M]^+$. **MP:** 126.8-127.2°C (Literature[45]: 128-130°C).

Synthesis of 1,4-bis(benzyloxy)-2-nitrobenzene – 14:

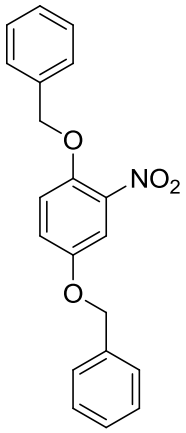

From Grynkiewicz *et al*.[45] Concentrated HNO_3 (2.10 mL) was diluted to 8 mL with glacial AcOH, and the solution was added to **13** (8.90 g, 30.7 mmol) stirred in glacial AcOH (40 mL). The reaction mixture was heated to 50°C for 10 min, at which point the starting material dissolved and the product started precipitating out of the bright yellow solution. After 1.5 h, the reaction mixture was allowed to cool to room temperature and was left to stir overnight. The resulting precipitate was filtered, washed with AcOH and H_2O, and dried over vacuum to give **14** (9.53 g, 93%) as a brilliant yellow solid.

^{1}H NMR (300 MHz, $CDCl_3$) δ: 7.48/7.12/7.04, ABX system, $^3J_{AB}$ 9.1 Hz, $^4J_{BX}$ 3.0 Hz, 3H, Ar-*H*; 7.45-7.34, m, 10H, Bn-*H*; 5.18, s, 2H, Ar-CH_2-O-; 5.05, s, 2H, Ar-CH_2-O-. **^{13}C NMR (75 MHz, $CDCl_3$) δ:** 152.5, 146.5, 140.6, 136.2, 136.1, 128.9, 128.8, 128.5, 128.3, 127.7, 127.3, 121.6, 117.5, 111.4, 72.1, 71.2. **MS (ESI, +ve):** *m*/*z* 358.0 $[M+Na]^+$. **MP:** 81.9-82.3°C (Literature[45]: 81-82.5°C).

Synthesis of 4-benzyloxy-2-nitrophenol – 15:

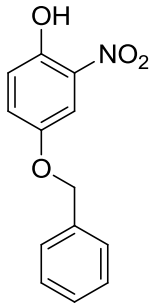

From Grynkiewicz *et al*.[45] Compound **14** (25.3 g, 75.4 mmol) was dissolved in EtOH-free $CHCl_3$ (50 mL) and the solution was treated with TFA (7.70 mL, 99.9 mmol). The reaction mixture was stirred at room temperature for 2 d, during which time the reaction was monitored by ^{1}H NMR spectroscopy. On completion, the mixture was neutralised using 5 M aqueous KOH solution. A further 100 mL of $CHCl_3$ was added to the reaction mixture, and the aqueous layer was removed by separation. The organic layer was washed repeatedly with dilute aqueous K_2CO_3 solution until the aqueous phase was a pale orange colour. Diethyl ether (225 mL) was added to the $CHCl_3$ solution, and was basified with 70 mL of 5 M KOH solution. The resulting red precipitate was collected over vacuum, before acidification with 2 M HCl, which turned the red precipitate yellow. The product was extracted from the aqueous mixture with Et_2O (4 × 200 mL). The organic fractions were combined and the solvent removed by rotary evaporation to yield **15** as a crude brown solid (16.8 g, 91%). Recrystallisation from boiling MeOH followed by the addition of cold water gave a cloudy yellow solution, which overnight became a yellow precipitate in an orange solution. The precipitate was filtered, washed with water and dried over vacuum to yield **15** (14.2 g, 77%), as a bright orange-yellow solid.

^{1}H NMR (400 MHz, $CDCl_3$) δ: 10.32, s, 1H, Ar-O*H*; 7.61/7.29/7.10, AMX system, $^3J_{AM}$ 9.2 Hz, $^4J_{MX}$ 3.1 Hz, 3H, Ar-*H*; 7.40, m, 5H, Bn-*H*; 5.07, s, 2H, Ar-CH_2-O-. **^{13}C NMR (75 MHz, $CDCl_3$) δ:** 151.8, 150.3, 136.0, 133.2, 128.9, 128.5, 128.0, 127.7, 121.0, 107.5, 71.1. **MS (EI):** *m*/*z* 245 $[M]^+$. **MP:** 68.4-68.7°C (Literature[45]: 67-70°C).

Synthesis of 1,2-bis(4-benzyloxy-2-nitrophenoxy)ethane – 16:

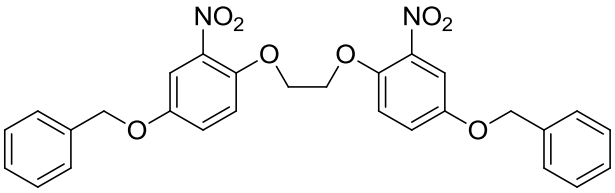

Adapted from Crossley *et al.*[46] Compound **15** (5.00 g, 20.4 mmol) was dissolved in DMF (10 mL), K_2CO_3 (3.39 g, 24.5 mmol) was added and the reaction stirred at room temperature. 1,2-Dichloroethane (803 µL, 10.2 mmol) was added and the reaction mixture was heated at 120°C for 1 d in a sealed pressure vessel. Once the reaction was allowed to cool, water (20 mL) was added and the mixture allowed to stir for a further 30 min. The mixture was acidified with 2 M HCl solution, Et_2O (20 mL) was added to dissolve any starting material, and the mixture was filtered to collect precipitated product, which was further washed with Et_2O and dried over a water aspirator to give **16** (5.27 g, quant.), as a yellow-beige powder.

^{1}H NMR (300 MHz, $CDCl_3$) δ: 7.45, m, 2H, Ar-*H*; 7.42-7.34, m, 10H, Bn-*H*; 7.18, m, 4H, Ar-*H*; 5.07, s, 4H, Ar-CH_2-O-; 4.44, s, 4H, -O-CH_2CH_2-O-. **^{13}C NMR (75 MHz, $CDCl_3$) δ:** 153.0, 146.6, 140.7, 136.1, 128.9, 128.5, 127.7, 121.8, 118.5, 111.3, 71.1, 70.2. **MS (ESI, +ve):** *m*/*z* 538.9 $[M+Na]^+$. **MP:** 183.0-184.1°C (Literature[46]: 184-185°C).

Synthesis of 1,2-bis(4-benzyloxy-2-aminophenoxy)ethane – 17:

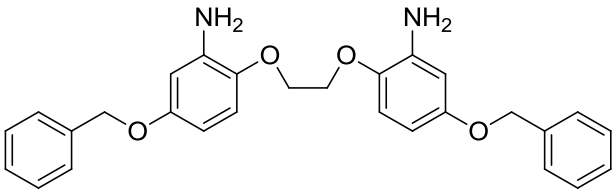

Dinitro compound **16** (5.00 g, 9.68 mmol) was dissolved in glacial AcOH (200 mL) and stirred for 10 min. Zinc powder (6.33 g, 96.8 mmol) was added slowly to the solution and allowed to stir overnight. The reaction mixture turned from yellow to deep red during this time. On completion, cold water was added to the solution and the resulting grey precipitate was collected. The precipitate was dissolved in CH_2Cl_2, dried ($MgSO_4$) and filtered to remove the

drying agent and remaining zinc powder. The solvent was removed under reduced pressure to give **17** (4.38 g, 99%), as a solid that darkened quickly in light.

^{1}H NMR (300 MHz, $CDCl_3$) δ: 7.45-7.18, m, 10H, Bn-*H*; 6.76/6.39/6.30, ABX system, $^3J_{AX}$ 8.7 Hz, $^4J_{AB}$ 2.9 Hz, 6H, Ar-*H*; 4.98, s, 4H, Ar-CH_2-O-; 4.70, br s, 4H, -NH_2; 4.26, 4H, s, -O-CH_2CH_2-O-. **^{13}C NMR (75 MHz, $CDCl_3$) δ:** 154.5, 141.1, 138.2, 137.6, 128.7, 128.0, 127.6, 114.5, 103.8, 103.4, 70.6, 68.9. **MS (ESI, +ve):** *m/z* 457.1 $[M+H]^+$. **MP:** 160.4-161.0°C (decomp.) (Literature[46]: 160-161°C (decomp.)).

Synthesis of tetraethyl 1,2-bis(*o*-amino-*p*-benzyloxyphenoxy)ethane-*N*,*N*,*N*',*N*'-tetraacetate – 18:

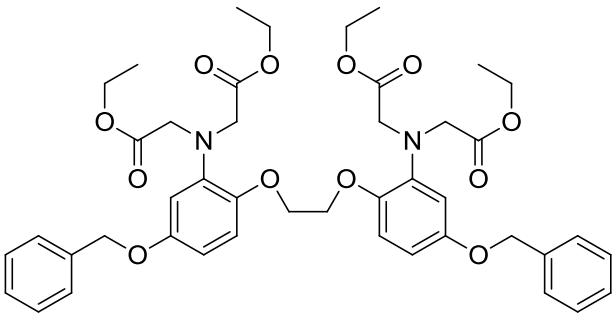

Bis-aniline **17** (600 mg, 1.31 mmol), DIPEA (2.52 mL, 14.5 mmol) and NaI (98 mg, 0.65 mmol) were stirred in toluene (20 mL) and ethyl bromoacetate (1.50 mL, 13.5 mmol) was added slowly. The reaction mixture was refluxed at 120°C for 2 d. After cooling, toluene (50 mL) was added, and the organic phase was washed with water (2 × 50 mL). The solvent was removed by rotary evaporation to give crude **18** (1.03 g) as a brown oil. The product was purified by running through a silica plug (40% EtOAc/hexane) to remove baseline material and give pure tetraethyl ester **18** (777 mg, 74%) as a light brown solid.

^{1}H NMR (400 MHz, $CDCl_3$) δ: 7.34, m, 10H, Bn-*H*; 6.77/6.50/6.47, ABX system, $^3J_{AX}$ 8.7 Hz, $^4J_{AB}$ 2.9 Hz, 6H, Ar-*H*; 4.97, s, 4H, Ar-CH_2-O-; 4.18, s, 4H, -O-CH_2CH_2-O-; 4.14, s, 8H, -N-CH_2-CO_2-; 4.07, q, ^3J 7.2 Hz, 8H, -O-C$H_2$$CH_3$; 1.17, t, ^3J 7.2 Hz, 12H, -O-CH_2CH_3. **^{13}C NMR (100 MHz, $CDCl_3$) δ:** 171.4 (*C*=O), 153.8, 144.9, 140.7, 137.4, 128.5, 127.9, 127.5, 115.0, 107.4, 106.7, 70.5, 68.2, 60.8, 53.6, 14.2. **MS (ESI, +ve):** *m/z* 823.2 $[M+Na]^+$. **HRMS (ESI, +ve):** *m/z* 801.3605 $[M+H]^+$, $C_{44}H_{52}N_2O_{12}$ required *m/z* 801.3593; *m/z* 823.3427 $[M+Na]^+$, $C_{44}H_{52}N_2O_{12}$ required *m/z* 823.3412. **MP:** 96.0-96.8°C.

Synthesis of tetraethyl 1,2-bis(*o*-amino-*p*-hydroxyphenoxy)ethane-*N*,*N*,*N*',*N*'-tetraacetate (dihydroxy-BAPTA tetraethyl ester) – 19:

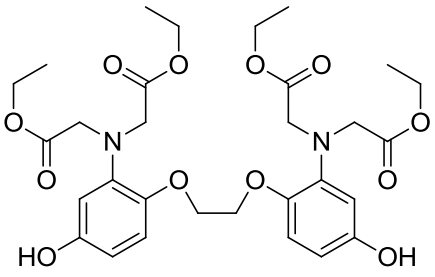

Benzyl-protected compound **18** (1.60 g, 2.00 mmol) was dissolved in THF (15 mL) and a suspension of 5% Pd/C (164 mg) in 3 mL of THF was added. The reaction was purged with nitrogen, and a hydrogen balloon was applied. The reaction was monitored by TLC. On completion, the reaction mixture was filtered through celite, and the product washed through with EtOAc. The solvent was removed *in vacuo* to give a brown oil (1.81 g). The crude oil was purified by column chromatography (50% EtOAc/hexane to 100% EtOAc), yielding pure **19** (932 mg, 75%), as a pale brown powder. Single crystals of **19**$(H_2O)_{1.5}$ suitable for X-ray crystallography were grown by vapor diffusion from methanol, using hexane as the precipitant.

^{1}H NMR (400 MHz, $CDCl_3$) δ: 6.61/6.35/6.27, ABX system, $^3J_{AX}$ 8.6 Hz, $^4J_{AB}$ 2.8 Hz, 6H, Ar-*H*; 5.43, s, 2H, Ar-O*H*; 4.13, s, 8H, -N-CH_2-CO_2-; 4.12, s, 4H, -O-CH_2CH_2-O-; 4.09, q, ^3J 7.1 Hz, 8H, -C$H_2$$CH_3$; 1.18, t, ^3J 7.1 Hz, 12H, -CH_2CH_3. **^{13}C NMR (75 MHz, $CDCl_3$) δ:** 171.8 (*C*=O), 150.9, 144.2, 140.6, 115.9, 108.1, 106.9, 68.2, 61.0, 53.8, 14.2. **MS (ESI, +ve):** *m/z* 621.3 $[M+H]^+$, 643.1 $[M+Na]^+$. **HRMS (ESI, +ve):** *m/z* 621.2652 $[M+H]^+$, $C_{30}H_{40}N_2O_{12}$ required *m/z* 621.2654; *m/z* 643.2474 $[M+Na]^+$, $C_{30}H_{40}N_2O_{12}$ required *m/z* 643.2473. **MP:** 94.4-95.0°C. **X-ray crystal data:** For **19**$(H_2O)_{1.5}$: $C_{30}H_{43}N_2O_{13.5}$, M = 647.66, colourless prism, 0.25 × 0.10 × 0.10 mm^3, triclinic, space group P -1, a = 10.1025(3), b = 11.8819(4), c = 15.3910(5) Å, α = 103.639(2)°, β = 101.782(2)°, γ = 108.034(2)°, V = 1628.57(9) Å^3, Z = 2, D_c = 1.321 g/cm^3, F_{000} = 690, T = 123(2) K, $2\theta_{max}$ = 50.0°, 20090 reflections collected, 5598 unique (R_{int} = 0.0304). Final *GoF* = 1.070, *R1* = 0.0566, *wR2* = 0.1159, *R* indices based on 4681 reflections with I>2σ(I) (refinement on F^2), 487 parameters, 9 restraints. Lp and absorption corrections applied, μ = 0.104 mm^{-1}.

Synthesis of 1,2-bis(*o*-amino-*p*-hydroxyphenoxy)ethane-*N*,*N*,*N*',*N*'-tetraacetic acid (dihydroxy-BAPTA acid) – 20:

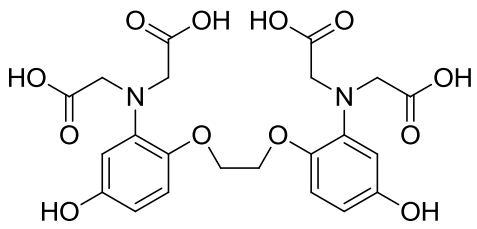

Ester **19** (100 mg, 0.161 mmol) was dissolved in hot MeOH (2 mL) and the solution was treated with a concentrated solution of KOH (72 mg, 1.28 mmol) in H_2O (0.5 mL). The reaction was heated at 60°C for 1 h, then the solvent was removed by rotary evaporation. The residue was dissolved in H_2O (10 mL) and the solution was acidified with concentrated HCl to pH 2, forming a brown precipitate. The product was extracted with EtOAc (100 mL), dried over $MgSO_4$, filtered and the solvent removed *in vacuo* to give **20** (45 mg, 55%), as a pale brown powder.

^{1}H NMR (400 MHz, $CDCl_3$) δ: 12.39, br s, 4H, -CO_2H; 8.84, br s, 2H, Ar-O*H*; 6.75, d, ^3J 8.3 Hz, 2H, Ar-*H*; 6.20, m, 4H, Ar-*H*; 4.06, s, 4H, -O-CH_2CH_2-O-; 4.02, s, 8H, -N-CH_2-CO_2-. **^{13}C NMR (100 MHz, $CDCl_3$) δ:** 172.4 (*C*=O), 152.1, 142.3, 140.5, 117.3, 106.8, 105.7, 68.7, 53.4. **MS (ESI, -ve):** *m*/*z* 507.0 [M-H]$^-$. **MP:** 162.8-164.2°C (decomp.).

Synthesis of diPEG-BAPTA tetraethyl ester – 21:

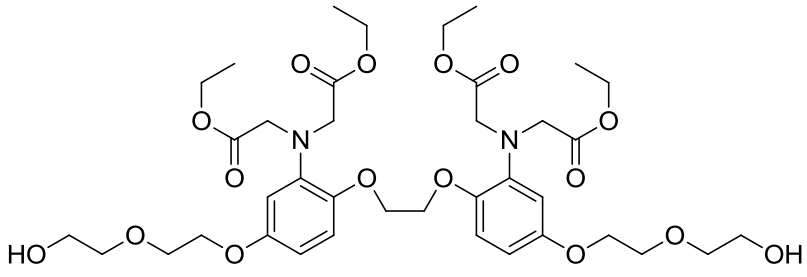

Compound **19** (201 mg, 0.324 mmol) was dissolved in DMF (2 mL), and K_2CO_3 (180 mg, 1.30 mmol) and 2-(2-chloroethoxy)ethanol (342 µL, 3.24 mmol) were added. The reaction mixture was heated to 110°C for 7 d and monitored by TLC. When all starting material had appeared to be consumed, the product was extracted with EtOAc and washed with H_2O and the solvent was removed to give a brown oil (256 mg). Purification by column chromatography (2% to 5% MeOH/EtOAc) afforded the polyether **21** (78 mg, 30%), as an off-white solid.

^{1}H NMR (400 MHz, $CDCl_3$) δ: 6.77/6.48/6.42, ABX system, $^3J_{AX}$ 8.7 Hz, $^4J_{AB}$ 2.9 Hz, 6H, Ar-*H*; 4.19, s, 4H, Ar-O-CH_2CH_2-O-Ar; 4.15, s, 8H, -N-CH_2-CO_2-; 4.09, q, ^3J 7.2 Hz, 8H, -C$H_2$$CH_3$; 4.05, t, ^3J 4.9 Hz,

4H, Ar-O-C*H*$_2$CH$_2$-O-; 3.81, t, ^3J 4.7 Hz, 4H, -O-C*H*$_2$CH$_2$-O-; 3.75, m, 4H, -O-C*H*$_2$CH$_2$-O-; 3.65, t, ^3J 4.5 Hz, 4H, -O-C*H*$_2$CH$_2$-O-; 2.20, br s, 2H, -O*H*; 1.18, t, ^3J 7.1 Hz, 12H, -CH$_2$C*H*$_3$. **^{13}C NMR (75 MHz, CDCl$_3$) δ:** 171.4 (*C*=O), 153.7, 145.1, 140.7, 115.3, 107.5, 106.7, 72.7, 69.9, 68.3, 68.1, 61.9, 60.9, 53.7, 14.2. **MS (ESI, +ve):** *m*/*z* 819.0 [M+Na]$^+$. **HRMS (ESI, +ve):** *m*/*z* 797.3694 [M+H]$^+$, $C_{38}H_{56}N_2O_{16}$ required *m*/*z* 797.3703; *m*/*z* 819.3517 [M+Na]$^+$, $C_{38}H_{56}N_2O_{16}$ required *m*/*z* 819.3522. **MP:** 56.2-57.6°C.

Synthesis of 1,2,3,4,6-penta-*O*-acetyl-β-D-glucose – 22:

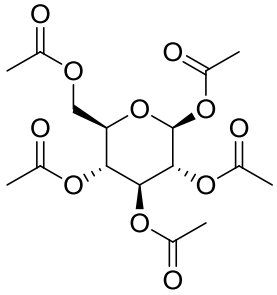

From Vogel.[53] α-D-Glucose (1.85 g, 10.3 mmol) and anhydrous NaOAc (1.50 g, 18.3 mmol) were ground together with a mortar and pestle and placed in a round bottom flask. Acetic anhydride (20 mL) was added and the reaction mixture was stirred and heated at reflux for 7 h, before pouring in 100 mL of crushed ice. The product was extracted with EtOAc (2 × 100 mL), washed with H_2O (2 × 100 mL) and saturated $NaHCO_3$ solution (200 mL), and the organic phase was dried over $MgSO_4$, filtered and concentrated *in vacuo* to give a cream precipitate. The solid was filtered over a water aspirator and washed with H_2O. The cream powder (3.18 g) was recrystallised from hot MeOH, filtered and washed thoroughly with ice-cold MeOH to give **22** (2.04 g, 51%), as a white powder.

^{1}H NMR (400 MHz, CDCl$_3$) δ: 5.71, d, ^3J 8.3 Hz, 1H, -C*H*-; 5.25, t, ^3J 9.4 Hz, 1H, -C*H*-; 5.14, dd, ^3J 9.4, 2.2 Hz, 1H, -C*H*-; 5.11, dd, ^3J 9.5, 3.8 Hz, 1H, -C*H*-; 4.28, dd, ^2J 12.5 Hz, ^3J 4.5 Hz, 1H, -C*H*$_2$-; 4.11, dd, ^2J 12.5 Hz, ^3J 2.2 Hz, 1H, -C*H*$_2$-; 3.83, ddd, ^3J 10.0, 4.5, 2.2 Hz, 1H, -C*H*-; 2.11, s, 3H, -OCO-C*H*$_3$; 2.08, s, 3H, -OCO-C*H*$_3$; 2.03, s, 6H, -OCO-C*H*$_3$; 2.01, s, 3H, -OCO-C*H*$_3$. **^{13}C NMR (100 MHz, CDCl$_3$) δ:** 170.7 (*C*=O), 170.2 (*C*=O), 169.5 (*C*=O), 169.4 (*C*=O), 169.1 (*C*=O), 91.8, 73.0, 72.9, 70.4, 67.9, 61.6, 20.9, 20.8, 20.7. **MS (ESI, +ve):** *m*/*z* 413.1 [M+Na]$^+$. **MP:** 130.8-131.3°C (Literature[53]: 131-132°C).

Synthesis of acetate-protected diglucose-BAPTA tetraethyl ester – 23:

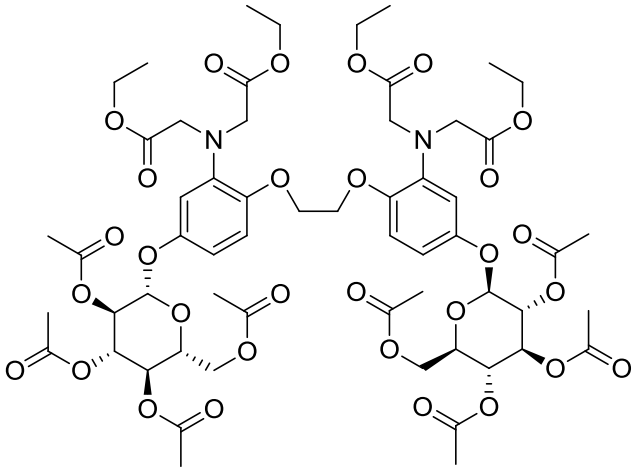

Adapted from Salvador *et al*.[54] Compound **19** (194 mg. 0.313 mmol) and glucose pentaacetate **22** (371 mg, 0.950 mmol) were dissolved in dry CH_2Cl_2 (8 mL) and 4 Å sieves were added. Boron trifluoride diethyl etherate (240 µL, 0.1.89 mmol) was added to the reaction mixture and the reaction was stirred at room temperature under Ar. When all starting material appeared by TLC (vanillin stain) to have been consumed after 6 d, more CH_2Cl_2 (100 mL) was added and the reaction mixture was filtered. The filtrate was washed with 1 M HCl solution (100 mL), saturated $NaHCO_3$ solution (100 mL) and H_2O (100 mL). The organic phase was dried over $MgSO_4$, filtered and the solvent removed *in vacuo* to give a thick brown oil (476 mg). Purification by column chromatography (2% MeOH/CH_2Cl_2 to 5% MeOH/CH_2Cl_2) yielded **23** (197 mg, 49%), as a thick, pale yellow oil.

^{1}H NMR (400 MHz, $CDCl_3$) δ: 6.74, m, 2H, Ar-*H*; 6.52, m, 4H, Ar-*H*; 5.3-5.0, m, 6H, -C*H*-; 4.92, d, ^3J 7.6 Hz, 2H, -C*H*-; 4.25, m, 4H, -CH_2-; 4.18, s, 4H, -O-CH_2CH_2-O-; 4.10, s, 8H, -N-CH_2-CO_2-; 4.06, q, ^3J 7.1 Hz, 8H, -C$H_2$$CH_3$; 3.79, ddd, ^3J 9.9, 4.7, 2.4 Hz, 2H, -C*H*-; 2.07, s, 6H, -OCO-CH_3; 2.05, s, 6H, -OCO-CH_3; 2.03, s, 6H, -OCO-CH_3; 2.01, s, 6H, -OCO-CH_3; 1.16, t, ^3J 7.1 Hz, 12H, -CH_2CH_3. **^{13}C NMR (100 MHz, $CDCl_3$) δ:** 171.3 (*C*=O), 170.8 (*C*=O), 170.4 (*C*=O), 169.5 (*C*=O), 169.4 (*C*=O), 151.9, 146.5, 140.6, 114.7, 109.8, 109.6, 100.3, 72.9, 72.1, 71.3, 68.3, 68.0, 62.1, 62.0, 60.9, 20.9, 20.8, 20.7, 14.2. **MS (ESI, +ve):** *m/z* 1281.2 $[M+H]^+$, 1303.2 $[M+Na]^+$. **HRMS (ESI, +ve):** *m/z* 1281.4541 $[M+H]^+$, $C_{58}H_{76}N_2O_{30}$ required *m/z* 1281.4556; *m/z* 1303.4371 $[M+Na]^+$, $C_{58}H_{76}N_2O_{30}$ required *m/z* 1303.4375.

2.9 References

1. Shi, P.; Gal, J.; Kwinter, D. M.; Liu, X.; Zhu, H., *Biochim. Biophys. Acta* **2010**, *1802*, 45-51.
2. Mattson, M. P., *Aging Cell* **2007**, *6*, 337-350.
3. Carriedo, S. G.; Yin, H. Z.; Weiss, J. H., *J. Neurosci.* **1996**, *16*, 4069-4079.

4. Rothstein, J. D.; Jin, L.; Dykes-Hoberg, M.; Kuncl, R. W., *Proc. Natl. Acad. Sci. USA* **1993**, *90*, 6591-6595.

5. Rothstein, J. D.; Dykes-Hoberg, M.; Pardo, C. A.; Bristol, L. A.; Jin, L.; Kuncl, R. W.; Kanai, Y.; Hediger, M. A.; Wang, Y.; Schielke, J. P.; Welty, D. F., *Neuron* **1996**, *16*, 675-686.

6. Cozzolino, M.; Ferri, A.; Carrì, M. T., *Antioxid. Redox Sign.* **2008**, *10*, 405-444.

7. Bendotti, C.; Carrì, M. T., *Trends Mol. Med.* **2004**, *10*, 393-400.

8. Greger, I. H.; Ziff, E. B.; Penn, A. C., *Trends Neurosci.* **2007**, *30*, 407-416.

9. Mayer, M. L., *Curr. Opin. Neurobiol.* **2005**, *15*, 282-288.

10. Zhu, L. P.; Yu, X. D.; Ling, S.; Brown, R. A.; Kuo, T. H., *Cell Calcium* **2000**, *28*, 107-117.

11. Lafon-Cazal, M.; Pietri, S.; Culcasi, M.; Bockaert, J., *Nature* **1993**, *364*, 535-537.

12. Kruman, I. I.; Pedersen, W. A.; Springer, J. E.; Mattson, M. P., *Exp. Neurol.* **1999**, *160*, 28-39.

13. Stout, A. K.; Raphael, H. M.; Kanterewicz, B. I.; Klann, E.; Reynolds, I. J., *Nat. Neurosci.* **1998**, *1*, 366-373.

14. Reynolds, I.; Hastings, T., *J. Neurosci.* **1995**, *15*, 3318-3327.

15. Dugan, L.; Sensi, S.; Canzoniero, L.; Handran, S.; Rothman, S.; Lin, T.; Goldberg, M.; Choi, D., *J. Neurosci.* **1995**, *15*, 6377-6388.

16. Rattray, M.; Bendotti, C., *Exp. Neurol.* **2006**, *201*, 15-23.

17. MacDermott, A. B.; Mayer, M. L.; Westbrook, G. L.; Smith, S. J.; Barker, J. L., *Nature* **1986**, *321*, 519-522.

18. Masliah, E.; Hansen, L.; Alford, M.; Deteresa, R.; Mallory, M., *Ann. Neurol.* **1996**, *40*, 759-766.

19. Dykens, J. A., *J. Neurochem.* **1994**, *63*, 584-591.

20. Schmid, R. W.; Reilley, C. N., *Anal. Chem.* **1957**, *29*, 264-268.

21. Tsien, R. Y., *Biochemistry* **1980**, *19*, 2396-2404.

22. Martell, A. E.; Smith, R. M. *Critical Stability Constants, Vol. 1*, Plenum Press: New York, 1974.

23. Harrison, S. M.; Bers, D. M., *Biochim. Biophys. Acta* **1987**, *925*, 133-143.

24. Unthank, J. K. Novel 'Dual-Action' Agents for the Treatment and Prevention of Neurodegenerative Disorders. PhD Thesis, Monash University, Melbourne, 2006.

25. Hardie, R. C., *Cell Calcium* **2005**, *38*, 547-556.

26. Amoroso, S.; D'Alessio, A.; Sirabella, R.; Di Renzo, G.; Annunziato, L., *J. Neurosci. Res.* **2002**, *68*, 454-462.

27. Yoshida, A.; Ueda, T.; Takauji, R.; Liu, Y. P.; Fukushima, T.; Inuzuka, M.; Nakamura, T., *Biochem. Biophys. Res. Commun.* **1993**, *196*, 927-934.

28. Thaler, C. D.; Haimo, L. T., *J. Cell Biol.* **1990**, *111*, 1939-1948.

29. Tonkikh, A.; Janus, C.; El-Beheiry, H.; Pennefather, P. S.; Samoilova, M.; McDonald, P.; Ouanounou, A.; Carlen, P. L., *Exp. Neurol.* **2006**, *197*, 291-300.

30. Tymianski, M.; Sattler, R.; Bernstein, G.; Jones, O. T., *Cell Calcium* **1997**, *22*, 111-120.

31. Wie, M. B.; Koh, J. Y.; Won, M. H.; Lee, J. C.; Shin, T. K.; Moon, C. J.; Ha, H. J.; Park, S. M.; Kim, H. C., *Prog. Neuropsychopharmacol. Biol. Psychiatry* **2001**, *25*, 1641-1659.

32. Tymianski, M.; Wallace, M. C.; Spigelman, I.; Uno, M.; Carlen, P. L.; Tator, C. H.; Charlton, M. P., *Neuron* **1993**, *11*, 221-235.

33. Tsien, R. Y., *Nature* **1981**, *290*, 527-528.

34. Macfarlane, K. J. Small Molecules & Peptide Nucleic Acids for the Treatment and Prevention of Neurodegeneration. PhD Thesis, Monash University, Melbourne, 2004.

35. Cheema, S. S.; Langford, S.; Cheung, N. S.; Beart, P. M.; Macfarlane, K. J.; Mulcair, M. Agents and Methods for the Treatment of Disorders Associated with Oxidative Stress. U.S. Patent Application US2005/0288359 A1, December 29, 2005.

36. Crans, D.; Clark, T.; von Ragué Schleyer, P., *Tetrahedron Lett.* **1980**, *21*, 3681-3684.

37. Viehe, H. G.; Janousek, Z.; Merenyi, R.; Stella, L., *Acc. Chem. Res.* **1985**, *18*, 148-154.

38. Gaudiano, G.; Koch, T. H., *Chem. Res. Toxicol.* **1991**, *4*, 2-16.

39. Turner, B. J. Toxic Mechanisms and Therapeutic Strategies in a Transgenic Mouse Model of Human Familial Amyotrophic Lateral Sclerosis. PhD Thesis, Howard Florey Institute of Experimental Physiology & Medicine, Melbourne, 2005.

40. Pethig, R.; Kuhn, M.; Payne, R.; Adler, E.; Chen, T. H.; Jaffe, L. F., *Cell Calcium* **1989**, *10*, 491-498.

41. London, R. E.; Rhee, C. K.; Murphy, E.; Gabel, S.; Levy, L. A., *Am. J. Physiol. Cell Physiol.* **1994**, *266*, C1313-C1322.

42. Katerinopoulos, H. E.; Iatridou, H.; Foukaraki, E.; Malekzadeh, M. N.; Kuhn, M. A.; Haugland, R. P. Benzazolylcoumarin-Based Ion Indicators. U.S. Patent 5,501,980, March 26, 1996.

43. Gressel, J.; Michaeli, D.; Kampel, V.; Amsellem, Z.; Warshawsky, A., *J. Agric. Food Chem.* **2002**, *50*, 6353-6360.

44. Gee, K. R.; Archer, E. A.; Lapham, L. A.; Leonard, M. E.; Zhou, Z.-L.; Bingham, J.; Diwu, Z., *Bioorg. Med. Chem. Lett.* **2000**, *10*, 1515-1518.

45. Grynkiewicz, G.; Poenie, M.; Tsien, R. Y., *J. Biol. Chem.* **1985**, *260*, 3440-3450.

46. Crossley, R.; Goolamali, Z.; Sammes, P. G., *J. Chem. Soc. Perkin Trans. 2* **1994**, 1615-1623.

47. Vorndran, C.; Minta, A.; Poenie, M., *Biophys. J.* **1995**, *69*, 2112-2124.

48. Robitaille, P.-M. L.; Jiang, Z., *Biochemistry* **1992**, *31*, 12585-12591.

49. Polt, R.; Porreca, F.; Szabò, L. Z.; Bilsky, E. J.; Davis, P.; Abbruscato, T. J.; Davis, T. P.; Harvath, R.; Yamamura, H. I.; Hruby, V. J., *Proc. Natl. Acad. Sci. USA* **1994**, *91*, 7114-7118.

50. Bell, G. I.; Burant, C. F.; Takeda, J.; Gould, G. W., *J. Biol. Chem.* **1993**, *268*, 19161-19164.

51. Pardridge, W. M.; Boado, R. J.; Farrell, C. R., *J. Biol. Chem.* **1990**, *265*, 18035-18040.

52. Fernández, C.; Nieto, O.; Fontenla, J. A.; Rivas, E.; Ceballos, M. L. d.; Fernández-Mayoralas, A., *Org. Biomol. Chem.* **2003**, *1*, 767-771.

53. Vogel, A. I. *Vogel's Textbook of Practical Organic Chemistry*, 5th ed.; Longman Singapore Publishers: Singapore, 1989.

54. Salvador, L. A.; Elofsson, M.; Kihlberg, J., *Tetrahedron* **1995**, *51*, 5643-5656.

55. Toshima, K.; Tatsuta, K., *Chem. Rev.* **1993**, *93*, 1503-1531.

56. Liu, H.-M.; Yan, X.; Li, W.; Huang, C., *Carbohyd. Res.* **2002**, *337*, 1763-1767.

57. Liégeois, C.; Lermusieau, G.; Collin, S., *J. Agric. Food Chem.* **2000**, *48*, 1129-1134.

58. Liu, Z.-Q., *Chem. Rev.* **2010**, *110*, 5675-5691.

59. Quideau, S.; Deffieux, D.; Douat-Casassus, C.; Pouységu, L., *Angew. Chem. Int. Ed.* **2011**, *50*, 586-621.

60. Obrenovich, M. E.; Li, Y.; Parvathaneni, K.; Yendluri, B. B.; Palacios, H. H.; Leszek, J.; Aliev, G., *CNS Neurol. Disord. Drug Targets* **2011**, *10*, 192-207.

61. Di Domenico, F.; Foppoli, C.; Coccia, R.; Perluigi, M., *Biochim. Biophys. Acta* **2012**, *1822*, 737-747.

62. Ignat, I.; Volf, I.; Popa, V. I., *Food Chem.* **2011**, *126*, 1821-1835.

63. Sheldrick, G. M., *Acta Crystallogr.* **1990**, *A46*, 467-473.

64. Sheldrick, G. M. *SHELXL-97, Computer Program for Crystal Sructure Refinement*, University of Göttingen: Göttingen, Germany, 1997.

65. Barbour, L. J., *J. Supramol. Chem.* **2001**, *1*, 189-191.

66. Gunduz, T.; Gunduz, N.; Kilic, Z.; Kilic, E.; Kenar, A., *Analyst* **1988**, *113*, 965-968.

CHAPTER THREE

CHROMANOL SYNTHETIC METHODS

3.1 Introduction

While it has been established that BAPTA acts as an antioxidant in both the presence and absence of Ca^{2+} ions,[1,2] it may be hypothesised that the installation of a chromanol core based on the structure of vitamin E could further improve antioxidant function and therefore act as a more promising candidate for targeting factors contributing to oxidative stress and neurodegeneration. In order to incorporate both the antioxidant chromanol core of vitamin E and the Ca^{2+}-binding functionality of BAPTA into one compound as planned, a series of 2,5,7-trimethylchromanol compounds incorporating functionalisation at the C2 and C8 positions was proposed, as shown generally in Figure 3.1. For our purposes, R^1 and R^2 in the figure below could be varied to incorporate Ca^{2+}-binding functionality mimicking BAPTA.

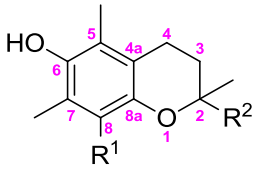

Figure 3.1 General structure indicating C2/C8 functionalisation of a chromanol.

If a convergent approach towards the synthesis of compounds of this class could be applied, it would allow installation of varied functional groups at the time of chroman formation, thereby allowing a number of targets to be synthesised from a common intermediate and negating yield problems associated with lengthy synthetic routes and functional group transformations.

There are a large number of chroman synthetic techniques currently utilised in the literature, particularly for synthesis of vitamin E.[3-17] One such method employs the reaction of hydroquinone with γ-methyl-γ-vinylbutyrolactone (**25**) in the presence of boron trifluoride diethyl etherate or zinc chloride to give a carboxylic acid functionalised chroman (Method A in Scheme 3.1). This method has been used to synthesise α-CEHC (R^1 ,R^2, $R^3 = CH_3$) and LLU-α (R^1 = H; R^2, $R^3 = CH_3$), believed to be metabolites of α- and γ-tocopherol, respectively.[3-6] While the starting lactone **25** is readily made from ethyl levulinate,[3] and the resulting acid can be further functionalised as esters or amides if desired, this synthesis has limitations due to the inability to vary the chain off the C2 position to any large extent.

A similar Lewis acid-promoted synthesis for chroman formation involves the reaction between trimethylhydroquinone and 3,6-dihydro-4-methyl-2H-pyran (**26**) *via* Friedel-Crafts alkylation (Method B).[7] The alkene used in this reaction can be synthesised in two steps from tetrahydropyran-4-one.[18] Once again, this synthetic route does not allow for much variability of

C2 functionalisation, although it could provide an efficient and convergent synthesis of the target synthesised in Chapter Four.

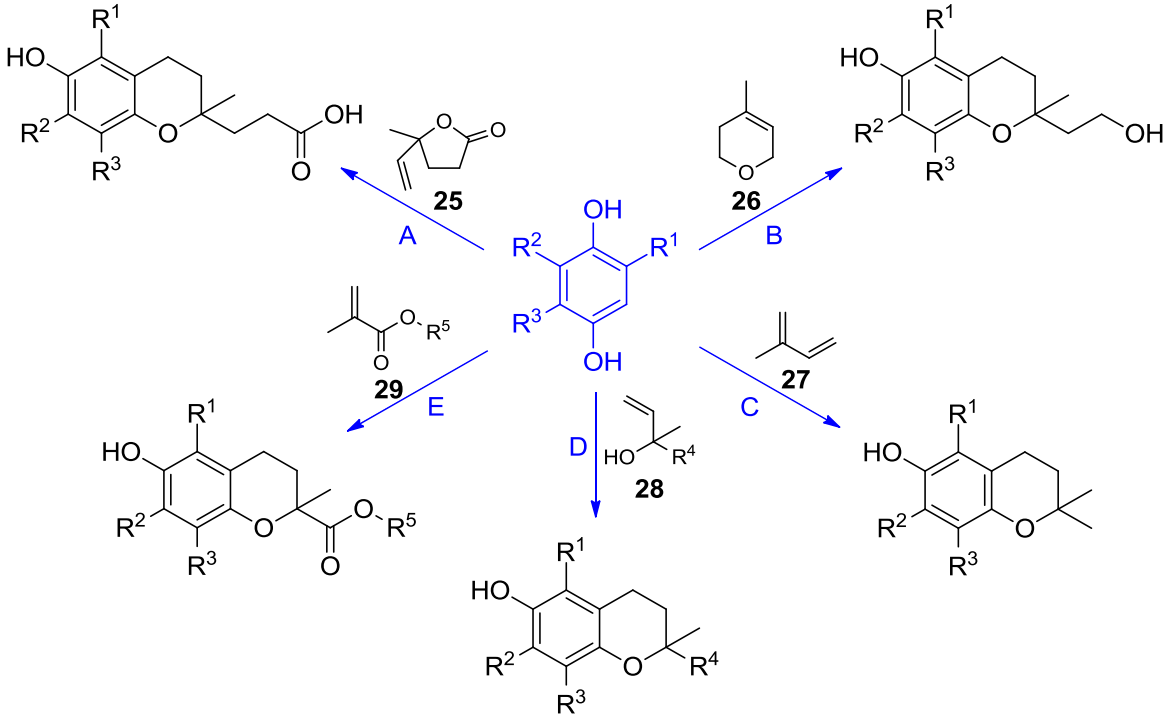

Scheme 3.1[3-17] Synthetic techniques towards chroman formation, showing methods A to E.

Perhaps a more restrictive method of chroman synthesis involves the alkylation of a hydroquinone with isoprene (**27**), often catalysed by Amberlyst 15, to yield a series of 2,2-dimethylchromans (Method C).[8-10] While the synthesis itself is straight-forward, it allows little by way of further functionalisation at the C2 position, and therefore is not a useful synthesis for the purposes of this thesis.

A more promising process for chroman synthesis involves the condensation reaction of a hydroquinone with a variety of functionalised allylic alcohol compounds (**28**), as shown in Method D in Scheme 3.1.[11-14] While this method is convergent and allows installation of a number of R-groups at the C2 position – making it a popular method for the production of vitamin E and its derivatives – synthesis of the alcohol precursors can be difficult and lengthy.[14,19]

Reaction of trimethylhydroquinone (R^1, R^2, $R^3 = CH_3$) with a methacrylate ester (**29**) and paraformaldehyde in the presence of organic acid and a secondary amine base produces a chroman with ester functionality at the C2 position (Method E),[15-17] in a protocol first established in a patent by Tamura in 2003.[17] The method appears promising for the introduction of various substituents at the C2 position, however no literature since that time has

described successful synthesis using other methallyl reactants. It is possible that the reaction relies on the electron-withdrawing properties of methyl methacrylate for its success.

Given that the methyl methacrylate reaction appeared promising, further examination of the literature revealed a patent by Fukumoto *et al.*,[20] which described the reaction of a phenol with paraformaldehyde and an alkene in the presence of organic acid and a secondary amine is used to produce a chroman compound, as shown generally in Scheme 3.2.

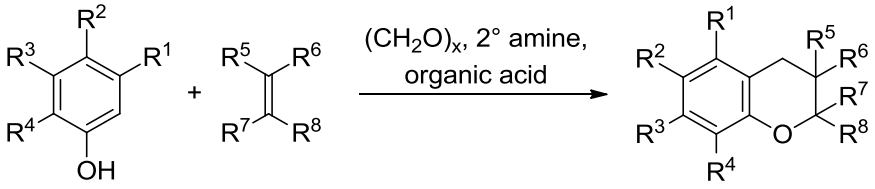

Scheme 3.2

Of particular interest to this project is a reaction involving acetate-protected trimethylhydroquinone with a methallyl reagent to give a protected chromanol, shown in Scheme 3.3. This method can be employed to synthesise vitamin E acetate, using 2,6,10,14-tetramethyl-1-pentadecene [R = $((CH_2)_3CHCH_3)_3CH_3$] as the alkene, however a wide range of other alkenes would be suitable, in order to create a variety of chroman compounds.

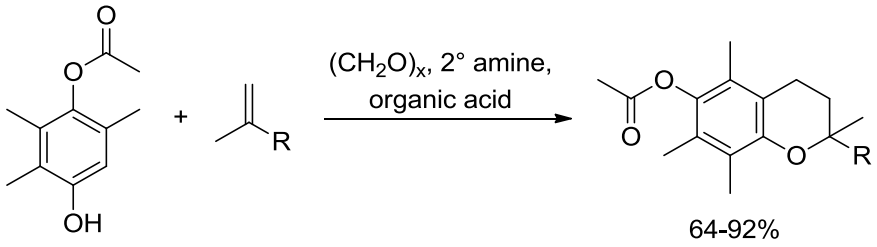

Scheme 3.3

The principle of this method is to use readily available, inexpensive starting materials to produce chromans in high yield and a simple manner. Variation of the synthetic method may allow for functionalisation directly off the chroman at the C8 position.

One of the key intermediates to the desired dual action targets is the alcohol **30** (Scheme 3.4). Subsequent alkylation of this alcohol and functionalisation at the C8 position would allow for the synthesis of new series of targets, shown generally as **31** and **32**. The following chapter describes efforts made towards exploring chroman synthesis.

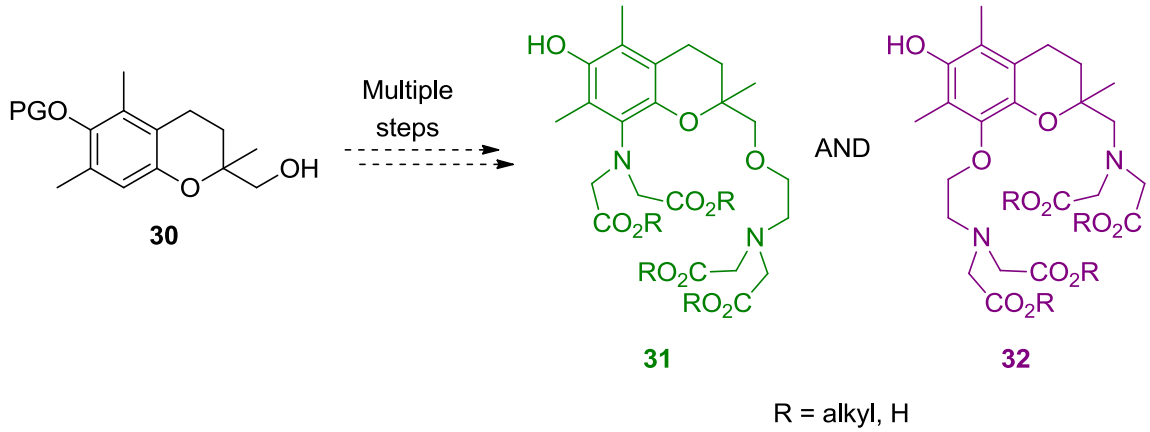

Scheme 3.4

3.2 Chromanol synthesis using methallyl reagents and paraformaldehyde

The synthesis of advanced chromans **35** and **36** from commercially available trimethylhydroquinone is shown in Scheme 3.5. The hydroquinone was first protected as the acetate to stop possible oxidation to the undesirable benzoquinone derivatives during alkylation. The monoprotected hydroquinone **34** was formed in high yield over two steps. Firstly, trimethylhydroquinone was diacetylated using acetic anhydride and Et_3N to give bis-acetate **33** in good (93%) yield. High resolution mass spectrometry (ESI) supported bis-acetylation of the hydroquinone, with peaks at *m/z* 237.1124 and *m/z* 259.0943, attributed to the $[M+H]^+$ and $[M+Na]^+$ ions, respectively. Nuclear magnetic resonance spectroscopy supported product formation, with new peaks at 2.33 and 2.30 ppm in the ^1H NMR spectrum, corresponding to the new different acetyl groups, and two distinct carbonyl signals in the ^{13}C NMR spectrum at 169.5 and 168.9 ppm respectively.

The diacetate **33** was regioselectively deprotected using sodium dithionite and potassium carbonate, adapted from a procedure by Snuparek *et al.*,[21] to give the monoacetate **34** in excellent yield (Scheme 3.5). Deprotection was supported by high resolution ESI mass spectrometry, with major peaks at *m/z* 195.1020 and *m/z* 217.0845, corresponding to the $[M+H]^+$ and $[M+Na]^+$ ions, as well as the loss of the one methyl singlet in the ^1H NMR spectrum and carbonyl and methyl carbon signals in the ^{13}C NMR spectrum. Reaction of **34** with 2-methyl-2-propen-1-ol, paraformaldehyde, dibutylamine and acetic acid in a pressure tube for two days gave the chroman **35** as a pale brown solid,[20] in quantitative yield with no purification necessary.

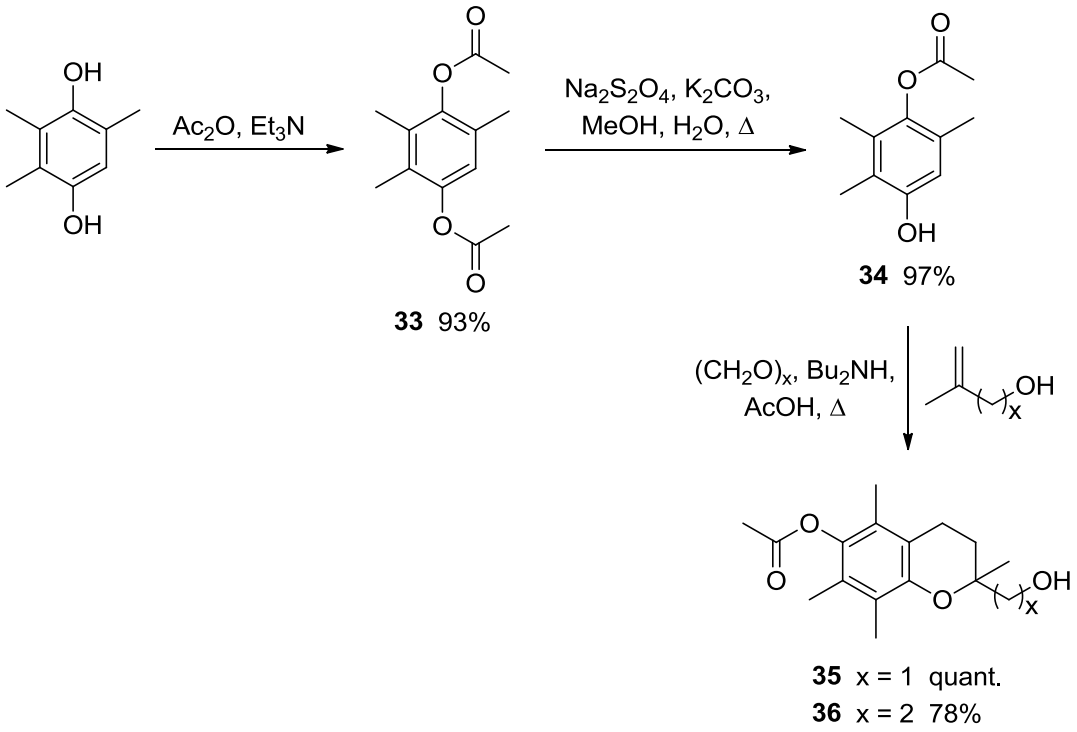

Scheme 3.5

Formation of **35** was supported by the presence of a major peak at *m*/*z* 301.1 by low resolution mass spectrometry (ESI), attributed to $[M+Na]^+$. The absence of a ^1H NMR resonance at 6.35 ppm as well as new peaks corresponding to newly installed pyran (2.65 and 2.02/1.73 ppm) and methyl protons (1.23 ppm) were also evidence of formation of the chroman structure, in addition to new distinctive AB system resonances at 3.65 and 3.58 ppm due to the methylene protons adjacent to the C2 carbon. Literature indicates that both the organic acid and base are required for formation of the expected product, a reaction hypothesised to progress *via* an intermediate.[20] The reaction is likely to proceed by *ortho*-directed electrophilic aromatic substitution, resulting in a high yield of pure product from the selective substitution of the aromatic proton *ortho* to the phenol, due to the presence of the three aromatic methyl groups.

Protected chromanol **36** was similarly formed from **34**, by replacing 2-methyl-2-propan-1-ol with 3-methyl-3-buten-1-ol under similar conditions (Scheme 3.5).[20] On completion, purification by column chromatography gave the desired product in 78% yield. Product formation was similarly supported by the disappearance of a resonance in the ^1H NMR spectrum at 6.35 ppm, as well as the presence of peaks attributable to newly installed protons. High resolution ESI mass spectrometry showed peaks at *m*/*z* 315.1570 and *m*/*z* 331.1302, corresponding to $[M+Na]^+$ and $[M+K]^+$, respectively.

While syntheses of chromans **35** and **36** were efficient, with yields after three steps of 90% and 70% respectively, in order for the target chromans to be formed (unsubstituted at C8), the previous syntheses were adapted using a dimethyl derivative of protected hydroquinone **34**. Firstly, hydroquinone **37** was synthesised *via* three different routes, each with varying degrees of success. Firstly, from commercially available 2,6-dimethylbenzoquinone, reduction using zinc powder and acetic acid yielded the hydroquinone in good yield on workup (Scheme 3.6).[22] Alternatively, 2,6-dimethylbenzoquinone was converted to the hydroquinone by reduction with sodium dithionite in 79% yield, after recrystallisation.[23] The reaction is easily monitored as it proceeds with a loss of the yellow colour of the quinone. Thirdly, the least successful attempt to synthesise 2,6-dimethylhydroquinone **37** was *via* the oxidation of 3,5-dimethylphenol using potassium persulfate in alkaline solution.[24] Although perhaps the cheapest synthesis, the reaction was low yielding, albeit with large quantities of starting material recovered, and required large volumes of solvent for extraction of both the recovered starting material and desired product. Proton NMR spectroscopy was used to support the formation of **37** in each case. In particular, a six-proton singlet at 2.06 ppm was seen, attributed to the two equivalent methyl groups. A two-proton signal at 6.32 ppm corresponded to the two equivalent aromatic protons, which differed from both the starting quinone and 3,5-dimethylphenol.

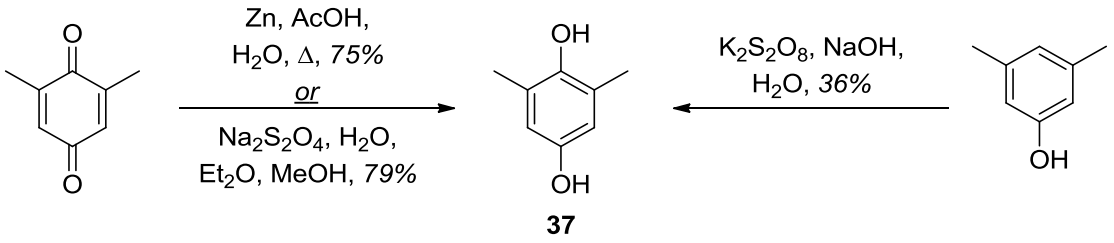

Scheme 3.6

From 2,6-dimethylhydroquinone **37**, the monoprotected dimethylhydroquinone **39** was formed in two steps (Scheme 3.7). 2,6-Dimethylhydroquinone **37** was acetylated using acetic anhydride and triethylamine to give bis-protected compound **38** in quantitative yield, then regioselective deprotection using sodium dithionite and potassium carbonate gave the monoacetate **39** in 98% yield.[21] Similar to the deprotection of **33** to form **34**, the deprotection of **38** to form **39** occurred in excellent yield and high regioselectivity, due to the steric hindrance of the aromatic methyl groups preventing removal of the second acetate group. Deprotection was supported by the loss of relevant signals in ^{1}H and ^{13}C NMR spectra, in particular the proton singlet resonance at 2.26 ppm and the carbonyl signal in the carbon spectrum at 168.8 ppm. Cleavage of only one ester was also supported by low resolution ESI mass spectrometry, with a positive ion peak at

m/z 202.9 and negative ion peak at m/z 178.9, attributable to the $[M+Na]^+$ and $[M-H]^-$ ions, respectively.

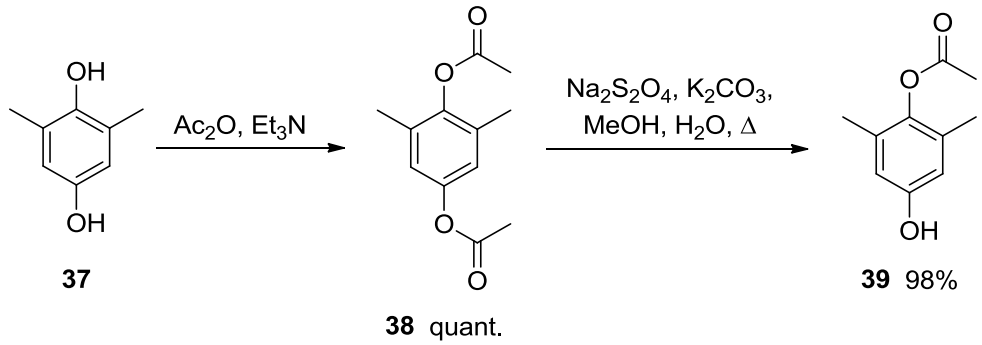

Scheme 3.7

X-ray crystallography of **39** (Figure 3.2) shows the intermolecular hydrogen bonding of the structure (O2 to H2 distance: 1.92 Å), which exists in an orthorhombic crystal system with space group $P2_12_12_1$. Crystals of **39** suitable for analysis were grown by slow evaporation from ethyl acetate.

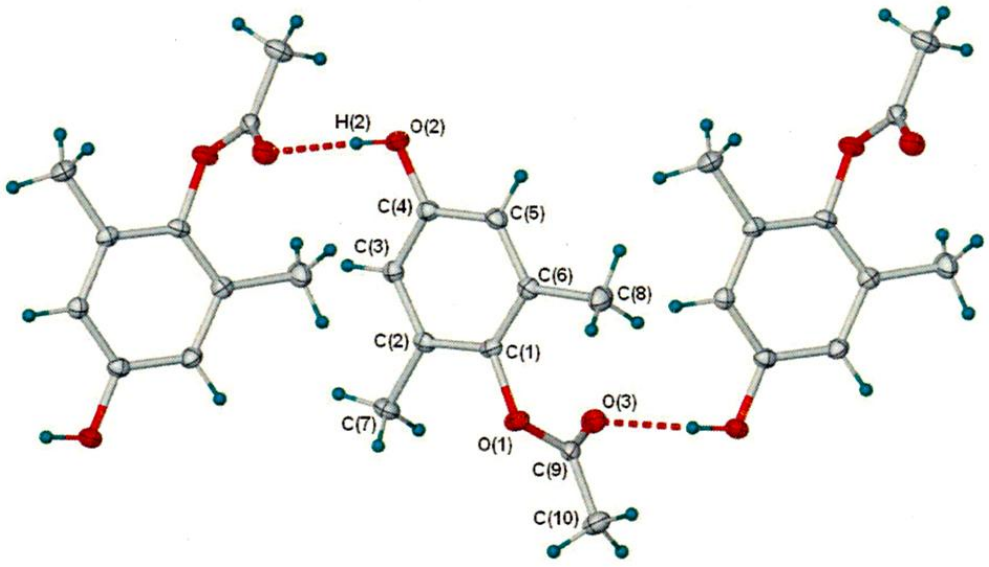

Figure 3.2 Molecular diagram of **39** as shown with 50% thermal ellipsoids and hydrogen atoms as spheres of arbitrary size. Only one molecule is unique, the remaining two are generated by symmetry. Individual molecules are associated by hydrogen bonds into a linear chain, which has a right handed helical structure. The non-centrosymmetric space group $P2_12_12_1$ implies only right handed helices are present, in the absence of a heavy atom, the choice of the direction of rotation was arbitrary. Friedel opposites were merged prior to the final refinement.

Following Fukumoto's synthesis, chromans **40** and **41** were synthesised (Scheme 3.8) from **39** in low yield (27% and 6%, respectively), after purification by column chromatography.[20] Repeated attempts and efforts towards optimisation could not improve on these yields, however TLC analysis and column chromatography indicated numerous byproducts, possibly resulting from second alkylation of the aromatic ring. This is not possible in compounds **35** and **36** where the methyl group at C8 acts to block this position from further attack. Formation of chroman **40** was supported by high resolution ESI mass spectrometry, with major peaks at m/z 265.1438 and m/z 287.1258, corresponding to the $[M+H]^+$ and $[M+Na]^+$ ions, respectively. In the ^1H NMR spectrum, pyran, methylene and methyl resonances of the expected product were observed, as well as a reduction in the integration and a downfield shift of the aromatic resonance from 6.44 to 6.55 ppm. In addition, whereas a single aromatic methyl resonance was observed for the starting material, representative of six protons, two aromatic methyl peaks were observed in the spectrum of the product, at 2.05 and 1.99 ppm, each integrating to three protons.

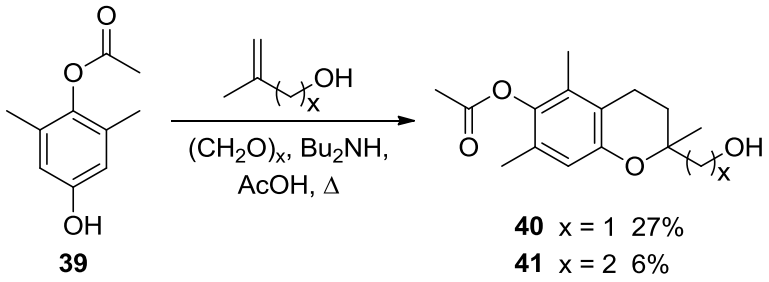

Scheme 3.8

Similar characteristic properties were observed as a means of identifying the production of chroman **41**, with an observed $[M+Na]^+$ peak at m/z 301.3 using positive low resolution ESI mass spectrometry, and an $[M-H]^-$ peak in the high resolution negative spectrum at m/z 277.1446. Formation of the pyran ring was supported by the presence of a triplet at 2.63 ppm and broad multiplet at around 1.7 to 2.0 ppm, whilst the reduction of integration and upfield shift of the aromatic proton peak from 6.44 to 6.52 ppm, as well as the presence of two separate aromatic methyl peaks at 2.07 and 2.00 ppm indicated alkylation of the aromatic ring. It is likely that the low yields of **40** and **41** were due to the probable second alkylation of the aromatic ring on addition of paraformaldehyde in each case, although no byproducts could be isolated and characterised.

Under the appropriate conditions, chromans may also be formed by the alkylation of unprotected hydroquinones. In a similar method to Fukumoto's synthesis, Tamura[17] described the synthesis of a series of chromans with ester functionalisation at the C2 position, derived

from the reaction of unprotected trimethylhydroquinone with paraformaldehyde and small chain methacrylate esters in the presence of organic acid (Scheme 3.9).

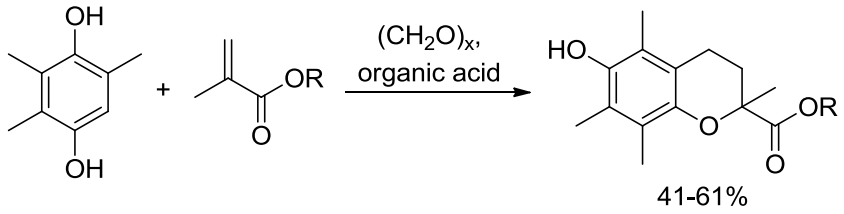

Scheme 3.9

With this method, the unprotected hydroquinone is used, since the absence of amine in the reaction prevents the oxidation of the hydroquinone to the corresponding benzoquinone. Some literature has reported the use of secondary amine bases, however resulting in lower yields of the chromanol product.[15-17] Conversely, reaction of the unprotected hydroquinone and a methacrylate ester in the absence of an organic acid significantly lowers the product yield.[17] The ability to use the unprotected hydroquinone may lie in the electron-withdrawing properties of the methacrylate esters, since no literature has described successful chroman synthesis using other methallyl reactants.

In an effort towards exploring this technique, reactions under the above conditions were carried out using both trimethylhydroquinone and 2,6-dimethylhydroquinone (**37**), with methyl methacrylate as the alkene and acetic acid as the organic acid catalyst (Scheme 3.10).[17]

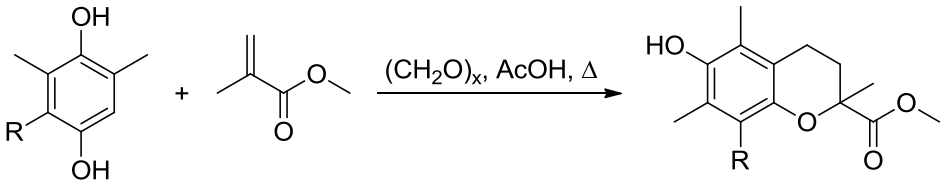

Scheme 3.10

While the trimethyl chroman **42** was obtained in moderate yield, the dimethyl product **43** was isolated in an unoptimised yield of 2%. Again, the resultant yield was attributed in part to the two aromatic positions at which alkylation could occur. Formation of chroman **42** was supported by the absence of any aromatic proton NMR signal of the starting material at around 6.5 ppm, and the presence of distinctive multiplets at 2.64/2.52 ppm and 2.42/1.87 ppm, attributed to the C4 and C3 protons, respectively, indicative of chroman formation. Mass

spectrometry (ESI) also supported chroman formation, with an $[M+H]^+$ peak at m/z 265.2. Chroman **42** is the acetate-protected ester of a well-known water soluble vitamin E derivative Trolox™ (shown in Figure 3.3).[25] Hydrolysis of the methyl ester would allow for an overall two-step synthesis of the commercially available compound, in moderate yield.

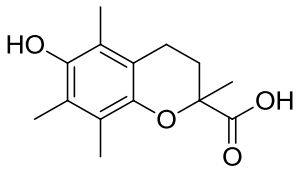

Figure 3.3 Trolox™

Characterisation of chroman **43** was similarly discerned, with a high resolution mass spectrum peak at m/z 251.1277, attributable to the $[M+H]^+$ ion, as well as ^{1}H NMR spectrum multiplets at 2.64/2.52 ppm and 2.42/1.87 ppm, characteristic of chroman formation. Also present in the ^{1}H NMR spectrum were two distinguishable inequivalent aromatic methyl peaks at 2.19 and 2.08 ppm, integrating to three protons each, compared to six equivalent protons in the hydroquinone starting material.

In a further effort towards determining the validity of this method in the functionalisation of a wide variety of chroman targets, a reaction under the above conditions (Scheme 3.10) was carried out this time using 3-methyl-3-buten-1-ol as the alkene (Scheme 3.11).[17] Although the reaction progressed until the hydroquinone was consumed, none of the expected product **44** was isolated or indicated by mass spectrometry or NMR spectroscopy. This supports the theory that a methacrylate ester alkene is required when using the unprotected hydroquinone.

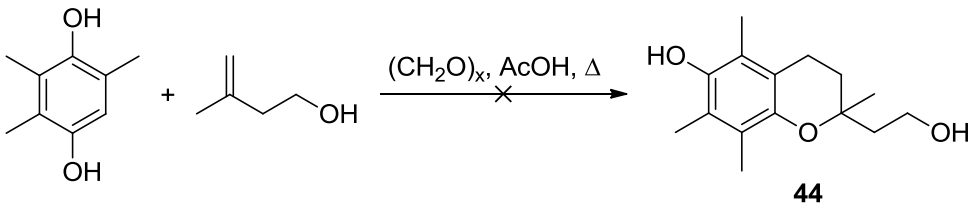

Scheme 3.11

Tamura's method, while potentially useful in the synthesis of Trolox™, did not present itself as a suitable pathway for the synthesis of a wider range of chromans with varied functionality.

3.3 Chromanol synthesis *via* a butoxymethyl intermediate

Given the low yields of mono-alkylation of protected hydroquinone **39**, a need to find a method of selective electrophilic aromatic alkylation at only one position on the aromatic ring was required. Further examination of the literature uncovered a simple two-step synthesis by Monoe *et al.*,[26] whereby reaction of a phenol compound (containing at least one unsubstituted ortho position), paraformaldehyde and an alcohol in the presence of an acid and a secondary amine gave an alkoxymethylphenol compound (shown generally as **45** in Scheme 3.12). Subsequent neat reaction of this compound with a carbon-carbon double bond containing reagent gave a series of chromans with selected functionality off the C2 position.

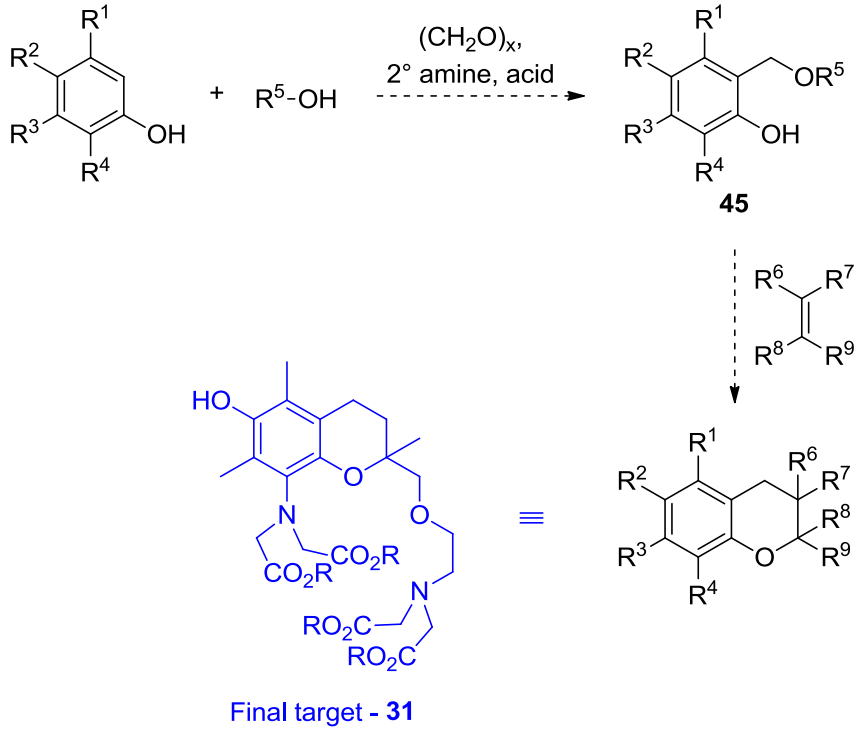

Scheme 3.12

Scheme 3.12 shows a methodology for producing a variety of chromans using the alkoxymethylphenol method. This method is stated in the literature to be inappropriate for alkene reagents that contain an unprotected alcohol within the molecule or an electron-withdrawing group bound to the carbon-carbon double bond.[26] It is anticipated that use of this synthetic method *via* alkoxymethylphenol **45** would allow for the desired functionalisation at the C2 position required for the subsequent synthesis of the generalised target **31**.

In terms of our synthetic scheme, C8 should be unsubstituted, however in order to explore this chemistry we began by using mono-protected trimethylhydroquinone (**34**), paraformaldehyde and *n*-butanol, in the presence of dibutylamine and acetic acid (Scheme 3.13).[26] The protected hydroquinone starting material was preferred given the tendency of hydroquinones to oxidise to corresponding benzoquinones under some conditions, while *n*-butanol was used as the alcohol in this case, since it has been found that butoxymethylphenol products were formed in higher yields than other alkoxy derivatives attempted.[26] The reagents were combined and heated overnight at 100°C, and produced the butoxy product **46** in quantitative yield upon workup. Product formation was supported in the ^{1}H NMR spectrum by the absence of the aromatic proton resonance at 6.35 ppm and presence of a benzylic peak at 4.73 ppm, integrating to two protons. Also present were triplets at 3.56 and 0.93 ppm and multiplets at 1.63 and 1.39 ppm, all attributable to the butoxy group. High resolution ESI mass spectrometry gave a peak at m/z 303.1569, representing the $[M+Na]^+$ ion.

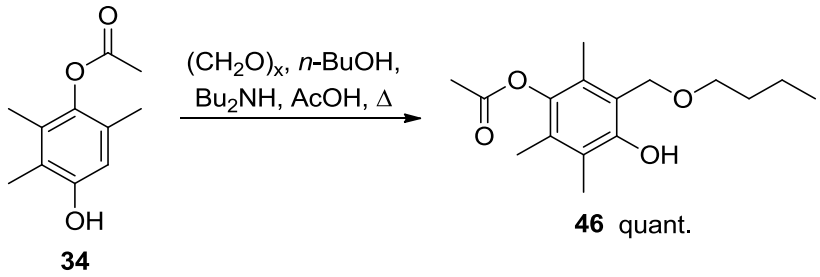

Scheme 3.13

The resulting product is valuable, due to the possible ability to form a wide range of 5,7,8-trimethyl chroman-2-ol compounds, depending on the alkene added in the next step. Since 3-methyl-3-buten-1-ol and 2-methyl-2-propen-1-ol contain unprotected alcohols, which were thought to lead to undesirable side reactions,[26] chroman formation using the acetate of 3-methyl-3-buten-1-ol with **46** was attempted. 3-Methylbut-3-enyl acetate **47** was synthesised by the slow addition of acetic anhydride to 3-methyl-3-buten-1-ol in the presence of triethylamine, and the product was formed in high yield after workup (Scheme 3.14).

Using the ester **47**, solvent-free reaction with butoxymethyl compound **46** and subsequent purification by column chromatography gave both the expected product **48** in good yield and the hydrolysed alcohol **36**, obtained previously *via* another method, as the minor product (Scheme 3.14).[26] The ^{1}H NMR spectrum of the diacetate **48** supported product formation, with the losses of butyl chain resonances and the benzyl resonance at 4.73 ppm observed, as well as new pyran ring proton resonances at 2.62 ppm and 1.8 to 2.0 ppm. A new

acetate proton peak at 2.04 ppm, integrated to three protons, was also present in the spectrum. A high resolution ESI mass spectrum of **48** gave an $[M+Na]^+$ peak, at m/z 357.1674.

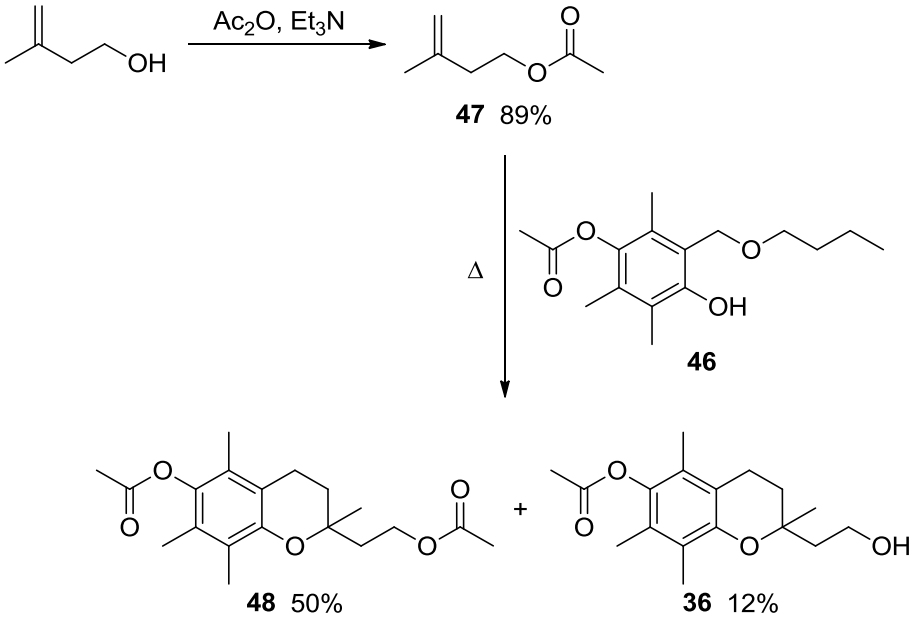

Scheme 3.14

Since the unprotected alcohol **36** was formed in the reaction, we hypothesised that chroman synthesis may be achieved using the unprotected alkenols 2-methyl-2-propen-1-ol and 3-methyl-3-buten-1-ol, despite literature suggesting otherwise,[26] thus removing two synthetic steps. Using the same method as in Scheme 3.14, neat reaction of butoxymethyl compound **46** and either 2-methyl-2-propen-1-ol or 3-methyl-3-buten-1-ol produced the expected alcohols **35** and **36** in quantitative and 69% yield, respectively (Scheme 3.15).[26]

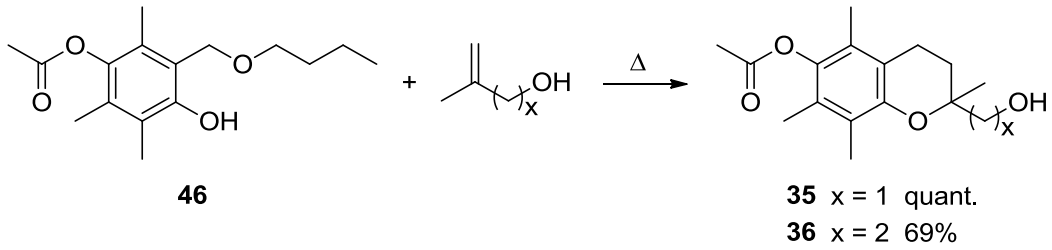

Scheme 3.15

Given the success of chroman formation using alkenol reagents, it was proposed that reaction of a protected butoxymethyl hydroquinone with a wide range of alkenyl reagents would allow installation of various functional groups off the C2 position of the chroman, using a simplified,

general method, shown in Scheme 3.16. For the purposes of determining general viability of this method, the group R^1 in the scheme below was first limited to a methyl group, however at a later stage it was expected that the dimethylbutoxy derivative (where R^1 = H) would be required, to allow further functionalisation off the C8 position of the chroman.

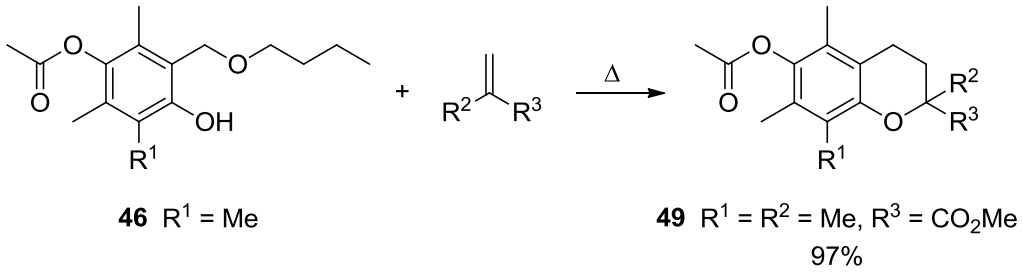

46 R^1 = Me

49 $R^1 = R^2$ = Me, $R^3 = CO_2Me$
97%

Scheme 3.16

Reaction of compound **46** and methyl methacrylate under solvent-free conditions resulted in the formation of the chroman **49**, in excellent yield (Scheme 3.16).[26] Product formation was supported by ^{1}H NMR spectroscopy, with the absence of butyl resonances, as well as new peaks corresponding to the pyran ring, and a singlet corresponding to the methyl ester at 3.66 ppm, integrating to three protons. Formation of **49** was also supported by low resolution ESI mass spectrometry, with major peaks at *m*/*z* 307.2 and *m*/*z* 329.2, corresponding to the $[M+H]^+$ and $[M+Na]^+$ ions, respectively. Chroman **49** is also the acetate-protected methyl ester of Trolox™ (Figure 3.3). Simple hydrolysis of both esters would allow for an overall four-to-five step synthesis of the commercially available compound, in good yield, compared to the original literature 5-step synthesis with 66% overall yield.[25]

Having shown that reaction with methyl methacrylate, an alkene containing an electron-withdrawing group adjacent to the carbon-carbon double bond, was successful for chroman formation, it was proposed that the deactivated phthalimide derivative of 3-methyl-3-buten-1-ol (**51** in Scheme 3.17) may also be a worthwhile candidate for this method of chroman formation, installing nitrogen functionality for subsequent Ca^{2+}-chelating capability as a derivative of BAPTA. Esterification of 3-methyl-3-buten-1-ol with *p*-toluenesulfonyl chloride proceeded in the presence of 4-dimethylaminopyridine (DMAP) and triethylamine, and the reaction, forming tosyl ester **50**, was achieved in good yield (Scheme 3.17).

From ester **50**, a substitution reaction using potassium phthalimide yielded the phthalimide product **51** in high yield. Formation of the new product was supported by ^{1}H NMR spectroscopy, with the absence of the distinctive tosyl signals, as well as new resonances at 7.82 and 7.69 ppm attributable to the phthalimide aromatic protons.

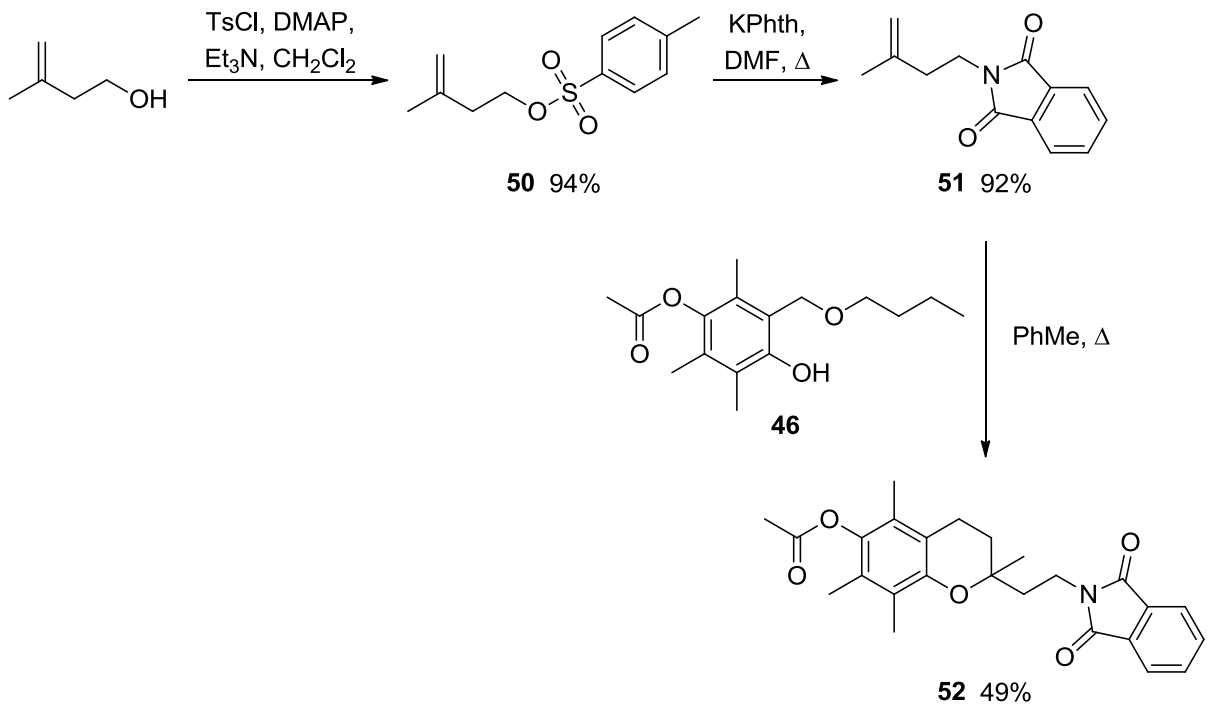

Scheme 3.17

While decomposition of the phthalimide **51** to form the resulting amine may be possible using hydrazine hydrate in the second step of a Gabriel synthesis, it was decided that retaining the deactivating phthalimide functionality would be advantageous, due to the decreased chance of possible side reactions involving an amino group occurring. From **51**, reaction with butoxymethyl compound **46** in toluene was conducted in a sealed pressure tube (Scheme 3.17), to give the phthalimide derivative **52** in 49% yield after purification by column chromatography.[26] Formation of compound **52** was supported by the absence of butyl chain resonances in the proton NMR spectrum, as well as the presence of C3 and C4 proton resonances of the newly formed chroman at 1.90 and 2.64 ppm, respectively. High resolution ESI mass spectrometry also evinced formation of **52**, with a major peak at *m*/*z* 444.1784, attributable to the $[M+Na]^+$ ion expected for the molecular formula of $C_{25}H_{27}NO_5$.

The validity of the butoxymethyl pathway for chroman synthesis relies on the ability of butoxymethyl compounds such as **46** to react with various alkenes, and therefore install numerous R-groups off the C2 position, thus allowing for easy functionalisation using readily available and easily synthesisable starting materials (Scheme 3.16). It was noted that full examination of this method could not occur without investigation of the reactivity of allyl compounds such as allyl alcohol, devoid of a methyl group off the carbon-carbon double bond. One advantage of using this class of compounds, should the synthesis be viable, would be that

these allyl compounds tend to be more readily available and cheaper than the corresponding methallyl analogues.

Neat reaction of butoxymethyl compound **46** with allyl alcohol produced notable results (Scheme 3.18), with both the formation of the expected chroman **53** as a minor product as well as allyloxy derivative **54** as the major isolable product.[26] Chroman **53** was identified by ^{1}H NMR spectroscopy, with multiplets at 2.69 and 1.82 ppm, attributable to the newly formed pyran ring, while **54** was identified by the presence of peaks at 5.94, 5.32, and 5.26 ppm, with distinctive splitting indicative of an allyl group. A benzyl resonance at 4.75 ppm was still present, similar to the starting material, however resonances attributable to the butyl chain were absent. Low resolution ESI mass spectrometry indicated the two products were isomers, due to the presence of peaks attributable to a molecular mass of 264 daltons in both cases.

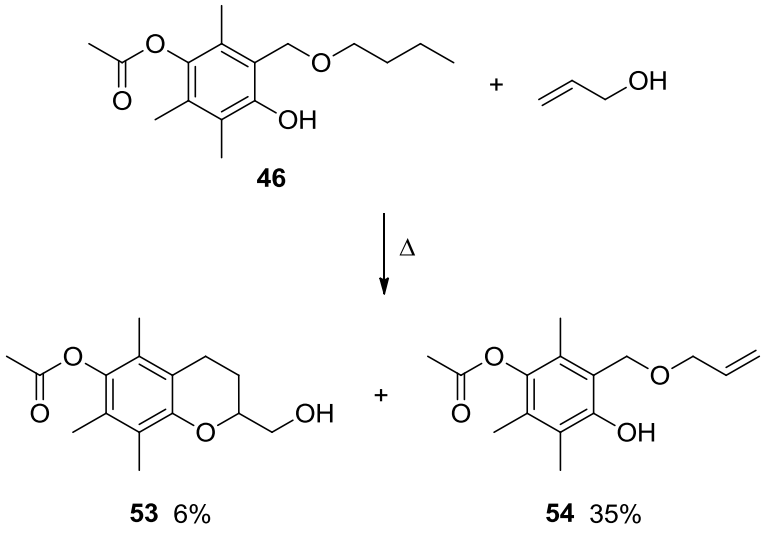

Scheme 3.18

The reason for the production of the allyl derivative **54**, instead of the expected chroman, must lie in the importance of the methyl group. Since the problem is likely to be electronic rather than steric, as chroman synthesis favours the methyl derivative, it is hypothesised that the reaction may proceed *via* a carbocation intermediate. In a proposed mechanism for both the production of a chroman as well as the allyl isomer (Scheme 3.19), it is suggested that protonation of the butoxy group and subsequent loss of butanol leads to intermediate **55a** and its carbocation canonical form **55b**. Nucleophilic attack of **55a** by an alkene can lead to a carbocation intermediate, which would depend on the stability of the carbocation – in the case of methallyl derivatives, tertiary carbocations would be formed, stabilising the intermediate, and allowing an intramolecular reaction to proceed.

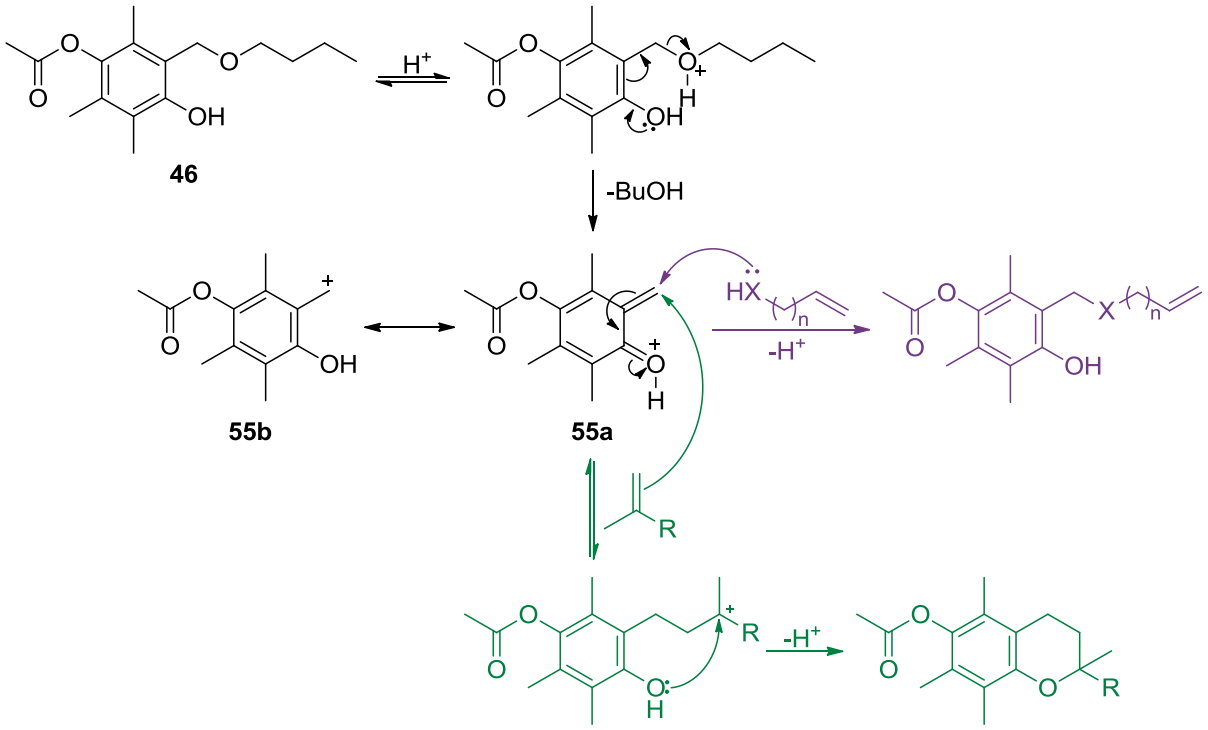

Scheme 3.19

If the vinyl methyl group was not present, however, a much less stable secondary carbocation would form *via* this mechanism, and it is likely that such an intermediate would not be stable enough to ensure chroman formation – instead, if the reactant could act as a nucleophile, it would attack **55a**, leading to the allyl derivative. If the reactant could not act as a nucleophile, it is possible that either the chroman or perhaps another product will form, even in the absence of the methyl group. The proposed mechanism is supported by the presence of a peak of m/z 207.1 found in the low resolution mass spectrum of butoxymethyl compound **46**, attributable to either **55a** or **55b**, suggesting that such a carbocation would be stable under these reaction conditions.

Given this hypothesis, by acetylating allylamine, the resulting deactivated acetamide would likely have diminished nucleophilic capability, and may not follow the nucleophilic reaction pathway in the same way as allyl alcohol. In order to first form the acetamide, reaction of allylamine and acetic anhydride proceeded at 0°C (Scheme 3.20), and *N*-allylacetamide **56** was produced in excellent yield after fractional distillation at reduced pressure.[27] Subsequent solvent-free reaction of the acetamide with **46** at 150°C produced the unexpected product **57** with an unoptimised yield of 20%.[26] The remainder of the reaction mixture contained one or more unidentifiable byproducts missing allyl and benzyl protons by NMR spectroscopy.

Formation of product **57** was supported by high resolution mass spectrometry, with a peak at *m*/*z* 328.1524, attributable to the $[M+Na]^+$ ion. Formation was also supported by proton NMR spectroscopy, with resonances attributable to the acetyl group at 2.04 ppm, as well as peaks distinctive of the allyl group, at 5.80, 5.31, 5.23 and 3.86 ppm, complete with appropriate splitting patterns. Interestingly, two broad singlets appeared in the NMR spectrum at 4.64 and 4.52 ppm, attributable to the two benzyl protons.

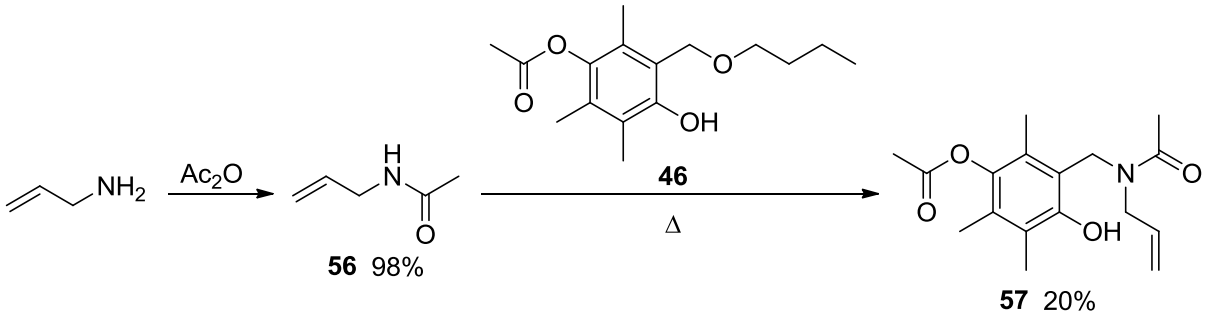

Scheme 3.20

Temperature-dependent proton NMR studies have shown that with an increase in temperature from -20°C to 30°C, the benzyl proton resonances broaden from an AB quartet to two broad singlets (Figure 3.4 overleaf), indicating some rigidity in the structure of **57** at lower temperatures.

The formation of the allylacetamide compound **57**, despite the reduced nucleophilic character of the nitrogen atom of acetamide **56**, indicates that even slight nucleophilic character of the reactant renders the allyl product pathway more favourable than chroman formation (Scheme 3.19). Future studies examining the behaviour of non-heteroatom allyl derivatives may provide further insight into the behaviour of these alkenes under the above conditions.

While reaction of alkenes with the trimethylbutoxy compound **46** have provided insight into the mechanism of chroman formation *via* this route, ultimately the aim of this synthetic pathway would be to improve yields of chromans with an aromatic proton at the C8 position. Following a similar method as for the synthesis of **46**, reaction of mono-protected dimethylhydroquinone **39** with paraformaldehyde and butanol in the presence of acetic acid and dibutylamine at 100°C gave both the mono-alkylated and bis-alkylated products **58** and **59**, as well as recovered starting material (Scheme 3.21).[26]

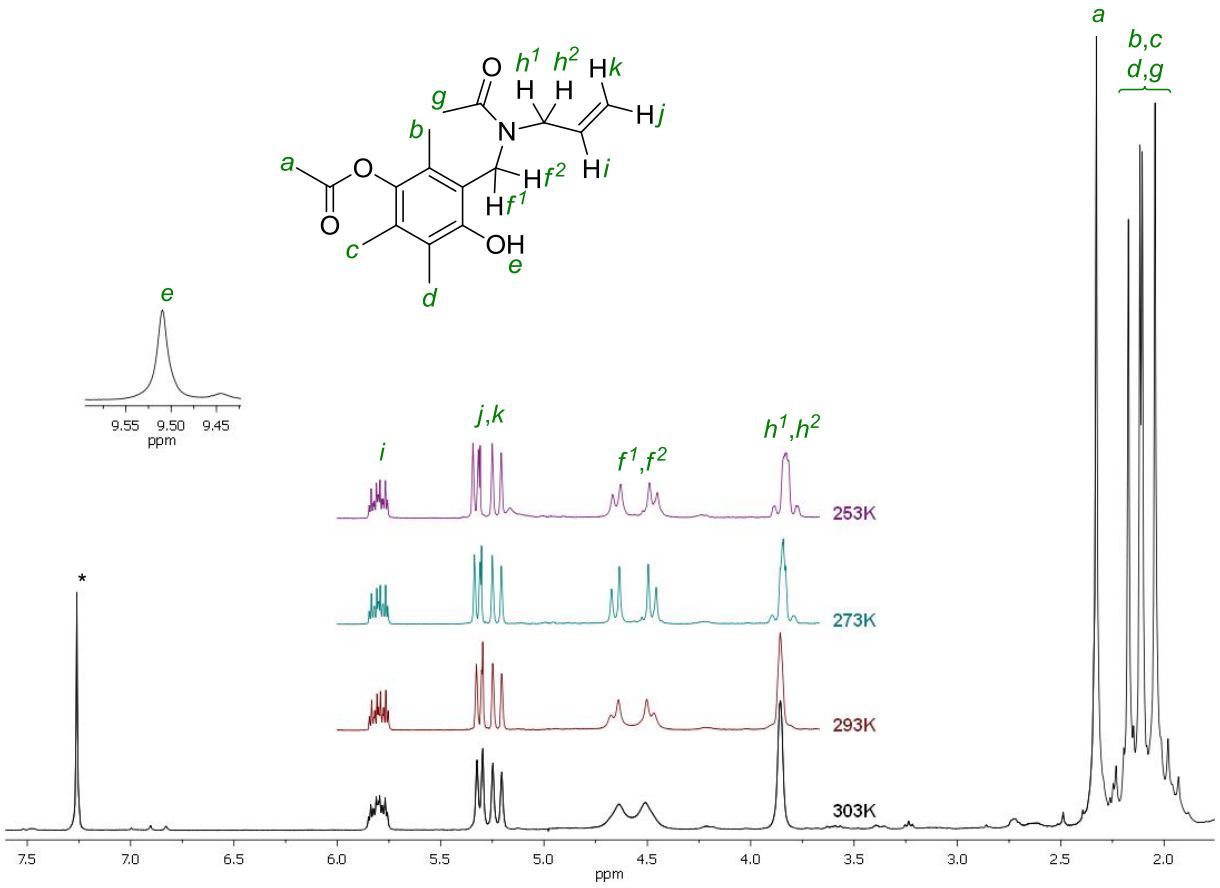

Figure 3.4 300 MHz variable temperature ^{1}H NMR spectra of **57** in $CDCl_3$ showing temperature-dependent behaviour. * Denotes residual solvent peaks.

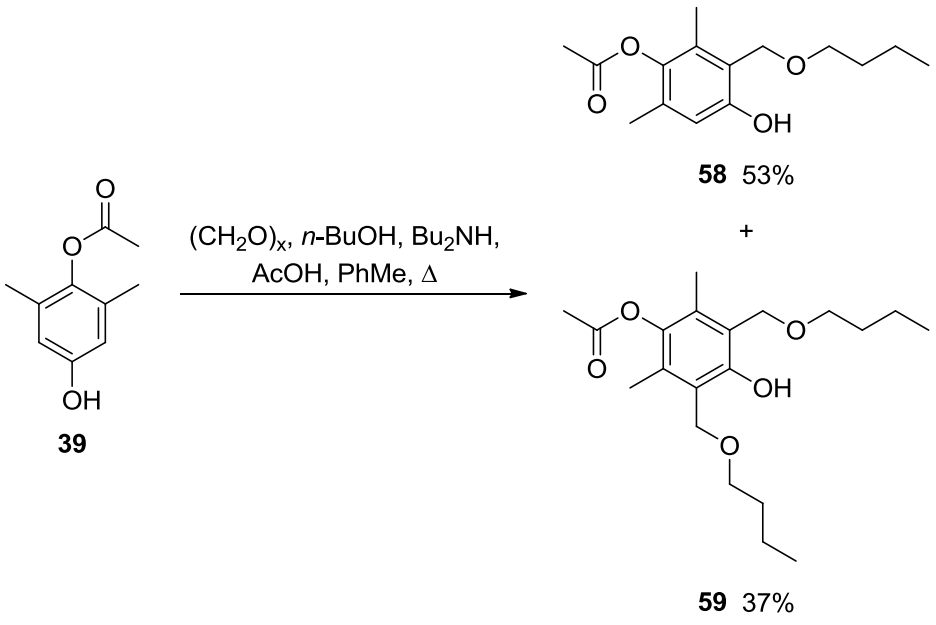

Scheme 3.21

During optimisation of this reaction, it became clear that the mono-alkylated product was most favourably formed when reaction occurred under dilute conditions. Formation of the desired product **58** was supported by high resolution ESI mass spectrometry, with a majors peaks at *m*/*z* 284.1857 and *m*/*z* 305.1149, attributable to the $[M+NH_4]^+$ and $[M+K]^+$ species, respectively. A peak was also present at *m*/*z* 265.2 in the negative low resolution mass spectrum, corresponding to the $[M-H]^-$ ion. Proton NMR spectroscopy supported mono-alkylation, with an aromatic proton resonance at 6.60 ppm, integrating to one proton, as well as a benzyl peak at 4.74 ppm and butyl resonances integrating to the appropriate number of protons. Formation of the isolated bis-alkylated product **59** was supported by high resolution ESI mass spectrometry, with a major peak at *m*/*z* 375.2144, corresponding to $[M+Na]^+$, and a peak in the low resolution negative spectrum of *m*/*z* 351.3, attributable to $[M-H]^-$.

Since a series of chromans with an aromatic proton at the C8 position were required, chroman synthesis was attempted using the dimethylbutoxy compound **58** using the same method as for the trimethyl derivative. Neat reaction of **58** with both 2-methyl-2-propen-1-ol and 3-methyl-3-buten-1-ol at 150°C gave previously synthesised chromans **40** and **41**, with yields of 67% and 31%, respectively (Scheme 3.22).[26] Proton NMR spectra of both compounds matched those obtained from previous syntheses, however the absence of butyl chain resonances in both cases also supported complete conversion using this method.

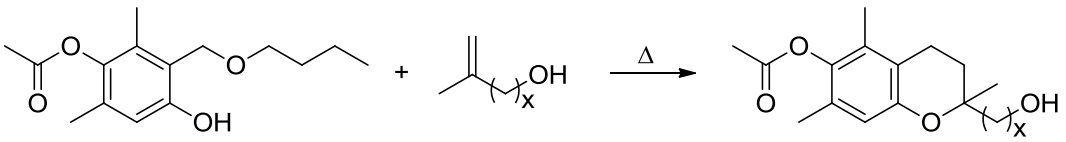

58

40 x = 1 67%
41 x = 2 31%

Scheme 3.22

Additionally synthesised using the above method was phthalimide product **60**, albeit in low yield (Scheme 3.23).[26] Butoxymethyl compound **58** and phthalimide **51** were dissolved in toluene, and heated to 150°C in a pressure tube. After cooling and distillation of the excess solvent, the crude product was purified by column chromatography to give pure **60**, with an unoptimised yield of 10% (12% recovered yield). The reaction proved to be inefficient, with more starting material recovered than product isolated. This is likely to be due to the presence of the toluene required to solvate the reaction; further reaction optimisation may require the investigation of neat reaction to form chroman **60**.

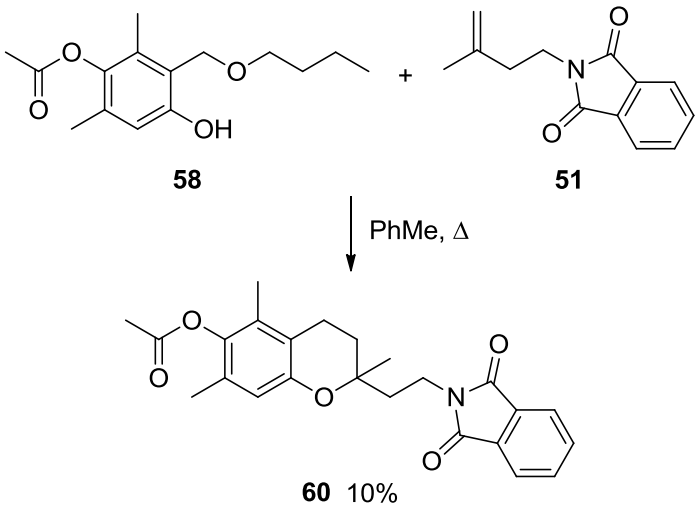

Scheme 3.23

Product formation was supported by the absence of butyl chain signals in the ^{1}H NMR spectrum, as well as peaks at 4.72 and 4.66 ppm, attributable to the vinyl protons of the alkene starting material. Proton resonances attributable to the newly formed pyran ring were present, as well as a carbon signal at 74.3 ppm, supporting the presence of the quaternary C2 carbon in the product. High resolution ESI mass spectrometry also supported formation of the phthalimide product, with a peak at *m*/*z* 425.2072, representative of a $[M+NH_4]^+$ ion.

By comparing the yields of chromans **35**, **36**, **40** and **41** (Table 3.1), using both one-step and two-step (*via* the butoxymethyl derivative) methods (Scheme 3.24), it can be seen that while the trimethyl products **35** and **36** formed from **34** were produced in equal or higher yields by the single-step method by Fukumoto *et al*.,[20] the dimethyl products **40** and **41** were formed in better yields from **39** when synthesised *via* the butoxymethyl method by Monoe *et al*.[26] This could be due to the ability to control the mono-alkylation of the protected hydroquinone more carefully than in the one-pot method, using dilution effects.

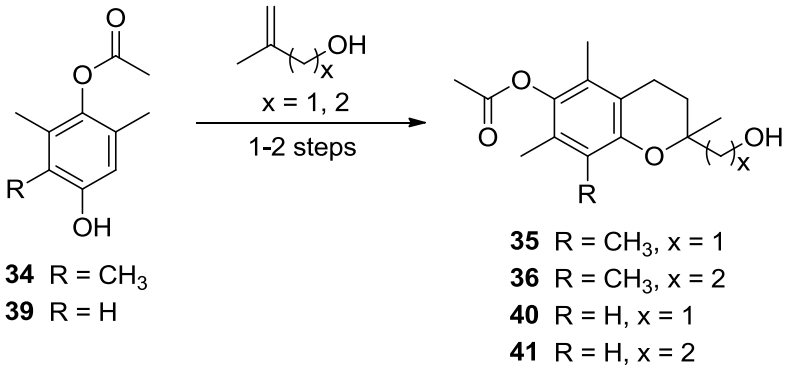

Scheme 3.24

Table 3.1 Comparison of yields obtained using two methods, from mono-protected di- and trimethylhydroquinone (**34** and **39**).

	Direct	**Butoxymethyl**
35	quant.	quant.
36	78%	69%
40	27%	36%
41	6%	16%

3.4 Chromanol synthesis *via* a bromination pathway

Despite the improved yields of chromans **40** and **41** *via* the butoxymethyl method, there was still a need for a more efficient method of forming chromans with the option of functionalising at the C8 position later. We hypothesised that "blocking" one aromatic position of the hydroquinone starting material with bromine (*i.e.* **61**) and subsequently alkylating using the conditions described herein should give a series of bromochromans in relatively high yield (Scheme 3.25). It was envisaged that these chromans would be able to be further functionalised at the C8 position if by nothing more than reducing the bromide out using nickel boride or similar reagents.

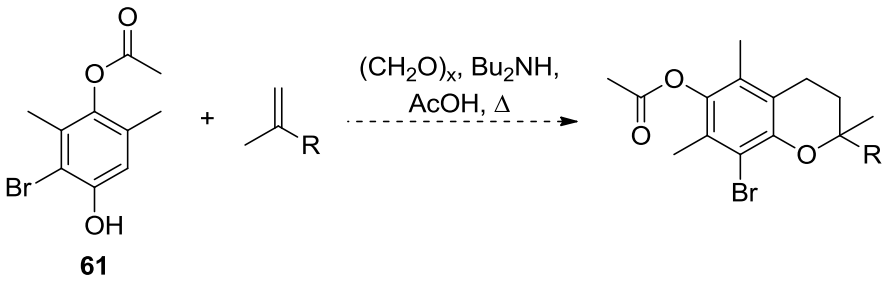

Scheme 3.25

From **38**, two attempts were made to synthesise the bis-protected, brominated hydroquinone **62** (Scheme 3.26), which could be deprotected at a later stage for use in chroman synthesis. One method involved the dropwise addition of a solution of bromine in glacial acetic acid to a solution of starting material **38** in acetic acid followed by removal of the solvent by rotary evaporation.[28] The second method involved stirring the bis-protected hydroquinone **38** and ferric bromide in chloroform, with bromine added dropwise on ice, before warming to room temperature. The reaction was monitored by thin layer chromatography until the starting

material had appeared to be consumed, with subsequent workup.[29] In both cases, the doubly brominated, mono-protected compound **63** was formed, with some starting material recovered, but **62** was not isolated.

Formation of the undesired product **63** was supported, amongst others, by negative high resolution ESI mass spectrometry, with $[M-H]^-$ peaks at m/z 334.8925, m/z 336.8904 and m/z 338.8885, in the expected isotopic pattern for a compound containing two bromine atoms. It is hypothesised that bromination of the fully protected hydroquinone failed because the *ortho* acetate group deactivates electrophilic aromatic substitution, while the combined steric bulk of the acetate and methyl groups may hinder reaction with bromine. The actual product was likely to have formed due to eventual deprotection of some of the starting material, which would then be subjected to a large excess of bromine in solution, thus leading to the doubly brominated species. Reduction of **63** using a nickel boride method was performed to give previously synthesised mono-protected hydroquinone **39** (Scheme 3.26).[30] Pure product was obtained in excellent yield, thereby allowing use of the compound for further applications.

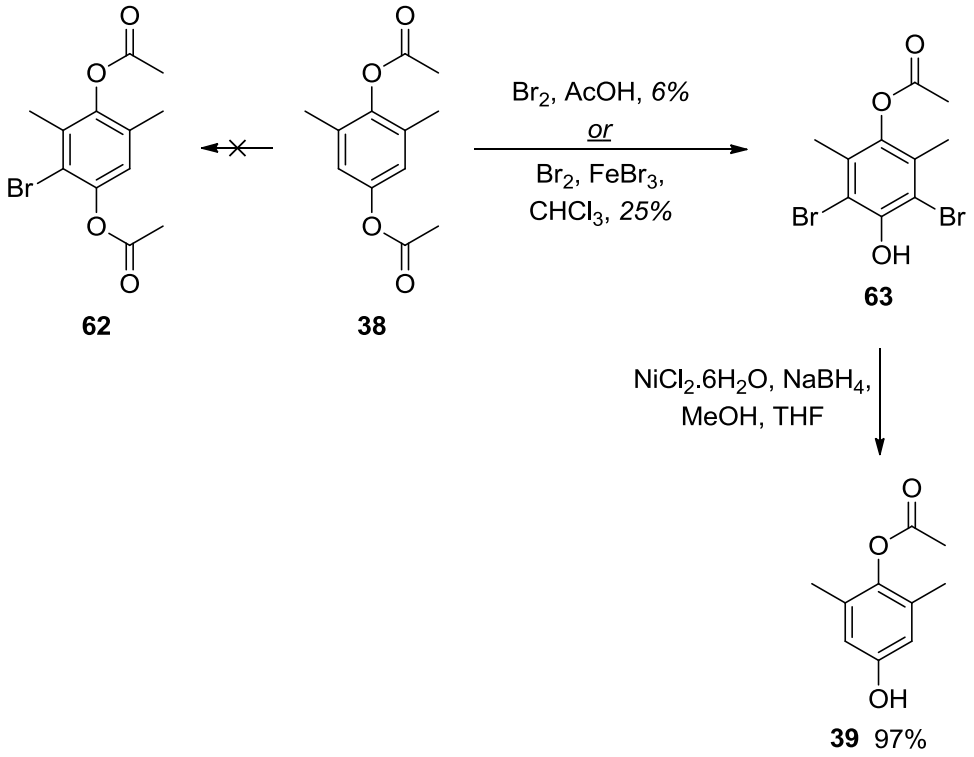

Scheme 3.26

Given that the synthesis of **62** from the bromination of bis-acetylated **38** had been unsuccessful, bromination of the unprotected hydroquinone was attempted. From 2,6-dimethylhydroquinone, following the literature, treatment with bromine in glacial acetic

anhydride gave the brominated product **64** in 72% yield (Scheme 3.27),[28] and formation of the product was evinced by negative low resolution mass spectrometry, with a bromine isotopic pattern at *m*/*z* 214.9 and 216.9, attributable to the [M-H]$^-$ ion. The ^{1}H NMR spectrum also supported product formation, with two inequivalent peaks corresponding at the aromatic methyl groups at 2.15 and 1.98 ppm, integrating to three protons each, as well as a lone aromatic proton signal at 6.45 ppm, integrating only one proton. Subsequent acetylation of **64** with acetic anhydride in the presence of triethylamine gave the diacetate product **62** in high yield (Scheme 3.27).

From bis-acetylated compound **62**, selective deprotection proceeded by the addition of sodium dithionite and aqueous potassium carbonate to give mono-acetylated bromo compound **61** in 80% yield (Scheme 3.27).[21] Formation of the bromo compound was supported by negative high resolution ESI mass spectrometry, with major peaks at *m*/*z* 256.9820 and *m*/*z* 258.9800, in the expected isotopic ratio for bromine, attributable to the [M-H]$^-$ ion. Proton NMR spectroscopy also supported formation of **61**, with inequivalent aromatic methyl peaks at 2.21 and 2.08 ppm, integrating to three protons each, and a singlet at 6.74 ppm integrating to one proton, indicating a lone aromatic proton.

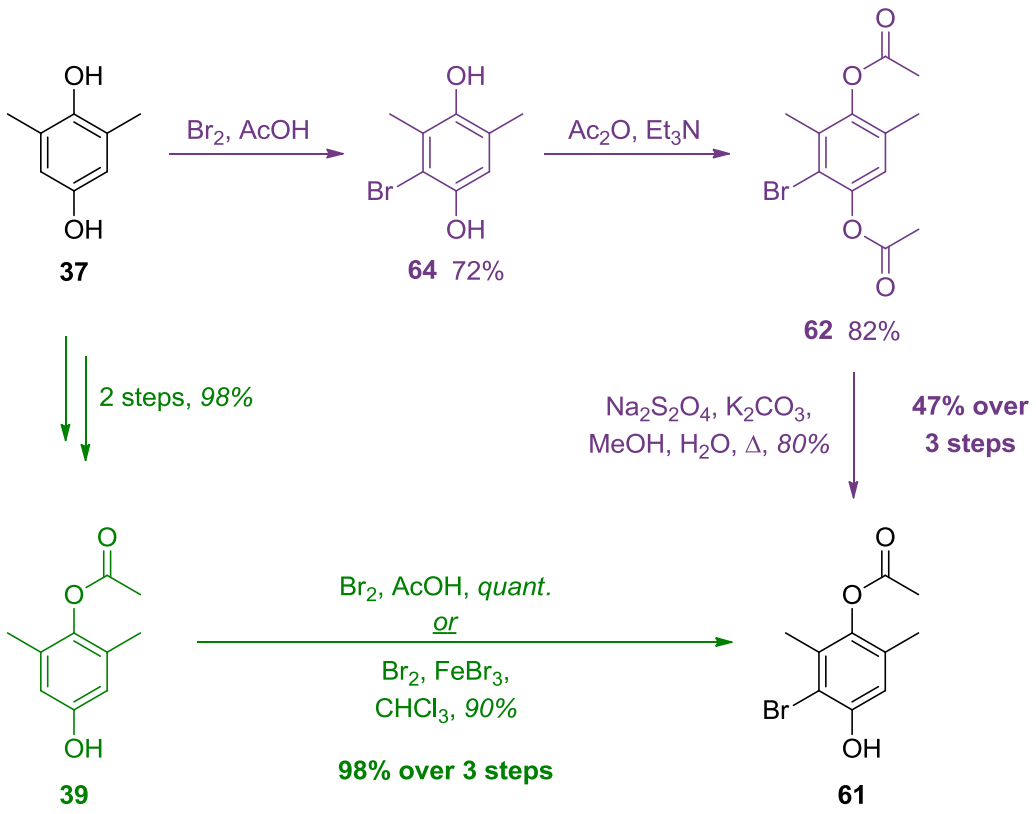

Scheme 3.27

Since mono-protected hydroquinone **39** had already successfully been synthesised in excellent yield, bromination of this compound to form **61** was also attempted. Methods previously used in the attempted aromatic bromination of **38** (Scheme 3.26) – dropwise addition of a solution of bromine in acetic acid; reaction with bromine in the presence of ferric bromide – were employed, as shown in Scheme 3.27.[28,29] In both cases, a high yield of the expected product was isolated. It is believed that the bromination of the mono-protected hydroquinone **39** proceeded in higher yields than both the unprotected (**37**) and bis-protected (**38**) derivatives due to the presence of both the unprotected phenol group, which allows promotion of the electrophilic aromatic substitution, as well as the presence of an acetate protecting group preventing the formation of benzoquinone derivatives. Overall, the three-step synthesis of **61** from **37** proceeded in a higher yield *via* mono-protected hydroquinone **39** (98%) than *via* bromo compounds **64** and **62** (47%).

X-ray crystallography of **61** (Figure 3.5 and Figure 3.6) shows the intermolecular hydrogen bonding of the structure, which exists in a monoclinic crystal system with space group $P2_1/c$. Crystals of **61** suitable for analysis were grown by vapor diffusion from chloroform and hexane.

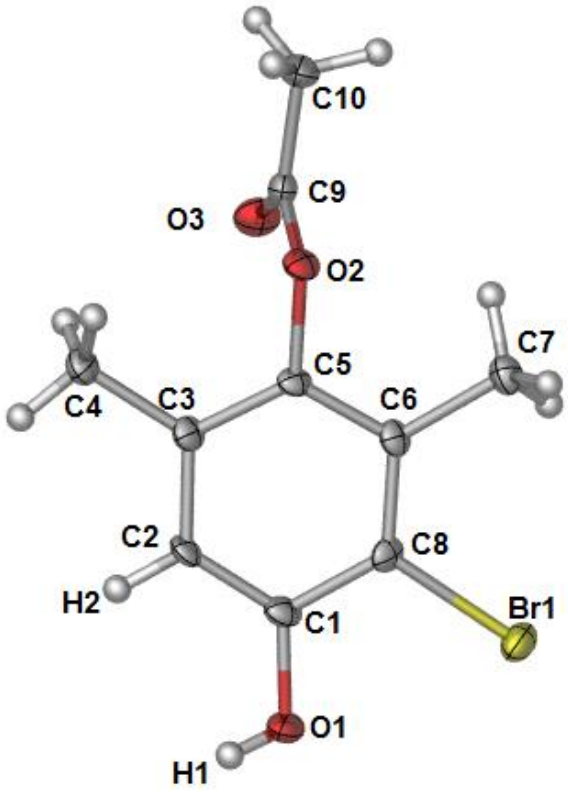

Figure 3.5 Molecular diagram of **61** as shown with 50% thermal ellipsoids and hydrogen atoms as spheres of arbitrary size.

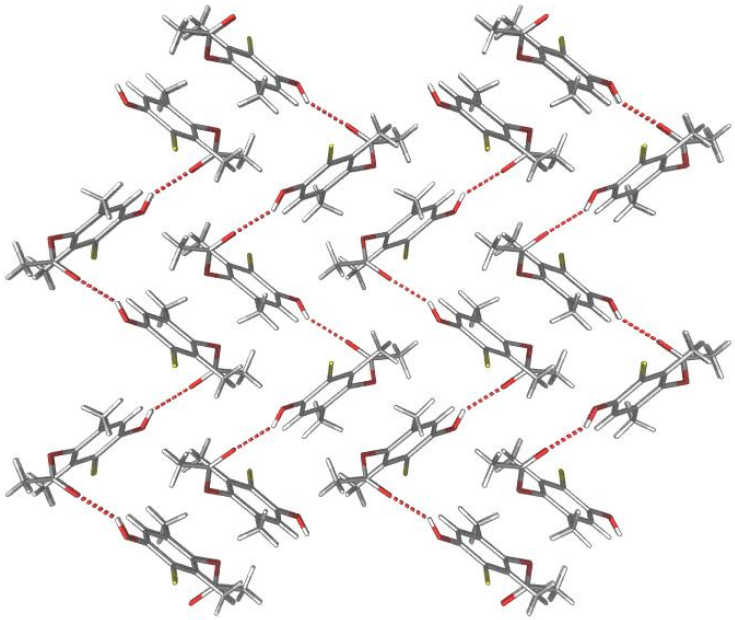

Figure 3.6 Looking down the *a* axis of **61**. The packing system is a result of hydrogen bonding (O3 to H1 distance: 1.985 Å), giving a herringbone pattern down the *a* axis.

From mono-acetylated bromo compound **61**, chroman formation under standard conditions gave bromo chroman compounds **65** and **66**, in 79% and 99% yield, respectively (Scheme 3.28). Formation of both products were supported by the usual ^{1}H NMR resonances attributable to chroman formation, especially the distinctive C3/C4 splitting patterns at around 1.8 ppm and 2.6 ppm, as well as the absence of the aromatic proton signal at 6.74 ppm in the starting material. High resolution mass spectrometry also supported formation of **65**, with $[M+NH_4]^+$ ions peaks at *m*/*z* 360.0807 and *m*/*z* 362.0788 in the expected isotopic pattern. The formation of **66** was similarly discerned, with major peaks at *m*/*z* 357.0693 and *m*/*z* 359.0674, corresponding to the $[M+H]^+$ ions.

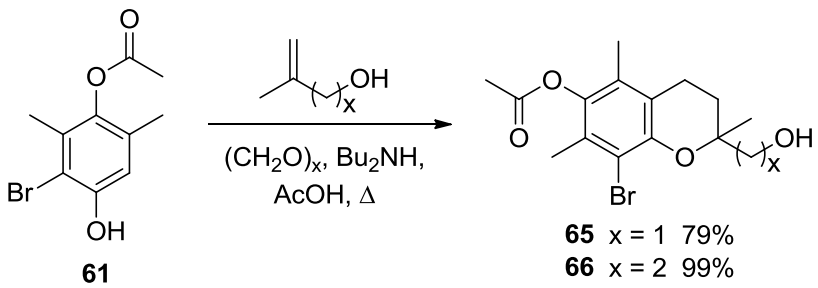

Scheme 3.28

Several attempts were made to debrominate **65** to produce chroman **40** (Scheme 3.29). Methods of Kiehlmann[31], lithiation[32] or nickel boride reduction[30] failed to give much in the way of moderate to high yield. In each case, the reaction was difficult to monitor by thin layer chromatography, due to the very similar polarities of the two compounds.

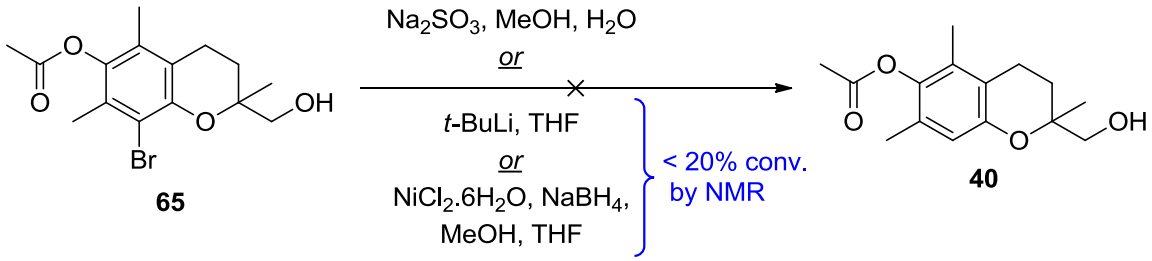

Scheme 3.29

Debromination was eventually achieved through hydrogenation in the presence of 10% palladium on charcoal and triethylamine (Scheme 3.30).[33] Chroman **65** was stirred for four days under these conditions and after workup and the crude product was passed through a silica plug (ethyl acetate), to obtain **40** in quantitative yield. Chroman **41** was similarly synthesised from the bromo precursor **66**, in 76% yield.

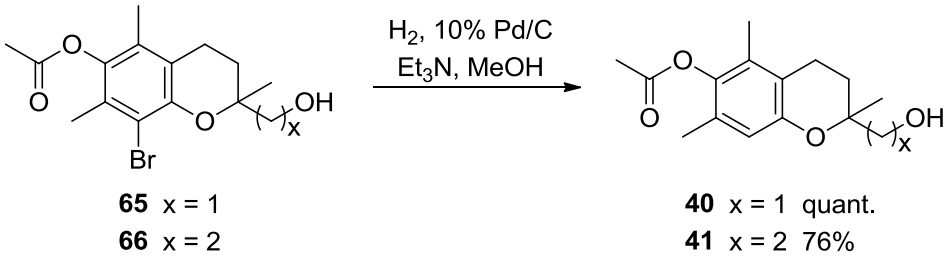

Scheme 3.30

Using the established protocol for forming chromans using the bromination method, various R-groups at the C2 and C8 positions could be theoretically installed to give a wide range of targets. Given this ability, targets **A** and **B** were envisaged, mimicking the Ca^{2+}-encapsulating cavity of BAPTA (shown in green in Scheme 3.31).

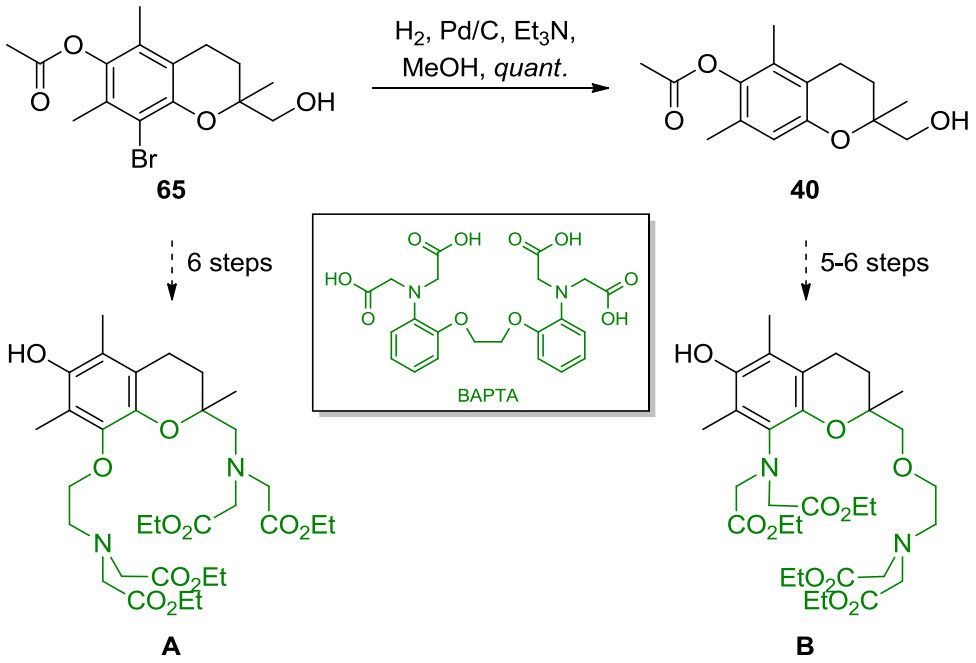

Scheme 3.31

3.5 Methods towards the synthesis of target **A**

With the synthetic plan in Scheme 3.31 in mind and with brominated chroman **65** in hand, attempts were made to install amine functionality in the 2-position of the chroman. Firstly, reaction of chroman **65** with *p*-toluenesulfonyl chloride gave the tosyl ester **67** in quantitative yield (Scheme 5.2). Formation of the ester was supported by high resolution ESI mass spectrometry, with an $[M+Na]^+$ peak at m/z 519.0444, as well as ^{1}H NMR signals at 8.80/7.33 ppm and 2.44 ppm attributable to the new aromatic and methyl protons, respectively, in addition to a downfield shift of AB system resonances from 3.64/3.58 ppm to 4.03/3.92 ppm corresponding to the methylene protons adjacent to the tosyl group.

Attempted substitution reactions of **67** with potassium phthalimide in dimethylformamide did not yield the phthalimide product **68** shown in Scheme 3.32, despite attempted optimisation of reaction conditions. It was proposed that the reaction did not proceed due to the steric hindrance of the bulky tosyl group in close proximity to the quaternary C2 carbon position, a factor that has plagued other research within our group. Alternatively, the attempted formation of **69** by the substitution of the tosylate with an azide group – a smaller nucleophile with less steric bulk – was unsuccessful under varied conditions (Scheme 3.32).

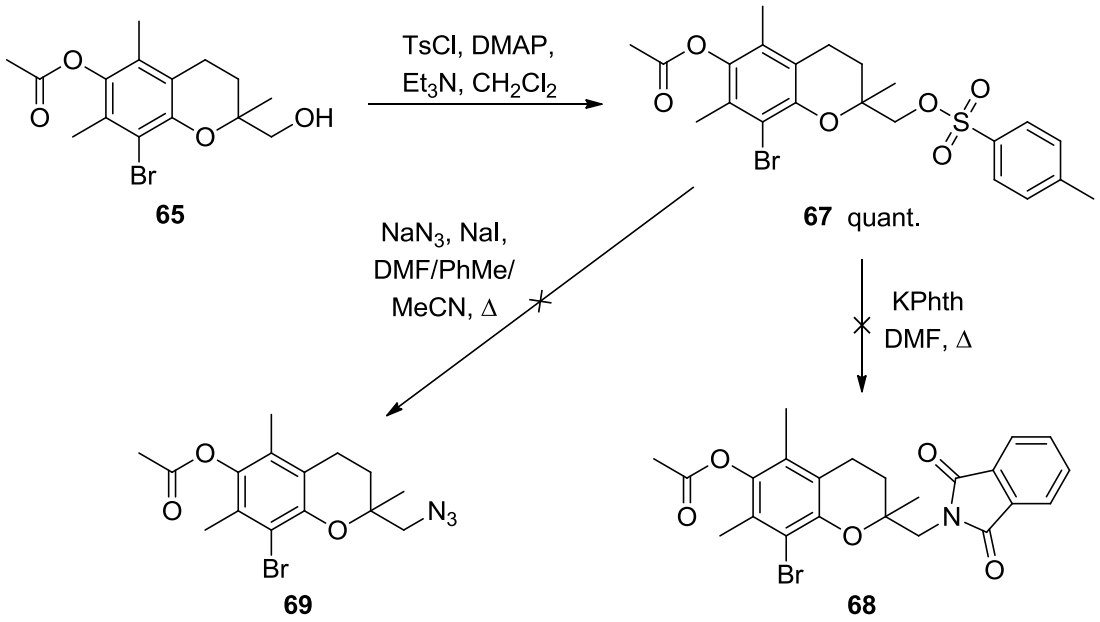

Scheme 3.32

To overcome the steric problem of substitution of the tosyl ester, it was therefore proposed that chroman formation using deactivated phthalimide **71** (in Scheme 3.33) may be a worthwhile candidate pathway to forming phthalimide **68**. The phthalimide methallyl precursor was synthesised in 2 steps (Scheme 3.33). Formation of the tosyl ester **70** of 2-methyl-2-propen-1-ol was attempted from the starting alcohol and *p*-toluenesulfonyl chloride, using a catalytic combination of triethylamine and 4-dimethylaminopyridine, however this only gave a negligible conversion to the expected tosyl ester **70**, as indicated by ^{1}H NMR spectroscopy.

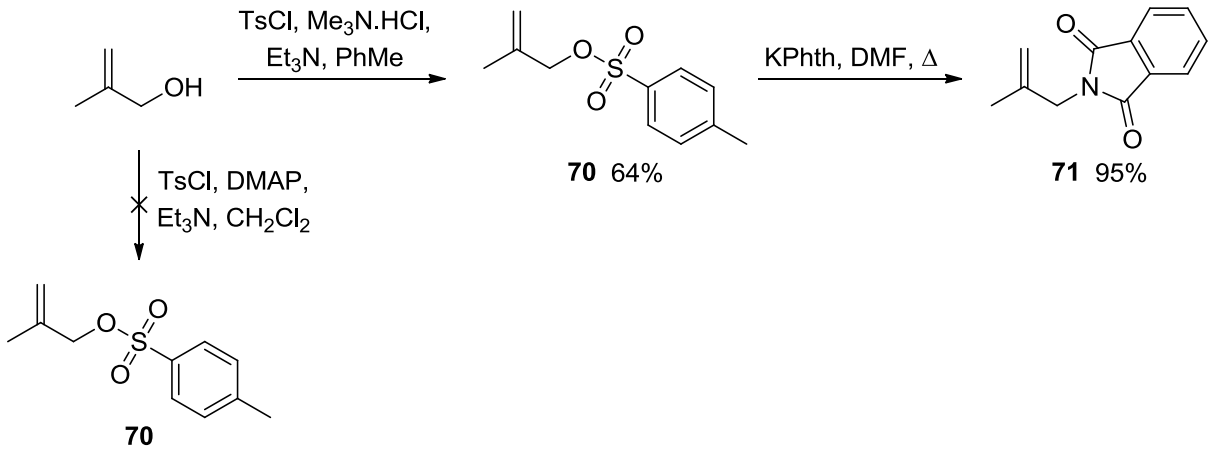

Scheme 3.33

An alternative synthesis using trimethylamine hydrochloride and triethylamine as catalytic agents for the esterification proceeded from 2-methyl-2-propen-1-ol to give **70** in 64% yield (Scheme 3.33),[34] with product formation supported by a mass spectrometry peak at *m*/*z* 249.0, indicating the $[M+Na]^+$ ion, as well as the AB system in the ^{1}H NMR spectrum at 7.78 and 7.33 ppm attributable to the new tosyl group protons, indicating that esterification had taken place. The esterification of the alcohol with *p*-toluenesulfonyl chloride was catalysed by trimethylamine formed *in situ* from trimethylamine hydrochloride and triethylamine. As triethylamine is a stronger base than trimethylamine, the equilibrium of Scheme 3.34 lies to the right, driving the formation of trimethylamine and triethylamine hydrochloride. Once formed, trimethylamine reacts with *p*-toluenesulfonyl chloride to form the sulfoniumammonium salt adduct, which may react readily with 2-methyl-2-propen-1-ol to form ester **70**, regenerating methylamine hydrochloride (Scheme 3.35).[34]

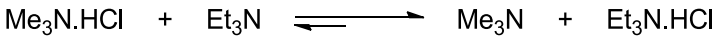

Scheme 3.34

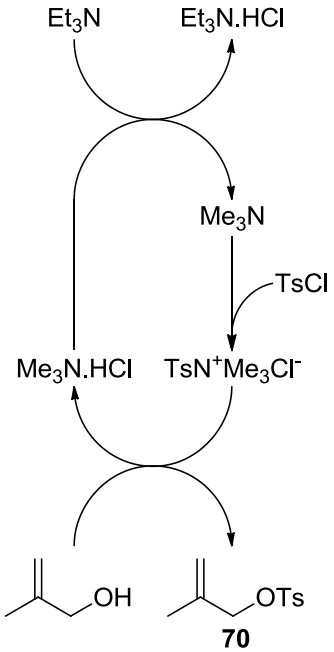

Scheme 3.35[34]

From the ester **70**, substitution using potassium phthalimide in dimethylformamide gave the phthalimide product **71** in 95% yield (Scheme 3.33). Formation of **71** was supported by ^{1}H NMR spectroscopy, with the absence of resonances at 7.78, 7.33 and 2.44 ppm, attributable to the

tosyl protons, and new complex multiplets at 7.84 and 7.73 ppm representing the new phthalimide group.

Attempted reaction of brominated hydroquinone **61**, methallyl phthalimide **71** and paraformaldehyde in the presence of acetic acid and dibutylamine did not give the expected product **68** (Scheme 3.36), however thin layer chromatography indicated that the bromo starting material **61** had been consumed. A similar reaction between previously synthesised phthalimide **51** and **61** to form **72** was also attempted, however the same problem arose.

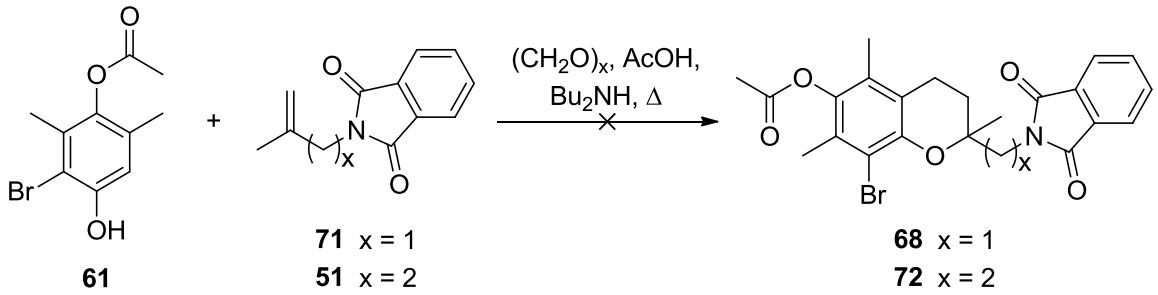

Scheme 3.36

In both cases, ^{1}H NMR spectroscopy of the crude reaction mixture showed an absence of the aromatic proton resonance at 6.74 ppm, indicating consumption of **61**, however ESI mass spectrometry showed neither of the expected products. Instead, strong peaks occurred in both mass spectra at m/z 400.0 and m/z 402.0, with the characteristic isotopic pattern of a compound containing a single bromine. Given the common mass formed from the attempted reaction of **61** with different phthalimide alkene substrates, it was hypothesised that the product resulted from a side reaction of the brominated hydroquinone either with itself or with the paraformaldehyde. The formation of expected products in the case of reaction with 2-methyl-2-propen-1-ol and 3-methyl-3-buten-1-ol, as well as the absence of the mass spectrum peaks at m/z 400 and m/z 402 in these reactions suggest that the phthalimide may play a promoting role in the side reaction without acting as a reactant itself.

Alternatively, it was proposed that the alkyl amine of the target could be installed *via* acetamide-containing alkenes. Like a phthalimide protecting group, an acetamide deactivates the nitrogen and may be readily removed at a later point in time. Alkenes **73** and **74** were synthesised from their corresponding phthalimide compounds **71** and **51** (Scheme 3.37) by firstly decomposing the phthalimide groups using hydrazine hydrate to form the primary amines, followed by acetylation using acetic anhydride in the presence of triethylamine. In both cases, the desired acetamide was synthesised in low yield after two steps.

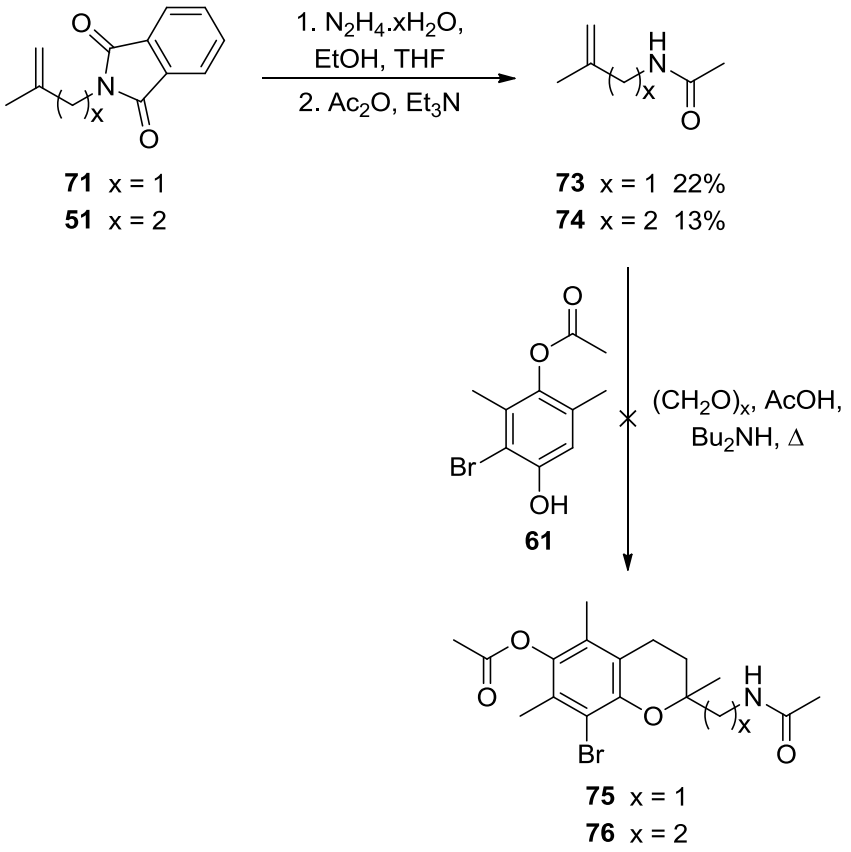

Scheme 3.37

Formation of acetamide **73** was supported by mass spectrometry, with major peaks at *m*/*z* 114.1 and 136.1, corresponding to the $[M+H]^+$ and $[M+Na]^+$ ions. In the ^1H NMR spectrum, evidence of the conversion included the loss of aromatic proton multiplets at 7.86 and 7.74 ppm, presence of an acetamide methyl proton peak at 1.97 ppm, as well as an upfield shift of the methylene proton peak from a singlet at 4.22 ppm to a doublet at 3.74 ppm. Formation of acetamide **74** was similarly supported, with major mass spectrum peaks at *m*/*z* 128.1 and 150.1, corresponding to the $[M+H]^+$ and $[M+Na]^+$ ions. The ^1H NMR spectrum displayed a new acetamide peak at 1.92 ppm, as well as upfield shifts of the ethylene proton triplets from 3.80 and 2.39 ppm to 3.32 and 2.17 ppm, respectively.

From the newly formed alkenes, reaction with mono-protected bromo hydroquinone **61**, paraformaldehyde, dibutylamine and acetic anhydride both solvent free and in toluene did not produce the expected products **75** and **76** (Scheme 3.37). In both cases, peaks in the mass spectra corresponding to the expected products appeared in the crude mixture, however attempts at purification isolated neither **75** nor **76**.

Functionalisation of the C2 chain was alternatively attempted by derivatisation of alcohol **66**. Attempted esterification using two equivalents of *p*-toluenesulfonyl chloride in dichloromethane with an excess of triethylamine and a catalytic amount of 4-dimethylaminopyridine yielded the unexpected doubly tosylated compound **77** after purification, in 73% yield (Scheme 3.38). Monitoring by thin layer chromatography had shown complete consumption of both starting materials, which was unexpected due to the excess of *p*-toluenesulfonyl chloride added. Formation of the undesired product was supported by peaks in the high resolution mass spectrum at *m*/*z* 645.0592 and 647.0568, in an isotopic pattern typical of a molecule with one bromine, attributable to the $[M+Na]^+$ ion. Proton NMR spectroscopy also supported tosylation at two positions, with the presence of four aromatic proton doublets in the ^1H NMR spectrum, all integrating to two protons, as well as two new aromatic methyl proton resonances at 2.46 and 2.42 ppm and the absence of an acetate proton resonance around 2.3 ppm.

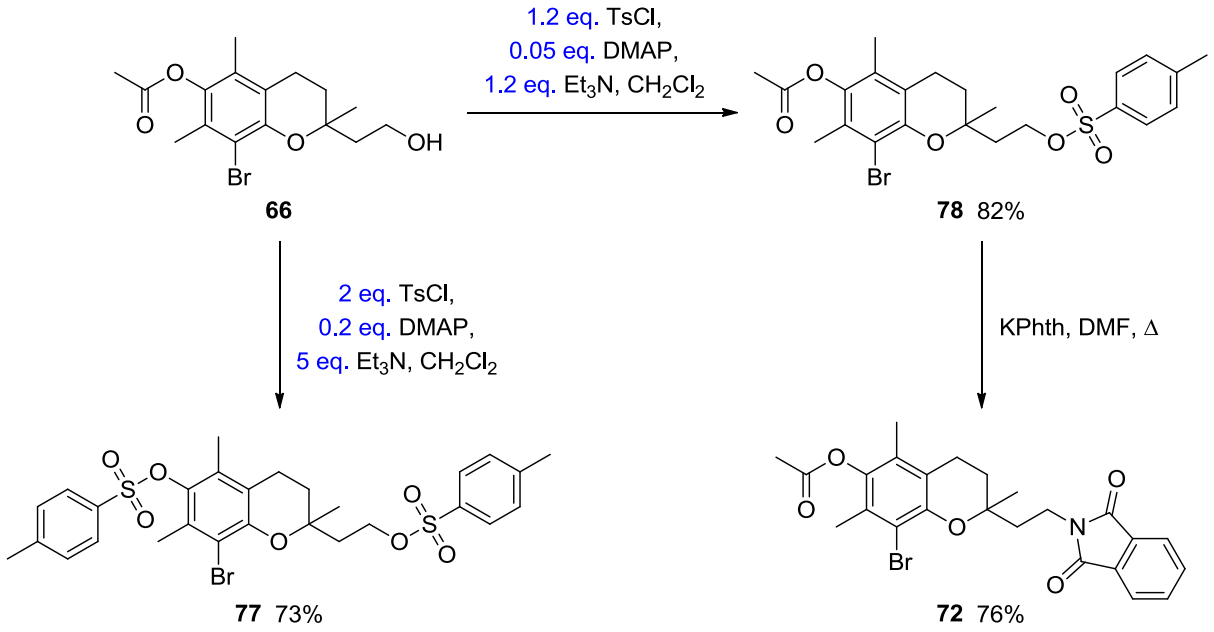

Scheme 3.38

It was hypothesised that the addition of an excess of base to the reaction may have promoted the cleavage of the acetate protecting group, leading to a free phenol, which would then react with the excess of *p*-toluenesulfonyl chloride to form the product **77**. Another reaction was attempted, this time with only 1.2 equivalents of both the *p*-toluenesulfonyl chloride and triethylamine and a smaller proportion of 4-dimethylaminopyridine, and the reaction was monitored frequently by thin layer chromatography, which appeared to show formation of **77**

once again, however on completion of the reaction and purification by column chromatography, the expected product **78** was isolated in 82% yield. Esterification at only one position was supported by the presence of only two aromatic proton doublets in the ^{1}H NMR spectrum, at 7.78 and 7.31 ppm, as well as retention of the acetate peak at 2.33 ppm. High resolution mass spectrometry also supported formation of the expected product, with major peaks at *m*/*z* 533.0602 and 535.0582, attributed to the $[M+Na]^+$ ion, in an isotopic pattern appropriate for one bromine.

From ester **78**, a substitution reaction using potassium phthalimide in the dimethylformamide gave the desired phthalimide product **72** (Scheme 3.38) in 76% yield. Complete substitution was supported by ^{1}H NMR spectroscopy, with the absence of aromatic proton resonances at 7.78 and 7.31 ppm and aromatic methyl peak at 2.43 ppm, and the presence of new multiplets at 7.82 and 7.69 ppm. High resolution mass spectrometry also supported product formation, with major $[M+Na]^+$ peaks at *m*/*z* 533.0602 and 535.0582, with an isotopic pattern expected for one bromine.

From compound **72**, it is anticipated that oxidation of the aryl bromine, Williamson ether synthesis and subsequent deprotection and alkylation of the nitrogens would give target **79** in approximately four steps, as shown in Scheme 3.39.

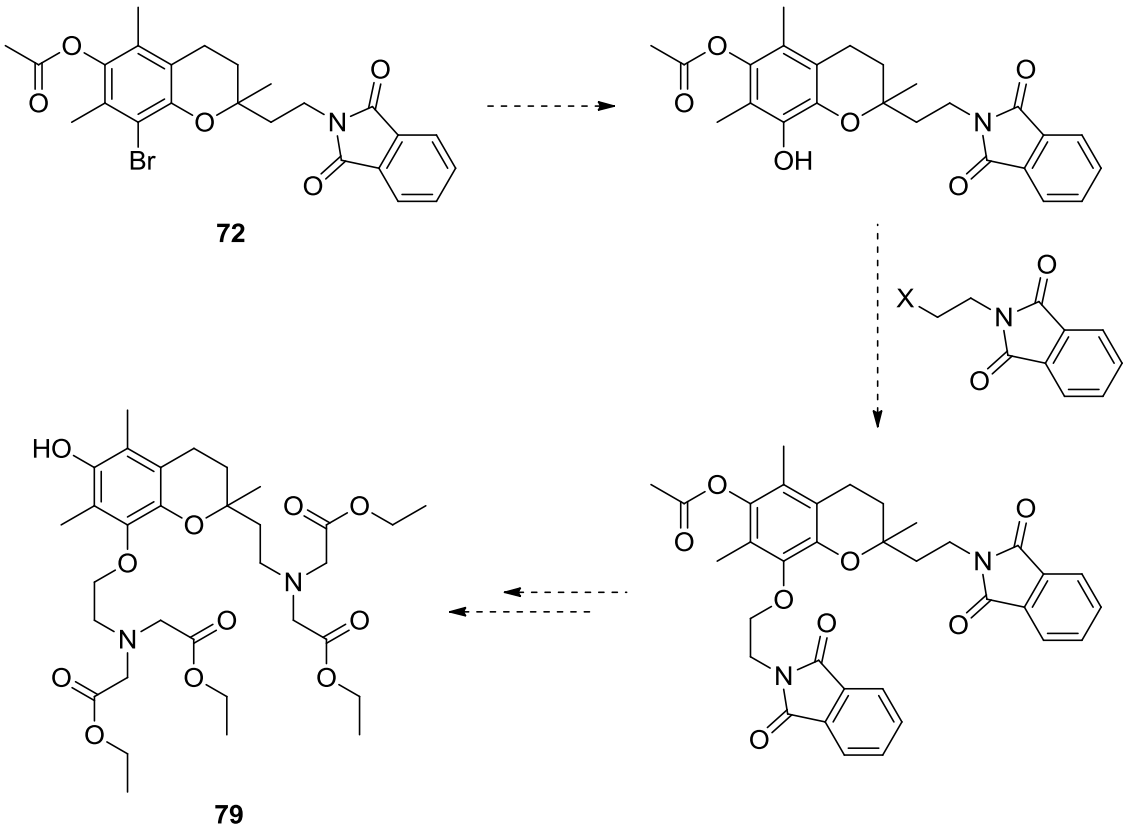

Scheme 3.39

3.6 Methods towards the synthesis of target **B**

In order to achieve the synthesis of target **B**, it was envisaged that alkylation of the alcohol would first be necessary to deactivate that portion of the compound, followed by nitration of the C8 carbon and subsequent functionalisation. A phthalimide group was deemed to be the best way to install the desired functionality, not only because decomposition of this group with form the amine required in later steps, but also because the group should be unreactive to nitrating conditions.

Firstly, the phthalimido alkyl precursor **80** was prepared from 2-chloroethanol. Substitution using potassium phthalimide in dimethylformamide produced **80** in 93% yield after workup (Scheme 3.40). From **80**, esterification using *p*-toluenesulfonyl chloride in the presence of triethylamine and 4-dimethylaminopyridine gave the ester **81** in 39% yield. Successful esterification was supported by new ^{1}H NMR spectroscopy resonances at 7.67 and 7.14 ppm with an AA'XX' splitting pattern attributable to new aromatic protons, as well as a new aromatic methyl resonance at 2.30 ppm and an observed downfield shift of methylene protons adjacent to the ester. Formation of **81** was also supported by a peak in the low resolution ESI at *m*/*z* 368.1, corresponding to the $[M+Na]^+$ ion.

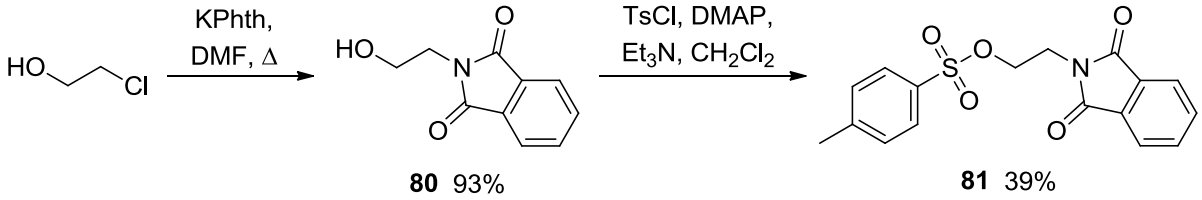

Scheme 3.40

With compound **81** in hand, the etherification to form alkylated chromans **82** and **83** was attempted. Three different methods were attempted for the etherification of ester **81** with chromans **40** and **41** (Scheme 3.41). Firstly, reaction of each chroman with **81** in the presence of bulky bases 1,4-diazabicyclo[2.2.2]octane (DABCO) and 1,8-diazabicycloundec-7-ene (DBU) was attempted.[35] A second method involved the use of potassium *tert*-butoxide in *tert*-butanol[36] and a third, use of sodium hydride in dry THF, was also attempted, in order to determine if a nucleophilic base would work, despite the likelihood of deacetylation. In each case none of the expected product was observed by mass spectrometry, and in the case of the sodium hydride, some evidence of deacetylation was observed in the mass spectrum, as expected for the use of a nucleophilic base.

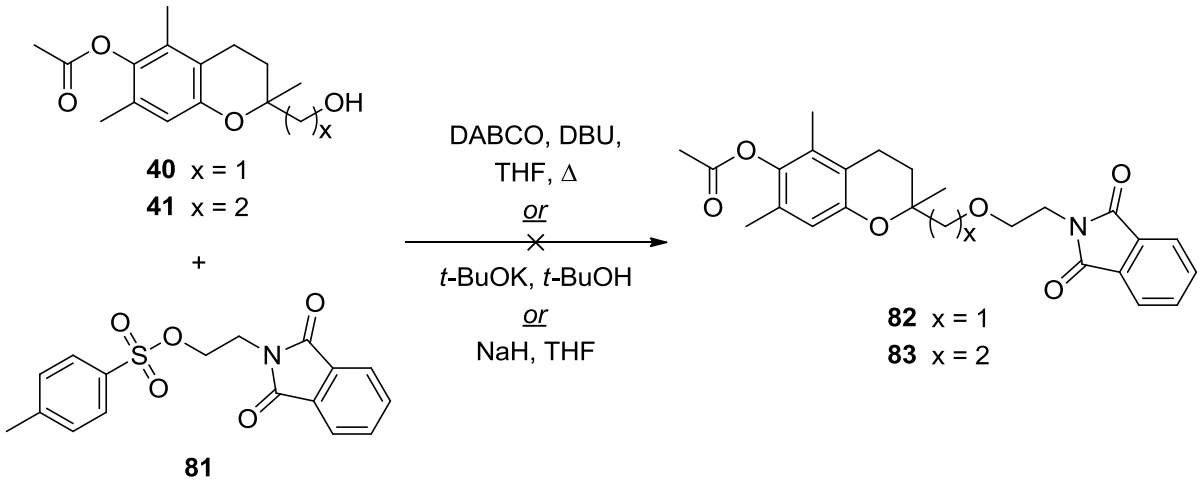

Scheme 3.41

Based on the assumption that once again steric problems were involved, specifically that the electrophile **81** was too bulky for the desired reactions to succeed, chloro derivative **85** was synthesised in two steps (Scheme 3.42). Firstly, from 2-chloroethanol, esterification using *p*-toluenesulfonyl chloride in the presence of 4-dimethylaminopyridine and triethylamine was performed, giving **84** in 80% yield, without the need for further purification. The product was identified by new AX signals in the ^{1}H NMR spectrumat 7.78 and 7.35 ppm and a new methyl peak at 2.43 ppm integrating to three protons, as well as a downfield shift of one of the methylene proton peaks from ~3.8 to 4.22 ppm. Low resolution mass spectrometry (ESI) also supported formation of **84**, with an $[M+Na]^+$ ion peak at m/z 257.1.

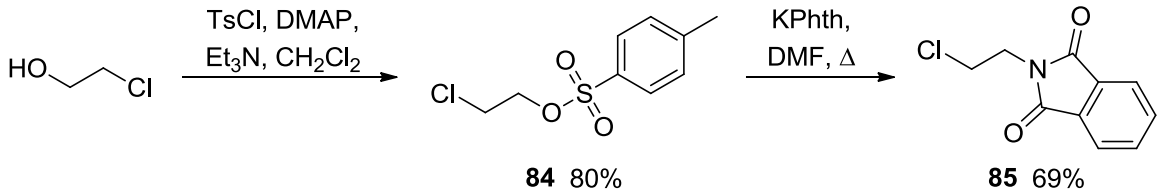

Scheme 3.42

From the ester, substitution with potassium phthalimide in dimethylformamide produced the phthalimide **85** in 69% yield (Scheme 3.42). None of the product resulting from the substitution of the chloride was observed spectroscopically, indicating that tosylate was a much better leaving group than the chloride. Total conversion the product **85** was supported primarily by the absence of distinctive aromatic peaks at 7.78 and 7.35 ppm in the ^{1}H NMR spectrum, as well as the absence of the aromatic methyl peak at 2.42 ppm. An upfield shift of one methylene

proton peak was also observed, from 4.22 ppm to 4.04 ppm, consistent with the conversion of the tosyl ester to the phthalimide.

The newly formed chloro compound **85** was used as a means of forming compound **82** on reaction with chroman **40** (Scheme 3.43). Attempted reaction of the two starting materials in the presence of DABCO and DBU[35] yielded none of the expected product, despite a new major spot being observed by thin layer chromatography, and a similar result was observed on attempted reaction of **40** and **85** using sodium hydride as the base, with no peak in the mass spectrum observed even for the deacetylated product of etherification.

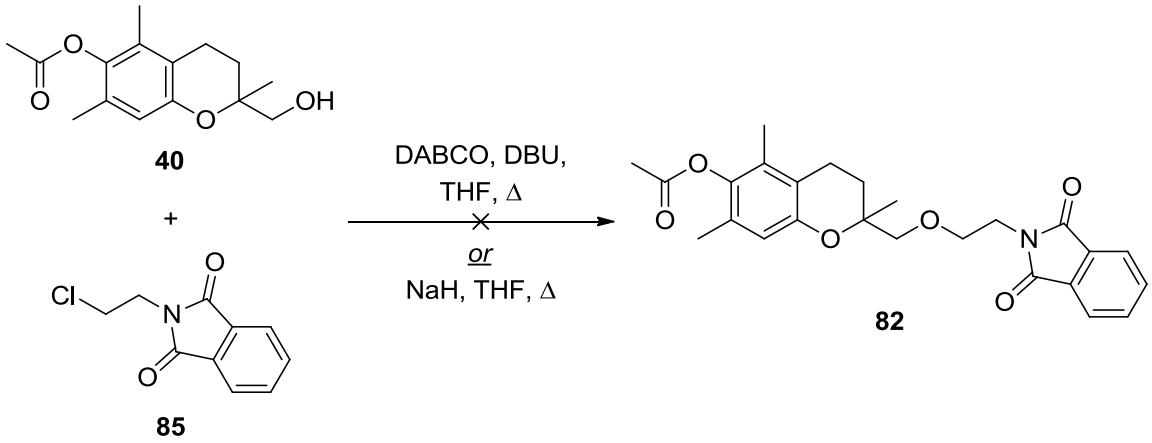

Scheme 3.43

At this point, an obvious alternative to the etherification of a previously formed chroman was to synthesise an alkene with the desired side chain already present, for reaction with bromo compound **61** to form a chroman with the required functionality off the C2 position (shown generally in Scheme 3.44).

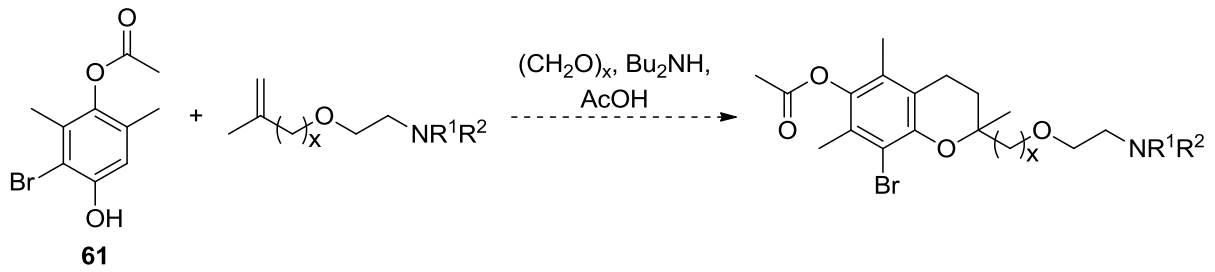

Scheme 3.44

In order to proceed with the synthetic route shown generally in Scheme 3.44, several attempts to form an appropriate functionalised ether were performed. Reaction of

2-methyl-2-propen-1-ol with two equivalents of sodium hydride to form the sodium alkoxide, followed by the addition of chloro compound **85** (Scheme 3.45),[37] did not form the expected ether **86**, rather *N*-vinylphthalimide (**88**), a byproduct formed from the elimination of hydrochloric acid from **85**. Similarly, reaction of 3-methyl-3-buten-1-ol with two equivalents of sodium hydride and phthalimide **85** yielded *N*-vinylphthalimide **88** instead of the expected longer chain ether **87** (Scheme 3.45). Both times, the elimination is expected to have occurred due to the excess of sodium hydride used. Formation of undesired product **88** was supported by low resolution ESI mass spectrometry, with a major peak at m/z 174.0 corresponding to the $[M+H]^+$ ion, as well as a distinctive AMX splitting pattern in the ^{1}H NMR spectrum at 6.87, 6.08 and 5.04 ppm, attributable to the vinyl protons. Repeating both experiments using 1.1 equivalents of sodium hydride,[37] as well as potassium *tert*-butoxide in *tert*-butanol,[36] recovered only starting material phthalimide **85** (Scheme 3.45).

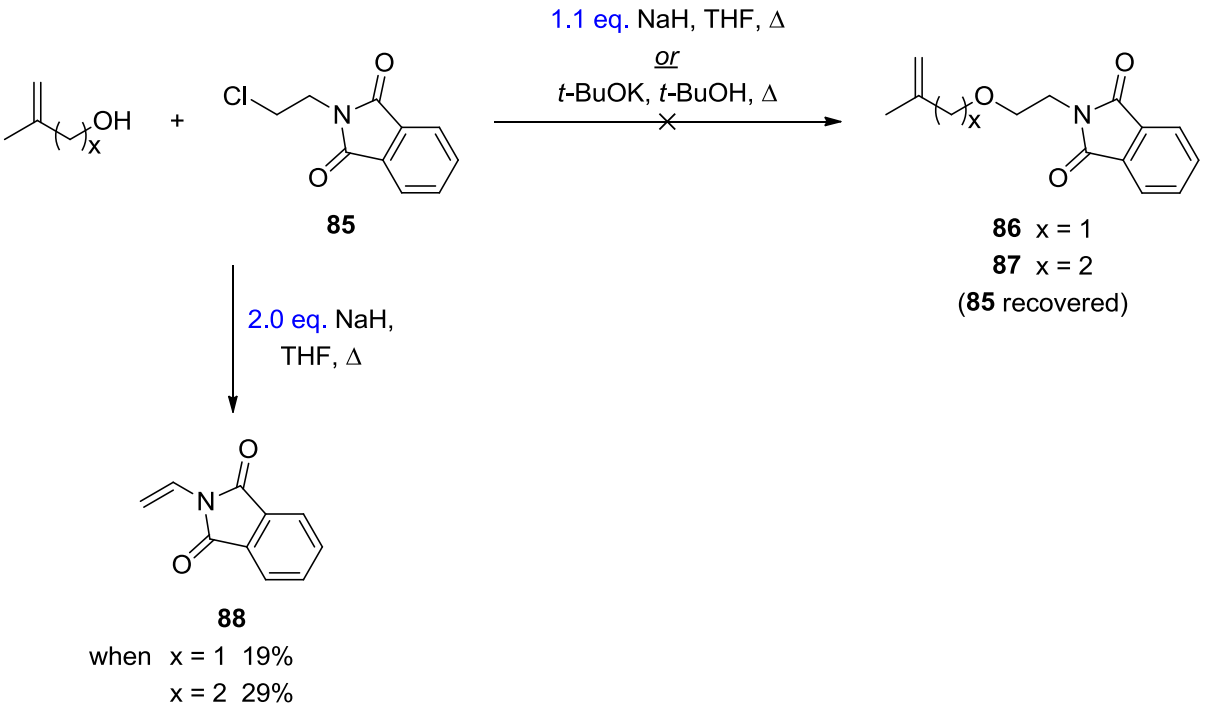

Scheme 3.45

In an alternative method towards the formation of ether **86**, attempted reaction of tosyl ester **70** with alcohol **80** in the presence of either sodium hydride in dry tetrahydrofuran or potassium *tert*-butoxide in *tert*-butanol did not yield the expected product, instead undergoing a side reaction to form previously synthesised phthalimide **71** (Scheme 3.46).[36,37]

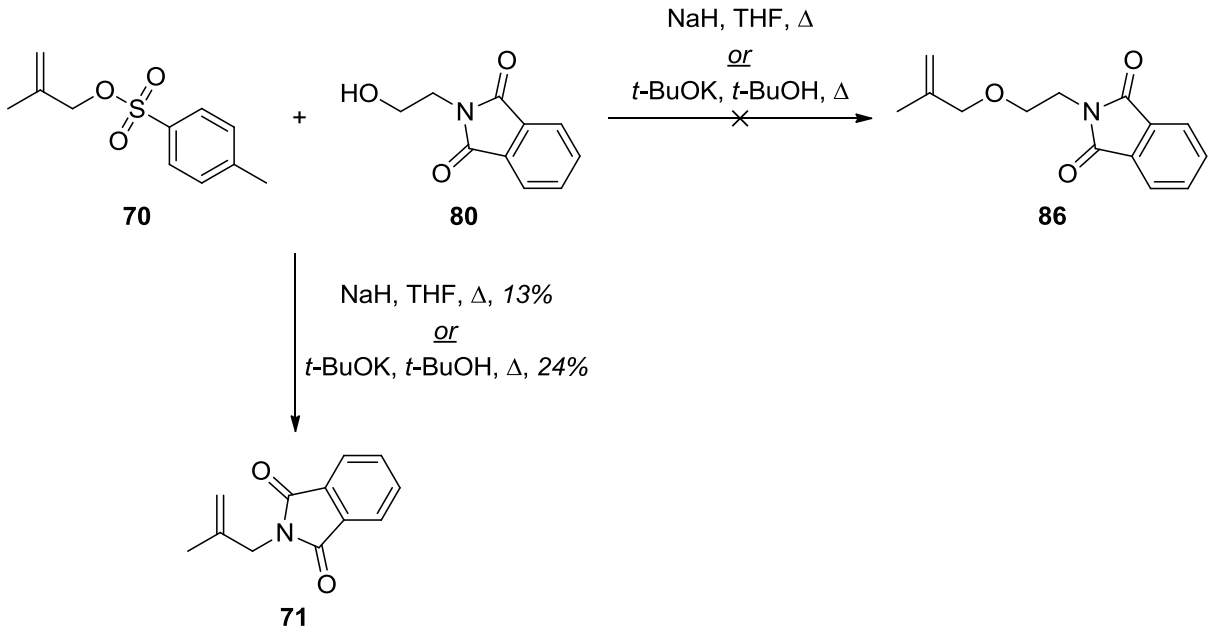

Scheme 3.46

Given that an alcohol should be more likely than an alkyl chain to deprotonate – although the phthalimide may play a promoting part – it is hypothesised that alcohol **80**, on deprotonation, undergoes a side reaction to eliminate a phthalimide anion, which may attack ester **70** to form **71** (Scheme 3.47).

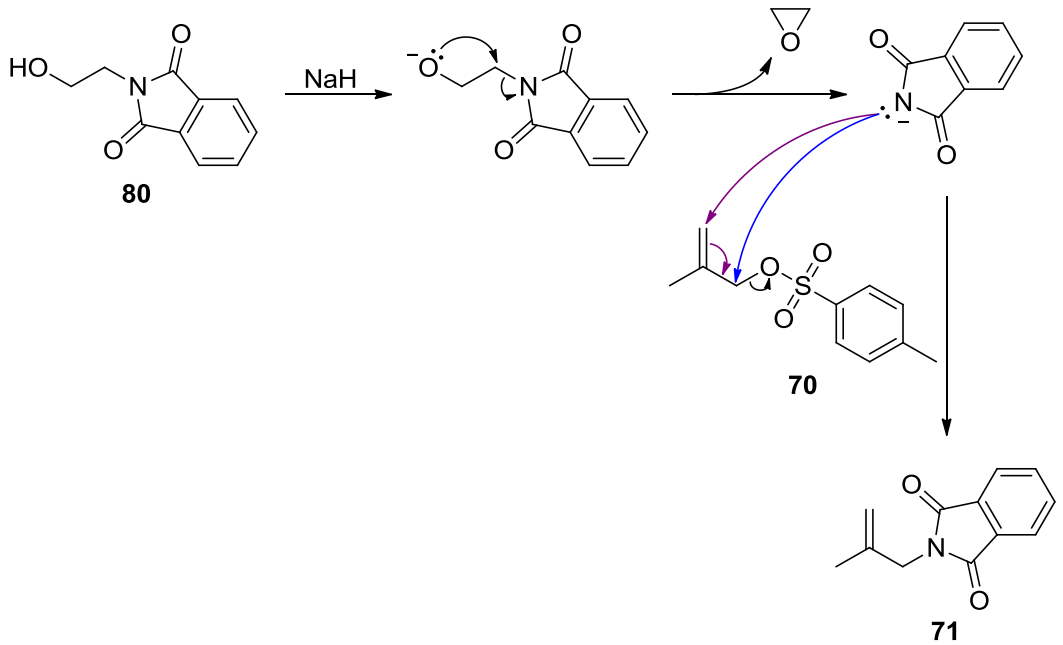

Scheme 3.47

Given that all attempts form to form a methallyl ether with an installed phthalimide group had failed, formation of an acetamide methallyl ether was attempted instead. Reaction of ester **70** with commercially available *N*-(2-hydroxyethyl)acetamide and sodium hydride in dry tetrahydrofuran formed the expected ether **89** in 36% yield after purification (Scheme 3.48).[37] Formation of **89** was supported by high resolution mass spectrometry, with a $[M+H]^+$ peak at m/z 158.1176. Proton and carbon NMR spectroscopy both also supported product formation, with the absence of resonances attributable to the tosyl group of **70**, as well as an upfield shift of the methylene resonance of ester **70** from 4.42 to 3.85 ppm.

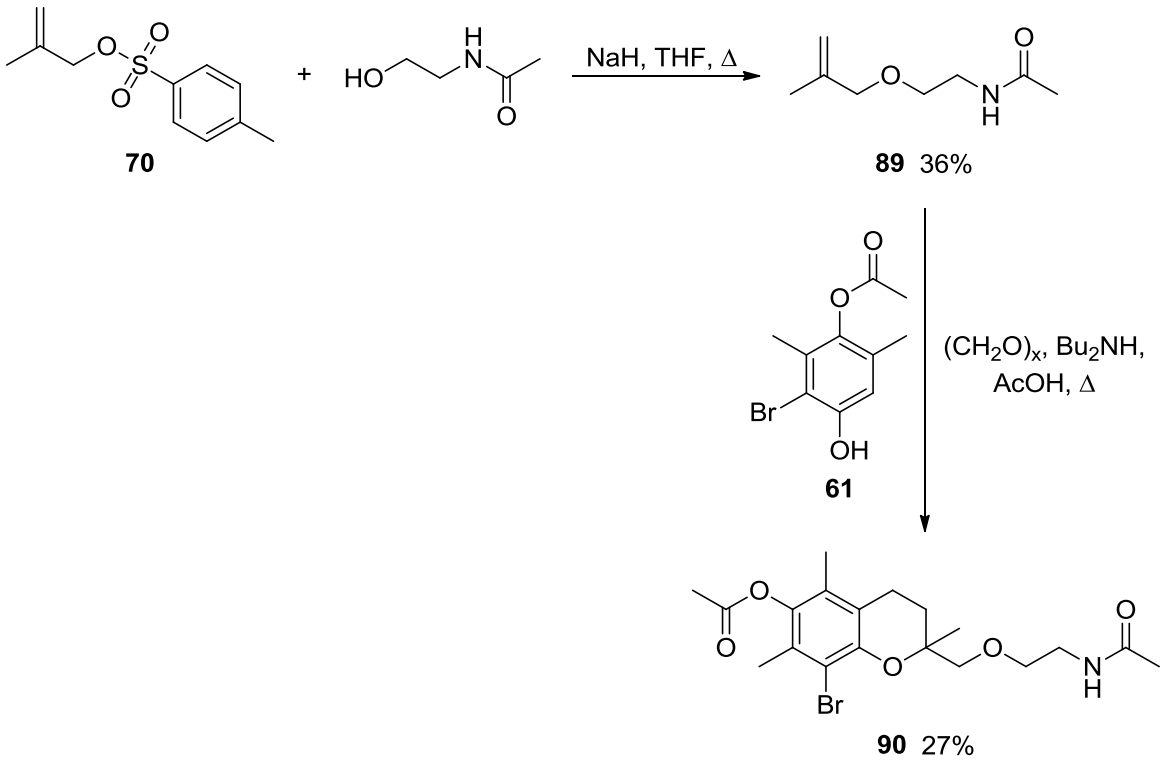

Scheme 3.48

From ether **89**, reaction with phenol **61** and paraformaldehyde in the presence of acetic acid and dibutylamine[20] produced the chroman **90** in 27% yield after purification by column chromatography. The ether **89** was used as the limiting reagent in this reaction because excess **61** was easier to remove by chromatography. Product formation was supported by the absence of the aromatic proton and vinyl proton peaks at around 6.74, 4.91 and 4.87 ppm, as well as the presence of the distinctive triplet at 2.65 ppm, indicative of the C4 protons of the chroman. High resolution ESI mass spectrometry also supported the formation of **90**, with peaks at m/z 428.1072 and m/z 430.1055 in a typical single bromine isotopic pattern, corresponding to the $[M+H]^+$ adduct.

With compound **90** in hand, it is anticipated that conversion of the aryl bromine to an aniline, hydrolysis of the acetate and acetamide groups and subsequent alkylation of the nitrogens would give target **B** (**91**), as shown in Scheme 3.49.

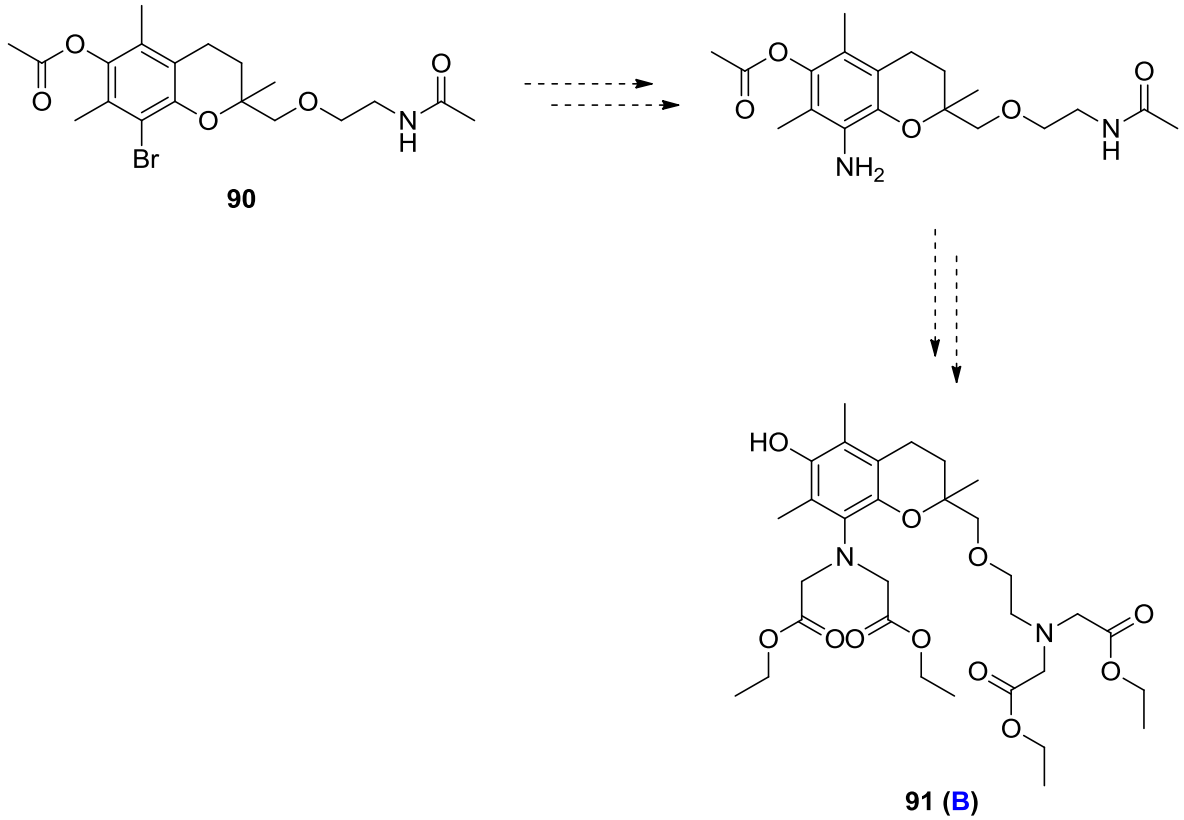

90 **91 (B)**

Scheme 3.49

3.7 Conclusion

In summary, we have explored various methods of chroman synthesis, introducing varied functionality off the C2 position, whilst allowing functionalisation at the C8 position. Synthesis of mono-protected tri- and dimethylhydroquinone allowed reaction with paraformaldehyde and various alkenes to form a variety of chromans functionalised at the C2 position. Chroman synthesis was also achieved *via* reaction of various alkenes with butoxymethyl intermediates, offering a slight increase in overall yields of 2,5,7-trimethyl chromans compared to the one-step reaction in each case.

Given the low yields of expected chromans obtained by reaction with mono-acetylated dimethylhydroquinone **39**, brominated analogue **61** was synthesised, allowing reaction with paraformaldehyde and various alkenes in a manner and yields similar to trimethylhydroquinone derivatives, however retaining the ability for further functionalisation at the C8 position. Bromo

chromans were synthesised in high yields and subsequently were successfully debrominated under reductive conditions to give C8-unsubstituted chromans.

At this point, two pathways towards the synthesis of vitamin E/BAPTA hybrids were envisaged. The first pathway, towards the synthesis of target **A**, involved attempts to install nitrogen functionality on the C2 chain by synthesising phthalimide intermediate **68**. While efforts to synthesise the desired intermediate – as well as acetamide derivatives – failed, the longer chained analogue **72** was successfully produced from bromo chroman **66**. It is expected that target **A** may be formed in approximately four steps from **72**.

The second pathway involved efforts towards the synthesis of target **B**. Several failed attempts were made to form phthalamidyl-functionalised C2 chains *via* etherification with chromans, thus it was alternatively hypothesised that the desired functionality could be installed by reacting functionalised alkenes with bromo intermediate **61**. Attempts to form phthalimidyl alkenes using etherification reactions all failed, often producing undesired byproducts, however acetamide **89** was successfully synthesised, allowing reaction with bromo intermediate **61** to form chroman **90**, which contained the desired backbone for future formation of target **B** (**91**).

3.8 Experimental details

Synthesis of 2,3,5-trimethyl-1,4-phenylene diacetate – 33:

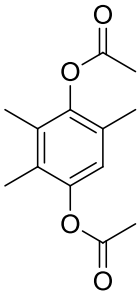

Trimethylhydroquinone (3.00 g, 19.7 mmol) was stirred in Ac_2O (7 mL) at room temperature, and Et_3N (2 mL) was added, turning the cloudy suspension to clear yellow solution. The reaction mixture was stirred overnight. On completion, water (40 mL) was added, and a pale yellow precipitate formed. The solid was filtered, washed with water and dried over vacuum to give **33** (4.34 g, 93%), a cream solid.

^{1}H NMR (300 MHz, $CDCl_3$) δ: 6.76, s, 1H, Ar-*H*; 2.33, s, 3H, -OCO-C*H*$_3$; 2.30, s, 3H, -OCO-C*H*$_3$; 2.12, s, 3H, Ar-C*H*$_3$; 2.07, s, 3H, Ar-C*H*$_3$; 2.06, s, 3H, Ar-C*H*$_3$. **^{13}C NMR (75 MHz, $CDCl_3$) δ:** 169.5 (*C*=O), 168.9 (*C*=O), 146.6, 145.9, 130.3, 128.4, 127.5, 121.3, 20.8, 20.5, 16.3, 13.2, 12.9. **MS (ESI, +ve):** *m/z* 259.1 $[M+Na]^+$. **HRMS (ESI, +ve):** *m/z* 237.1124 $[M+H]^+$, $C_{13}H_{16}O_4$ required *m/z* 237.1121; *m/z* 259.0943 $[M+Na]^+$, $C_{13}H_{16}O_4$ required *m/z* 259.0941. **MP:** 107.2-108.2°C (Literature[38]: 109-110°C).

Synthesis of 4-hydroxy-2,3,6-trimethylphenyl acetate – 34:

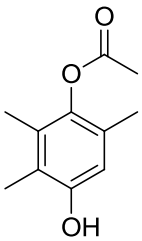

Adapted from Snuparek *et al.*[21] Diacetate **33** (1.00 g, 4.23 mmol) was dissolved in hot MeOH (4.5 mL), and $Na_2S_2O_4$ (55 mg, 0.32 mmol) and a solution of K_2CO_3 (155 mg, 1.12 mmol) in water (6 mL) were added slowly. The reaction was heated at 40°C for 1 h, then cooled to room temperature and allowed to stir overnight. Upon addition of 6 mL of cold (5°C) water the product precipitated, and was then filtered, washed with cold water and dried over vacuum to give **34** (794 mg, 97%), as a cream powder.

^{1}H NMR (300 MHz, $CDCl_3$) δ: 6.35, s, 1H, Ar-*H*; 5.28, s, 1H, Ar-O*H*; 2.34, s, 3H, -OCO-CH_3; 2.08, s, 3H, Ar-CH_3; 2.04, s, 3H, Ar-CH_3; 2.03, s, 3H, Ar-CH_3. **^{13}C NMR (75 MHz, $CDCl_3$) δ:** 170.3 (*C*=O), 151.4, 141.6, 129.6, 127.4, 121.6, 114.7, 20.6, 16.3, 13.1, 11.9. **MS (ESI, +ve):** *m/z* 194.8 $[M+H]^+$, 216.9 $[M+Na]^+$. **HRMS (ESI, +ve):** *m/z* 195.1020 $[M+H]^+$, $C_{11}H_{14}O_3$ required *m/z* 195.1016; *m/z* 217.0845 $[M+Na]^+$, $C_{11}H_{14}O_3$ required *m/z* 217.0835. **MP:** 106.3-107.3°C (Literature[39]: 106-107°C).

Synthesis of 2-(hydroxymethyl)-2,5,7,8-tetramethylchroman-6-yl acetate – 35:

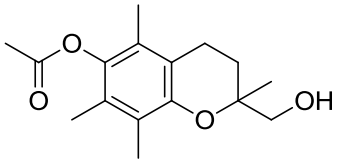

Method 1: Following Fukumoto *et al.*[20] Mono-protected hydroquinone **34** (1.00 g, 5.15 mmol), 2-methyl-2-propen-1-ol (2.18 mL, 25.8 mmol), 80% (w/w) paraformaldehyde (230 mg, 6.13 mmol), Bu_2NH (100 µL, 0.59 mmol) and glacial AcOH (150 µL, 2.6 mmol) were heated to 150°C in a pressure tube and the reaction was monitored by TLC (20% EtOAc/hexane). After 2 d, the reaction was allowed to cool, and the excess 2-methyl-2-propen-1-ol was distilled off to give **35**, (1.43 g, quant.), as a pale brown solid. *Method 2*: Adapted from Monoe *et al.*[26] Butoxymethyl compound **46** (200 mg, 0.713 mmol) and 2-methyl-2-propen-1-ol (200 µL, 2.36 mmol) were stirred neat in a pressure tube and heated to 150°C. The reaction was monitored by TLC, and when all starting material was observed to have been consumed after 2.5 d, the reaction was cooled, transferred into a round bottom flask with 5 mL of toluene. Solvent and excess 2-methyl-2-propen-1-ol were removed under reduced pressure to give the resulting chroman **35** (199 mg, quant.), as a pale brown solid. Product was pure by ^{1}H NMR spectroscopy and did not require further purification.

^{1}H NMR (300 MHz, $CDCl_3$) δ: 3.65/3.58, AB system, ^2J 10.7 Hz, 2H, -CH_2OH; 2.65, m, 2H, -CH_2CH$_2$-; 2.33, s, 3H, -OCO-CH_3; 2.10, s, 3H, Ar-CH_3; 2.03, s, 3H, Ar-CH_3; 2.02/1.73, m/m, 1H/1H, -CH$_2$CH_2-; 1.99, s, 3H, Ar-CH_3; 1.23, s, 3H, -CH_3. **^{13}C NMR (100 MHz, $CDCl_3$) δ:** 169.8 (*C*=O), 148.9, 141.2, 127.1, 125.3, 123.1, 117.5, 75.7, 69.4, 27.6, 20.9, 20.6, 20.2, 13.0, 12.2, 12.0. **MS (ESI, +ve):** *m/z* 279.1, $[M+H]^+$, 301.1 $[M+Na]^+$. **HRMS (ESI, +ve):** *m/z* 279.1588 $[M+H]^+$, $C_{16}H_{22}O_4$ required *m/z* 279.1591. **MP:** 87.1-88.6°C.

Synthesis of 2-(2-hydroxyethyl)-2,5,7,8-tetramethylchroman-6-yl acetate –36:

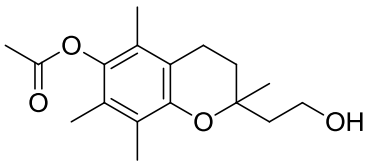

Method 1: Following Fukumoto *et al.*[20] Mono-protected hydroquinone **34** (813 mg, 4.19 mmol), 3-methyl-3-buten-1-ol (4.23 mL, 41.9 mmol), 80% (w/w) paraformaldehyde (173 mg, 4.61 mmol), Bu_2NH (71 µL, 0.42 mmol) and glacial AcOH (120 µL, 2.1 mmol) were heated to 150°C in a pressure tube and the reaction was monitored by TLC (20% EtOAc/hexane). After 2 d, the reaction was allowed to cool, and the excess 3-methyl-3-buten-1-ol was distilled off to give a brown oil. Purification by column chromatography (30%-50% EtOAc/hexane) gave chroman **36**, (956 mg, 78%), as a pale yellow oil that solidified to a cream solid over time. *Method 2*: Adapted from Monoe *et al.*[26] Butoxymethyl compound **46** (200 mg, 0.713 mmol) and 3-methyl-3-buten-1-ol (238 µL, 2.36 mmol) were stirred neat in a pressure tube and heated to 150°C. The reaction was monitored by TLC, and when all starting material was observed to have been consumed after 3 d, the reaction was cooled, transferred into a round bottom flask with 10 mL of toluene. Solvent and excess 3-methyl-3-buten-1-ol were removed under reduced pressure to give a brown oil. Purification by column chromatography (20% EtOAc/hexane to 50% EtOAc/hexane) gave the expected product **36** (143 mg, 69%), as a cream solid.

^{1}H NMR (300 MHz, $CDCl_3$) δ: 3.75, t, ^3J 6.7 Hz, 2H, -CH$_2$CH_2OH; 2.99, br s, 1H, -O*H*; 2.56, t, ^3J 6.7 Hz, 2H, -CH_2CH$_2$-; 2.25, s, 3H, -OCO-CH_3; 2.03, s, 3H, Ar-CH_3; 1.97, s, 3H, Ar-CH_3; 1.93, s, 3H, Ar-CH_3; 1.90-1.65, m, 4H, -CH$_2$CH_2-/-CH_2CH$_2$OH; 1.22, s, 3H, -CH_3. **^{13}C NMR (75 MHz, $CDCl_3$) δ:** 169.2 (*C*=O), 148.5, 140.7, 126.5, 124.8, 122.4, 117.0, 74.7, 58.2, 41.8, 31.2, 23.4, 20.1, 20.0, 12.5, 11.6, 11.5. **MS (ESI, +ve):** *m/z* 293.3 $[M+H]^+$, 315.3 $[M+Na]^+$. **HRMS (ESI, +ve):** *m/z* 315.1570 $[M+Na]^+$, $C_{17}H_{24}O_4$ required *m/z* 315.1567; *m/z* 331.1302 $[M+K]^+$, $C_{17}H_{24}O_4$ required *m/z* 331.1306. **MP:** 74.4-75.8°C.

Synthesis of 2,6-dimethylhydroquinone – 37:

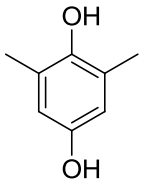

Method 1: Adapted from Emerson and Smith.[22] 2,6-Dimethylbenzoquinone (3.00 g, 22.0 mmol) was dissolved in glacial AcOH (18 mL), and water (9 mL) and Zn powder (3.00 g, 45.9 mmol) were added, forming a dark red solution. The mixture was heated at reflux until colourless (~45 min), then diluted with 10 mL of boiling water. The reaction mixture was decanted and filtered, and the remaining Zn powder was heated further with boiling water (30 mL), and decanted and filtered again. Product precipitated from the darkening filtrates on cooling to ~0°C overnight. The precipitate was filtered, washed (H_2O) and dried *in vacuo* to give 2,6-dimethylhydroquinone **37** (2.27 g, 75%), as cream needles. *Method 2*: Adapted from Carpino *et al*.[23] Sodium dithionite (26.1 g, 150 mmol) was dissolved in water (180 mL) and a solution of 2,6-dimethylbenzoquinone (5.95 g, 37.5 mmol) in a mixture of Et_2O (90 mL) and MeOH (55 mL) was slowly added at room temperature. After vigorous stirring for 15 min, the mixture was placed in a separating funnel and the layers were allowed to separate. The ether phase was removed and the aqueous phase was extracted twice with 65 mL portions of ether. The combined ether extracts were washed with H_2O (100 mL) and brine (100 mL), dried ($MgSO_4$), filtered and the solvent removed under reduced pressure to give a tan solid. The product was recrystallised from hot $CHCl_3$ and filtered over vacuum to give 2,6-dimethylhydroquinone **37** (4.06 g, 79%), a cream solid. *Method 3*: From Baker and Brown.[24] 3,5-Dimethylphenol (50.0 g, 409 mmol) was dissolved in 10% NaOH solution (820 mL, 2.05 mol), and a saturated aqueous solution of potassium persulfate (112 g, 414 mmol) was added slowly over 3 h, not allowing the reaction mixture to rise above 20°C. As the potassium persulfate was added, the solution darkened from colourless to dark brown. The reaction mixture was left stirring overnight, after which time the reaction mixture was acidified to pH 3 using 6 M HCl solution. The solution was extracted with 300 mL portions of Et_2O until the organic phase was a pale yellow colour. The organic extracts were combined, washed with H_2O, dried ($MgSO_4$), filtered and the solvent removed *in vacuo* to give recovered 3,5-dimethylphenol (19.70 g), as a brown solid. The remaining acidic aqueous solution was further acidified with 6 M HCl solution to pH 1, and the product was extracted with 300 mL portions of Et_2O until the organic phase was a pale yellow colour. These organic extracts were combined, washed with H_2O, dried ($MgSO_4$), filtered and the solvent removed *in vacuo* to give 2,6-dimethylhydroquinone **37** (20.5 g, 36%; recovered yield: 60%), as a brown solid.

^{1}H NMR (300 MHz, $CDCl_3$/d_6-DMSO) δ: 6.32, s, 2H, Ar-*H*; 5.29, br s, 2H, Ar-O*H*; 2.06, s, 6H, Ar-CH_3. **^{13}C NMR (75 MHz, $CDCl_3$/d_6-DMSO) δ:** 149.7, 145.6, 125.2, 114.8, 16.4. **MS (EI):** *m*/*z* 138 $[M]^+$. **MP:** 150.9-152.3°C (Literature[40]: 153-154°C).

Synthesis of 2,6-dimethyl-1,4-phenylene diacetate – 38:

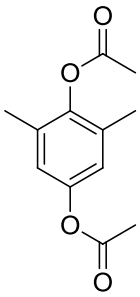

2,6-Dimethylhydroquinone **37** (5.00 g, 36.2 mmol) was stirred in Ac_2O (28 mL) at room temperature, and Et_3N (7.5 mL) was added, turning the cloudy suspension to clear yellow solution. The reaction mixture was stirred for 4 d. On completion, water (150 mL) was added, and the product was extracted with $CHCl_3$ (2 × 100 mL), washed with H_2O (2 × 100 mL), dried with $MgSO_4$, filtered and the solvent removed *via* rotary evaporation to give **38** (8.04 g, quant.), as a pale brown solid. Product was used in subsequent reactions without further purification.

^{1}H NMR (300 MHz, $CDCl_3$) δ: 6.80, s, 2H, Ar-*H*; 2.33, s, 3H, -OCO-C*H*$_3$; 2.26, s, 3H, -OCO-C*H*$_3$; 2.14, s, 3H, Ar-C*H*$_3$. **^{13}C NMR (75 MHz, $CDCl_3$) δ:** 169.6 (*C*=O), 168.8 (*C*=O), 147.9, 145.8, 131.5, 121.4, 21.2, 20.5, 16.5. **MS (ESI, +ve):** *m/z* 245.0 $[M+Na]^+$. **MP:** 91.5-93.4°C (Literature[38]: 92-93°C).

Synthesis of 4-hydroxy-2,6-dimethylphenyl acetate – 39:

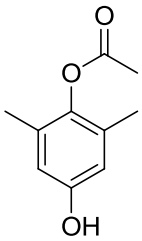

Method 1: Adapted from Snuparek *et al.*[21] Bis-protected hydroquinone **38** (7.75 g, 34.9 mmol) was stirred in MeOH (33 mL) at 50°C, before cooling to 35°C, and $Na_2S_2O_4$ (435 mg, 2.50 mmol) and a solution of K_2CO_3 (1.21 g, 8.75 mmol) in water (45 mL) were added slowly. The reaction was stirred at 40°C for 1 h, then cooled to room temperature. Upon addition of 50 mL of cold (5°C) water, the product precipitated, and the reaction mixture was left to stir overnight. The thick white precipitate that was formed was filtered and washed with H_2O to give product **39** (6.16 g, 98%), a white powder. *Method 2*: Adapted from Back *et al.*[30] Dibromo compound **63** (113 mg, 0.334 mmol) was dissolved in a mixture of 4.5 mL of MeOH and 1.5 mL of THF. Nickel chloride hexahydrate was added, and the reaction was cooled to 0°C. Sodium borohydride was added slowly in portions, and H_2 gas evolved from the reaction. When the reaction settled, the mixture was heated at reflux for 5 h, after which time the reaction appeared by TLC to be complete. The reaction mixture was filtered and the product washed through with EtOAc. The filtrate, a cloudy white mixture, was concentrated by rotary evaporation to give a pale yellow solid (87 mg). The residue was taken up in EtOAc and washed with H_2O, before drying over $MgSO_4$, filtration and removal of solvent *in vacuo* to give debrominated product **39** (58 mg, 97%), as a cream solid. Crystals of **39** suitable for X-ray crystallography were grown by slow evaporation from ethyl acetate.

^{1}H NMR (300 MHz, $CDCl_3$) δ: 6.44, s, 2H, Ar-*H*; 5.31, s, 1H, Ar-O*H*; 2.32, s, 3H, -OCO-CH_3; 2.07, s, 6H, -CH_3. **^{13}C NMR (75 MHz, $CDCl_3$) δ:** 170.0 (*C*=O), 153.3, 141.8, 131.1, 115.3, 20.6, 16.5. **MS (ESI, +ve):** *m*/*z* 202.9 $[M+Na]^+$. **MS (ESI, -ve):** *m*/*z* 178.9 $[M-H]^-$. **MP:** 109.6-110.2°C (Literature[41]: 104-105°C). **X-ray crystal data:** $C_{10}H_{12}O_3$, M = 180.20, colourless prism, 0.25 × 0.20 × 0.13 mm^3, orthorhombic, space group $P2_12_12_1$, a = 7.1666(4), b = 11.4345(6), c = 11.6327(6) Å, $\alpha = \beta = \gamma$ = 90.00°, V = 953.26(9) Å^3, Z = 4, D_c = 1.256 g/cm^3, F_{000} = 384, T = 123(2) K, $2\theta_{max}$ = 58.0°, 5270 reflections collected, 1467 unique (R_{int} = 0.0207]). Final *GoF* = 1.076, *R1* = 0.0330, *wR2* = 0.0831, *R* indices based on 1344 reflections with I>2σ(I) (refinement on F^2), 125 parameters, 0 restraints. Lp and absorption corrections applied, μ = 0.092 mm^{-1}.

Synthesis of 2-(hydroxymethyl)-2,5,7-trimethylchroman-6-yl acetate – 40:

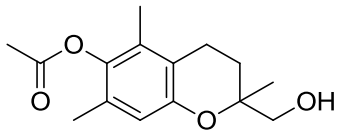

Method 1: Adapted from Fukumoto *et al.*[20] Mono-protected hydroquinone **39** (200 mg, 1.11 mmol), 2-methyl-2-propen-1-ol (470 µL, 5.54 mmol), 80% (w/w) paraformaldehyde (46 mg, 1.23 mmol), Bu_2NH (57 µL, 0.34 mmol) and glacial AcOH (32 µL, 0.56 mmol) were combined in a pressure tube, degassed with N_2 for 30 min, and heated to 150°C. After 2 d, the reaction was allowed to cool, toluene (5 mL) was added, and solvents were distilled off *in vacuo* to give a brown oil. Purification by column chromatography (50% EtOAc/hexane) yielded **40**, (80 mg, 27%), as a pale brown oil. *Method 2*: Adapted from Monoe *et al.*[26] Butoxymethyl compound **58** (1.00 g, 3.77 mmol) and 2-methyl-2-propen-1-ol (1.05 mL, 12.4 mmol) were stirred neat in a pressure tube and heated to 150°C. The reaction was monitored by TLC, and when all starting material was observed to have been consumed after 8 d, the reaction was cooled, transferred into a round bottom flask with 3 mL of toluene. Solvent and excess 2-methyl-2-propen-1-ol were removed under reduced pressure to give the resulting chroman **40** (669 mg, 67%), as a pale brown oil. Product was pure by ^{1}H NMR spectroscopy and did not require purification. *Method 3 (attempted)*: Adapted from Kiehlmann *et al.*[31] A solution of chroman **65** (43 mg, 0.13 mmol) in MeOH (3 mL) was added to a solution of anhydrous Na_2SO_3 (95 mg, 0.754 mmol) in the H_2O (2.5 mL) and the flask was shaken for 10 min. After this time, the solvent was removed by rotary evaporation at 40°C and the reaction mixture underwent extraction with EtOAc (4 × 10 mL) and was washed with H_2O (20 mL) and the organic phased dried ($MgSO_4$), filtered and concentrated under reduced pressure to give a brown oil (43 mg). Proton NMR showed only starting material. *Method 4 (attempted)*: Adapted from Boyer *et al.*[32] Chroman **65** (107 mg, 0.312 mmol) was dissolved in dry THF (2 mL) and cooled to -75°C under Schlenk conditions. tert-Butyl lithium (420 µL, 0.714 mmol) was added and the reaction stirred for

30 min, during which time a pale yellow precipitate formed, before the reaction mixture was warmed to room temperature and stirred overnight. Diethyl ether (10 mL) and H_2O (1 mL) were added to the reaction flask, the organic phase was separated and the aqueous phase was extracted with diethyl ether (2 × 10 mL). The combined organic phase was washed with brine (30 mL), dried ($MgSO_4$), filtered and the solvent removed by rotary evaporation to give a cloudy pale brown oil (111 mg). The ^{1}H NMR spectrum showed 20% conversion to the debrominated chroman **40**. *Method 5 (attempted)*: Adapted from Back *et al*.[30] Chroman **65** (47 mg, 0.14 mmol) was dissolved in 3 mL of MeOH and 1 mL of THF, $NiCl_2.6H_2O$ (326 mg, 1.37 mmol) was added and the solution was cooled to 0°C. Sodium borohydride (156 mg, 4.12 mmol) was added slowly over 2 h and the reaction mixture bubbled vigorously. The reaction was allowed to warm to room temperature overnight, over which time a black solid formed. The reaction mixture was heated at reflux for 2 d, during which time the reaction was monitored by TLC. When the starting material had appeared to be consumed, the reaction was allowed to cool and filtered through celite and the solvent removed under reduced pressure to give a pale yellow solid (77 mg). Proton NMR showed only partial (< 20%) conversion to the debrominated compound **40**. *Method 6*: Adapted from Rey *et al*.[33] Bromo chroman **65** (1.24 g, 3.60 mmol) was stirred in MeOH (20 mL), and Et_3N (2.0 mL) was added, dissolving the starting material. To the solution, 10% Pd/C (126 mg) was added, and the reaction vessel was purged with nitrogen, before a H_2 balloon was applied. The reaction was stirred at room temperature for 4 d, and on completion, the reaction mixture was filtered through celite and washed with MeOH, and the solvent was removed by rotary evaporation, to give a greyish yellow solid (1.51 g). Chromatography using a silica plug (ethyl acetate) gave chroman **40** (950 mg, quant.), as a pale yellow oil.

^{1}H NMR (300 MHz, $CDCl_3$) δ: 6.54, s, 1H, Ar-*H*; 3.60/3.54, AB system, ^2J 11.4 Hz, 2H, -C*H*$_2$OH; 2.62, m, 2H, -C*H*$_2$CH$_2$-; 2.31, s, 3H, -OCO-C*H*$_3$; 2.05, s, 3H, Ar-C*H*$_3$; 2.02/1.71, m/m, 1H/1H, -CH$_2$C*H*$_2$-; 1.99, s, 3H, Ar-C*H*$_3$; 1.22, s, 3H, -C*H*$_3$. **^{13}C NMR (100 MHz, $CDCl_3$) δ:** 169.6 (*C*=O), 150.9, 141.5, 128.9, 128.7, 118.2, 116.7, 75.8, 69.1, 27.6, 20.6, 20.5, 20.0, 16.4, 12.3. **MS (ESI, +ve):** *m*/*z* 287.3 $[M+Na]^+$. **HRMS (ESI, +ve):** *m*/*z* 265.1438 $[M+H]^+$, $C_{15}H_{20}O_4$ required *m*/*z* 265.1434; *m*/*z* 287.1258 $[M+Na]^+$, $C_{15}H_{20}O_4$ required *m*/*z* 287.1254.

Synthesis of 2-(2-hydroxyethyl)-2,5,7-trimethylchroman-6-yl acetate – 41:

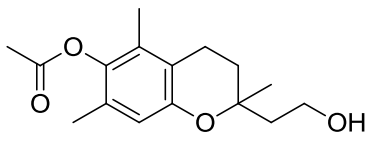

Method 1: Adapted from Fukumoto *et al*.[20] Mono-protected hydroquinone **39** (200 mg, 1.11 mmol), 3-methyl-3-buten-1-ol (470 µL, 5.54 mmol), 80% (w/w) paraformaldehyde (46 mg,

1.23 mmol), Bu_2NH (57 µL, 0.34 mmol) and glacial AcOH (32 µL, 0.56 mmol) were combined in a pressure tube, degassed with N_2 for 30 min, and heated to 150°C. After 2 d, the reaction was allowed to cool, toluene (5 mL) was added, and solvents were distilled off *in vacuo* to give a brown oil. Purification by column chromatography (50% EtOAc/hexane) yielded **41**, (20 mg, 6%), as a yellow oil. *Method 2*: Adapted from Monoe *et al*.[26] Butoxymethyl compound **58** (222 mg, 0.834 mmol) and 3-methyl-3-buten-1-ol (278 µL, 2.75 mmol) were stirred neat in a pressure tube and heated to 150°C. The reaction was monitored by TLC, and when all starting material was observed to have been consumed after 4 d, the reaction was cooled, transferred into a round bottom flask with 5 mL of toluene. Solvent and excess 3-methyl-3-buten-1-ol were removed under reduced pressure to give a brown oil (231 mg). Purification by column chromatography (50% EtOAc/hexane) yielded chroman **41** (73 mg, 31%), as a yellow oil. *Method 3*: Adapted from Rey *et al*.[33] Bromo chroman **66** (420 mg, 1.18 mmol) was stirred in MeOH (6.5 mL), and Et_3N (0.7 mL) was added, dissolving the starting material. To the solution, 10% Pd/C (42 mg) was added, and the reaction vessel was purged with nitrogen, before a H_2 balloon was applied. The reaction was stirred at room temperature for 5 d, and on completion, the reaction mixture was filtered through celite and washed with MeOH, and the solvent was removed by rotary evaporation, to give chroman **41** (250 mg, 76%) as a yellow oil.

^{1}H NMR (300 MHz, $CDCl_3$) δ: 6.52, s, 1H, Ar-*H*; 3.87, m, 2H, -CH_2CH_2OH; 2.63, t, ^3J 6.3 Hz, 2H, -CH_2CH_2-; 2.32, s, 3H, -OCO-CH_3; 2.07, s, 3H, Ar-CH_3; 2.00, s, 3H, Ar-CH_3; 1.97-1.72, m, 4H, -CH_2CH_2-/-CH_2CH_2OH; 1.30, s, 3H, -CH_3. **^{13}C NMR (75 MHz, $CDCl_3$) δ:** 169.7 (*C*=O), 150.9, 141.8, 129.1, 128.9, 118.3, 116.9, 76.2, 59.4, 42.1, 31.8, 23.8, 20.8, 20.5, 16.6, 12.5. **MS (ESI, +ve):** *m/z* 301.3 $[M+Na]^+$. **MS (ESI, -ve):** *m/z* 277.3 $[M-H]^-$. **HRMS (ESI, -ve):** *m/z* 277.1446 $[M-H]^-$, $C_{16}H_{22}O_4$ required *m/z* 277.1445.

Synthesis of methyl 6-hydroxy-2,5,7,8-tetramethylchroman-2-carboxylate – 42:

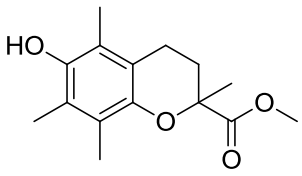

From Tamura.[17] Trimethylhydroquinone (500 mg, 3.29 mmol), methyl methacrylate (1.76 mL, 16.5 mmol), 80% (w/w) paraformaldehyde (247 mg, 6.58 mmol) and glacial AcOH (95 µL, 1.7 mmol) were combined in a pressure tube. The reaction mixture was degassed with N_2, and heated at 180°C for 3 h, after which time the reaction was cooled to room temperature, forming a precipitate. The product was filtered, washed with cold MeOH and dried over vacuum to give ester **42** (490 mg, 56%), as a cream powder.

^{1}H NMR (400 MHz, $CDCl_3$) δ: 4.20, br s, 1H, Ar-O*H*; 3.67, s, 3H, -O-CH_3; 2.64/2.52, m/m, 1H/1H, -CH_2CH_2-; 2.42/1.87, m/m, 1H/1H, -CH_2CH_2-; 2.18, s, 3H, Ar-CH_3; 2.16, s, 3H, Ar-CH_3; 2.07, s, 3H, Ar-CH_3; 1.60, s, 3H, -CH_3. **^{13}C NMR (75 MHz, $CDCl_3$) δ:** 174.6 (*C*=O), 145.7, 145.4, 122.8, 121.3, 118.5, 117.1, 77.4, 52.5, 30.8, 25.6, 21.1, 12.4, 12.0, 11.4. **MS (ESI, +ve):** *m/z* 265.2 $[M+H]^+$, 287.2 $[M+Na]^+$. **MP:** 161.8-162.9°C (Literature[42]: 162-164°C).

Synthesis of methyl 6-hydroxy-2,5,7-trimethylchroman-2-carboxylate – 43:

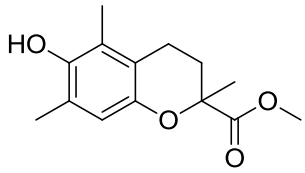

Adapted from Tamura.[17] 2,6-Dimethylhydroquinone **37** (200 mg, 1.45 mmol), methyl methacrylate (775 µL, 7.25 mmol), 80% (w/w) paraformaldehyde (61 mg, 1.63 mmol) and glacial AcOH (42 µL, 0.73 mmol) were combined in a pressure tube. The reaction mixture was degassed with N_2, and heated at 180°C for 33 h, during which time the reaction was monitored by TLC. When all starting material appeared to have been consumed, the reaction mixture was cooled to room temperature, giving a brown oil. The oil was transferred into an RBF with 5 mL of toluene and 5 mL of MeOH, and solvent was removed by rotary evaporation, to give a pale brown solid (203 mg). Purification by column chromatography (20% EtOAc/hexane) gave 8 mg (2%) of ester **43**, as a cream solid.

^{1}H NMR (400 MHz, $CDCl_3$) δ: 6.61, s, 1H, Ar-*H*; 4.23, br s, 1H Ar-O*H*; 3.69, s, 3H, -O-CH_3; 2.64/2.52, m/m, 1H/1H, -CH_2CH_2-; 2.42/1.87, m/m, 1H/1H, -CH_2CH_2-; 2.19, s, 3H, Ar-CH_3; 2.08, s, 3H, Ar-CH_3; 1.58, s, 3H, -CH_3. **^{13}C NMR (100 MHz, $CDCl_3$) δ:** 174.4 (*C*=O), 147.2, 146.0, 122.6, 121.9, 117.9, 116.1, 77.4, 52.6, 30.7, 25.4, 20.9, 16.2, 11.5. **MS (ESI, +ve):** *m/z* 273.2 $[M+Na]^+$. **HRMS (ESI, +ve):** *m/z* 251.1277 $[M+H]^+$, $C_{14}H_{18}O_4$ required *m/z* 251.1278; *m/z* 273.1099 $[M+Na]^+$, $C_{14}H_{18}O_4$ required *m/z* 273.1097. **MP:** 106.4-108.2°C.

Attempted synthesis of 2-(2-hydroxyethyl)-2,5,7,8-tetramethylchroman-6-ol – 44:

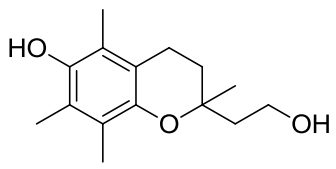

Adapted from Tamura.[17] Trimethylhydroquinone (500 mg, 3.29 mmol), 3-methyl-3-buten-1-ol (1.66 mL, 16.4 mmol), 80% (w/w) paraformaldehyde (248 mg, 6.61 mmol) and glacial AcOH (95 µL, 1.7 mmol) were combined in a pressure tube. The reaction mixture was degassed with N_2, and heated at 180°C for 3.5 h, during which time the reaction was

monitored for the consumption of the hydroquinone. The reaction was cooled to room temperature and the excess 3-methyl-3-buten-1-ol was removed by rotary evaporation. The product was filtered, washed with cold MeOH and dried over vacuum to give a white solid (79 mg). The filtrate was extracted with EtOAc, washed with H_2O and concentrated *in vacuo* to give a brown oil (581 mg). Neither residue appeared to be the desired product **44** by mass spectrometry or ^{1}H NMR spectroscopy.

Synthesis of 3-(butoxymethyl)-4-hydroxy-2,5,6-trimethylphenyl acetate – 46:

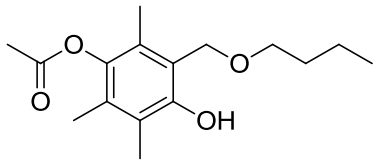

From Monoe *et al.*[26] Protected hydroquinone **34** (1.00 g, 5.15 mmol), 80% (w/w) paraformaldehyde (220 mg, 5.86 mmol), *n*-butanol (3.00 mL, 32.8 mmol), Bu_2NH (87 µL, 0.52 mmol) and glacial AcOH (148 µL, 2.57 mmol) were combined in a pressure tube, which was heated at 100°C overnight. On completion, the reaction flask was cooled, and 10 mL toluene was added. The organic solvent was washed with H_2O (2 × 10 mL), and the organic solvent was removed under reduced pressure to give pure **46** (1.44 g, quant.), as a pale brown waxy solid.

^{1}H NMR (400 MHz, $CDCl_3$) δ: 8.24, s, 1H, Ar-O*H*; 4.73, s, 2H, Ar-C*H*$_2$-O-; 3.56, t, ^3J 6.5 Hz, -O-C*H*$_2$(CH$_2$)$_2$CH$_3$; 2.32, s, 3H, -OCO-CH$_3$; 2.16, s, 3H, Ar-C*H*$_3$; 2.04, s, 3H, Ar-C*H*$_3$; 2.00, s, 3H, Ar-C*H*$_3$; 1.63, m, 2H, -O-CH$_2$C*H*$_2$CH$_2$CH$_3$; 1.39, m, 2H, -O-(CH$_2$)$_2$C*H*$_2$CH$_3$; 0.93, t, ^3J 7.4 Hz, 3H, -O-(CH$_2$)$_3$C*H*$_3$. **^{13}C NMR (100 MHz, $CDCl_3$) δ:** 169.4 (*C*=O), 152.3, 140.7, 128.9, 124.2, 122.4, 118.0, 70.7, 68.9, 31.5, 20.3, 19.2, 13.7, 13.0, 12.0, 11.6. **MS (ESI, +ve):** *m/z* 303.2 [M+Na]$^+$. **HRMS (ESI, +ve):** *m/z* 303.1569 [M+Na]$^+$, $C_{16}H_{24}O_4$ required *m/z* 303.1567. **MP:** 52.7-55.2°C.

Synthesis of 3-methylbut-3-enyl acetate – 47:

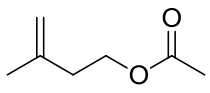

3-Methyl-3-buten-1-ol (5.0 mL, 50 mmol) and Ac_2O (23 mL, 240 mmol) were stirred in a round bottom flask and cooled to 0°C. Triethylamine (14 mL, 100 mmol) was added to the solution. The reaction was stirred and slowly allowed to warm to room temperature, and was left overnight, over which time the solution had turned from clear and colourless to a dark brown colour. The product was extracted with CH_2Cl_2, washed with H_2O, dried ($MgSO_4$), and filtered. The filtrate solvent was removed at room temperature by rotary

evaporation to give **47** (5.65 g, 89%), as a dark brown oil. ^{1}H NMR spectroscopy indicated pure product, which was used in subsequent reactions without further purification.

^{1}H NMR (300 MHz, $CDCl_3$) δ: 4.73, s, 1H, C=C-*H*; 4.67, s, 1H, C=C-*H*; 4.11, t, ^{3}J 6.9 Hz, 2H, -CH_2CH_2-O-; 2.27, t, ^{3}J 6.9 Hz, 2H, -CH_2CH_2-O-; 1.97, s, 3H, -OCO-CH_3; 1.69, s, C=C-CH_3. **^{13}C NMR (75 MHz, $CDCl_3$) δ:** 170.9 (*C*=O), 141.7, 112.2, 62.6, 36.7, 22.4, 20.8.

Synthesis of 2-(6-acetoxy-2,5,7,8-tetramethylchroman-2-yl)ethyl – 48:

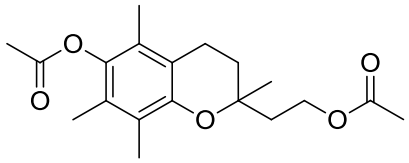

Adapted from Monoe *et al.*[26] Butoxymethyl compound **46** (400 mg, 1.43 mmol) and 3-methylbut-3-enyl acetate **47** (610 mg, 4.76 mmol) were stirred neat in a pressure tube and heated to 150°C. The reaction was monitored by TLC, and when all starting material was observed to have been consumed after 40 h, the reaction was cooled, transferred into a round bottom flask with toluene (10 mL). Solvent and excess 3-methylbut-3-enyl acetate were removed under reduced pressure to give a clear, pale brown oil. Purification by column chromatography (20% EtOAc/hexane to 100% EtOAc) gave the expected product **48** (237 mg, 50%), as a clear yellow oil. The hydrolysed alcohol **36** (52 mg, 12%) was also isolated during purification.

^{1}H NMR (300 MHz, $CDCl_3$) δ: 4.27, m, 2H, -CH_2CH_2-O-; 2.62, t, ^{3}J 6.8 Hz, 2H, -CH_2CH_2-; 2.33, s, 3H, Ar-OCO-CH_3; 2.10, s, 3H, Ar-CH_3; 2.04, s, 3H, aliphatic -OCO-CH_3; 2.03, s, 3H, Ar-CH_3; 1.99, s, 3H, Ar-CH_3; 2.0-1.8, m, -CH_2CH_2-O-/-CH_2CH_2-; 1.30, s, 3H, -CH_3. **^{13}C NMR (75 MHz, $CDCl_3$) δ:** 171.1 (*C*=O), 169.6 (*C*=O), 148.9, 141.0, 127.0, 125.1, 123.2, 117.1, 73.8, 60.8, 38.1, 31.7, 24.2, 21.0, 20.5, 20.4, 13.0, 12.1, 11.9. **MS (ESI, +ve):** *m/z* 357.3 $[M+Na]^+$. **HRMS (ESI, +ve):** *m/z* 357.1674 $[M+Na]^+$, $C_{19}H_{26}O_5$ required *m/z* 357.1672.

Synthesis of methyl 6-acetoxy-2,5,7,8-tetramethylchroman-2-carboxylate – 49:

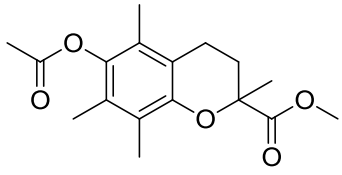

Adapted from Monoe *et al.*[26] Butoxymethyl compound **46** (200 mg, 0.713 mmol) and methyl methacrylate (252 µL, 2.36 mmol) were stirred neat in a pressure tube and heated to 150°C. The reaction was monitored by TLC, and when all starting material was

observed to have been consumed after 2 d, the reaction was cooled, and excess methyl methacrylate was removed under reduced pressure to give the ester **49** (211 mg, 97%), as a pale brown waxy solid.

^{1}H NMR (400 MHz, $CDCl_3$) δ: 3.66, s, 3H, -O-C*H*$_3$; 2.65/2.42, m/m, 1H/1H, -C*H*$_2$CH$_2$-; 2.32, s, 3H, -OCO-C*H*$_3$; 2.18, s, 3H, Ar-C*H*$_3$; 2.05/1.86, 1H/1H, -CH$_2$C*H*$_2$-; 2.04, s, 3H, Ar-C*H*$_3$; 1.61, s, 3H, -C*H*$_3$. **^{13}C NMR (100 MHz, $CDCl_3$) δ:** 174.1 (*C*=O), 169.0 (*C*=O), 152.4, 141.4, 127.1, 124.9, 123.0, 117.1, 77.3, 52.3, 30.2, 25.4, 20.8, 20.5, 12.9, 12.0, 11.8. **MS (ESI, +ve):** *m*/*z* 307.2 $[M+H]^+$, 329.2 $[M+Na]^+$. **MP:** 103.5-104.3°C (Literature[42]: 104-105°C).

Synthesis of 3-methylbut-3-enyl 4-methylbenzenesulfonate – 50:

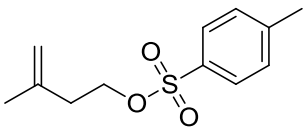

3-Methyl-3-buten-1-ol (5.00 mL, 49.5 mmol), DMAP (1.21 g, 9.90 mmol) and Et_3N (14.0 mL, 101 mmol) were dissolved in CH_2Cl_2 (20 mL), and the reaction mixture was stirred and cooled to 0°C. *p*-Toluenesulfonyl chloride (18.9 g, 99.2 mmol) was added slowly over 5 min, after which time the mixture thickened, requiring a further 5 mL of CH_2Cl_2 to be added to the flask. The reaction was allowed to warm to room temperature overnight. After 24 h, the solvent was removed by rotary evaporation, and the product extracted with EtOAc (100 mL). The organic phase was washed with saturated aqueous solutions of NH_4Cl (100 mL) and brine (100 mL), followed by washing with water (2 × 100 mL). The organic solvent was dried with $MgSO_4$, filtered, and the solvent removed *in vacuo* to give ester **50** (11.13 g, 94%), a pale, clear yellow oil.

^{1}H NMR (300 MHz, $CDCl_3$) δ: 7.79/7.33, AA'XX' system, ^3J 8.3 Hz, 4H, Ts-*H*; 4.79, m, 1H, C=C-*H*; 4.67, m, 1H, C=C-*H*; 4.13, t, ^3J 6.9 Hz, 2H, -CH$_2$C*H*$_2$-O-; 2.45, s, 3H, Ar-C*H*$_3$; 2.35, t, ^3J 6.8 Hz, 2H, -C*H*$_2$CH$_2$-O-; 1.66, s, 3H, C=C-C*H*$_3$. **^{13}C NMR (75 MHz, $CDCl_3$) δ:** 144.7, 140.1, 133.1, 129.8, 127.7, 112.9, 68.5, 36.6, 22.1, 21.4. **MS (ESI, +ve):** *m*/*z* 263.2 $[M+Na]^+$.

Synthesis of *N*-(3-methylbut-3-enyl)phthalimide – 51:

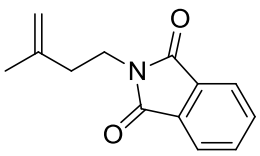

Ester **50** (7.65 g, 31.8 mmol) was dissolved in DMF (30 mL) and potassium phthalimide salt (12.0 g, 64.8 mmol) was added. The resulting slurry was stirred at room temperature for 3 d, after which time ^{1}H NMR spectroscopy showed approximately 70% conversion. The reaction was then stirred at 100°C

for 24 h until conversion was complete. The reaction mixture was filtered while hot to remove excess potassium phthalimide salt, and 150 mL of CH_2Cl_2 was added to the filtrate, forming a gel-like precipitate. The mixture was washed with saturated $NaHCO_3$ solution (150 mL) and H_2O (150 mL), and the solvent was dried over $MgSO_4$, filtered and removed under reduced pressure to give a concentrated yellow solution in DMF. Water was added and the flask cooled to promote precipitation, and the resulting solid was filtered and washed with H_2O to give a cream solid (8.2 g). Purification by column chromatography (20% EtOAc/hexane) gave phthalimide **51** (6.30 g, 92%), as a white solid.

^{1}H NMR (300 MHz, $CDCl_3$) δ: 7.82, m, 2H, Phth-*H*; 7.69, m, 2H, Phth-*H*; 4.73, m, 1H, C=C-*H*; 4.67, m, 1H, C=C-*H*; 3.82, t, ^3J 7.2 Hz, 2H, -CH_2CH_2-N-; 2.40, t, ^3J 7.1 Hz, -CH_2CH_2-N-; 1.81, s, 3H, -CH_3. **^{13}C NMR (75 MHz, $CDCl_3$) δ:** 167.7 (*C*=O), 141.8, 133.5, 131.9, 122.8, 112.4, 36.1, 36.0, 21.7. **MS (ESI, +ve):** *m*/*z* 238.2 $[M+Na]^+$. **MP:** 49.5-51.1°C (Literature[43]: 51-52°C).

Synthesis 2-(2-phthalimidylethyl)-2,5,7,8-tetramethylchroman-6-yl acetate – 52:

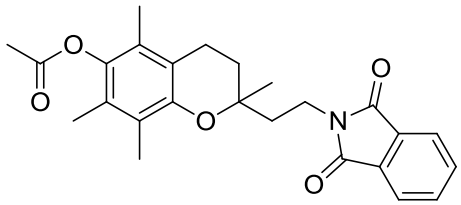

Adapted from Monoe *et al.*[26] Butoxymethyl compound **46** (212 mg, 0.740 mmol) and phthalimide **51** (526 mg, 2.44 mmol) were dissolved in toluene (0.5 mL), and the reaction mixture was stirred and heated to 150°C in a pressure tube for 2 d. The reaction was monitored by TLC. On cooling to room temperature, 10 mL of toluene was added, transferred into an RBF and the solvent was removed by rotary evaporation, to give a pale brown solid (720 mg). Purification by column chromatography (20% EtOAc/hexane to 100% EtOAc) yielded phthalimide **52** (154 mg, 49%), as a white solid.

^{1}H NMR (300 MHz, $CDCl_3$) δ: 7.81, m, 2H Phth-*H*; 7.68, m, 2H, Phth-*H*; 3.90, t, ^3J 8.3 Hz, 2H, -CH_2CH_2-N-; 2.64, t, ^3J 6.6 Hz, 2H, -CH_2CH_2-; 2.32, s, 3H, -OCO-CH_3; 2.07, s, Ar-CH_3; 2.01, s, 3H, Ar-CH_3; 1.98, s, 3H, Ar-CH_3; 1.90, m, 4H, -CH_2CH_2-N-/-CH_2CH_2-; 1.33, s, 3H, -CH_3. **^{13}C NMR (75 MHz, $CDCl_3$) δ:** 169.7 (*C*=O), 168.3 (*C*=O), 149.0, 141.0, 133.9, 132.4, 127.0, 125.1, 123.3, 123.2, 117.2, 74.0, 38.6, 33.6, 31.0, 23.7, 20.6, 20.5, 13.0, 12.2, 11.9. **MS (ESI, +ve):** *m*/*z* 422.2 $[M+H]^+$, 444.2 $[M+Na]^+$. **HRMS (ESI, +ve):** *m*/*z* 444.1784 $[M+Na]^+$, $C_{25}H_{27}NO_5$ required *m*/*z* 444.1781. **MP:** 160.2-160.9°C.

Synthesis of 2-(hydroxymethyl)-5,7,8-trimethylchroman-6-yl acetate (53) and 3-((allyloxy)methyl)-4-hydroxy-2,5,6-trimethylphenyl acetate (54):

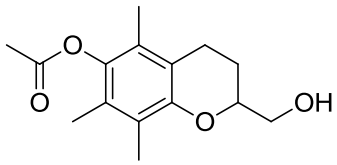

53

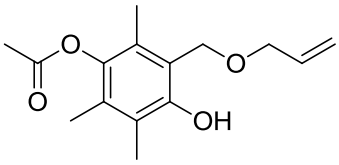

54

Adapted from Monoe *et al.*[26] Butoxymethyl compound **46** (200 mg, 0.713 mmol) and allyl alcohol (160 µL, 2.35 mmol) were stirred and heated to 150°C in a pressure tube for 2 d, and monitored by TLC. When starting material had been consumed, the vessel was cooled to room temperature and the solvent and excess allyl alcohol were removed by rotary evaporation to give a brown oil. Purification by column chromatography (20% EtOAc/hexane to 100% EtOAc) gave the expected chroman **53** (12 mg, 6%), as a pale yellow oil, and allyl ether **54** (67 mg, 35%), as a pale yellow oil.

*Characterisation of **53**:* **^{1}H NMR (300 MHz, $CDCl_3$) δ:** 4.30, m, 1H, -C*H*-; 3.80, m, 2H, -CH_2OH; 2.69, m, 2H, -CH_2CH_2-; 2.33, s, 3H, -OCO-CH_3; 2.12, s, 3H, Ar-CH_3; 2.04, 2H, 3H, Ar-CH_3; 1.98, s, 3H, Ar-CH_3; 1.82, m, 2H, -CH_2CH_2-. **^{13}C NMR (100 MHz, $CDCl_3$) δ:** 169.8 (*C*=O), 150.2, 141.4, 127.1, 125.6, 122.9, 118.5, 75.7, 65.9, 23.8, 22.9, 20.7, 13.0, 12.2, 12.0. **MS (ESI, +ve):** *m*/*z* 265.3 $[M+H]^+$, 287.3 $[M+Na]^+$. **HRMS (ESI, +ve):** *m*/*z* 265.1436 $[M+H]^+$, $C_{15}H_{20}O_4$ required *m*/*z* 265.1434.

*Characterisation of **54**:* **^{1}H NMR (300 MHz, $CDCl_3$) δ:** 7.92, br s, 1H, Ar-O*H*; 5.94, ddt, ^3J 16.7, 10.4, 5.6 Hz, 1H, C=C*H*-CH_2; 5.32, dq, ^3J 17.2 Hz, ^2J 1.5 Hz, 1H, C=C-*H*; 5.26, dq, ^3J 10.4 Hz, ^2J 1.3 Hz, 1H, C=C-*H*; 4.75, s, 2H, Ar-CH_2-O-; 4.08, dt, ^3J 5.7 Hz, ^4J 1.3 Hz, 2H, OCH_2-CH=CH_2; 2.32, s, 3H, -OCO-CH_3; 2.16, s, 3H, Ar-CH_3; 2.05, s, 3H, Ar-CH_3; 2.01, s, 3H, Ar-CH_3. **^{13}C NMR (75 MHz, $CDCl_3$) δ:** 169.5 (*C*=O), 152.5, 141.1, 133.6, 129.4, 124.7, 122.8, 118.4, 118.0, 71.4, 67.9, 20.5, 13.2, 12.2, 11.8. **MS (ESI, +ve):** *m*/*z* 287.1 $[M+Na]^+$. **MS (ESI, -ve):** *m*/*z* 263.1 $[M-H]^-$. **HRMS (ESI, +ve):** *m*/*z* 287.1249 $[M+Na]^+$, $C_{15}H_{20}O_4$ required *m*/*z* 287.1254.

Synthesis of *N*-allylacetamide – 56:

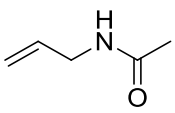

From Stille and Becker.[27] Acetic anhydride (10.7 mL, 113 mmol) was stirred to 0°C and allylamine (5.00 mL, 66.6 mmol) was added dropwise, with stirring. When all allylamine had been added and gas evolution had subsided, the

reaction mixture was heated to 100°C for 90 min. After this time, fractional distillation under reduced pressure (100°C at 10 mmHg) isolated the acetamide **56** (6.45 g, 98%), as a colourless oil.

^{1}H NMR (400 MHz, $CDCl_3$) δ: 6.67, s, 1H, -N*H*; 5.69, ddt, ^3J 17.2, 10.3, 5.6 Hz, 1H, C=C*H*-CH_2; 5.04, dq, ^3J 17.2 , ^2J 1.6 Hz, 1H, C=C-*H*; 4.97, dq, ^3J 10.3 Hz, ^2J 1.5 Hz, 1H, C=C-*H*; 3.71, tt, ^3J 5.7 Hz, ^4J 1.6 Hz, -CH_2-; 1.87, s, 3H, -NCO-CH_3. **^{13}C NMR (75 MHz, $CDCl_3$) δ:** 170.3 (*C*=O), 134.2, 115.8, 41.8, 22.8. **MS (ESI, +ve):** *m/z* 122.1 $[M+Na]^+$.

Synthesis of 3-((*N*-allylacetamido)methyl)-4-hydroxy-2,5,6-trimethylphenyl acetate – 57:

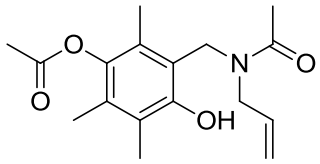

Adapted from Monoe *et al*.[26] Butoxymethyl compound **46** (200 mg, 0.698 mmol) and *N*-allylacetamide **56** (228 mg, 2.30 mmol) were combined in a pressure tube, degassed with N_2, and heated to 150°C for 2.5 d. The reaction was monitored by TLC. On consumption of starting material, the reaction was cooled, to give a yellow solid. The product was dissolved in EtOAc (50 mL), washed with H_2O (50 mL) and the solvent removed under reduced pressure to give a pale yellow solid (242 mg). Purification by column chromatography (20% EtOAc/hexane to 100% EtOAc) gave allylacetamide **57** (43 mg, 20%), as a yellow oil.

^{1}H NMR (400 MHz, $CDCl_3$) δ: 9.51, br s, 1H, Ar-O*H*; 5.80, ddt, ^3J 17.2, 10.5, 4.4 Hz, 1H, C=C*H*-CH_2; 5.31, dq, ^3J 10.4 Hz, ^2J 0.7 Hz, 1H, C=C-*H*; 5.23, dq, ^3J 17.3 Hz, ^2J 0.7 Hz, 1H, C=C-*H*; 4.64, br s, 1H, Ar-C*H*-N-; 4.52, br s, 1H, Ar-C*H*-N-; 3.86, s, 2H, NCH_2-CH=C; 2.33, s, 3H, -OCO-CH_3; 2.17, s, 3H, Ar-CH_3; 2.12, s, 3H, Ar-CH_3; 2.11, s, 3H, Ar-CH_3; 2.04, s, 3H, NCO-CH_3. **^{13}C NMR (75 MHz, $CDCl_3$) δ:** 174.0 (*C*=O), 169.7 (*C*=O), 152.8, 140.7, 131.6, 130.2, 126.0, 123.5, 118.3, 117.1, 50.1, 41.6, 29.8, 21.0, 20.6, 13.4, 12.6. **MS (ESI, +ve):** *m/z* 306.2 $[M+H]^+$, 328.3 $[M+Na]^+$. **HRMS (ESI, +ve):** *m/z* 328.1524 $[M+Na]^+$, $C_{17}H_{23}NO_4$ required *m/z* 328.1519.

Synthesis of 3-(butoxymethyl)-4-hydroxy-2,6-dimethylphenyl acetate (58) and 3,5-bis(butoxymethyl)-4-hydroxy-2,6-dimethylphenyl acetate (59):

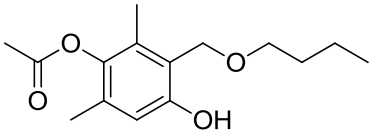

58

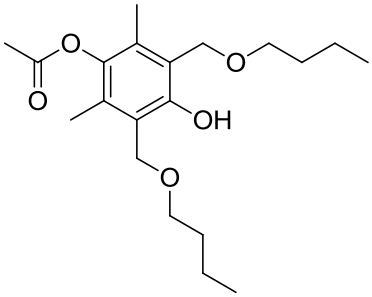

59

Adapted from Monoe *et al.*[26] Mono-acetoxy dimethylhydroquinone **39** (1.00 g, 5.55 mmol) and 80% (w/w) paraformaldehyde (206 mg, 5.49 mmol) were dissolved in toluene (53 mL), and *n*-butanol (3.30 mL, 36.1 mmol), Bu_2NH (94 µL, 0.55 mmol) and glacial AcOH (160 µL, 2.78 mmol) were added to the reaction mixture, which was stirred and heated to 100°C, and monitored by TLC. When the reaction had appeared to stop progressing after 5.5 d, the reaction mixture was cooled to room temperature, and the solvent removed *in vacuo* to give a brown oil (1.18 g). Purification by column chromatography (20% EtOAc/hexane to 100% EtOAc) recovered starting material (203 mg), butoxymethyl compound **58** (778 mg, 53%; recovered yield: 66%), as pale brown solid, and bis-alkylated product **59** (354 mg, 37%), as a yellow oil.

*Characterisation of **58**:* **^{1}H NMR (400 MHz, $CDCl_3$) δ:** 8.07, br s, 1H, Ar-O*H*; 6.60, s, 1H, Ar-*H*; 4.74, s, 2H, Ar-CH_2-O-; 3.56, t, ^3J 6.5 Hz, 2H, -O-CH_2(CH_2)$_2$$CH_3$; 2.31, s, 3H, -OCO-$CH_3$; 2.08, s, 3H, Ar-C$H_3$; 2.00, s, 3H, Ar-C$H_3$; 1.63, m, 2H, -O-$CH_2CH_2$$CH_2$$CH_3$; 1.40, m, 2H,-O-($CH_2$)$_2CH_2$$CH_3$; 0.93, t, ^3J 7.4 Hz, 3H, -O-(CH_2)$_3$CH_3. **^{13}C NMR (100 MHz, $CDCl_3$) δ:** 169.5 (*C*=O), 154.3, 141.1, 130.7, 127.7, 118.9, 116.3, 71.1, 69.2, , 31.7, 20.5, 19.4, 16.5, 13.9, 12.3. **MS (ESI, +ve):** *m*/*z* 289.2 $[M+Na]^+$, 305.2 $[M+K]^+$. **MS (ESI, -ve):** *m*/*z* 265.2 $[M-H]^-$. **HRMS (ESI, +ve):** *m*/*z* 284.1857 $[M+NH_4]^+$, $C_{15}H_{22}O_4$ required *m*/*z* 284.1856; *m*/*z* 305.1149 $[M+K]^+$, $C_{15}H_{22}O_4$ required *m*/*z* 305.1150. **MP:** 58.1-59.2°C.

*Characterisation of **59**:* **^{1}H NMR (400 MHz, $CDCl_3$) δ:** 8.42, s, 1H, Ar-O*H*; 4.66, br s, 4H, Ar-CH_2-O-; 3.52, t, ^3J 6.7 Hz, 4H, -O-CH_2(CH_2)$_2$$CH_3$; 2.32, s, 3H, -OCO-$CH_3$; 2.08, s, 6H, Ar-C$H_3$; 1.59, m, 4H, -O-$CH_2CH_2$$CH_2$$CH_3$; 1.38, m, 4H,-O-($CH_2$)$_2CH_2$$CH_3$; 0.91, t, ^3J 7.4 Hz, 6H, -O-(CH_2)$_3$CH_3. **^{13}C NMR (100 MHz, $CDCl_3$) δ:** 169.5 (*C*=O), 153.4, 141.2, 129.3, 120.6, 70.5, 66.5, 31.9, 20.5, 19.4, 14.0, 12.5. **MS (ESI, +ve):** *m*/*z* 375.3 $[M+Na]^+$. **MS (ESI, -ve):** *m*/*z* 351.3 $[M-H]^-$. **HRMS (ESI, +ve):** *m*/*z* 375.2144 $[M+Na]^+$, $C_{20}H_{32}O_5$ required *m*/*z* 375.2142.

Synthesis of 2-(2-phthalimidylethyl)-2,5,7-trimethylchroman-6-yl acetate – 60:

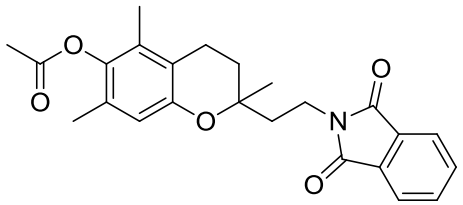

Adapted from Monoe *et al.*[26] Butoxymethyl compound **58** (213 mg, 0.800 mmol) and phthalimide **51** (568 mg, 2.64 mmol) were dissolved in toluene (0.5 mL), and the reaction mixture was stirred and heated to 150°C in a pressure tube for 8 d. The reaction was monitored by TLC, and the reaction was stopped when all starting material appeared to have been consumed. On cooling to room temperature, toluene (3 mL) was added, the solution transferred into an RBF and the solvent was removed by rotary evaporation, to give a brown solid (619 mg). Purification by column chromatography (20% EtOAc/hexane to 100% EtOAc) yielded phthalimide **60** (32 mg, 10%; recovered yield: 12%), as a cream solid.

^{1}H NMR (300 MHz, $CDCl_3$) δ: 7.82, m, 2H, Phth-*H*; 7.69, m, 2H, Phth-*H*; 6.28, s, 1H, Ar-*H*; 3.86, m, 2H, -CH_2CH_2-N-; 2.62, m, 2H, -CH_2CH_2-; 2.30, s, 3H, -OCO-CH_3; 2.08/1.86, m/m, 2H/2H, -CH_2CH_2-/-CH_2CH_2-N-; 1.98, s, 3H, Ar-CH_3; 1.96, s, 3H, Ar-CH_3; 1.35, s, 3H, -CH_3. **^{13}C NMR (75 MHz, $CDCl_3$) δ:** 169.5 (*C*=O), 168.3 (*C*=O), 150.9, 141.3, 133.9, 132.5, 128.7, 128.5, 123.3, 117.8, 116.7, 74.3, 37.5, 33.6, 31.2, 23.7, 20.6, 20.3, 16.4, 12.3. **MS (ESI, +ve):** *m/z* 430.1 $[M+Na]^+$. **HRMS (ESI, +ve):** *m/z* 425.2072 $[M+NH_4]^+$, $C_{24}H_{25}NO_5$ required *m/z* 425.2071. **MP:** 106.6-109.1°C.

Synthesis of 3-bromo-4-hydroxy-2,6-dimethylphenyl acetate – 61:

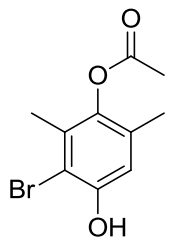

Method 1: Adapted from Snuparek *et al.*[21] Diacetate **62** (113 mg, 0.375 mmol) was dissolved in hot MeOH (3 mL), and both $Na_2S_2O_4$ (7 mg, 40 μmol) and a solution of K_2CO_3 (20 mg, 0.14 mmol) in water (2 mL) were added slowly. The reaction was heated at 45°C for 1.5 h, then cooled to room temperature and allowed to stir overnight. After addition of 10 mL of cold water, the product was extracted with EtOAc (2 × 25 mL), washed with H_2O (2 × 50 mL), dried over $MgSO_4$, and filtered. Removal of solvent by rotary evaporation afforded **61** (78 mg, 80%), as a pale brown solid. *Method 2*: Adapted from Smith and Wiley.[28] Mono-protected hydroquinone **39** (1.05 g, 5.80 mmol) was dissolved in glacial AcOH (25 mL), and a solution of Br_2 (312 μL, 6.09 mmol) in glacial AcOH (8 mL) was added dropwise. The reaction was stirred at room temperature overnight, before rapid removal of the solvent by rotary evaporation to give brominated product

61 (1.50 g, quant.), as a pale yellow solid. *Method 3*: Adapted from Friedli and Shechter.[29] Protected hydroquinone **39** (100 mg, 0.555 mmol) was dissolved in $CHCl_3$ (5 mL), and $FeBr_3$ (33 mg, 0.112 mmol) was added. The reaction mixture was cooled to 0°C, before dropwise addition of a solution of Br_2 (28.5 µL, 0.556 mmol) in 1 mL $CHCl_3$. The reaction was stirred at room temperature for 3 d, monitored by TLC. On completion, H_2O was added, and the product was extracted with EtOAc, washed with H_2O, dried over $MgSO_4$, filtered and the solvent removed by rotary evaporation to give **61** (129 mg, 90%), as a pale brown solid. Crystals of **61** suitable for X-ray crystallography were grown by vapor diffusion from chloroform, using hexane as the precipitant.

^{1}H NMR (300 MHz, $CDCl_3$) δ: 6.74, s, 1H, Ar-*H*; 5.57, s, 1H, Ar-O*H*; 2.33, s, 3H; -OCO-C*H*$_3$; 2.21, s, 3H, Ar-C*H*$_3$; 2.08, s, 3H, Ar-C*H*$_3$. **^{13}C NMR (75 MHz, $CDCl_3$) δ:** 169.3 (*C*=O), 150.2, 141.6, 130.8, 130.6, 114.9, 110.6, 20.5, 17.1, 16.5. **MS (ESI, -ve):** *m/z* 256.9 $[M-H]^-$ (^{79}Br), 259.0 $[M-H]^-$ (^{81}Br). **HRMS (ESI, -ve):** *m/z* 256.9820 $[M-H]^-$, $C_{10}H_{11}{}^{79}BrO_3$ required *m/z* 256.9813; *m/z* 258.9800 $[M-H]^-$, $C_{10}H_{11}{}^{81}BrO_3$ required *m/z* 258.9793. **MP:** 96.5-98.1°C. **X-ray crystal data:** $C_{10}H_{11}BrO_3$, M = 259.10, colourless prism, 0.30 × 0.20 × 0.10 mm^3, monoclinic, space group $P2_1/c$, a = 9.0829(19), b = 8.984(2), c = 13.158(3) Å, $\alpha = \gamma = 90.00°$, β = 99.576(7)°, V = 1058.7(4) Å^3, Z = 4, D_c = 1.626 g/cm^3, F_{000} = 520, T = 123(2) K, $2\theta_{max}$ = 55.0°, 6283 reflections collected, 2381 unique (R_{int} = 0.0642). Final *GoF* = 0.991, *R1* = 0.0490, *wR2* = 0.1096, *R* indices based on 1501 reflections with I>2σ(I) (refinement on F^2), 131 parameters, 0 restraints. Lp and absorption corrections applied, μ = 3.861 mm^{-1}.

Synthesis of 2-bromo-3,5-dimethyl-1,4-phenylene diacetate – 62:

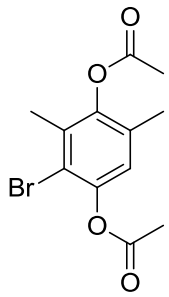

The brominated hydroquinone **64** (200 mg, 0.921 mmol) was stirred in Ac_2O (5.0 mL) as a suspension, and Et_3N (1.0 mL) was added, dissolving the starting material, as a pale yellow solution. The solution was stirred at room temperature overnight, turning a dark brown colour. On completion, 10 mL of H_2O was added, forming a precipitate. The product was filtered and the filtrate filtered a second time. The two precipitates were analysed and combined to give bromo compound **62** (228 mg, 82%), as a pale brown powder.

^{1}H NMR (400 MHz, $CDCl_3$) δ: 6.89, s, 1H, Ar-*H*; 2.34, s, 3H, -OCO-C*H*$_3$; 2.33, s, 3H, -OCO-C*H*$_3$; 2.26, s, 3H, Ar-C*H*$_3$; 2.12, s, 3H, Ar-C*H*$_3$. **^{13}C NMR (100 MHz, $CDCl_3$) δ:** 168.7 (*C*=O), 168.4 (*C*=O), 146.2,

146.1, 132.4, 130.6, 122.6, 116.6, 20.9, 20.5, , 17.1, 16.5. **MS (ESI, +ve):** *m/z* 322.9 $[M+Na]^+$ (^{79}Br), 324.9 $[M+Na]^+$ (^{81}Br). **HRMS (ESI, +ve):** *m/z* 322.9886 $[M+Na]^+$, $C_{12}H_{13}{}^{79}BrO_4$ required *m/z* 322.9895; *m/z* 324.9867 $[M+Na]^+$, $C_{12}H_{13}{}^{81}BrO_4$ required *m/z* 324.9874. **MP:** 115.1-115.7°C.

Synthesis of 3,5-dibromo-4-hydroxy-2,6-dimethylphenyl acetate – 63:

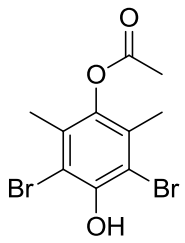

Method 1: Adapted from Smith and Wiley.[28] Bis-protected hydroquinone **38** (251 mg, 1.13 mmol) was dissolved in glacial AcOH (3.14 mL) at room temperature. A solution of Br_2 (61 µL, 1.19 mmol) in glacial AcOH (565 µL) was added dropwise to the reaction mixture, which was stirred for 5 h, after which time the solvent was removed rapidly (15-20 min) by rotary evaporation, yielding a brown oil (296 mg). Purification by column chromatography (20% EtOAc/hexane) produced 115 mg of unreacted **38** and product **63** (24 mg, 6%; recovered yield: 12%), as a pale yellow oil. Mass spectrometry (ESI) showed none of the expected mono-brominated product **62**. *Method 2*: Adapted from Friedli and Shechter.[29] Bis-protected hydroquinone **38** (174 mg, 0.783 mmol) was dissolved in $CHCl_3$ (3 mL), and $FeBr_3$ (300 mg, 1.02 mmol) was added. The reaction mixture was cooled to 0°C and Br_2 (60 µL, 1.17 mmol) was added dropwise. The reaction was allowed to warm to room temperature, and stirred for 3 d, monitored by TLC. When starting material appeared to be consumed, H_2O (3 mL) was added, and the product was extracted with EtOAc (2 × 5 mL), washed with H_2O (10 mL), dried over $MgSO_4$, and filtered. Solvent was removed under reduced pressure to give a red-brown oil (203 mg). Purification by column chromatography (20% EtOAc/hexane) gave **63** (67 mg, 25%), as pale yellow crystals.

^{1}H NMR (400 MHz, $CDCl_3$) δ: 5.95, s, 1H, Ar-O*H*; 2.34, s, 3H, -OCO-CH_3; 2.21, s, 6H, Ar-CH_3. **^{13}C NMR (75 MHz, $CDCl_3$) δ:** 168.9 (*C*=O), 147.7, 141.3, 130.7, 110.0, 20.5, 17.3. **MS (ESI, -ve):** *m/z* 334.8 $[M-H]^-$ (^{79}Br), 336.8 $[M-H]^-$ (^{79}Br,^{81}Br), 338.9 $[M-H]^-$ (^{81}Br). **HRMS (ESI, -ve):** *m/z* 334.8925 $[M-H]^-$, $C_{10}H_{10}{}^{79}Br_2O_3$ required *m/z* 334.8918; *m/z* 336.8904 $[M-H]^-$, $C_{10}H_{10}{}^{79}Br{}^{81}BrO_3$ required *m/z* 336.8898; *m/z* 338.8885 $[M-H]^+$, $C_{10}H_{10}{}^{81}Br_2O_3$ required *m/z* 338.8878. **MP:** 151.4-152.4°C.

Synthesis of 2-bromo-3,5-dimethylbenzene-1,4-diol – 64:

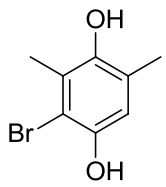

From Smith and Wiley.[28] 2,6-Dimethylhydroquinone **37** (204 mg, 1.48 mol) was dissolved in glacial AcOH (4.1 mL), to which a solution of Br_2 (79 µL, 1.5 mmol) in glacial AcOH (0.7 mL) was added dropwise. After 5 h, the solvent was removed rapidly on a rotary evaporator to give 251 mg of a pale orange powder. The product was recrystallised from hot 40% EtOH solution to give bromo compound **64** (230 mg, 72%), as a cream powder.

^{1}H NMR (400 MHz, $CDCl_3$/d_6-DMSO) δ: 7.51, s, 1H, Ar-O*H*; 6.80, s, 1H, Ar-O*H*; 6.45, s, 1H, Ar-*H*; 2.15, s, 3H, Ar-CH_3; 1.98, s, 3H, Ar-CH_3. **^{13}C NMR (100 MHz, $CDCl_3$/d_6-DMSO) δ:** 146.5, 145.9, 125.5, 124.8, 114.6, 109.9, 16.4, 16.4. **MS (ESI, -ve):** *m*/*z* 214.9 $[M-H]^-$ (^{79}Br), 216.9 $[M-H]^-$ (^{81}Br). **MP:** 142.0-142.8°C (decomp.) (Literature[28]: 145-146°C).

Synthesis of 8-bromo-2-(hydroxymethyl)-2,5,7-trimethylchroman-6-yl acetate – 65:

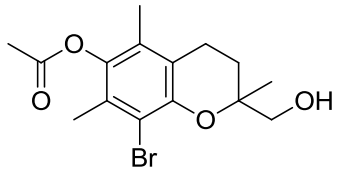

Adapted from Fukumoto *et al*.[20] Protected bromohydroquinone **61** (1.01 g, 3.89 mmol), 2-methyl-2-propen-1-ol (1.65 mL, 19.5 mmol), 80% (w/w) paraformaldehyde (160 mg, 4.26 mmol), Bu_2NH (66 µL, 0.389 mmol) and glacial AcOH (112 µL, 1.95 mmol) were combined in a pressure tube, and heated at 150°C for 2 d. The solvent was removed *in vacuo* to give a thick, dark brown oil (1.70 g). Purification by column chromatography (35% EtOAc/hexane) gave chroman **65** (1059 mg, 79%), as pale yellow crystals.

^{1}H NMR (300 MHz, $CDCl_3$) δ: 3.64/3.58, AB system, ^2J 11.5 Hz, 2H, -CH_2OH; 2.65, m, 2H, -CH_2CH_2-; 2.38, br s, 1H, -O*H*; 2.32, s, 3H, -OCO-CH_3; 2.19, s, 3H, Ar-CH_3; 1.97, s, 3H, Ar-CH_3; 1.93/1.74, m/m, 1H/1H, -CH_2CH_2-; 1.26, s, 3H, -CH_3. **^{13}C NMR (75 MHz, $CDCl_3$) δ:** 169.2 (*C*=O), 147.8, 141.2, 129.1, 127.7, 119.2, 112.0, 77.3, 68.9, 27.5, 20.5, 20.4, 20.3, 16.8, 12.4. **MS (ESI, +ve):** *m*/*z* 365.0 $[M+Na]^+$ (^{79}Br), 367.0 $[M+Na]^+$ (^{81}Br). **HRMS (ESI, +ve):** *m*/*z* 360.0807 $[M+NH_4]^+$, $C_{15}H_{19}{}^{79}BrO_4$ required *m*/*z* 360.0810; *m*/*z* 362.0788 $[M+NH_4]^+$, $C_{15}H_{19}{}^{81}BrO_4$ required *m*/*z* 362.0790. **MP:** 99.0-101.4°C.

Synthesis of 8-bromo-2-(2-hydroxyethyl)-2,5,7-trimethylchroman-6-yl acetate – 66:

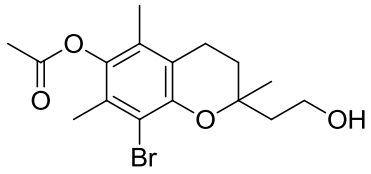

Adapted from Fukumoto *et al.*[20] Protected bromo-hydroquinone **61** (752 mg, 2.90 mmol), 3-methyl-3-buten-1-ol (2.93 mL, 29.0 mmol), 80% (w/w) paraformaldehyde (121 mg, 3.22 mmol), Bu_2NH (49 μL, 0.29 mmol) and glacial AcOH (83 μL, 1.4 mmol) were combined in a pressure tube, and heated at 150°C for 4 d. The solvent was removed *in vacuo* to give a thick, dark brown oil (1.47 g). Purification by silica plug (EtOAc) gave chroman **66** (1.03 mg, 99%), as a pale brown oil.

^{1}H NMR (300 MHz, $CDCl_3$) δ: 3.96/3.79, m/m, 1H/1H, -CH_2CH_2OH; 2.62, t, ^3J 6.7 Hz, 2H, -CH_2CH_2-; 2.29, s, 3H, -OCO-CH_3; 2.16, s, 3H, Ar-CH_3; 1.94, s, 3H, Ar-CH_3; 1.77, m, 4H, -CH_2CH_2-/-CH_2CH_2OH; 1.27, s, 3H, -CH_3. **^{13}C NMR (100 MHz, $CDCl_3$) δ:** 169.2 (*C*=O), 147.5, 141.2, 129.1, 127.8, 118.9, 111.9, 77.6, 58.8, 42.2, 31.8, 22.4, 20.6, 20.4, 16.8, 12.3. **MS (ESI, +ve):** *m/z* 379.1 $[M+Na]^+$ (^{79}Br), 381.0 $[M+Na]^+$ (^{81}Br). **HRMS (ESI, +ve):** *m/z* 357.0693 $[M+H]^+$, $C_{16}H_{21}{}^{79}BrO_4$ required *m/z* 357.0701; *m/z* 359.0674 $[M+H]^+$, $C_{16}H_{21}{}^{81}BrO_4$ required *m/z* 359.0681.

Synthesis of 8-bromo-2,5,7-trimethyl-2-(tosyloxymethyl)chroman-6-yl acetate – 67:

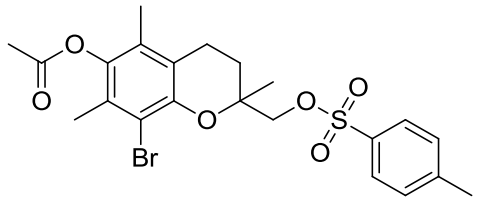

Bromo chroman **65** (2.82 g, 8.21 mmol), DMAP (205 mg, 1.68 mmol) and Et_3N (2.30 mL, 16.5 mmol) were stirred in CH_2Cl_2 (75 mL), and the reaction mixture was cooled to 0°C. *p*-Toluenesulfonyl chloride (3.13 g, 16.4 mmol) was added slowly in portions, and the mixture was allowed to warm slowly to RT, and was stirred for 5 d, with monitoring by TLC. When all starting material had appeared to be consumed, the reaction mixture was washed with aqueous NH_4Cl solution, brine and H_2O, before drying over $MgSO_4$, filtering and removal of solvent by rotary evaporation to give a brown oil (4.50 g). Silica plug chromatography (50% EtOAc/hexane) gave **67** (4.08 g, quant.) as a pale yellow crystalline solid.

^{1}H NMR (400 MHz, $CDCl_3$) δ: 8.80/7.33, AA'XX' system, ^3J 8.2 Hz, 4H, Ts-*H*; 4.03/3.92, AB system, ^3J 9.7 Hz, 2H, -CH_2-O-; 2.58, m, 2H, -CH_2CH_2-; 2.44, s, 3H, Ar-CH_3; 2.33, s, 3H, -OCO-CH_3;

2.19, s, 3H, Ar-CH_3; 1.98/1.81, m/m, 2H, -CH_2CH_2-; 1.94, s, 3H, Ar-CH_3; 1.33, s, 3H, -CH_3. **^{13}C NMR (75 MHz, $CDCl_3$) δ:** 169.1 (*C*=O), 147.4, 145.0, 141.3, 132.6, 130.0, 129.4, 128.0, 127.7, 118.6, 111.9, 74.9, 60.4, 27.7, 22.1, 21.6, 20.4, 20.0, 16.9, 12.3. **MS (ESI, +ve):** *m/z* 518.9 $[M+Na]^+$ (^{79}Br), 520.9 $[M+Na]^+$ (^{81}Br). **HRMS (ESI, +ve):** *m/z* 519.0444 $[M+Na]^+$, $C_{22}H_{25}{}^{79}BrO_6S$ required *m/z* 519.0453; *m/z* 521.0433 $[M+Na]^+$, $C_{22}H_{25}{}^{81}BrO_6S$ required *m/z* 521.0432. **MP:** 107.1-109.7°C.

Attempted synthesis of 8-bromo-2-(phthalimidylmethyl)-2,5,7-trimethylchroman-6-yl acetate – 68:

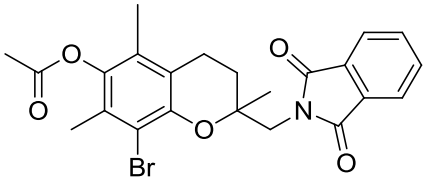

Method 1: Ester **67** (58 mg, 0.12 mmol) was dissolved in DMF (2 mL) and potassium phthalimide (108 mg, 0.583 mmol) was added. The reaction was stirred and heated at 120°C, with monitoring by TLC. After 7 d, the reaction was cooled to RT and H_2O was added. The reaction mixture was extracted with CH_2Cl_2, washed with H_2O, dried ($MgSO_4$), filtered and solvent was removed by rotary evaporation, giving a yellow oil. Water was added to the oil to precipitate the apparent product and cooled overnight. The precipitate was filtered and washed with H_2O to give a beige solid (17 mg). Mass spectrometry and ^{1}H NMR spectroscopy indicated only starting material. *Method 2*: Adapted from Fukumoto *et al.*[20] Protected bromo-hydroquinone **61** (204 mg, 0.787 mmol), alkene phthalimide **71** (212 mg, 1.05 mmol), 80% (w/w) paraformaldehyde (33 mg, 0.88 mmol), Bu_2NH (13 µL, 77 µmol), glacial AcOH (23 µL, 0.40 mmol) and toluene (2 mL) were combined in a pressure vessel, which was heated to 100°C for 18 h, after which time TLC indicated that the bromo starting material had been consumed. Solvent was removed *in vacuo* to give a brown oil (494 mg). Mass spectrometry of the crude mixture showed major peaks at *m/z* 400.1 and 402.1, in an isotopic pattern consistent with one bromine. No bromo hydroquinone **61** or expected product **68** were detected.

Attempted synthesis of 2-(azidomethyl)-8-bromo-2,5,7-trimethylchroman-6-yl acetate – 69:

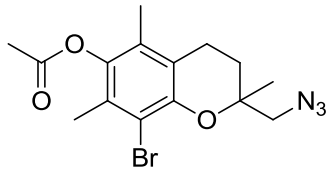

Tosyl ester **67** was dissolved in either DMF, toluene or acetonitrile, and NaN_3 (4 equiv.) and NaI (0.2 equiv.) were added. The reaction mixture was stirred and heated at 90°C for 2 d, during which time progress was monitored by ESI mass spectrometry. After 2 d, each reaction was stopped, and no product was observed by mass spectrometry.

Synthesis of 2-methylallyl 4-methylbenzenesulfonate – 70:

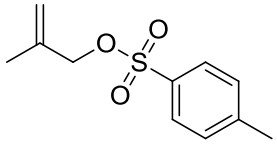

Method 1 (attempted): 2-Methyl-2-propen-1-ol (5.00 mL, 59.1 mmol) was dissolved in CH_2Cl_2 (20 mL), and DMAP (1.44 g, 11.8 mmol) and Et_3N (16.5 mL, 119 mmol) were added. The reaction mixture was stirred and cooled to 0°C, and *p*-toluenesulfonyl chloride (22.5 g, 118 mmol) was added over 5 min, while the reaction was kept cool (not above 4°C). During the addition of *p*-toluenesulfonyl chloride, some fumes were formed, despite maintaining a low temperature, and the mixture thickened, requiring a further 5 mL of CH_2Cl_2 to be added to the flask. The reaction mixture was stirred and allowed to warm to room temperature overnight. Monitoring by TLC was difficult, due to the starting material being too volatile to appear on the plate. After 24 h stirring, the solvent was removed by rotary evaporation, and the presumed product was extracted with EtOAc, and washed with saturated aqueous solutions of NH_4Cl and brine, followed by washing with H_2O. The solvent was dried over $MgSO_4$ and filtered, and the solvent removed under reduced pressure to give a white solid (2.82 g). Characterisation by ^1H NMR spectroscopy showed only *p*-toluenesulfonyl chloride, not the expected product **70**. *Method 2*: From Yoshida *et al.*[34] 2-Methyl-2-propen-1-ol (3.00 mL, 35.4 mmol) was stirred in toluene (95 mL), and $Me_3N.HCl$ (350 mg, 3.66 mmol) and Et_3N (9.9 mL, 71 mmol) were added. The reaction mixture cooled to 0°C, followed by the slow addition of *p*-toluenesulfonyl chloride (10.1 g, 53.2 mmol). As the reaction mixture thickened, a further 25 mL of toluene was added. The reaction was stirred and kept cool with stirring for 1 h, before being allowed to warm to room temperature and stirred overnight. On completion, H_2O (100 mL) was added to the reaction and the product was extracted with EtOAc (2 × 100 mL) and washed with saturated aqueous NH_4Cl solution (2 × 250 mL), brine (250 mL) and H_2O (250 mL), dried with $MgSO_4$ and filtered. Removal of the solvent by rotary evaporation gave a yellow oil (8.77 g). Purification by

column chromatography (hexane to 10% EtOAc/hexane) gave ester **70** (5.13 g, 64%), as a colourless oil.

^{1}H NMR (300 MHz, $CDCl_3$) δ: 7.78/7.33, AA'XX' system, ^3J 8.3 Hz, 4H, Ts-*H*; 4.98, m, 1H, C=C-*H*; 4.93, m, 1H, C=C-*H*; 4.42, s, 2H, -CH_2-; 2.44, s, 3H, Ar-CH_3; 1.68, s, 3H, -CH_3. **^{13}C NMR (75 MHz, $CDCl_3$) δ:** 144.9, 138.1, 133.4, 129.9, 128.0, 115.7, 73.8, 21.7, 19.1. **MS (ESI, +ve):** *m*/*z* 249.0 $[M+Na]^+$.

Synthesis of *N*-(2-methylallyl)phthalimide – 71:

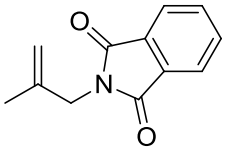

Method 1: Ester **70** (316 mg, 1.40 mmol) was dissolved in DMF (5 mL) and potassium phthalimide (520 mg, 2.81 mmol) was added. The reaction was heated at 100°C overnight. Water was added to the reaction on completion, the product was extracted with CH_2Cl_2 and washed with H_2O, dried over $MgSO_4$ and filtered. Solvent was removed *in vacuo* to give a yellow oil, from which the product was precipitated with H_2O, filtered and washed with H_2O to give **71** (265 mg, 95%), as a cream powder. *Method 2*: Adapted from Goff *et al*.[37] A 60% dispersion of NaH in oil (25 mg, 0.63 mmol), washed twice with hexane, was stirred in 2 mL of dry THF under N_2. A solution of phthalimide **80** (104 mg, 0.544 mmol) in 2 mL of dry THF was added dropwise to the suspension. Once H_2 gas formation subsided, the reaction mixture was stirred at room temperature for 10 min. Tosyl ester **70** (143 mg, 0.632 mmol) was dissolved in 2 mL of dry THF, and this solution was added dropwise to the reaction mixture, and the reaction was stirred at room temperature for 2 d under N_2, then heated at 80°C overnight, monitored by TLC. A further 15 mg of NaH in 2 mL dry THF was added to the reaction mixture after this time, and the reaction was heated at 80°C for a further 1 d, accompanied with a colour change of the cloudy reaction mixture from white to pale yellow, after which time TLC indicated no tosyl ester starting material was remaining. Water (10 mL) was slowly added to the reaction mixture (gas evolution) and the product was extracted with EtOAc (2 × 50 mL), washed with H_2O (2 × 50 mL), dried over $MgSO_4$ and filtered. Concentration of the filtrate by rotary evaporation yielded a yellow oily solid (29 mg). Purification by column chromatography (20% EtOAc/hexane) did not isolate either of the starting materials **70** or **80** or the expected product **86**, however phthalimide **71** (16 mg, 13%) was isolated, as a cream powder. *Method 3*: Adapted from Obert *et al*.[36] To a solution of *t*-BuOK (62 mg, 0.55 mmol) in *t*-BuOH (10 mL) under N_2, phthalimide **80** (101 mg, 0.528 mmol) was added, producing a cloudy white mixture. A solution of ester **70** (104 mg, 0.460 mmol) in 4 mL of *t*-BuOH was added slowly, turning the reaction mixture a pale pink colour. The reaction was heated at reflux

overnight, before workup with the addition of H_2O (10 mL). The reaction mixture was extracted with EtOAc (2 × 20 mL), washed with H_2O (2 × 20 mL), dried with $MgSO_4$, filtered and the solvent removed *in vacuo* to give a cream waxy solid (65 mg). Purification by column chromatography (20% EtOAc/hexane) yielded phthalimide **71** (22 mg, 24%), as a pale yellow solid.

^{1}H NMR (300 MHz, $CDCl_3$) δ: 7.86, m, 2H, Phth-*H*; 7.74, m, 2H, Phth-*H*; 4.89, m, 1H, C=C-*H*; 4.82, m, 1H, C=C-*H*; 4.22, s, 2H, -CH_2-; 1.78, s, 3H, -CH_3. **^{13}C NMR (75 MHz, $CDCl_3$) δ:** 168.2 (*C*=O), 139.5, 134.1, 132.3, 123.5, 112.2, 43.4, 20.5. **MS (ESI, +ve):** *m*/*z* 202.1 $[M+H]^+$. **MP:** 86.2-88.5°C (Literature[44]: 88.5-90°C).

Synthesis of 8-bromo-2-(2-phthalimidylethyl)-2,5,7-trimethylchroman-6-yl acetate – 72:

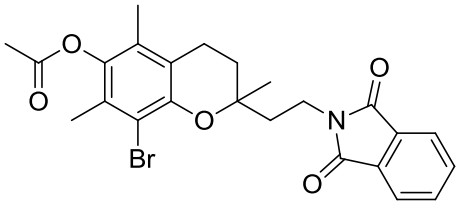

Method 1 (attempted): Adapted from Fukumoto *et al.*[20] Protected bromo-hydroquinone **61** (208 mg, 0.803 mmol), alkene phthalimide **51** (365 mg, 1.70 mmol), 80% (w/w) paraformaldehyde (33 mg, 0.88 mmol), Bu_2NH (14 µL, 82 µmol), glacial AcOH (23 µL, 0.40 mmol) and toluene (2 mL) were combined in a pressure vessel, which was heated to 100°C for 20 h, after which time TLC had indicated that the bromo starting material had been consumed. Solvent was removed *in vacuo* to give a brown oil. Mass spectrometry of the crude mixture showed major peaks at *m*/*z* 400.2 and 402.0, in an isotopic pattern consistent with one bromine present. No bromo hydroquinone **61** or expected product **72** were detected. *Method 2 (attempted*, *solvent-free)*: Protected bromo-hydroquinone **61** (31 mg, 0.12 mmol), alkene **51** (52 mg, 0.24 mmol), 80% (w/w) paraformaldehyde (6 mg, 0.2 mmol), Bu_2NH (2 µL, 0.01 mmol) and glacial AcOH (4 µL, 0.07 mmol) were combined in a pressure tube and the reaction mixture was heated at 150°C for 1 hour. Thin layer chromatography at this time indicated consumption of bromo compound **37**, and the low resolution mass spectrum had major peaks at *m*/*z* 400.2 and 402.3, consistent with the presence of one bromine. Heating of the reaction mixture for a further 1 h gave the same results. *Method 3*: Ester **78** (384 mg, 0.751 mmol) was dissolved in DMF (7 mL) and potassium phthalimide (168 mg, 0.907 mmol) was added. The reaction mixture was heated at 100°C overnight, after which time the reaction was cooled to room temperature and filtered. The filtrate was extracted with EtOAc, washed twice with H_2O, dried ($MgSO_4$), filtered and the solvent removed *in vacuo* to give a pale yellow solid (312 mg). The solid was filtered and

washed with H_2O to remove excess DMF, giving phthalimide **72** (276 mg, 76%), a pale yellow powder.

^{1}H NMR (400 MHz, $CDCl_3$) δ: 7.82, m, 2H, Phth-*H*; 7.69, m, 2H, Phth-*H*; 3.94, m, 2H, -CH_2CH_2-N-; 2.67, m, 2H, -CH_2CH_2-; 2.32, s, 3H, -OCO-CH_3; 2.18, s, 3H, Ar-CH_3; 2.04/1.85, m/m, 2H/2H, -CH_2CH_2-/-CH_2CH_2-N-; 1.97, s, 3H, Ar-CH_3; 1.38, s, 3H, -CH_3. **^{13}C NMR (100 MHz, $CDCl_3$) δ:** 169.4, 168.0, 148.0, 141.1, 134.0, 132.8, 129.2, 127.6, 123.3, 118.8, 112.3, 75.6, 38.2, 33.6, 31.0, 23.3, 20.7, 20.6, 17.0, 12.5. **MS (ESI, +ve):** *m/z* 486.0 $[M+H]^+$ (^{79}Br), 488.0 $[M+H]^+$ (^{81}Br), 507.9 $[M+Na]^+$ (^{79}Br), 509.9 $[M+Na]^+$ (^{81}Br). **HRMS (ESI, +ve):** *m/z* 486.0914 $[M+H]^+$, $C_{24}H_{24}{}^{79}BrNO_5$ required *m/z* 486.0916; *m/z* 488.0898 $[M+H]^+$, $C_{24}H_{24}{}^{81}BrNO_5$ required *m/z* 488.0896. **MP:** 170.8-172.7°C.

Synthesis of *N*-(2-methylallyl)acetamide – 73:

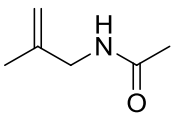

Phthalimide **71** (1.84 g, 9.14 mmol) was dissolved in THF (15 mL) and EtOH (35 mL) was added. The solution was cooled to 5°C, before the dropwise addition of hydrazine hydrate (4.45 mL, 91.5 mmol). The reaction was allowed to warm to room temperature and stirred for 3 h, during which time a white precipitate was formed. The precipitate was removed by filtration and washed with a small amount of THF. The filtrate was cooled in an ice bath, and Ac_2O (50 mL) and Et_3N (15 mL) were slowly added with stirring and left to warm to room temperature. The reaction was stirred at room temperature for 3 d. On completion, water was added to the reaction mixture and the product was extracted with EtOAc (2 × 200 mL), washed with saturated aqueous $NaHCO_3$ solution (4 × 100 mL) and H_2O (2 × 200 mL), and the organic phase was dried over $MgSO_4$, filtered and the solvent evaporated under reduced pressure to give a white oily solid (748 mg). The product was dissolved in CH_2Cl_2 and filtered to remove impurities before concentration *in vacuo* to give a white solid (672 mg). Purification by column chromatography (Et_2O, followed by EtOAc, flushed with 20% MeOH/EtOAc) gave acetamide **73** (225 mg, 22%), as a pale yellow oil.

^{1}H NMR (400 MHz, $CDCl_3$) δ: 6.15, br s, 1H, -N*H*; 4.78, m, 2H, -C=CH_2; 3.74, d, ^3J 6.0 Hz, 2H, -CH_2-; 1.97, s, 3H, -NCO-CH_3; 1.68, s, 3H, -CH_3. **^{13}C NMR (100 MHz, $CDCl_3$) δ:** 170.4 (*C*=O), 142.0, 110.9, 45.2, 23.1, 20.3. **MS (ESI, +ve):** *m/z* 114.1 $[M+H]^+$, 136.1 $[M+Na]^+$.

Synthesis of *N*-(3-methylbut-3-enyl)acetamide – 74:

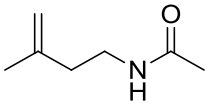

Phthalimide **51** (2.00 g, 9.30 mmol) was dissolved in THF (25 mL) and EtOH (45 mL) and the solution was cooled to 0°C, before the dropwise addition of hydrazine hydrate (4.52 mL, 92.9 mmol). The reaction was stirred at 0°C for 1 h, as a thick precipitate formed. A further 70 mL EtOH was added and the reaction was stirred at RT for 2 d. The reaction mixture was filtered to remove phthalhydrazide byproduct, which was washed with a small amount of EtOH. The filtrate was stirred and cooled to 0°C. Triethylamine (20 mL) and Ac_2O (65 mL) were added, as the reaction changed from colourless to a clear yellow solution. The reaction was allowed to warm to RT, and stirred for 3 d, over which time the yellow colour of the solution paled. The reaction was then heated at 100°C for 1 h, before cooling to RT and excess EtOH/THF was removed by rotary evaporation. The product was extracted from thee aqueous solution with EtOAc (2 × 300 mL), washed with H_2O (300 mL) and saturated $NaHCO_3$ solution (3 × 300 mL), before a further wash with H_2O (300 mL). The organic phase was dried over $MgSO_4$ and filtered to give a pinkish-brown oily solid (579 mg). Purification by column chromatography (EtOAc to 20% MeOH/EtOAc) gave **74** (154 mg, 13%) as a yellow oil.

^{1}H NMR (400 MHz, $CDCl_3$) δ: 5.80, br s, 1H, -N*H*; 4.77, m, 1H, -C=C-*H*; 4.69, m, 1H, -C=C-*H*; 3.32, q, ^3J 6.4 Hz, 2H, -CH_2CH_2-N-; 2.17, t, ^3J 6.8 Hz, 2H, -CH_2CH_2-N-; 1.92, s, 3H, -NCO-CH_3; 1.69, s, 3H, -CH_3. **^{13}C NMR (75 MHz, $CDCl_3$) δ:** 170.2 (*C*=O), 142.8, 112.4, 37.5, 37.2, 23.4, 22.1. **MS (ESI, +ve):** *m*/*z* 128.1 $[M+H]^+$, 150.1 $[M+Na]^+$. **HRMS (ESI, +ve):** *m*/*z* 150.0894 $[M+H]^+$, $C_7H_{13}NO$ required *m*/*z* 150.0889.

Attempted synthesis of 2-(acetamidomethyl)-2,5,7,8-tetramethylchroman-6-yl acetate – 75:

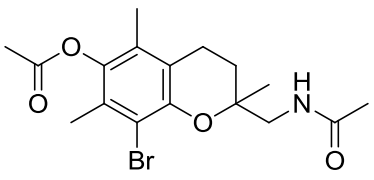

Adapted from Fukumoto *et al.*[20] Protected bromo-hydroquinone **61** (52 mg, 0.20 mmol), alkene **73** (34 mg, 0.30 mmol), 80% (w/w) paraformaldehyde (19 mg, 0.51 mmol), Bu_2NH (75 µL, 0.44 mmol) and glacial AcOH (100 µL, 1.74 mmol) were combined in a pressure vessel, which was heated to 150°C for 2 d, after which time TLC had indicated that the bromo starting material had been consumed. Solvent was removed *in vacuo* to give a brown oil. Mass spectrometry of the crude mixture showed some $[M+H]^+$ peaks at

m/*z* 384.1 and 386.1, in an isotopic pattern consistent with one bromine present, however no product was isolated on purification by column chromatography (EtOAc to 20% MeOH/EtOAc).

Attempted synthesis of 2-(2-acetamidoethyl)-2,5,7,8-tetramethylchroman-6-yl acetate – 76:

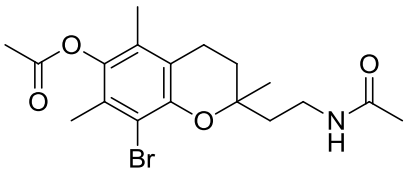

Adapted from Fukumoto *et al.*[20] Protected bromo-hydroquinone **61** (50 mg, 0.19 mmol), alkene **74** (36 mg, 0.28 mmol), 80% (w/w) paraformaldehyde (16 mg, 0.43 mmol), Bu_2NH (75 µL, 0.45 mmol) and glacial AcOH (100 µL, 1.74 mmol) were combined in a pressure vessel, which was heated at 150°C for 1 h, after which time TLC had indicated that the bromo starting material had been consumed. Solvent was removed *in vacuo* to give a brown oil. Mass spectrometry of the crude mixture showed peaks for the expected product at *m*/*z* 398.1/400.1, representing $[M+H]^+$ and *m*/*z* 420.1/422.1, corresponding to the $[M+Na]^+$ peak, both in a isotopic patterns consistent with one bromine present, however the ^1H NMR spectrum was inconclusive and attempted purification by column chromatography (EtOAc to 20% MeOH/EtOAc) gave three fractions, of which none appeared to be the expected product or the bromo starting material by ^1H NMR spectroscopy or mass spectrometry.

Synthesis of 8-bromo-2,5,7-trimethyl-2-(2-(tosyloxy)ethyl)chroman-6-yl 4-methylbenzenesulfonate – 77:

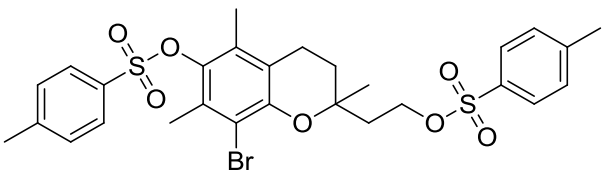

Alcohol **66** (271 mg, 0.759 mmol) was dissolved in CH_2Cl_2 (5 mL), and DMAP (21 mg, 0.17 mmol) and Et_3N (526 µL, 3.79 mmol) were added. The reaction mixture was cooled to 0°C, before the slow addition of *p*-toluenesulfonyl chloride (293 mg, 1.54 mmol). The reaction was slowly warmed to room temperature and stirred overnight, after which time the starting material had appeared by TLC to be consumed. The solvent was removed by rotary evaporation and the product was extracted with EtOAc. The organic phase was washed twice with saturated aqueous NH_4Cl solution, once each with brine and H_2O, dried over $MgSO_4$, filtered and the solvent removed under reduced pressure to give 399 mg of a pale brown oil. Purification by

column chromatography (20% EtOAc/hexane) gave pure **77** (346 mg, 73%), as a clear yellow oil.

^{1}H NMR (400 MHz, $CDCl_3$) δ: 7.79/7.35, AA'XX' system, ^3J 8.2 Hz, 4H, Ts-*H*; 7.76/7.30, AA'XX' system, ^3J 8.1 Hz, 4H, Ts-*H*; 4.36-4.22, m, 2H, -C*H*$_2$CH$_2$-O-; 2.54, t, ^3J 6.8 Hz, 2H, -C*H*$_2$CH$_2$-; 2.46, s, 3H, Ar-C*H*$_3$; 2.42, s, 3H, Ar-C*H*$_3$; 2.07, s, 3H, Ar-C*H*$_3$; 1.96, s, 3H, Ar-C*H*$_3$; 1.97/1.79, m/m, 2H/2H, -CH$_2$C*H*$_2$-/-C*H*$_2$CH$_2$-O-; 1.24, s, 3H, -C*H*$_3$. **^{13}C NMR (100 MHz, $CDCl_3$) δ:** 148.2, 145.5, 144.9, 140.4, 134.0, 133.0, 131.4, 130.3, 130.0, 129.9, 128.3, 128.0, 119.1, 112.5, 75.3, 66.7, 38.5, 31.5, 23.7, 21.8, 21.7, 20.6, 18.3, 13.9. **MS (ESI, +ve):** *m*/*z* 644.9 $[M+Na]^+$ (^{79}Br), 646.8 $[M+Na]^+$ (^{81}Br). **HRMS (ESI, +ve):** *m*/*z* 645.0592 $[M+Na]^+$, $C_{28}H_{31}{}^{79}BrO_7S_2$ required *m*/*z* 645.0592; *m*/*z* 647.0568 $[M+Na]^+$, $C_{28}H_{31}{}^{81}BrO_7S_2$ required *m*/*z* 647.0572.

Synthesis of 8-bromo-2,5,7-trimethyl-2-(2-(tosyloxy)ethyl)chroman-6-yl acetate – 78:

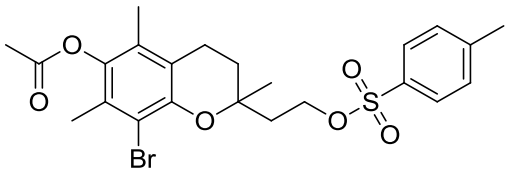

Alcohol **66** (359 mg, 1.00 mmol), DMAP (7 mg, 60 μmol) and Et_3N (167 μL, 1.20 mmol) were dissolved in CH_2Cl_2 (8 mL), and the reaction mixture was cooled to 0°C. *p*-Toluenesulfonyl chloride (232 mg, 1.22 mmol) was added slowly, and the reaction was allowed to warm to room temperature, with monitoring by TLC. The reaction was stirred overnight, after which time TLC indicated the consumption of starting material. On completion, solvent was removed by rotary evaporation, and the product was extracted with EtOAc, washed twice with saturated aqueous NH_4Cl solution and once each with brine and H_2O. The organic phase was dried with $MgSO_4$, filtered and solvent removed under reduced pressure to give a yellow oil (498 mg). Purification by column chromatography (20% EtOAc/hexane) gave pure **78** (421 mg, 82%), as a pale yellow oil.

^{1}H NMR (400 MHz, $CDCl_3$) δ: 7.78/7.31, AA'XX' system, ^3J 8.2 Hz, 4H, Ts-*H*; 4.35/4.26, m/m, 1H/1H, -CH$_2$C*H*$_2$-O-; 2.59, t, ^3J 6.4 Hz, 2H, -C*H*$_2$CH$_2$-; 2.43, s, 3H, Ar-C*H*$_3$; 2.33, s, 3H, -OCO-C*H*$_3$; 2.18, s, 3H, Ar-C*H*$_3$; 2.00/1.79, m/m, 2H/2H, -CH$_2$C*H*$_2$-/-C*H*$_2$CH$_2$-O-; 1.95, s, 3H, Ar-C*H*$_3$; 1.25, s, 3H, -C*H*$_3$. **^{13}C NMR (100 MHz, $CDCl_3$) δ:** 169.3 (*C*=O), 147.6, 144.9, 141.2, 133.1, 130.0, 129.3, 128.0, 127.7, 118.7, 112.1, 75.0, 66.9, 38.5, 31.6, 23.7, 21.7, 20.6, 20.5, 16.9, 12.4. **MS (ESI, +ve):** *m*/*z* 532.9 $[M+Na]^+$ (^{79}Br), 534.9 $[M+Na]^+$ (^{81}Br). **HRMS (ESI, +ve):** *m*/*z* 533.0602 $[M+Na]^+$,

$C_{23}H_{27}{}^{79}BrO_6S$ required m/z 533.0609; m/z 535.0582 $[M+Na]^+$, $C_{23}H_{27}{}^{81}BrO_6S$ required m/z 535.0589.

Synthesis of *N*-(2-hydroxyethyl)phthalimide – 80:

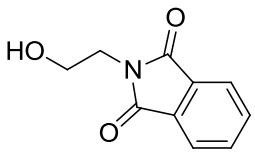

2-Chloroethanol (3.00 mL, 44.8 mmol) and potassium phthalimide salt (27.6 g, 149 mmol) were stirred in DMF (150 mL) at 100°C for 11 h, and stirred at RT for a further 6 d. After this time, the reaction mixture was filtered washed with CH_2Cl_2, and the filtrate was washed twice with saturated aqueous $NaHCO_3$ solution and once with H_2O. The organic extract was dried over $MgSO_4$, filtered and the solvent removed *in vacuo* to give a yellow oil. Product was precipitated out on addition of a small amount of H_2O, and the resulting precipitate was collected over vacuum, washed with H_2O and dried to give **80** (7.95 g, 93%), as a cream solid.

^{1}H NMR (400 MHz, $CDCl_3$) δ: 7.84, m, 2H, Phth-*H*; 7.73, m, 2H, Phth-*H*; 3.88, m, 4H, -CH_2CH_2OH. **^{13}C NMR (100 MHz, $CDCl_3$) δ:** 169.0 (*C*=O), 134.2, 132.1, 123.5, 61.2, 41.0. **MS (ESI, +ve):** m/z 214.0 $[M+Na]^+$. **MP:** 127.3-127.7°C (Literature[45]: 126.5-127.5°C).

Synthesis of 2-phthalimidylethyl 4-methylbenzenesulfonate – 81:

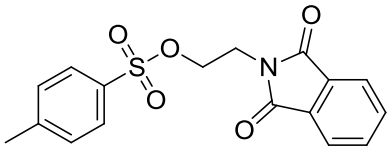

Phthalimide **80** (7.79 g, 40.7 mmol) was dissolved in CH_2Cl_2 (150 mL) and DMAP (1.00 g, 8.20 mmol) was added. After slow addition of Et_3N (11.5 mL, 82.6 mmol), the reaction mixture turned a clear, pale yellow colour, and was cooled to 0°C. *p*-Toluenesulfonyl chloride (16.0 g, 83.9 mmol) was added slowly in portions, and the reaction mixture turned a pale brown colour, then was allowed to warm to room temperature with stirring overnight. On completion, solvent was removed by rotary evaporator and the product was extracted with EtOAc, washed with aqueous NH_2Cl solution, brine and water. Then organic phase was dried over $MgSO_4$, filtered and the solvent removed *in vacuo* to give a cream solid (11.02 g). The crude product was purified by dissolving impurities in EtOAc, and collecting the solid by vacuum filtration to yield ester **81** (5.45 g, 39%), as a cream solid.

^{1}H NMR (300 MHz, $CDCl_3$) δ: 7.78, m, 2H, Phth-*H*; 7.71, m, 2H, Phth-*H*; 7.67/7.14, AA'XX' system, ^3J 8.3 Hz, 4H, Ts-*H*; 4.30, t, ^3J 5.4 Hz, 2H, -O-CH_2CH$_2$-N-; 3.91, t, ^3J 5.4 Hz, 2H, -O-CH$_2$CH_2-N-; 2.30, s, 3H, -CH_3. **^{13}C NMR (75 MHz, $CDCl_3$) δ:** 167.7 (*C*=O), 144.9, 135.6, 134.2, 130.0,129.9, 127.9, 123.4, 66.6, 37.0, 21.7. **MS (ESI, +ve):** *m*/*z* 368.1 $[M+Na]^+$. **MP:** 140.1-141.4°C (Literature[45]: 142°C).

Attempted synthesis of 2-((2-phthalimidylethoxy)methyl)-2,5,7-trimethylchroman-6-yl acetate – 82:

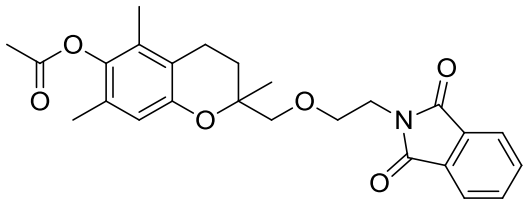

Method 1: Adapted from Zlatev *et al*.[35] Chroman **40** (62 mg, 0.23 mmol) and ester **81** (405 mg, 1.17 mmol) were dissolved in dry THF (3 mL) and 1,4-diazabicyclo[2.2.2]octane (53 mg, 0.47 mmol) and 1,8-diazabicycloundec-7-ene (88 µL, 0.59 mmol) were added the solution, which was heated at reflux under N_2 for 4 h. The reaction was cooled to RT and stirred for a further 3 d, after which time analysis by low resolution mass spectrometry indicated the presence of neither of the starting materials nor the desired product. *Method 2*: Adapted from Obert *et al*.[36] Chroman **40** (44 mg, 0.17 mmol) was dissolved in *tert*-butanol (2 mL) and stirred under Ar. Ester **81** (287 mg, 0.831 mmol) and potassium *tert*-butoxide (40 mg, 0.36 mmol) were added slowly the solution, which was stirred under Ar for 4 d, after which time the reaction mixture had turned solid. The product was extracted with EtOAc (10 mL), washed with brine (3 × 10 mL), the organic phase was dried with Na_2SO_4, filtered and the solvent was removed by rotary evaporation to give a cream solid (201 mg). The proton NMR spectrum of the solid showed mainly ester **81** was present, while low resolution mass spectrometry showed none of the expected product. *Method 3*: A 60% dispersion of NaH in oil (126 mg, 3.15 mmol), washed twice with hexane, was stirred in 2 mL of dry THF. To this suspension a solution of chroman **40** (82 mg, 0.31 mmol) and ester **81** (214 mg, 0.62 mmol) in dry THF (6 mL) was added slowly under N_2. The reaction mixture was stirred and heated to 80°C for 5 d, with monitoring by TLC. On completion, the reaction mixture was extracted with EtOAc, washed with H_2O, dried over $MgSO_4$ and the solvent was removed *in vacuo*. Proton NMR spectroscopy of the crude mixture showed possible deacetylation of chroman **82**. Mass spectrometry supported the lack of product formation, with a major peak at *m*/*z* 287.2, representing the $[M+Na]^+$ ion of the starting material, and a peak was present at *m*/*z* 245.2, for the deacetylated chroman. None of the desired product was observed in the spectrum. *Method 4*: Adapted from Zlatev *et al*.[35] Chroman **40** (53 mg, 0.20 mmol) and phthalimide compound **85** (84 mg, 0.40 mmol) were dissolved in dry THF

(2 mL). 1,4-Diazabicyclo[2.2.2]octane (45 mg, 0.40 mmol) and 1,8-diazabicycloundec-7-ene (75 μL, 0.50 mmol) were added the solution, which was heated at reflux under N_2 for 2 d. After this time a new major spot by TLC had been formed, so the reaction was cooled to RT. Water was added the reaction mixture, which was extracted with EtOAc, washed with H_2O, dried over $MgSO_4$, filtered and the solvent was removed *in vacuo* to give 57 mg of yellow oil. Attempted purification by column chromatography (20% EtOAc/hexane) yielded five fractions, none of which appeared by ^1H NMR or mass spectrometry to be the desired product. *Method 5*: A 60% dispersion of NaH in oil (30 mg, 1.0 mmol), washed twice with hexane, was stirred in 1 mL of dry THF. To this suspension a solution of chroman **40** (19 mg, 0.072 mmol) and phthalimide **85** (30 mg, 0.14 mmol) in dry THF (1.5 mL) was added slowly under N_2. The reaction mixture was stirred and heated at reflux overnight, and the reaction was stopped when a new major spot appeared by TLC. Mass spectrometry of the reaction mixture showed no peaks attributable to the expected product.

Attempted synthesis of 2-(2-(2-phthalimidylethoxy)ethyl)-2,5,7-trimethylchroman-6-yl acetate – 83:

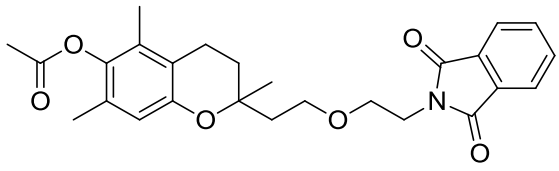

Method 1: Adapted from Zlatev *et al*.[35] Chroman **41** (12 mg, 0.043 mmol) and ester **81** (75 mg, 0.22 mmol) were dissolved in dry THF (2 mL) and 1,4-diazabicyclo[2.2.2]octane (13 mg, 0.11 mmol) and 1,8-diazabicycloundec-7-ene (17 μL, 0.11 mmol) were added the solution, which was heated at reflux under N_2 for 3 h. After this time chroman **41** appeared by TLC to have been consumed, so the reaction was cooled to RT. The reaction mixture was extracted with EtOAc, washed with H_2O, dried over Na_2SO_4, filtered and the solvent was removed *in vacuo* to give 123 mg of green-brown oily solid. Mass spectrometry indicated very little expected product formation, and primarily the starting chroman **41**. *Method 2*: A 60% dispersion of NaH in oil (26 mg, 0.65 mmol), washed twice with hexane, was stirred in 2 mL of dry THF. To this suspension a solution of chroman **41** (18 mg, 0.065 mmol) and ester **81** (45 mg, 0.13 mmol) in dry THF (3 mL) was added slowly under N_2. The reaction mixture was stirred and heated to 80°C for 5 d, with monitoring by TLC. On completion, the reaction mixture was extracted with EtOAc, washed with H_2O, dried over $MgSO_4$ and the solvent was removed *in vacuo*. Mass spectrometry supported the lack of product formation, with no peaks present for the desired product or either of the starting materials, and a peak was present at m/z 259.2, attributable to the $[M+Na]^+$ peak of deacetylated chroman.

Synthesis of 2-chloroethyl 4-methylbenzenesulfonate – 84:

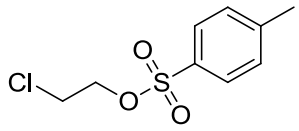

2-Chloroethanol (2.00 mL, 29.8 mmol) was dissolved in CH_2Cl_2 (120 mL), DMAP (735 mg, 6.02 mmol) and Et_3N (8.5 mL, 61 mmol) were added, and the reaction mixture was stirred and cooled to 0°C. *p*-Toluenesulfonyl chloride (6.86 g, 36.0 mmol) was added slowly in portions, and the reaction mixture was allowed to warm slowly to room temperature, and stirred overnight. The reaction was monitored by TLC. On completion, the solvent was removed by rotary evaporation, and the product extracted with EtOAc, and the organic phased was washed with aqueous NH_4Cl solution, brine and H_2O. On drying with $MgSO_4$ and filtration, the solvent was removed to give **84** as a colourless oil (5.63 g, 80%).

^{1}H NMR (400 MHz, $CDCl_3$) δ: 7.78/7.35, AA'XX' system, ^3J 8.2 Hz, 4H, Ts-*H*; 4.22, t, ^3J 5.9 Hz, 2H, $ClCH_2CH_2$-O-; 3.63, t, ^3J 5.9 Hz, 2H, $ClCH_2CH_2$-O-; 2.43, s, 3H, Ar-CH_3. **^{13}C NMR (100 MHz, $CDCl_3$) δ:** 145.3, 132.7, 130.0, 128.0, 69.1, 40.9, 21.7. **MS (ESI, +ve):** *m/z* 257.1 $[M+Na]^+$ (^{35}Cl), 259.0 $[M+Na]^+$ (^{37}Cl).

Synthesis of *N*-(2-chloroethyl)phthalimide – 85:

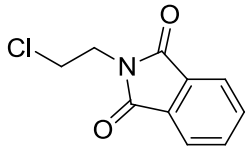

Ester **84** (5.63 g, 24.0 mmol) was dissolved in DMF (200 mL), and potassium phthalimide (4.45 g, 24.0 mmol) was added. The reaction was stirred and heated at 100°C overnight, after which time ^{1}H NMR spectroscopy of a small aliquot indicated that all of **84** had been consumed. On completion, H_2O (150 mL) was added and the product was extracted with CH_2Cl_2 (2 × 200 mL), washed with saturated aqueous $NaHCO_3$ solution (300 mL) and H_2O (300 mL), dried with $MgSO_4$, filtered and solvent removed *in vacuo* to give a yellow oil, from which the product was precipitated on addition of H_2O. The precipitate was filtered over vacuum, washed with H_2O and dried to give product **85** (3.46 mg, 69%), as a cream solid.

^{1}H NMR (300 MHz, $CDCl_3$) δ: 7.87, m, 2H, Phth-*H*; 7.73, m, 2H, Phth-*H*; 4.04, t, ^3J 6.4 Hz, 2H, $ClCH_2CH_2$-N-; 3.77, t, ^3J 6.4 Hz, 2H, $ClCH_2CH_2$-N-. **^{13}C NMR (75 MHz, $CDCl_3$) δ:** 168.1 (*C*=O), 134.3, 132.0, 123.6, 40.9, 39.6. **MS (ESI, +ve):** *m/z* 210.0 $[M+H]^+$ (^{35}Cl), 212.1 $[M+H]^+$ (^{37}Cl). **MP:** 78.7-80.1°C (Literature[46]: 79.5-81°C).

Attempted synthesis of *N*-(2-((2-methylallyl)oxy)ethyl)phthalimide – 86:

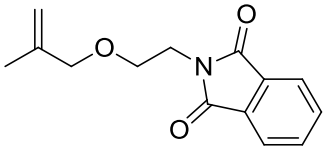

Method 1: Adapted from Goff *et al*.[37] A 60% dispersion of NaH in oil (103 mg, 2.58 mmol), washed twice with hexane, was stirred in 3 mL of dry THF under N_2. The suspension was cooled to ~5°C, and a solution of 2-methyl-2-propen-1-ol (200 µL, 2.36 mmol) in 1 mL of dry THF was slowly added. Once H_2 gas formation has subsided, the reaction mixture was stirred at 80°C for 3 h. After this time, the flask was cooled to 0°C, and a solution of phthalimide **85** (596 mg, 2.84 mmol) in dry THF (3 mL) was added dropwise. The pale cloudy yellow reaction mixture darkened to a deeper clear yellow, and the reaction was stirred at RT overnight. After 24 h, all starting material had appeared by TLC to have been consumed and a white precipitate had formed. Water (10 mL) was added and the reaction mixture was extracted with EtOAc (2 × 10 mL), washed with H_2O (2 × 20 mL), dried over $MgSO_4$ and filtered. The filtrate was concentrated *in vacuo* to give starting material phthalimide **85** (268 mg). None of the expected product **86** was identified. *Method 2*: Adapted from Obert *et al*.[36] Potassium *tert*-butoxide (160 mg, 1.43 mmol) was dissolved *tert*-butanol (13 mL) under N_2. 2-Methyl-2-propen-1-ol (121 µL, 1.43 mmol) and phthalimide **85** (249 mg, 1.19 mmol) were added and the reaction mixture was stirred at RT for 10 min, before heating at reflux for 2 d with monitoring by TLC. The reaction was cooled to RT before it was extracted with EtOAc (2 × 10 mL), washed with H_2O (20 mL), dried over $MgSO_4$, filtered and the solvent removed by rotary evaporation to give starting material phthalimide **85** (201 mg).

Attempted synthesis of *N*-(2-((3-methylbut-3-en-1-yl)oxy)ethyl)phthalimide – 87:

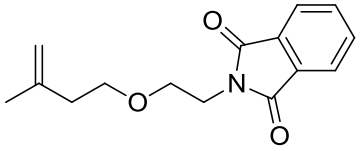

Adapted from Goff *et al*.[37] A 60% dispersion of NaH in oil (88 mg, 2.21 mmol), washed twice with hexane, was stirred in 3 mL of dry THF under N_2. The suspension was cooled to ~5°C, and a solution of 3-methyl-3-buten-1-ol (200 µL, 1.98 mmol) in 1 mL of dry THF was slowly added. Once H_2 gas formation has subsided, the reaction mixture was stirred at 80°C for 3 h. After this time, the flask was cooled to 0°C, and a solution of phthalimide **85** (499 mg, 2.38 mmol) in dry THF (3 mL) was added dropwise. The cloudy orange-brown reaction mixture clarified, and the reaction was stirred at RT for 2 d, after which time all starting material had appeared by TLC to have been consumed. Water (10 mL) was added and the reaction mixture was extracted with EtOAc (20 mL), washed with H_2O (2 × 20 mL), dried over $MgSO_4$ and filtered. The filtrate was concentrated *in vacuo* to give a yellow oily residue (291 mg). Characterisation by ^{1}H NMR

spectroscopy indicated the residue was a 3:2 mixture of starting material phthalimide **85** and *N*-vinylphthalimide (**88**). None of the expected product **87** was identified.

Synthesis of *N*-vinylphthalimide – 88:

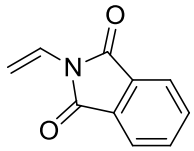

Method 1: Adapted from Goff *et al.*[37] A 60% dispersion of NaH in oil (133 mg, 3.33 mmol), washed twice with hexane, was stirred in 4 mL of dry THF under N_2. The suspension was cooled to ~5°C, and a solution of 2-methyl-2-propen-1-ol (138 µL, 1.63 mmol) in 1 mL of dry THF was slowly added. Once H_2 gas formation has subsided, the reaction mixture was stirred at reflux for 2 h. After this time, the flask was cooled in an ice bath, and a solution of phthalimide **85** (411 mg, 1.96 mmol) in dry THF (3 mL) was added dropwise. The very pale yellow solution darkened to a deeper yellow, and the reaction was stirred at RT overnight. After 24 h, all starting material had appeared by TLC to have been consumed. The reaction was filtered through celite and the product washed through with EtOAc. The solvent was removed by rotary evaporation to give a yellow solid (64 mg). Purification by column chromatography (20% EtOAc/hexane) yielded *N*-vinylphthalimide **88** (55 mg, 19%). None of the expected product **86** or phthalimide **85** was identified by ^{1}H NMR spectroscopy or mass spectrometry. *Method 2*: Adapted from Goff *et al.*[37] A 60% dispersion of NaH in oil (158 mg, 3.96 mmol), washed twice with hexane, was stirred in dry THF (3 mL) under N_2 gas. The mixture was cooled in an ice bath, and a solution of 3-methyl-3-buten-1-ol (200 µL, 1.98 mmol) in dry THF (1 mL) was added. When H_2 formation had subsided, the reaction mixture was heated at reflux for 2 h, followed by cooling in an ice bath. A solution of phthalimide **85** (512 mg, 2.44 mmol) in dry THF (3 mL) was added dropwise to the reaction mixture, which was then warmed slowly to room temperature and stirred under N_2 overnight, during which time the reaction colour changed from pale orange to a cloudy deep red. When all of phthalimide **85** appeared consumed by TLC, H_2O (10 mL) was added to the solution and the product was extracted with EtOAc (2 × 10 mL), washed with H_2O (20 mL), dried over $MgSO_4$ and filtered. The filtrate was concentrated by rotary evaporation to give a yellow crystalline solid (199 mg). Purification by column chromatography (20% EtOAc/hexane) yielded **88** (100 mg, 29%) as a white solid.

^{1}H NMR (400 MHz, $CDCl_3$) δ: 7.85, m, 2H, Phth-*H*; 7.73, m, 2H, Phth-*H*; 6.87/6.08/5.04, AMX system, $^3J_{AM}$ 16.3 Hz, $^3J_{AX}$ 9.9 Hz, 3H, N-C*H*=CH_2. **^{13}C NMR (75 MHz, $CDCl_3$) δ:** 166.6 (*C*=O), 134.6, 131.8, 123.9, 123.8, 104.6. **MS (ESI, +ve):** *m/z* 174.0 $[M+H]^+$. **MP:** 76.5-77.8°C (Literature[47]: 79°C).

Synthesis of *N*-(2-((2-methylallyl)oxy)ethyl)acetamide – 89:

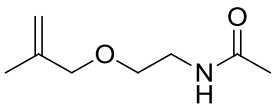

Adapted from Goff *et al.*[37] A 60% dispersion of NaH in oil (105 mg, 2.63 mmol), washed twice with hexane, was stirred in 2 mL of dry THF under N_2 gas. The suspension was cooled in an ice bath and a solution of *N*-(2-hydroxyethyl)acetamide (200 µL, 2.17 mmol) in dry THF (1 mL) was added dropwise. When H_2 gas evolution had subsided, a further 2 mL of dry THF was added to the flask and the reaction was warmed to room temperature and stirred for a further 3 h, during which time a white precipitate had formed in the clear solution. The reaction mixture was cooled in an ice bath and a solution of ester **70** (590 mg, 2.61 mmol) in dry THF (2 mL) was added dropwise, and the reaction was stirred at room temperature for 6 d, during which time the reaction was monitored by TLC (iodine stain). The reaction was cooled to room temperature and 20 mL of water was added, after which time the product separated as a pale yellow oil on top of the aqueous phase. The product was extracted with EtOAc (2 × 50 mL), washed with H_2O (2 × 50 mL), dried over $MgSO_4$, filtered and the solvent removed by rotary evaporation to give a clear pale yellow oil (167 mg). Purification by column chromatography (20% EtOAc/hexane to 100% EtOAc to 20% MeOH/EtOAc) gave ether **89** (124 mg, 36%), as a clear pale yellow oil.

^{1}H NMR (300 MHz, $CDCl_3$) δ: 6.01, br s, 1H, -N*H*-; 4.91, m, 1H, C=C-*H*; 4.87, m, 1H, C=C-*H*; 3.85, s, 2H, -CH_2-O-; 3.43, m, 4H, -O-CH_2CH_2-N-; 1.95, s, 3H, -NCO-CH_3; 1.69, s, 3H, -CH_3. **^{13}C NMR (75 MHz, $CDCl_3$) δ:** 170.2 (*C*=O), 142.0, 112.6, 75.1, 68.7, 39.5, 23.4, 19.5. **MS (ESI, +ve):** *m*/*z* 180.0 $[M+Na]^+$. **HRMS (ESI, +ve):** *m*/*z* 158.1176 $[M+H]^+$, $C_8H_{15}NO_2$ required *m*/*z* 158.1176.

Synthesis of 2-((2-acetamidoethoxy)methyl)-8-bromo-2,5,7-trimethylchroman-6-yl acetate – 90:

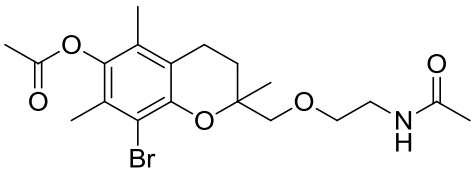

Adapted from Fukumoto *et al.*[20] Protected bromohydroquinone **61** (244 mg, 0.946 mmol), ether **89** (124 mmol, 0.789 mmol), 80% (w/w) paraformaldehyde (56 mg, 1.5 mmol), Bu_2NH (15 µL, 0.089 mmol) and glacial AcOH (25 µL, 0.43 mmol) were combined in a pressure tube, and heated at 150°C for 2 d. Progression of the reaction was monitored by TLC and mass spectrometry. On completion, EtOAc (20 mL) was added and the organic phase was washed with H_2O (20 mL), dried over $MgSO_4$, filtered and the solvent removed *in vacuo* to give a brown oil (234 mg).

Purification by column chromatography (100% CH_2Cl_2 to 10% MeOH/CH_2Cl_2) yielded pure **90** (92 mg, 27%), as a brown oil.

^{1}H NMR (400 MHz, $CDCl_3$) δ: 5.92, br s, 1H, -N*H*-; 3.67/3.62, m/m, 1H/1H, -O-CH_2CH$_2$-N-; 3.56/3.50, AB system, ^2J 10.4 Hz, 2H, -CH_2-O-; 3.45, m, 2H, -O-CH_2CH_2-N-; 2.65, t, ^3J 7.0 Hz, 2H, -CH_2CH$_2$-; 2.33, s, 3H; -OCO-CH_3; 2.20, s, 3H, Ar-CH_3; 1.98, s, 3H, Ar-CH_3; 1.93, s, 3H, -NCO-CH_3; 1.75, m, 2H, -CH$_2$CH_2-; 1.29, s, 3H, -CH_3. **^{13}C NMR (100 MHz, $CDCl_3$) δ:** 170.2, 169.3, 148.1, 141.0, 129.1, 127.6, 119.0, 112.5, 74.9, 70.5, 68.6, 39.4, 28.0, 23.2, 20.5, 20.4, 16.9, 12.4. **MS (ESI, +ve):** *m/z* 450.0 $[M+Na]^+$ (^{79}Br), 452.0 $[M+Na]^+$ (^{81}Br). **HRMS (ESI, +ve):** *m/z* 428.1072 $[M+H]^+$, $C_{19}H_{26}{}^{79}BrNO_5$ required *m/z* 428.1068; *m/z* 430.1055 $[M+H]^+$, $C_{19}H_{26}{}^{81}BrNO_5$ required *m/z* 430.1047.

3.9 References

1. Macfarlane, K. J. Small Molecules & Peptide Nucleic Acids for the Treatment and Prevention of Neurodegeneration. PhD Thesis, Monash University, Melbourne, 2004.

2. Cheema, S. S.; Langford, S.; Cheung, N. S.; Beart, P. M.; Macfarlane, K. J.; Mulcair, M. Agents and Methods for the Treatment of Disorders Associated with Oxidative Stress. U.S. Patent Application US2005/0288359 A1, December 29, 2005.

3. Wechter, W. J.; Kantoci, D.; Murray, E. D.; D'Amico, D. C.; Jung, M. E.; Wang, W.-H., *Proc. Natl. Acad. Sci. USA* **1996**, *93*, 6002-6007.

4. Kantoci, D.; Wechter, W. J.; Murray, E. D.; Dewind, S. A.; Borchardt, D.; Khan, S. I., *J. Pharmacol. Exp. Ther.* **1997**, *2822*, 648-656.

5. Pope, S. A. S.; Burtin, G. E.; Clayton, P. T.; Madge, D. J.; Muller, D. P. R., *Free Radic. Biol. Med.* **2002**, *33*, 807-817.

6. Mazzini, F.; Galli, F.; Salvadori, P., *Eur. J. Org. Chem.* **2006**, 5588-5593.

7. Fujita, Y.; Shiono, M.; Ejiri, K.; Saita, K., *Chem. Lett.* **1985**, 1399-1400.

8. Ahluwalia, V. K.; Arora, K. K.; Jolly, R. S., *J. Chem. Soc. Perkin Trans. 1* **1982**, 335-338.

9. Cichewicz, R. H.; Kenyon, V. A.; Whitman, S.; Morales, N. M.; Arguello, J. F.; Holman, T. R.; Crews, P., *J. Am. Chem. Soc.* **2004**, *126*, 14910-14920.

10. Kalena, G.; Jain, A.; Banerji, A., *Molecules* **1997**, *2*, 100-105.

11. Pope, S. A. S.; Burtin, G. E.; Clayton, P. T.; Madge, D. J.; Muller, D. P. R., *Bioorg. Med. Chem.* **2001**, *9*, 1337-1343.

12. Coman, S. M.; Pop, G.; Stere, C.; Parvulescu, V. I.; El Haskouri, J.; Beltrán, D.; Amorós, P., *J. Catal.* **2007**, *251*, 388-399.

13. Wehrli, P. A.; Fryer, R. I.; Metlesics, W., *J. Org. Chem.* **1971**, *36*, 2910-2912.

14. Muller, T.; Coowar, D.; Hanbali, M.; Heuschling, P.; Luu, B., *Tetrahedron* **2006**, *62*, 12025-12040.

15. Couladouros, E. A.; Moutsos, V. I.; Lampropoulou, M.; Little, J. L.; Hyatt, J. A., *J. Org. Chem.* **2007**, *72*, 6735-6741.

16. Hyatt, J. A., *Synth. Commun.* **2008**, *38*, 8-14.

17. Tamura, Y. Method for Producing 6-Hydroxy-2,5,7,8-Tetramethylcumarone-2-Carboxylic Acid Ester. Japanese Patent Application JP2003-146981, May 21, 2003.

18. Hodgson, D. M.; Stent, M. A. H. Substituted Alkene Diols. International Patent Application WO2003/018521 A1, March 6, 2003.

19. Mandai, T.; Yamaguchi, H.; Nishikawa, K.; Kawada, M.; Otera, J., *Tetrahedron Lett.* **1981**, *22*, 763-764.

20. Fukumoto, E.; Torihara, M.; Tamai, Y. Process for Producing Chroman. U.S. Patent 5,495,026, February 27, 1996.

21. Snuparek, V.; Polak, J.; Varga, I.; Kmetty, G. Preparation Method of 1,4-Benzendiol-2,3,5-Trimethyl-4-Acetate. Czech Patent CS239442, April 16, 1987.

22. Emerson, O. H.; Smith, L. I., *J. Am. Chem. Soc.* **1940**, *62*, 141-142.

23. Carpino, L. A.; Triolo, S. A.; Berglund, R. A., *J. Org. Chem.* **1989**, *54*, 3303-3310.

24. Baker, W.; Brown, N. C., *J. Chem. Soc.* **1948**, 2303 - 2307.

25. Scott, J.; Cort, W.; Harley, H.; Parrish, D.; Saucy, G., *J. Am. Oil Chem. Soc.* **1974**, *51*, 200-203.

26. Monoe, H.; Sato, J.; Kanehira, K.; Tamai, Y. Process for Producing Chromans. U.S. Patent 6,133,471, October 17, 2000.

27. Stille, J. K.; Becker, Y., *J. Org. Chem.* **1980**, *45*, 2139-2145.

28. Smith, L. I.; Wiley, P. F., *J. Am. Chem. Soc.* **1946**, *68*, 887-893.

29. Friedli, F. E.; Shechter, H., *Tetrahedron Lett.* **1985**, *26*, 1157-1158.

30. Back, T. G.; Yang, K.; Krouse, H. R., *J. Org. Chem.* **2002**, *57*, 1986-1990.

31. Kiehlmann, E.; van der Merwe, P. J.; Hundt, H. K. L., *Org. Prep. Proc. Int.* **1983**, *15*, 341-348.

32. Boyer, F.-D.; Beauhaire, J.; Martin, M. T.; Ducrot, P.-H., *Synthesis* **2006**, 3250-3260.

33. Rey, M.; Vergnani, T.; Dreiding, A. S., *Helv. Chim. Acta* **1985**, *68*, 1828-1834.

34. Yoshida, Y.; Sakakura, Y.; Aso, N.; Okada, S.; Tanabe, Y., *Tetrahedron* **1999**, *55*, 2183-2192.

35. Zlatev, I.; Vasseur, J.-J.; Morvan, F., *Tetrahedron* **2007**, *63*, 11174-11178.

36. Obert, E.; Bellot, M.; Bouteiller, L.; Andrioletti, F.; Lehen-Ferrenbach, C.; Boue, F., *J. Am. Chem. Soc.* **2007**, *129*, 15601-15605.

37. Goff, D. A.; Harris, R. N.; Bottaro, J. C.; Bedford, C. D., *J. Org. Chem.* **2002**, *51*, 4711-4714.

38. Skinner, W. A.; Parkhurst, R. M., *J. Chromatogr. A* **1964**, *13*, 69-73.

39. Tarabrin, M. B.; Chupin, V. V.; Bulychev, E. Y.; Evstigneeva, R. P., *Khim. Farm. Zh.* **1985**, *19*, 219-223.

40. James, T. H.; Snell, J. M.; Weissberger, A., *J. Am. Chem. Soc.* **1938**, *60*, 2084-2093.

41. Liu, F.; Liebeskind, L. S., *J. Org. Chem.* **1998**, *63*, 2835-2844.

42. Palozza, P.; Piccioni, E.; Avanzi, L.; Vertuani, S.; Calviello, G.; Manfredini, S., *Free Radic. Biol. Med.* **2002**, *33*, 1724-1735.

43. Machida, M.; Oda, K.; Kanaoka, Y., *Chem. Pharm. Bull.* **1984**, *32*, 75-84.

44. Adams, R.; Cairns, T. L., *J. Am. Chem. Soc.* **1939**, *61*, 2464-2467.

45. Peacock, D. H.; Dutta, U. C., *J. Chem. Soc.* **1934**, 1303-1305.

46. Sakellarios, E. J., *Helv. Chim. Acta* **1946**, *29*, 1675-1684.

47. Cox, M.; Prager, R. H.; Svensson, C. E., *Aust. J. Chem.* **2003**, *56*, 887-896.

CHAPTER FOUR

SYNTHESIS OF A VITAMIN E/BAPTA HYBRID

4.1 Introduction

In addition to the dual-action compounds and methods outlined in Chapter Three, synthesis of an alternative target incorporating the functionality of vitamin E and BAPTA, shown generally in Figure 4.1, was pursued.

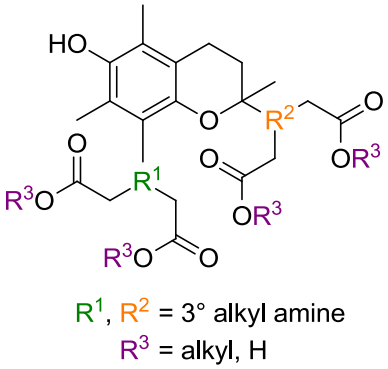

Figure 4.1 General vitamin E/BAPTA hybrid structure indicating C2/C8 functionalisation of a chromanol.

Work by Scott *et al.*[1] described the synthesis of (2*R*,4'*R*,8'*R*)-α-tocopherol (natural vitamin E) and (*2R*,3'*E*,7'*E*)-α-tocotrienol by means of first synthesising the 2,5,7,8-tetramethyl chromanol core, then functionalising the C2 acetal to form the phytyl tails of the target molecules. As shown overleaf in Scheme 4.1, acid-catalysed reaction of trimethylhydroquinone with methyl vinyl ketone and trimethyl orthoformate gives acetal **92**, from which acetylation yields protected chromanol **93**, as described in the literature.[1] Acid-catalysed hydrolysis of **93** leads to the mixture of ring-closed and ring-opened products **94a** and **94b** in equilibrium, of which **94b** may be subjected to nucleophilic attack by trimethyl phosphonoacetate in the presence of sodium hydride to give ester **95** *via* a Horner-Wadsworth-Emmons reaction.[1] The ester was then reduced using lithium aluminium hydride to produce the alcohol **44**, of which synthesis was attempted in Chapter Three by an alternate route.[2]

Using this methodology, and following work undertaken within our research group,[3] it is envisaged that general protected chroman alcohol analogue **96** may be synthesised in six steps from 2,6-dimethylhydroquinone (**37**), as shown in Scheme 4.2. From the alcohol intermediate **96**, functionality may be installed at the C8 position, allowing for Ca^{2+}-chelating BAPTA-like tetraacetate arms to be built, leading to the tetraethyl ester target.

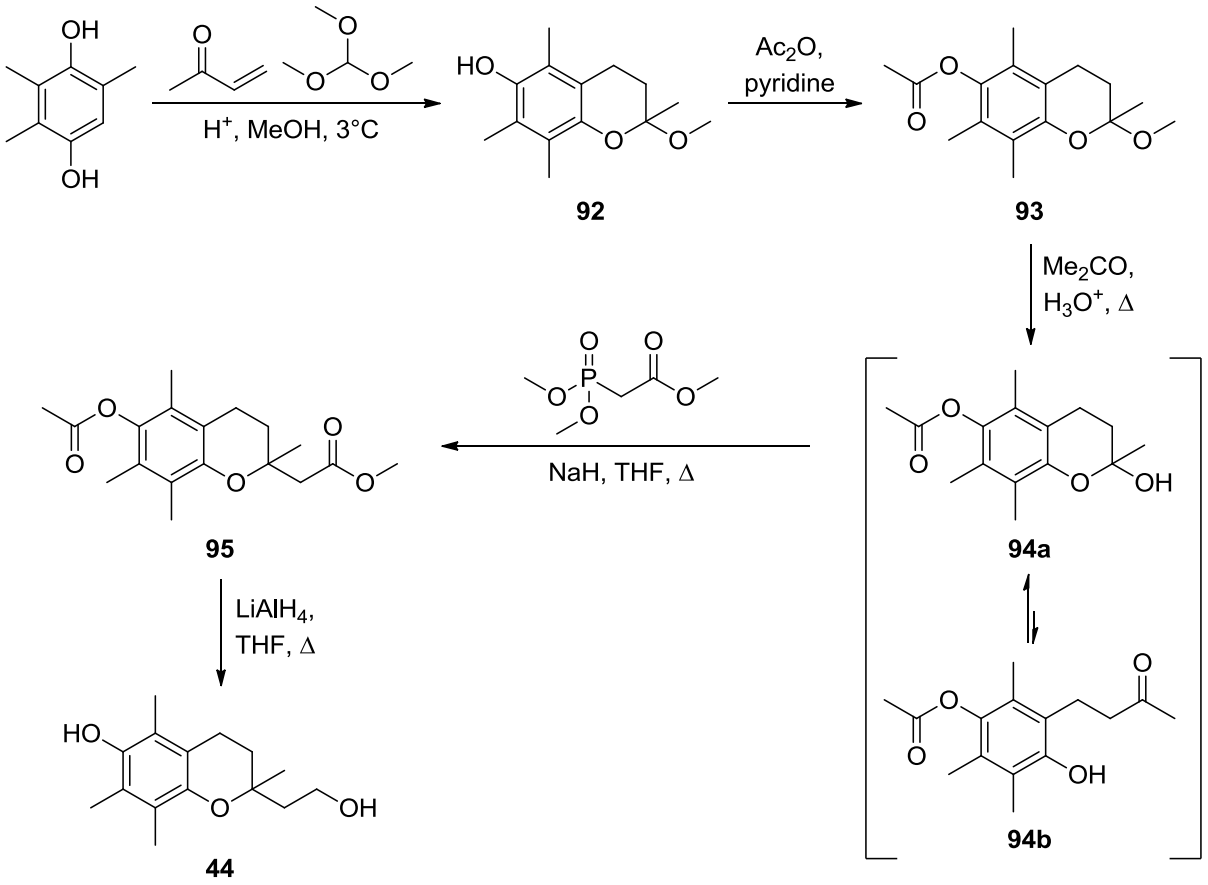

Scheme 4.1

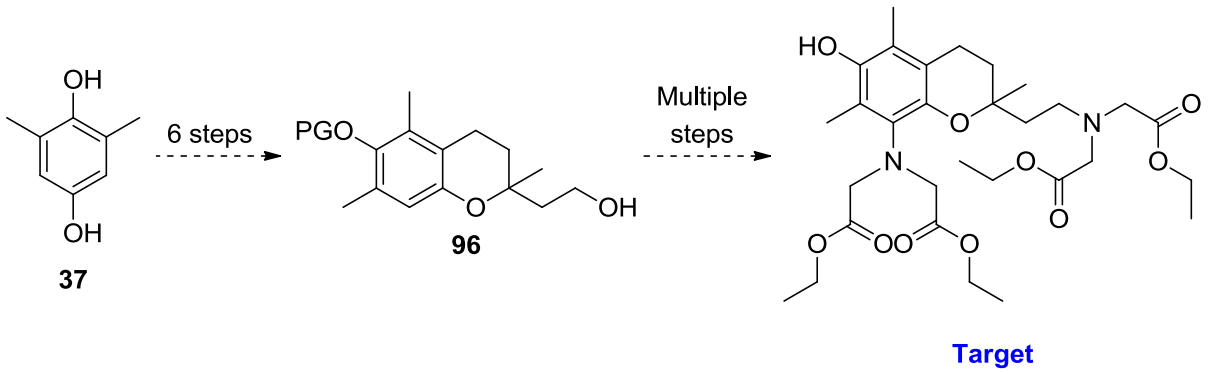

Scheme 4.2

4.2 Synthetic route to a vitamin E/BAPTA hybrid

Following Scott's method[1] and work undertaken within our research group,[3] reaction of the hydroquinone **37** with methyl vinyl ketone in the presence of trimethyl orthoformate and sulfuric acid resulted in the formation of the acetal **97** in good yield, as shown in Scheme 4.3. In

order to obtain the optimised yield of 84%, the methanol used as the solvent in the reaction was distilled before use, and the reaction temperature was maintained at 0°C to reduce the likelihood of a second alkylation at the C8 position. This appeared to give a clean reaction.

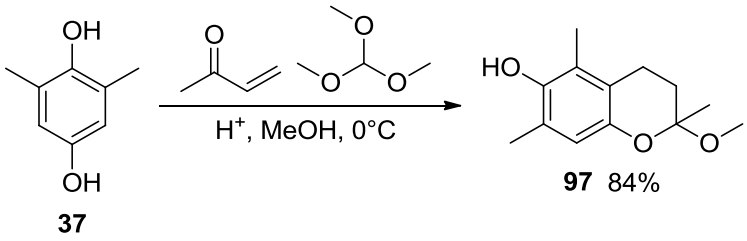

Scheme 4.3

Characterisation of **97** by ^{1}H NMR spectroscopy was consistent with the desired chroman structure, with the conversion from **37** evidenced by the aromatic proton resonance at 6.52 ppm integrating to only one proton and presence of singlets at 2.20 and 2.12 ppm indicative of the two inequivalent aromatic methyl proton peaks. New multiplets at 2.70/2.56 ppm and 2.11/1.79 ppm were also observed for the pyran ring protons, as well as singlets at 1.51 and 3.24 ppm attributable to the C2-methyl protons and methoxy protons, respectively. Carbon NMR spectroscopy similarly supported chroman formation, with peaks attributable to the newly formed pyran ring, in particular the two methylene carbons at 32.0 and 19.9 ppm, as well the presence of a peak at 49.0 ppm corresponding to the methoxy carbon resonance and an observed upfield shift of one aromatic methyl resonance from 16 ppm to 11.5 ppm.

With acetal **97** in hand, the next step was to protect the phenol by reaction with benzyl chloride, resulting in chromanol **98**. Choice of this protecting group was made due to the relatively inert benzyl ether formed, allowing reactions under a variety of conditions, including reduction by lithium aluminium hydride, without decomposition of the compound. It was also expected that the resulting benzyl ether could be readily cleaved at a later stage by hydrogenation leading to the target plus toluene, which could also be easily removed on workup.

Scheme 4.4 shows the protection of acetal **97** by the addition of an excess of benzyl chloride and potassium carbonate in acetonitrile, and the reaction mixture heated at reflux overnight to give **98** in quantitative yield.[4] The heterogeneous nature of the reaction, resulting from the low solubility of potassium carbonate in acetonitrile, meant that excess potassium carbonate could be removed from the reaction by filtration. Characterisation by low resolution ESI mass spectrometry supported the formation of the benzyl-protected acetal **98**, with m/z 335.4, attributable to $[M+Na]^{+}$. Four new resonances were observed by ^{13}C NMR spectroscopy, corresponding to the three different aromatic carbon environments of the benzyl

group at 128.6, 128.1, and 128.0 ppm respectively, as well as the benzylic carbon at 97.6 ppm.

Acetal **98** was subsequently hydrolysed to form the hemiacetal **99a** (Scheme 4.4),[1] which was used in subsequent reactions without further purification. Mass spectrometry (ESI) gave *m*/*z* 321.3, consistent with $[M+Na]^+$.

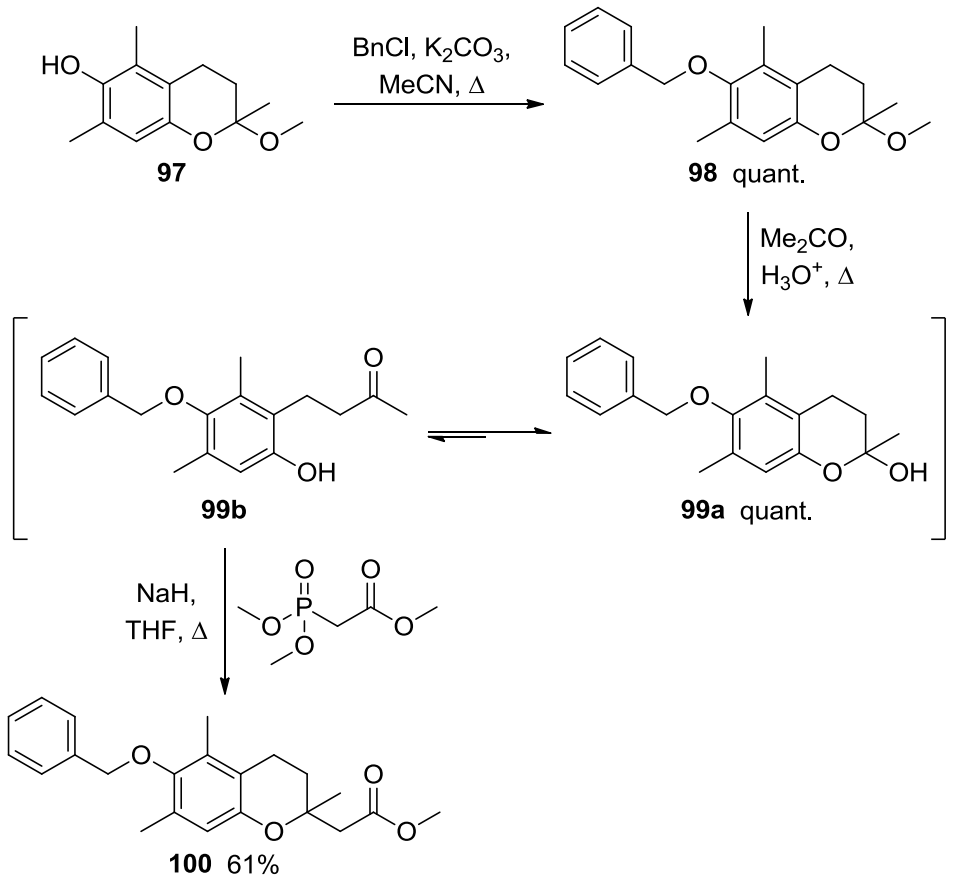

Scheme 4.4

Reaction of **99a** with trimethyl phosphonoacetate and sodium hydride in dry tetrahydrofuran formed ester **100**, *via* a Horner-Wadsworth-Emmons reaction.[1] The compound was obtained in 61% yield, after purification by column chromatography. Reaction of the phosphonoester with the ring-opened tautomer **99b** formed an intermediate oxaphosphetan, and subsequent ring-closing *via* a 1,4-addition afforded the ester **100** (Scheme 4.5).

The structure of **100** was supported by ^{1}H NMR spectroscopy, with a new peak at 3.70 ppm, integrating to three protons, assigned as the protons of the methyl ester. Low resolution ESI mass spectrometry gave a major peak at *m*/*z* 377.3, representing the $[M+Na]^+$ ion, whilst ^{13}C NMR spectroscopy showed a signal at 171.2 ppm, indicative of the carbonyl carbon present in the compound.

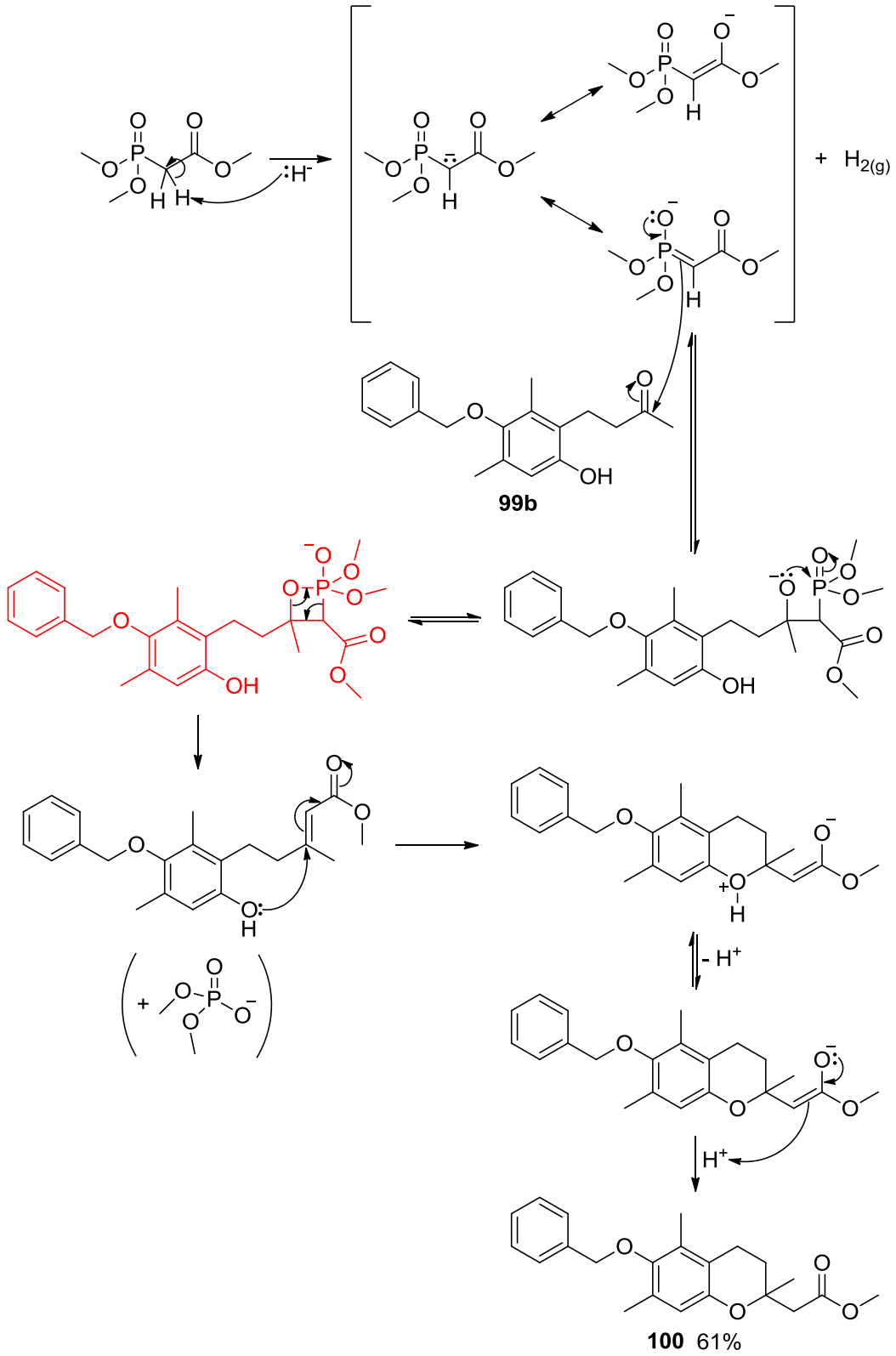

Scheme 4.5 Reaction of ring-opened **99b** with trimethyl phosphonoacetate to form ester **100**. The mechanism proceeds *via* an oxaphosphetan intermediate (**red**).

The next step in the synthetic scheme was to reduce the ester **100** to form the alcohol **101** (Scheme 4.6).[2] This was achieved by dropwise addition of a solution of **100** in dry tetrahydrofuran to a mixture of lithium aluminium hydride in dry tetrahydrofuran, and heating the heterogeneous mixture at reflux for two hours. After the aqueous workup, a good yield of oil (88%) was obtained. The ^{1}H NMR spectrum of the product obtained was more complicated than that of the starting ester, in particular the presence of the multiplets attributable to the -CH_2CH_2- protons at 3.88 and 1.84 ppm. The ^{13}C NMR spectroscopy signal at 171.2 ppm, attributed to the carbonyl of **100**, was also absent, indicating that the reduction was successful. Low resolution ESI mass spectrometry of **101** gave a strong signal at *m*/*z* 349.2, attributed to the $[M+Na]^+$ ion.

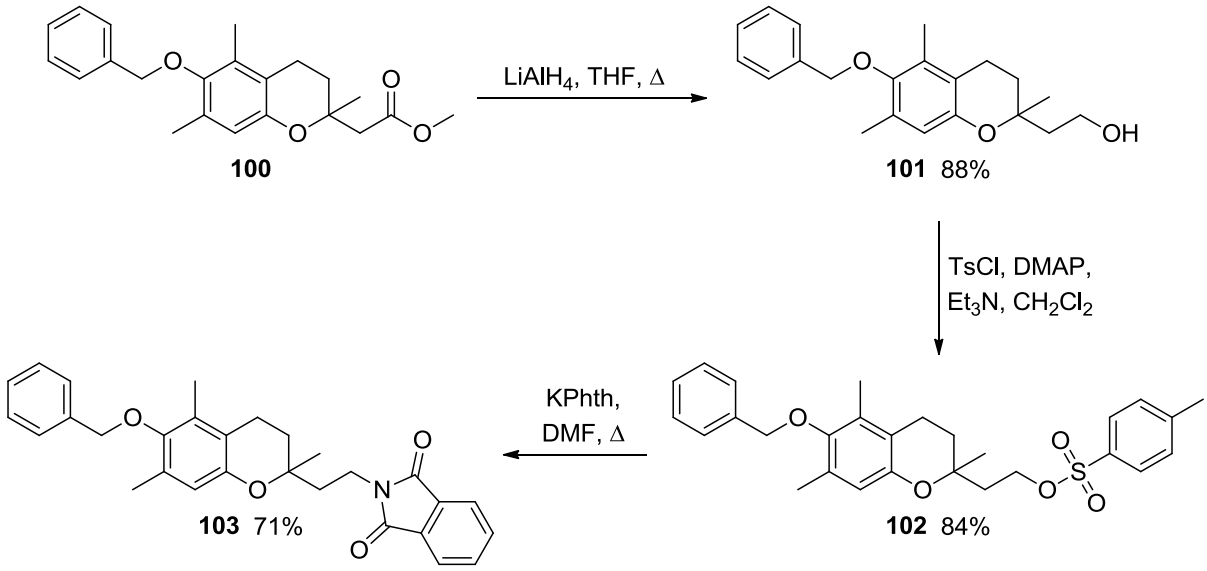

Scheme 4.6

From product **101**, two directions could have been taken to further functionalise the compound:

1) nitration of the chroman structure at the C8 position, which, after reduction, would produce the anilinic nitrogen; or
2) conversion of the alcohol to an amine by way of a Gabriel synthesis, which would first require substitution of the alcohol with a better leaving group (*e.g*. tosyl group), which could then be displaced with a phthalimide group, and deprotected to give the free amine.

Both synthetic routes were necessary to develop the amine groups of the target molecule; however functionalisation of the alkyl chain was attempted first. Previous unpublished studies within our group indicated the use of nitric acid to nitrate alcohol **101** at the C8 position could

cause unfavourable side reactions, such as elimination, and thus produce a low yield of the expected nitrated product. Alternatively nitration of a compound with a poor leaving group such as a phthalimide could remove complications arising from elimination.

Addition of *p*-toluenesulfonyl chloride and bases 4-dimethylaminopyridine (DMAP) and triethylamine to a solution of **101** in dichloromethane gave ester **102** in 84% yield (Scheme 4.6) after purification by column chromatography. Characterisation by high resolution mass spectrometry (ESI) indicated **102** had formed, with m/z 503.1871, consistent with the $[M+Na]^+$ ion. Addition of the tosyl group was also observed by ^{1}H NMR spectroscopy with signals attributable to the aromatic protons at 7.79 and 7.49 ppm, relating to the benzyl and tosyl protons collectively, as well as the tosyl methyl proton resonance at 2.45 ppm.

Substitution of the tosylate ester with a phthalimide group formed the first part of a Gabriel synthesis. With compound **102** in hand, reaction with potassium phthalimide in dimethylformamide afforded a white solid, in 71% yield, which was assigned as **103** after purification by column chromatography (Scheme 4.6). In the ^{1}H NMR spectrum of **103**, aromatic proton resonances were observed at 7.78 and 7.66 ppm, attributable to the phthalimide group, and resonances corresponding to the four aromatic and the methyl protons of the tosyl group were absent. An upfield shift of the resonance of the -CH_2CH_2-O- protons of **102** from 4.26 ppm to 3.93/3.80 ppm was also observed upon addition of the phthalimide group. Carbon NMR spectroscopy showed the carbon signal expected including the phthalimide carbonyl carbons, at 168.0 ppm. High resolution ESI mass spectrometry gave m/z 478.1994, attributed to $[M+Na]^+$.

Phthalimide **103**, dissolved in dichloromethane, was added to concentrated nitric in dichloromethane, and stirred at room temperature to afford **104**, a bright yellow powder, after purification by column chromatography, in quantitative yield (Scheme 4.7). Nitration of **103** was supported by the absence of the aromatic proton resonance at 6.22 ppm. High resolution ESI mass spectrometry gave the expected accurate mass result for $[M+Na]^+$ of m/z 523.1844. This is the first known example of nitration of the C8 position of a chromanol.

After synthesising **104**, the plan was to remove the phthalimide group to form the free amine, then reduce the nitro group to form the diamine, followed by alkylation to form the BAPTA arms of the structure. Firstly, decomposition of the phthalimide to form the free amine was attempted by dissolving **104** in absolute ethanol, followed by the dropwise addition of hydrazine hydrate (Scheme 4.7). The amine **105** was obtained in good yield (88%) and characterised by ^{1}H NMR spectroscopy, with the important difference being the removal of the phthalimide proton resonances. Carbon NMR spectroscopy also supported the structure of **105**, with the loss of some aromatic carbon resonances, as well as the loss of the carbonyl signal at 168.3 ppm. High resolution mass spectrometry (ESI) gave m/z 371.1957, attributed to $[M+H]^+$.

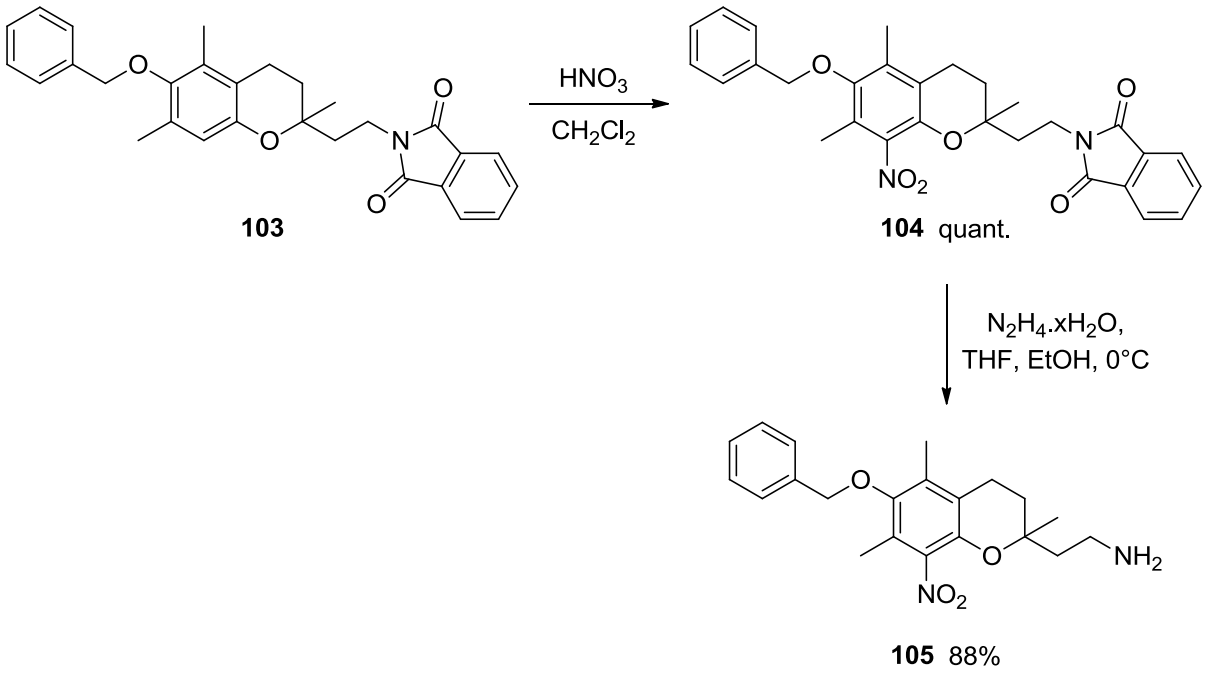

103 **104** quant. **105** 88%

Scheme 4.7

Reduction of the nitro group of **105** under hydrogenation conditions (Scheme 4.8) afforded aniline **106** in excellent yield. Product formation was supported by high resolution ESI mass spectrometry, with a major peak at *m*/*z* 341.2225, corresponding to the $[M+H]^+$ adduct of **106**. Alkylation of **106** under Finkelstein conditions using ethyl bromoacetate in the presence of sodium iodide and *N*,*N*-diisopropylethylamine (DIPEA) gave the tetraethyl ester **107** (Scheme 4.8) with an unoptimised yield of 18% after purification by column chromatography. Mono- and tri-alkylated intermediate species were observed by mass spectrometry in the remainder of the crude reaction mixture. Future optimisation of reaction conditions and purification may improve yield of the product.

Formation of **107** was supported by high resolution ESI mass spectrometry, with a $[M+Na]^+$ peak at *m*/*z* 707.3518, which agrees with the expected mass for the molecular formula of $C_{37}H_{52}N_2O_{10}$. Proton NMR spectroscopy also indicated the formation of **107**, with overlapping peaks at 4.15 and 1.25 ppm, corresponding to the new ethyl ester groups, as well as resonances at 3.80 and 3.57 ppm, indicative of the amino acetate protons. Figure 4.2 shows the proton NMR spectrum of **107**.

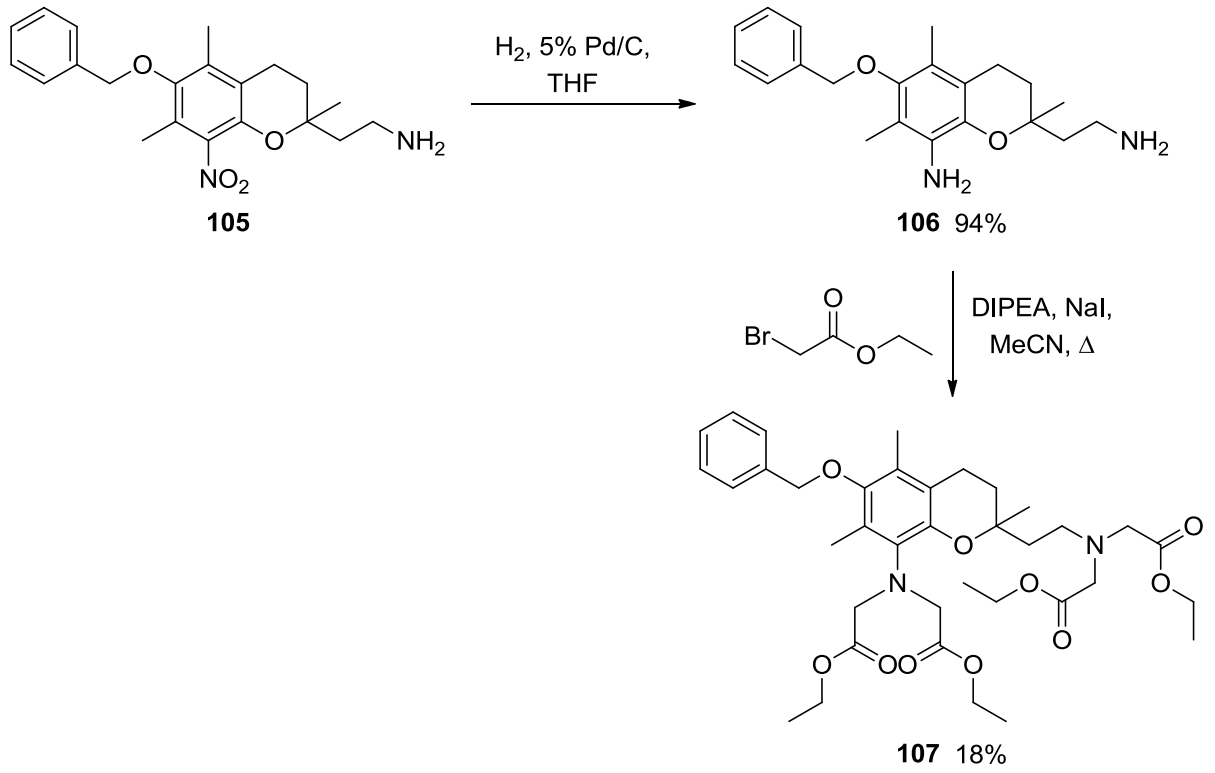

Scheme 4.8

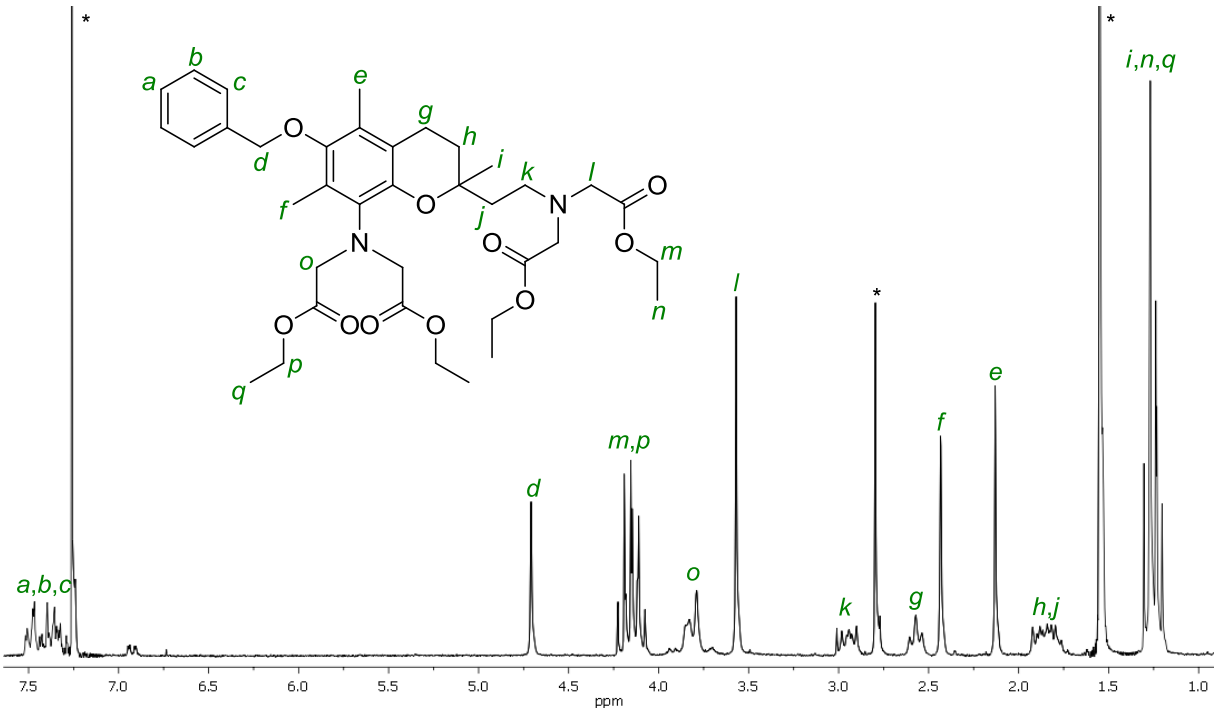

Figure 4.2 200 MHz ^{1}H NMR spectrum of **107** in $CDCl_3$ at 303K. * Denotes residual solvent peaks.

4.3 An alternate pathway towards the synthesis of the target

Given that acetate-protected alcohol **41** had previously been synthesised in Chapter Three from 2,6-dimethylhydroquinone *via* a bromo intermediate in much higher yield than the analogous benzyl-protected alcohol **101** over five steps (Scheme 4.9), it was decided that synthesis towards the dual-action target may also be approached using alcohol **41**. The benefit of following this synthetic pathway would be the ability to hydrolyse all esters in the one step, thus potentially eliminating a synthetic step.

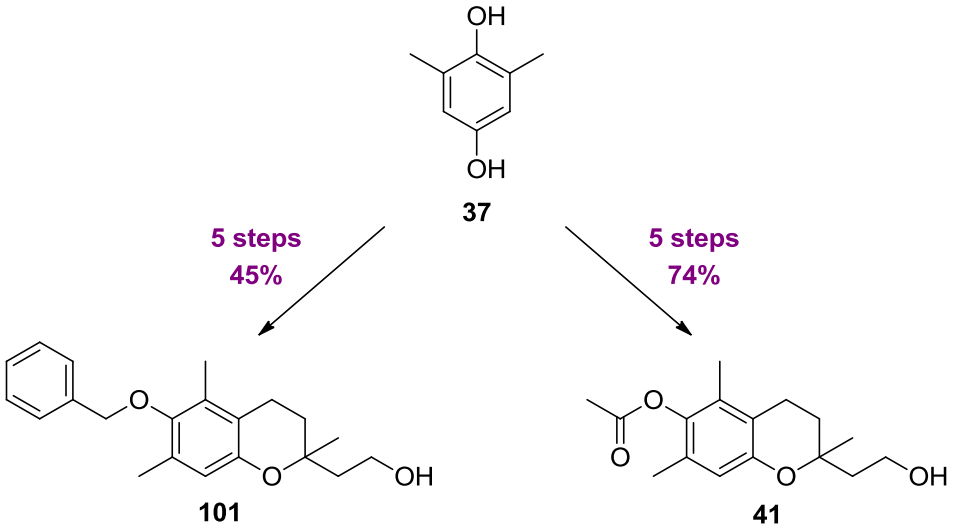

Scheme 4.9

Esterification of alcohol **41** using *p*-toluenesulfonyl chloride in the presence of bases 4-dimethylaminopyridine and triethylamine gave the expected product **108** in 76% yield (Scheme 4.10) after purification by column chromatography using 20% ethyl acetate in hexane as the eluent. Product formation was supported by a peak at *m/z* 455.1500 in the high resolution ESI mass spectrum, attributable to the $[M+Na]^+$ ion. Proton NMR spectroscopy also supported esterification, with new resonances at 7.76 and 7.31 ppm, and a visible downfield shift from 3.87 to 4.22 ppm of the multiplet corresponding to the methylene protons adjacent to the ester oxygen.

From the ester **108**, substitution using potassium phthalimide gave compound **60** as a pale yellow powder in 80% yield after purification (Scheme 4.10). Complete conversion was supported by the absence of the aromatic tosyl proton signals in the ^{1}H NMR spectrum at 7.76 and 7.31 ppm and the aromatic methyl peak at 2.43 ppm, as well the presence of new multiplets further downfield at 7.82 and 7.69 ppm. Compound **60** had been previously synthesised using another pathway in Chapter Three, *via* butoxymethyl intermediate **58**, leading to an overall yield

of 5% over four steps from **37**. The pathway pursued here in this chapter (shown in green in Scheme 4.10) produced **60** in an overall 45% yield over seven steps from **37**, thus providing a more efficient synthesis of **60**, despite the greater number of steps required.

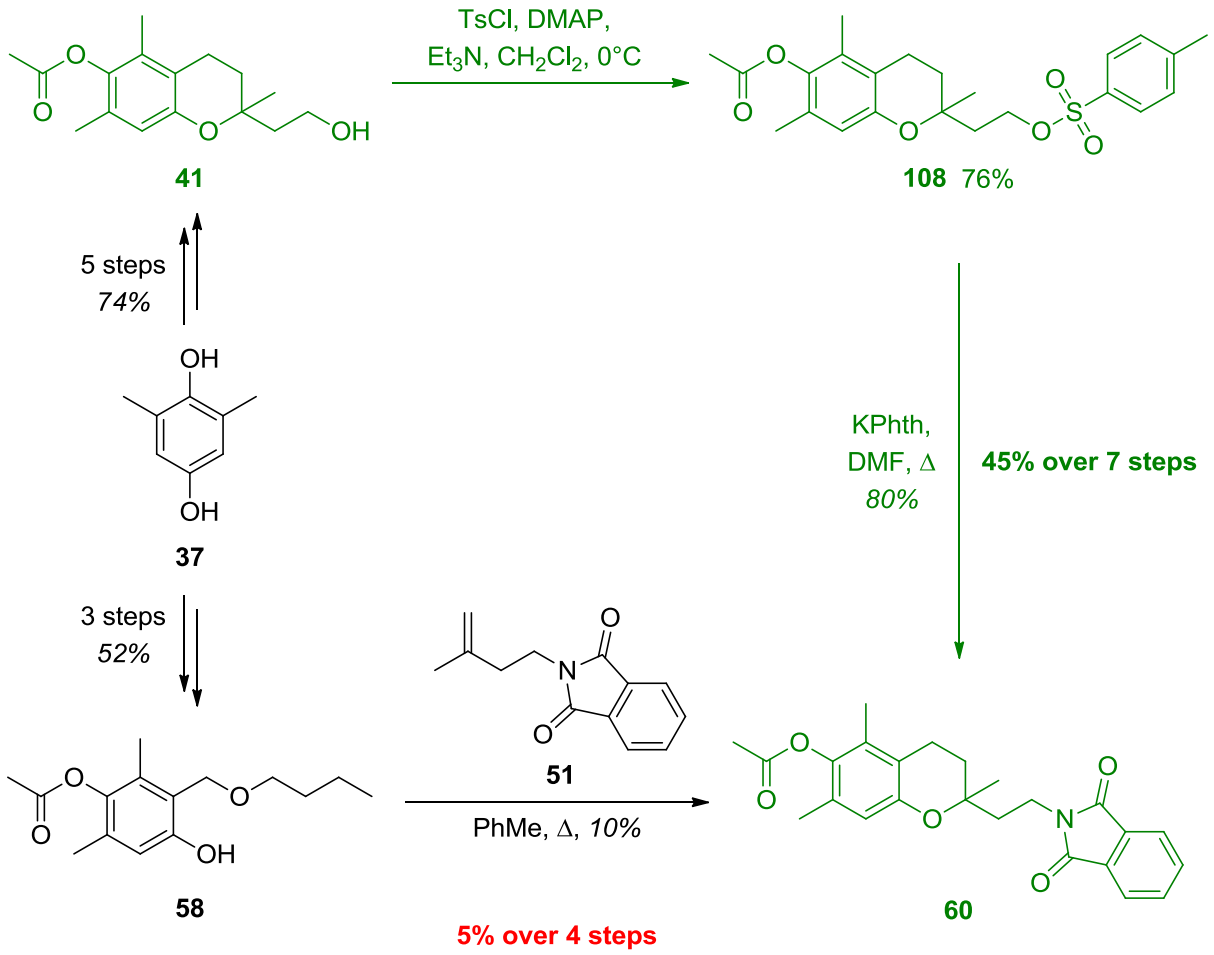

Scheme 4.10

From **60**, nitration in dichloromethane using concentrated nitric acid produced compound **109** in high yield (Scheme 4.11). Successful nitration was supported primarily by ^{1}H NMR spectroscopy, with the absence of the C8 aromatic proton signal of the starting material at 6.28 ppm, as well as a high resolution ESI mass spectrum peak at *m*/*z* 475.1471, corresponding to the $[M+Na]^+$ ion.

Subsequent treatment of **109** with hydrazine hydrate cleaved both the phthalimide group – as the second step of the Gabriel synthesis – and the acetate protecting group to give nitro amine compound **110** in 83% yield (Scheme 4.11). Formation of compound **110** was supported by high resolution ESI mass spectrometry, with a major peak at *m*/*z* 281.1501,

corresponding to $[M+H]^+$. Proton NMR spectroscopy also supported product formation, with the absence of acetyl and aryl protons at 2.3 and 7.7 ppm, respectively.

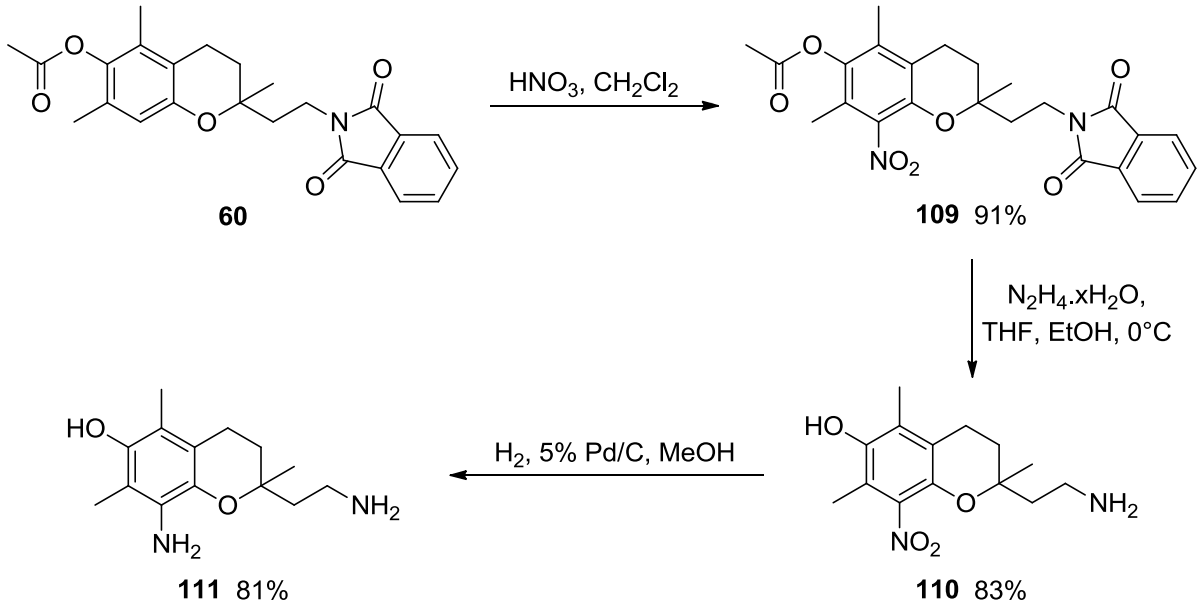

Scheme 4.11

Reduction of the nitro amine by hydrogenation (5% Pd/C) yielded aniline **111** in 81% yield (Scheme 4.11). Successful reduction to the diamine was supported by a major peak at m/z 251.1747 in the high resolution ESI mass spectrum, corresponding to the $[M+H]^+$ ion.

Alkylation of **111** using ethyl bromoacetate under Finkelstein conditions gave the target tetraethyl ester **112** with an unoptimised yield of 10% (Scheme 4.12). Successful tetra-alkylation was supported by high resolution ESI mass spectrometry, with peaks at m/z 595.3229 and m/z 617.1046, corresponding to the $[M+H]^+$ and $[M+Na]^+$ adducts of the product with a molecular formula of $C_{30}H_{46}N_2O_{10}$.

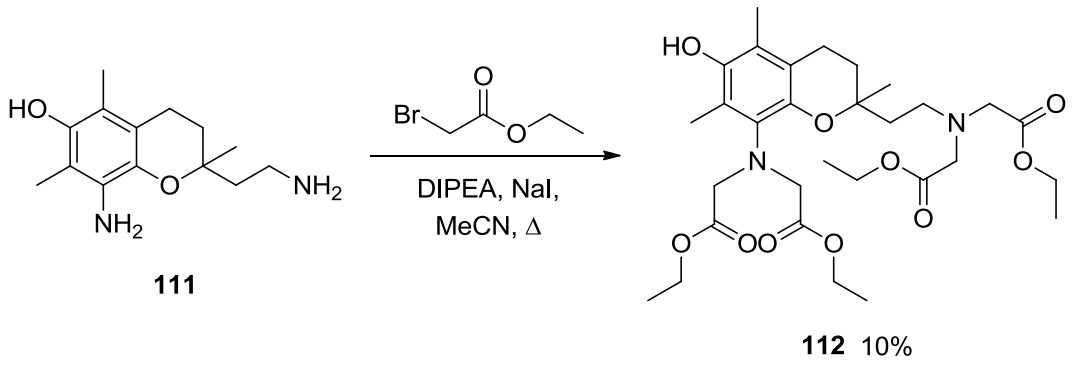

Scheme 4.12

The successful formation of **112** was also supported by ^{13}C NMR spectroscopy, with new resonances at 171.8 and 171.2 ppm, indicative of the two newly installed carbonyl groups, in addition to four distinct peaks at 14.4, 14.3, 11.5 and 11.3 ppm corresponding to the new ethyl ester groups. The remainder of the crude reaction mixture contained unidentified byproducts, although none of the mono-, di- or tri-alkylated intermediates were observed by mass spectrometry.

4.4 Aqueous antioxidant testing of candidates

The protocol employed to assess the antioxidant efficiency of the target molecules against lipid peroxidation was described in Chapter Two. Using the same method, the antioxidant efficiencies of **107** and **112** were determined and compared with vitamin E and both the acid and tetraethyl ester of BAPTA (Table 4.1).

Table 4.1 Antioxidant efficiencies calculated from the oxidation of linoleic acid.

Compound[a]	Efficiency (±5%)
Vitamin E[b]	91
3 (BAPTA ester)[c]	35
4 (BAPTA)[d]	79
107[b]	84
112[b]	95

[a] Final concentration of compounds was 33 μM
[b] Solubilised in methanol 33% (v/v)
[c] Solubilised in methanol 100% (v/v)
[d] Solubilised in dimethyl sulfoxide 33% (v/v)

Benzyl ether **107** exhibited high antioxidant efficiency compared to the BAPTA acid and tetraethyl ester, despite the protection of the phenol rendering the chromanol functionally inactive. The deprotected chromanol **112** exhibited even more potent antioxidant activity, higher than both vitamin E and BAPTA, indicating that the presence of the chelating side-chains, particularly the installation of the anilinic nitrogen *meta* to the phenol, did not appear to hinder antioxidant activity. This result supports the hypothesis that small molecule targets incorporating both a chromanol core based on vitamin E and Ca^{2+}-chelating functionality

analogous to BAPTA could prove suitable candidates for combating factors contributing to the pathogenesis of neurodegeneration. Further *in vitro* and *in vivo* studies would need to be performed in order to comprehensively assess the suitability of this class of compound in the prevention and treatment of neurodegeneration.

4.5 Conclusion

In summary, we have pursued two different pathways towards the synthesis of the pro-target. Reaction of 2,6-dimethylhydroquinone with methyl vinyl ketone and trimethyl orthoformate facilitated the construction of the chromanol core of the target molecule whilst leaving the C8 position available for further functionalisation. Protection of the chromanol and subsequent transformations, including a Horner-Wadsworth-Emmons reaction, yielded the benzyl-protected compound **107**. Overall, the synthesis was relatively inefficient, with a yield of 4% over eleven steps, and a further step required to deprotect **107** to give the target. A few of the reactions had low to moderate yields, while the alkylation of 2,6-dimethylhydroquinone **37** to form the acetal **97** and the Horner-Wadsworth-Emmons reaction of hemiacetal **99a** to form the ester **100** were not high yielding on a large scale. As a result, it was proposed that investigation of a more efficient synthetic pathway may be favourable for the synthesis of the target.

An alternative pathway towards the synthesis of the target **112** was undertaken from acetate-protected alcohol **41**, synthesised in Chapter Three, and following a similar sequence of reactions to those performed on the benzyl-protected series, the unprotected target **112** was synthesised in an overall yield of 3% over eleven steps from 2,6-dimethylhydroquinone. Most of the reactions in this pathway were high-yielding, giving an overall yield of 28% in the first ten steps, however the final alkylation step will require optimisation through refinement of reaction conditions and purification technique.

Aqueous antioxidant testing of final compounds **107** and **112** indicated antioxidant potency comparable with vitamin E and higher than BAPTA, while it is anticipated that these compounds would also exhibit Ca^{2+} binding similar to BAPTA, potentially allowing simultaneous targeting of factors contributing to both oxidative stress and disruption of Ca^{2+} homeostasis. Further *in vitro* and *in vivo* studies will be required to investigate the overall suitability of these compounds as candidates for the treatment and prevention of neurodegenerative disease.

4.6 Project summary

In summary, we have examined various pathways and methods towards the synthesis of "dual-action" candidates for treating motor neuron disease, incorporating both Ca^{2+}-chelating groups and antioxidant function based on BAPTA and vitamin E. While preliminary antioxidant testing indicates that some of the pro-drug candidates exhibit antioxidant efficiency comparable to vitamin E and higher than BAPTA, Ca^{2+} binding studies undertaken by isothermal titration calorimetry and antioxidant testing in the presence of Ca^{2+} should be undertaken in order to fully evaluate the potential of these candidates in synergistically targeting ROS and excess intracellular Ca^{2+}. Further functionalisation of the candidates – for example, the derivatisation of C4/C5/C7 chromanol positions, the incorporation of fluorescent tags, or the pursuit of benzofuran derivatives – may also provide possibilities in targeting the pathogenesis of motor neuron degeneration.

4.7 Experimental details

Synthesis of 2-(2-phthalimidylethyl)-2,5,7-trimethylchroman-6-yl acetate – 60:

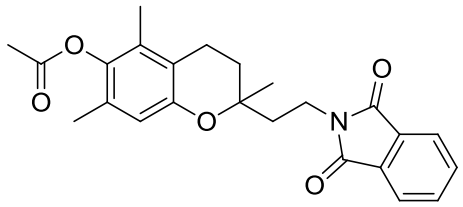

Ester **108** (1.77 g, 4.09 mmol) was dissolved in DMF (80 mL) and potassium phthalimide (1.53 g, 8.26 mmol) was added. The reaction was stirred and heated at 100°C overnight, with monitoring by TLC. On completion, H_2O was added to the reaction, and the product was extracted with CH_2Cl_2 (2 × 150 mL), washed with saturated aqueous $NaHCO_3$ solution (150 mL) and H_2O (150 mL), and the organic phase was dried over $MgSO_4$, filtered and solvent removed *in vacuo* to give a brown oil (2.15 g). Purification by column chromatography (50% EtOAc/hexane) gave pure phthalimide **60** (1.33 g, 80%), as a pale yellow powder.

^{1}H NMR (300 MHz, $CDCl_3$) δ: 7.82, m, 2H, Phth-*H*; 7.69, m, 2H, Phth-*H*; 6.28, s, 1H, Ar-*H*; 3.86, m, 2H, -CH_2CH_2-N-; 2.62, m, 2H, -CH_2CH_2-; 2.30, s, 3H, -OCO-CH_3; 2.08/1.86, m/m, 2H/2H, -CH_2CH_2-/-CH_2CH_2-N-; 1.98, s, 3H, Ar-CH_3; 1.96, s, 3H, Ar-CH_3; 1.35, s, 3H, -CH_3. **^{13}C NMR (75 MHz, $CDCl_3$) δ:** 169.5 (*C*=O), 168.3 (*C*=O), 150.9, 141.3, 133.9, 132.5, 128.7, 128.5, 123.3, 117.8, 116.7, 74.3, 37.5, 33.6, 31.2, 23.7, 20.6, 20.3, 16.4, 12.3. **MS (ESI, +ve):** *m*/*z* 430.1 $[M+Na]^+$. **HRMS (ESI, +ve):** *m*/*z* 425.2072 $[M+NH_4]^+$, $C_{24}H_{25}NO_5$ required *m*/*z* 425.2071. **MP:** 106.6-109.1°C.

Synthesis of 2-methoxy-2,5,7-trimethylchroman-6-ol – 97:

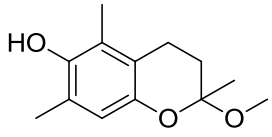

Adapted from Scott *et al.*[1] and Macfarlane.[3] 2,6-Dimethylhydroquinone **37** (500 mg, 3.62 mmol) and trimethyl orthoformate (550 µL, 5.02 mmol) were dissolved in dry MeOH (5 mL), and the reaction mixture was cooled on ice. Concentrated H_2SO_4 (100 µL) was added, followed by dropwise addition of methyl vinyl ketone (600 µL, 7.28 mmol). The reaction mixture was protected from light and stirred at 0°C for 1 h, before warming to room temperature with stirring for 4 h. Water was then added, and the resulting precipitate was washed with water and dried *in vacuo* to form **97** (672 mg, 84%) as a bright white crystalline powder.

^{1}H NMR (300 MHz, $CDCl_3$) δ: 6.52, s, 1H, Ar-*H*; 4.20, br s, 1H, Ar-O*H*; 3.24, s, 3H, -O-CH_3; 2.70/2.56, m/m, 1H/1H, -CH_2CH_2-; 2.20, s, 3H, Ar-CH_3; 2.12, s, 3H, Ar-CH_3; 2.11/1.79, m/m, 1H/1H, -CH_2CH_2-; 1.51, s, 3H, -CH_3. **^{13}C NMR (75 MHz, $CDCl_3$) δ:** 146.0, 145.9, 122.1, 121.9, 119.6, 116.1, 97.4, 49.0, 32.0, 23.2, 19.9, 16.1, 11.5. **MS (EI):** *m/z* 222 $[M]^+$. **MP:** 128.3-128.8°C (Literature[4]: 129-131°C).

Synthesis of 6-benzyloxy-2-methoxy-2,5,7-trimethylchroman – 98:

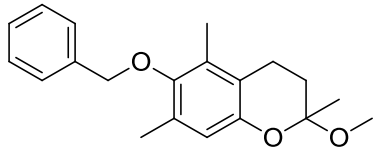

From Cohen *et al.*[4] Benzyl chloride (9.20 mL, 79.8 mmol), was added to a solution of **97** (3.53 g, 15.9 mmol) and K_2CO_3 (11.0 g, 79.6 mmol) in dry acetonitrile (100 mL). The reaction was protected from light and heated at reflux overnight. On completion, acetonitrile was added, the solution filtered and concentrated under high vacuum to give **98** (4.97 g, quant.) as a light brown oil. Product **98** was used in subsequent reactions without further purification.

^{1}H NMR (400 MHz, $CDCl_3$) δ: 7.51, m, 2H, Bn-*H*; 7.37, m, 3H, Bn-*H*; 6.59, s, 1H, Ar-*H*; 4.75, s, 2H, Ar-CH_2-O-; 3.28, s, 3H, -O-CH_3; 2.74/2.56, m/m, 1H/1H, -CH_2CH_2-; 2.28, s, 3H, Ar-CH_3; 2.20, s, 3H, Ar-CH_3; 2.14/1.82, m/m, 1H/1H, -CH_2CH_2- ; 1.55, s, 3H, -CH_3. **^{13}C NMR (75 MHz, $CDCl_3$) δ:** 149.6, 148.4, 138.1, 129.6, 129.5, 128.6, 128.1, 128.0, 119.7, 116.5, 97.6, 74.6, 49.1, 31.9, 23.2, 19.8, 16.5, 12.3. **MS (ESI, +ve):** *m/z* 335.4 $[M+Na]^+$.

Synthesis of 6-benzyloxy-2,5,7-trimethylchroman-2-ol – 99a:

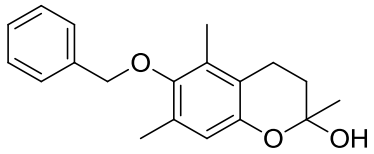

Adapted from Scott *et al*.[1] and Macfarlane.[3] Acetal **98** (4.98 g, 15.9 mmol) was dissolved in a mixture of acetone (30 mL), water (30 mL) and concentrated HCl (500 µL). Acetone was removed at reflux until the distilling head reached 98°C. The heat source was removed, and the solution cooled to room temperature. The product was extracted twice into EtOAc (2 × 50 mL), washed with H_2O (2 × 100 mL), dried over $MgSO_4$. After filtration and the solvent was removed under reduced pressure to give hemiacetal **99a** (4.75 g, quant.), as a brown oil. Product formation was supported by mass spectrometry.

MS (ESI, +ve): *m*/*z* 321.3 $[M+Na]^+$.

Synthesis of methyl 2-(6-benzyloxy-2,5,7-trimethylchroman-2-yl)acetate – 100:

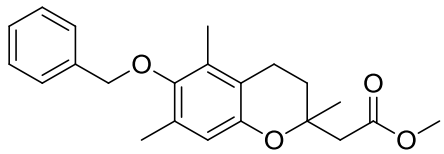

Adapted from Scott *et al*.[1] and Macfarlane.[3] 60% NaH in oil (1.40 g, 35.0 mmol) was washed twice with hexane and stirred in dry THF (120 mL), to which trimethyl phosphonoacetate (5.92 mL, 36.6 mmol) was added dropwise. Gas evolved from the reaction mixture. The reaction was stirred for 15 min before dropwise addition of **99a** (4.75 g, 15.9 mmol), pre-dissolved in dry THF (40 mL), forming a yellow solution. The solution heated at reflux for 16 d, during which time the reaction was monitored by TLC and a further 1.40 g of NaH and 5.92 mL of trimethyl phosphonoacetate in 50 mL dry THF was added to the reaction mixture. When the reaction was complete, solvent was removed under reduced pressure and Et_2O and H_2O were added to the flask, with vigorous stirring. The two phases were separated using a separating funnel. The ether layer was washed with H_2O, dried over $MgSO_4$, filtered and the solvent removed under reduced pressure to give a brown oil. Purification by column chromatography (20-50% EtOAc/hexane) afforded **100** (3.45 g, 61%), as a pale yellow oil.

^{1}H NMR (300 MHz, $CDCl_3$) δ: 7.48, m, 2H, Bn-*H*; 7.38, m, 3H, Bn-*H*; 6.52, s, 1H, Ar-*H*; 4.74, s, 2H, Ar-C*H*$_2$-O-; 3.70, s, 3H, -O-C*H*$_3$; 2.64, m, 4H, -C*H*$_2$CH$_2$-/-C*H*$_2$-CO$_2$-; 2.25, s, 3H, Ar-C*H*$_3$; 2.18, s, 3H, Ar-C*H*$_3$; 2.09/1.91, m/m, 1H/1H, -CH$_2$C*H*$_2$-; 1.43, s, 3H, -C*H*$_3$. **^{13}C NMR (75 MHz, $CDCl_3$) δ:** 171.2 (*C*=O), 149.2, 138.0, 130.0, 129.6, 128.6, 128.0, 127.9, 118.1, 116.9, 74.7, 73.8, 51.7, 43.7, 30.9, 25.0, 20.5, 16.5, 12.3. **MS (ESI, +ve):** *m*/*z* 377.3 $[M+Na]^+$.

Synthesis of 2-(6-benzyloxy-2,5,7-trimethylchroman-2-yl)ethanol – 101:

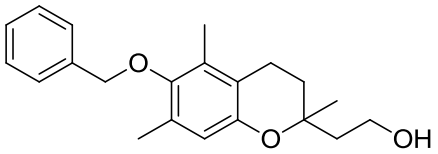

Adapted from Grisar *et al*.[2] and Macfarlane.[3] Ester **100** (1.40 g, 3.95 mmol) was dissolved in dry THF (6 mL) and added dropwise to a stirred suspension of $LiAlH_4$ (726 mg, 19.1 mmol) in dry THF (10 mL). The heterogeneous mixture was heated at reflux for 2 h, cooled and stirred at room temperature overnight. The reaction was cooled in an ice bath and quenched by dropwise addition of H_2O (20 mL) and then 2 M HCl (10 mL). Solvent was removed under reduced pressure and the product extracted in Et_2O (3 × 100 mL), washed with H_2O (300 mL) and saturated $NaHCO_3$ solution (300 mL), before drying over $MgSO_4$. Filtration and removal of solvent under reduced pressure produced alcohol **101** (1.14 g, 88%), as a clear yellow oil.

^{1}H NMR (300 MHz, $CDCl_3$) δ: 7.49, m, 2H, Bn-*H*; 7.38, m, 3H, Bn-*H*; 6.51, s, 1H, Ar-*H*; 4.74, s, 2H, Ar-C*H*$_2$-O-; 3.88, m, 2H, -CH_2C*H*$_2$OH; 2.63, t, ^3J 6.5 Hz, 2H, -C*H*$_2$$CH_2$-; 2.25, s, 3H, Ar-C*H*$_3$; 2.18, s, 3H, Ar-C*H*$_3$; 1.84, m, 4H, -C*H*$_2$$CH_2$OH/-$CH_2$C*H*$_2$-; 1.32, s, 3H, -C*H*$_3$. **^{13}C NMR (75 MHz, $CDCl_3$) δ:** 149.3, 149.1, 138.0, 130.0, 129.8, 128.6, 128.0, 127.9, 118.3, 116.8, 75.8, 74.7, 59.3, 41.8, 31.9, 23.5, 20.4, 16.5, 12.3. **MS (ESI, +ve):** *m/z* 327.2 $[M+H]^+$, 349.2 $[M+Na]^+$.

Synthesis of 2-(6-benzyloxy-2,5,7-trimethylchroman-2-yl)ethyl 4-methylbenzenesulfonate – 102:

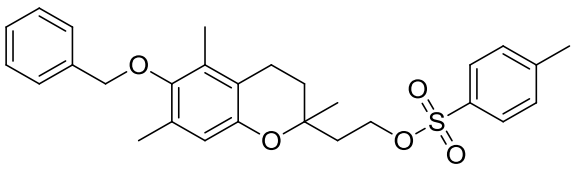

Alcohol **101** (1.60 g, 4.90 mmol), DMAP (110 mg, 0.90 mmol) and Et_3N (6.80 mL, 49.1 mmol) were dissolved in CH_2Cl_2 (15 mL). *p*-Toluenesulfonyl chloride (1.90 g, 10.0 mmol) was added and the solution stirred at room temperature overnight. On completion, the solvent was removed under reduced pressure and the product extracted into EtOAc, washed with NH_4Cl, brine and water, dried ($MgSO_4$), filtered and the solvent removed *in vacuo* to give **102** (1.99 g, 84%) as a yellow oil. The product was used in subsequent reactions without further purification.

^{1}H NMR (300 MHz, $CDCl_3$) δ: 7.79/7.49, AA'XX' system, ^3J 8.2 Hz, 4H, Ts-*H*; 7.35, m, 5H, Bn-*H*; 6.42, s, 1H, Ar-*H*; 4.73, s, 2H, Ar-C*H*$_2$-O-; 4.26, m, 2H, -CH_2C*H*$_2$-O-; 2.56, t, ^3J 6.8 Hz, 2H, -C*H*$_2$$CH_2$-;

2.45, s, 3H, Ar-CH_3; 2.24, s, 3H, Ar-CH_3; 2.05, s, 3H, Ar-CH_3; 1.97, m, 2H, -CH_2CH$_2$-O-; 1.80, t, ^3J 6.8 Hz, 2H, -CH$_2$CH_2-; 1.25, s, 3H, -CH_3. **^{13}C NMR (75 MHz, CDCl$_3$) δ:** 149.2, 144.9, 138.0, 133.3, 130.0, 129.7, 128.6, 128.0, 127.9, 118.0, 116.7, 74.7, 73.5, 67.0, 38.3, 31.7, 24.2, 21.8, 20.3, 16.5, 12.3. **MS (ESI, +ve):** *m/z* 481.3 [M+H]$^+$, 503.2 [M+Na]$^+$. **HRMS (ESI, +ve):** *m/z* 503.1871 [M+Na]$^+$, $C_{28}H_{32}O_5S$ required *m/z* 503.1863.

Synthesis of *N*-(2-(6-benzyloxy-2,5,7-trimethylchroman-2-yl)ethyl)phthalimide – 103:

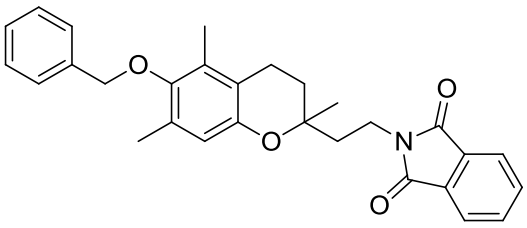

Ester **102** (1.95 g, 4.06 mmol) was dissolved in DMF (10 mL) and potassium phthalimide (3.75 g, 20.2 mmol) was added. The reaction was heated to 100°C for 3.5 h. Upon cooling to room temperature, 2 M HCl (30 mL) was added and the product extracted into $CHCl_3$, washed with 5 M aqueous KOH solution, then H_2O, and dried over $MgSO_4$. The solvent was removed *in vacuo* to yield **103** (1.31 g, 71%), as an off-white solid.

^{1}H NMR (400 MHz, CDCl$_3$) δ: 7.78, m, 2H, Phth-*H*; 7.66, m, 2H, Phth-*H*; 7.45, m, 2H, Bn-*H*; 7.34, m, 3H, Bn-*H*; 6.22, s, 1H, Ar-*H*; 4.68, s 2H, Ar-CH_2-O-; 3.93/3.80, m/m, 1H/1H, -CH$_2$CH_2-N-; 2.63, m, 2H, -CH_2CH$_2$-; 2.14, s, 3H, Ar-CH_3; 2.11, s, 3H, Ar-CH_3; 1.90/1.80, m/m, 4H, -CH_2CH$_2$-N-/-CH$_2$CH_2-; 1.36, s, 3H, -CH_3. **^{13}C NMR (100 MHz, CDCl$_3$) δ:** 168.0 (*C*=O), 149.2, 148.8, 137.9, 133.7, 132.3, 129.4, 129.3, 128.4, 127.7, 127.6, 123.0, 117.8, 116.5, 74.4, 73.8, 37.0, 33.4, 31.3, 29.6, 23.5, 20.1, 16.2, 12.1. **MS (ESI, +ve):** *m/z* 456.3 [M+H]$^+$, 478.2 [M+Na]$^+$. **HRMS (ESI, +ve):** *m/z* 478.1994 [M+Na]$^+$, $C_{29}H_{29}NO_4$ required *m/z* 478.1989. **MP:** 95.1-96.9°C.

Synthesis of *N*-(2-(6-benzyloxy-2,5,7-trimethyl-8-nitrochroman-2-yl)ethyl)phthalimide – 104:

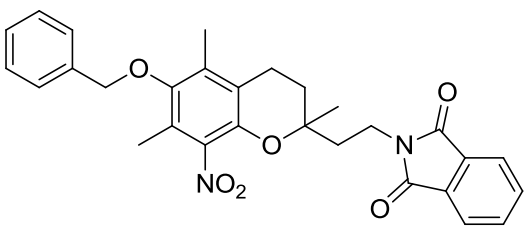

Phthalimide **103** (1.29 g, 2.82 mmol) was dissolved in CH_2Cl_2 (10 mL), and the solution was added dropwise to a vigorously stirred mixture of conc. HNO_3 (0.5 mL) in CH_2Cl_2 (150 mL). The reaction was stirred for 10 min, and turned a pale yellow colour. The reaction mixture was concentrated slowly *in vacuo* at room temperature to a third

of the original volume, and the reaction was monitored by TLC as the solution turned a bright yellow colour. On completion, water (30 mL) was added, and the two phases separated. The organic phase was washed with H_2O (30 mL), dried ($MgSO_4$), filtered, and the solvent removed to yield **104** (1.41 g, quant.) as a yellow solid.

^{1}H NMR (400 MHz, $CDCl_3$) δ: 7.82, m, 2H, Phth-*H*; 7.69, m, 2H, Phth-*H*; 7.40, m, 5H, Bn-*H*; 4.73, s, 2H, Ar-CH_2-O-; 3.83, m, 2H, -CH_2CH_2-N-; 2.67, m, 2H, -CH_2CH_2-; 2.19, s, 6H, Ar-CH_3; 1.8-2.1, m, 4H, -CH_2CH_2-N-/-CH_2CH_2-; 1.40, s, 3H, -CH_3. **^{13}C NMR (75 MHz, $CDCl_3$) δ:** 168.3 (*C*=O), 148.1, 141.3, 137.1, 134.0, 132.5, 132.3, 128.7, 128.4, 128.0, 123.3, 122.2, 120.1, 75.9, 75.3, 37.5, 33.4, 30.8, 23.6, 20.4, 12.6, 11.3. **MS (ESI, +ve):** *m/z* 501.3 $[M+H]^+$, 523.2 $[M+Na]^+$. **HRMS (ESI, +ve):** *m/z* 523.1844 $[M+Na]^+$, $C_{29}H_{28}N_2O_6$ required *m/z* 523.1840. **MP:** 125.6-127.8°C.

Synthesis of 2-(6-benzyloxy-2,5,7-trimethyl-8-nitrochroman-2-yl)ethanamine – 105:

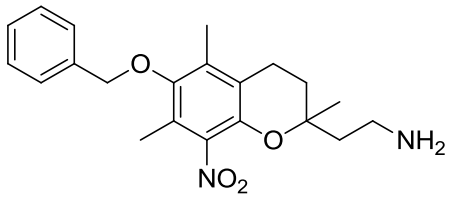

Nitro phthalimide compound **104** (437 mg, 0.873 mmol) was dissolved in THF (3 mL) and EtOH (20 mL) was added. After the solution was cooled to 0°C, hydrazine hydrate (425 μL, 8.73 mmol) was added dropwise, and the reaction mixture was allowed to warm slowly to room temperature was stirred for 3 d, monitored by TLC, during which time a precipitate formed. On completion, the reaction mixture was filtered to remove the phthalhydrazide byproduct and the product was washed through with EtOH. The filtrate was then concentrated under reduced pressure and the resulting crude solid dissolved in $CHCl_3$. The solution was again filtered to remove the byproduct and the filtrate concentrated *in vacuo* to give **105** (285 mg, 88%), as a bright yellow oil. The product was used in subsequent reactions without further purification.

^{1}H NMR (400 MHz, $CDCl_3$) δ: 7.39, m, 5H, Bn-*H*; 5.02, br s, 2H, -NH_2; 4.70, s, 2H, Ar-CH_2-O-; 2.98, m, 2H, -$CH_2CH_2NH_2$; 2.60, m, 2H, -CH_2CH_2-; 2.17, s, 3H, Ar-CH_3; 2.16, s, 3H, Ar-CH_3; 1.94, m, 4H, -CH_2CH_2-/-C$H_2CH_2NH_2$; 1.23, s, 3H, -CH_3. **^{13}C NMR δ (75 MHz, $CDCl_3$):** 148.0, 141.5, 137.0, 132.9, 132.6, 128.7, 128.3, 127.9, 122.1, 120.3, 76.6, 75.3, 38.8, 35.4, 31.3, 23.7, 20.4, 12.6, 11.3. **MS (ESI, +ve):** *m/z* 371.3 $[M+H]^+$, 393.3 $[M+Na]^+$. **HRMS (ESI, +ve):** *m/z* 371.1957 $[M+H]^+$, $C_{21}H_{26}N_2O_4$ required *m/z* 371.1965.

Synthesis of 2-(2-aminoethyl)-6-benzyloxy-2,5,7-trimethylchroman-8-amine – 106:

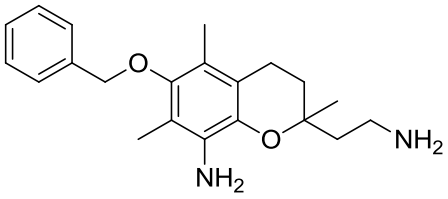

Nitro compound **105** (52 mg, 0.14 mmol) was dissolved in THF (2 mL), and 5% Pd/C (10 mg) was added to the solution. The reaction vessel was flushed with N_2, and a H_2 balloon was applied. The reaction mixture was stirred at room temperature for 2 d, during which time the reaction was monitored by mass spectrometry. When all starting material appeared to have been consumed, the reaction mixture was filtered through celite and the solvent was removed by rotary evaporation to give diamine **106** (45 mg, 94%), as a yellow oil. The product was used in subsequent reactions without purification.

^{1}H NMR (400 MHz, $CDCl_3$) δ: 7.39, m, 5H, Bn-*H*; 4.65, s, 2H, Ar-C*H*$_2$-O-; 3.94, br s, 4H, -N*H*$_2$; 3.11, br s, 2H, -$CH_2CH_2NH_2$; 2.55, m, 2H, -C*H*$_2$$CH_2$-; 2.08, s, 3H, Ar-C*H*$_3$; 2.05, s, 3H, Ar-C*H*$_3$; 1.93/1.71, m/m, 4H, -$CH_2CH_2$-/-C*H*$_2$$CH_2NH_2$; 1.20, s, 3H, Ar-C*H*$_3$. **^{13}C NMR (75 MHz, $CDCl_3$) δ:** 148.8, 137.9, 137.3, 131.8, 128.8, 128.5, 127.7, 127.1, 118.1, 114.2, 74.9, 74.5, 38.2, 35.9, 31.1, 23.4, 20.1, 11.5, 10.4. **MS (ESI, +ve):** *m/z* 341.4 $[M+H]^+$. **HRMS (ESI, +ve):** *m/z* 341.2225 $[M+H]^+$, $C_{21}H_{28}N_2O_2$ required *m/z* 341.2224.

Synthesis of diethyl 2,2'-((6-benzyloxy-2-(2-(bis(2-ethoxy-2-oxoethyl)amino)ethyl)-2,5,7-trimethylchroman-8-yl)azanediyl)diacetate – 107:

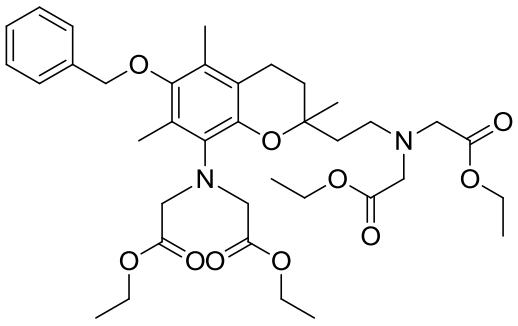

Diamine **106** (73 mg, 0.21 mmol) was dissolved in acetonitrile (8 mL), and NaI (18 mg, 0.12 mmol), DIPEA (410 µL, 2.35 mmol) and ethyl bromoacetate (240 µL, 2.16 mmol) were added. The reaction was heated at reflux for 4 d, with monitoring by mass spectrometry, after which time the reaction mixture was cooled to room temperature, filtered, and the product washed through with EtOAc (100 mL). The filtrate was washed with H_2O (2 × 100 mL), dried over $MgSO_4$, filtered and the solvent removed *in vacuo* to give a red-brown oil (134 mg). Purification by column chromatography (50% EtOAc/hexane to 100% EtOAc) isolated tetraethyl ester **107** (27 mg, 18%), as a clear yellow oil.

^{1}H NMR (200 MHz) δ: 7.40, m, 5H, Bn-*H*; 4.71, s, 2H, Ar-CH_2-O-; 4.17/4.13, q/q, ^3J 7.1 Hz, 8H, -O-CH_2CH$_3$; 3.80, m, 4H, -N-CH_2-CO$_2$-; 3.57, s, 4H, -N-CH_2-CO$_2$-; 2.95, m, 2H, -CH$_2$CH_2-N-; 2.57, t, ^3J 6.9 Hz, 2H, -CH_2CH$_2$-; 2.43, s, 3H, Ar-CH_3; 2.13, s, 3H, Ar-CH_3; 1.84, m, 4H, -CH$_2$CH_2-/-CH_2CH$_2$-N-; 1.25, m, 15H, -CH_3/-CH$_2$CH_3. **^{13}C NMR (100 MHz, CDCl$_3$) δ:** 171.8 (*C*=O), 171.3 (*C*=O), 148.7, 147.9, 138.1, 136.1, 130.1, 128.6, 127.9, 127.8, 127.2, 118.1, 74.8, 74.5, 60.7, 60.6, 60.4, 55.2, 49.7, 38.4, 31.1, 23.6, 20.6, 14.4, 14.3, 12.2, 12.0. **MS (ESI, +ve):** *m*/*z* 685.4 [M+H]$^+$, 707.4 [M+Na]$^+$. **HRMS (ESI, +ve):** *m*/*z* 707.3518 [M+Na]$^+$, $C_{37}H_{52}N_2O_{10}$ required *m*/*z* 707.3514.

Synthesis of 2,5,7-trimethyl-2-(2-(tosyloxy)ethyl)chroman-6-yl acetate – 108:

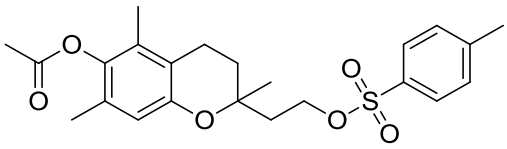

Alcohol **41** (1.52 g, 5.46 mmol) was dissolved in CH_2Cl_2 (50 mL), and DMAP (140 mg, 1.15 mmol) and Et_3N (1.52 mL, 10.9 mmol) were added. The reaction mixture was stirred and cooled to 0°C, and *p*-toluenesulfonyl chloride (2.08 g, 10.9 mmol) was added slowly to the reaction mixture. The reaction was allowed to warm to room temperature and stirred overnight, with monitoring by TLC. When all starting material had appeared to have been consumed, the product was taken up in EtOAc, and the resulting organic solution was washed twice with saturated aqueous NH_4Cl solution, once with brine and H_2O, and dried over $MgSO_4$, filtered and the solvent removed by rotary evaporation to give a brown oil (2.83 g). Purification by column chromatography (20% EtOAc/hexane to 100% EtOAc) isolated ester **108** (1.80 g, 76%), as a pale brown oil.

^{1}H NMR (300 MHz, CDCl$_3$) δ: 7.76/7.31, AA'XX' system, ^3J 8.2 Hz, 4H, Ts-*H*; 6.42, s, 1H, Ar-*H*; 4.22, m, 2H, -CH$_2$CH_2-O-; 2.53, t, ^3J 7.0 Hz, 2H, -CH_2CH$_2$-; 2.43, s, 3H, -OCO-CH_3; 2.30, s, 3H, Ar-CH_3; 2.04, s, 3H, Ar-CH_3; 1.96, s, 3H, Ar-CH_3; 1.95, m, 2H, -CH$_2$CH_2-/-CH_2CH$_2$-O-; 1.75, 2H, m, -CH$_2$CH_2-/-CH_2CH$_2$-O-; 1.22, s, 3H, -CH_3. **^{13}C NMR (75 MHz, CDCl$_3$) δ:** 169.5 (*C*=O), 150.7, 144.9, 141.5, 133.3, 130.0, 128.9, 128.6, 128.0, 117.8, 116.7, 73.7, 66.9, 38.4, 31.4, 24.2, 21.7, 20.6, 20.2, 16.4, 12.3. **MS (ESI, +ve):** *m*/*z* 455.1 [M+Na]$^+$. **HRMS (ESI, +ve):** *m*/*z* 455.1500, $C_{23}H_{28}O_6S$ required *m*/*z* 455.1499.

Synthesis of 2-(2-phthalimidylethyl)-2,5,7-trimethyl-8-nitrochroman-6-yl acetate – 109:

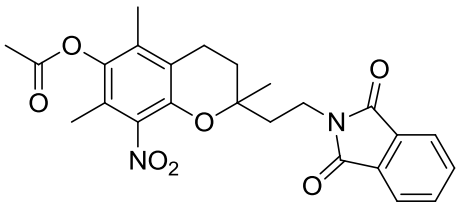

Phthalimide **60** (999 mg, 2.45 mmol) was dissolved in CH_2Cl_2 (30 mL), and the solution was added dropwise to a vigorously stirred mixture of conc. HNO_3 (475 µL) in CH_2Cl_2 (140 mL). The reaction was stirred at room temperature overnight, after which time TLC analysis indicated that the starting material had not fully been consumed. The reaction mixture was concentrated at 50°C by rotary evaporation to 20 mL, and stirred again overnight, with a precipitate forming in the reaction flask. On completion, the product was redissolved in CH_2Cl_2, washed with saturated aqueous $NaHCO_3$ solution and H_2O, dried with $MgSO_4$, filtered and the solvent removed under reduced pressure to give pure **109** (1.01 g, 91%), as a yellow powder.

^{1}H NMR (400 MHz, $CDCl_3$) δ: 7.74, m, 2H, Phth-*H*; 7.68, m, 2H, Phth-*H*; 3.81, m, 2H, -CH_2CH_2-N-; 2.67, m, 2H, -CH_2CH_2-; 2.33, s, 3H, -OCO-CH_3; 2.02, s, 3H, Ar-CH_3; 2.01, s, 3H, Ar-CH_3; 1.90, m, 4H, -CH_2CH_2-/-CH_2CH_2-N-; 1.38, s, 3H, -CH_3. **^{13}C NMR (75 MHz, $CDCl_3$) δ:** 168.9 (*C*=O), 168.3 (*C*=O), 142.9, 140.4, 134.0, 131.6, 130.2, 128.4, 123.4, 121.6, 120.0, 76.3, 37.5, 33.3, 30.5, 23.6, 20.5, 20.3, 12.7, 11.6. **MS (ESI, +ve):** *m/z* 453.0 $[M+H]^+$, 474.9 $[M+Na]^+$. **HRMS (ESI, +ve):** *m/z* 475.1471 $[M+Na]^+$, $C_{24}H_{24}N_2O_7$ required *m/z* 475.1476. **MP:** 88.2-91.6°C.

Synthesis of 2-(2-aminoethyl)-2,5,7-trimethyl-8-nitrochroman-6-ol – 110:

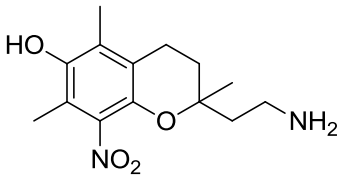

Compound **109** (190 mg, 0.42 mmol) was dissolved in THF (8 mL) and EtOH (22 mL) was added to the solution, which was cooled to 0°C before the dropwise addition of hydrazine hydrate (200 µL, 4.2 mmol). The reaction mixture was allowed to warm to room temperature and stirred overnight. The reaction was monitored by TLC, and on apparent consumption of **109**. On completion, the solvent was removed by rotary evaporation to give an orange solid (286 mg). The residue was dissolved in $CHCl_3$ and filtered to remove phthalhydrazide, and the solution was washed with several small portions of H_2O. The organic solvent was removed under reduced pressure to give product **110** (98 mg, 83%), as a yellow oil.

^{1}H NMR (400 MHz, $CDCl_3$) δ: 3.89, br s, 2H, -NH_2; 2.83, m, 2H, -$CH_2CH_2NH_2$, 2.59, t, ^3J 6.0 Hz, 2H, -CH_2CH_2-; 2.07, s, 3H, Ar-CH_3; 1.92, s, 3H, Ar-CH_3; 1.75, m, 4H, -CH_2CH_2-/-$CH_2CH_2NH_2$; 1.21, s, 3H,

-C*H*$_3$. **^{13}C NMR (100 MHz, CDCl$_3$) δ:** 145.3, 140.1, 138.5, 130.2, 128.3, 119.5, 76.2, 35.3, 31.6, 31.3, 23.6, 20.4, 12.1, 11.3. **MS (ESI, +ve):** *m*/*z* 281.2 [M+H]$^+$. **HRMS (ESI, +ve):** *m*/*z* 281.1501 [M+H]$^+$, $C_{14}H_{20}N_2O_4$ required *m*/*z* 281.1496.

Synthesis of 8-amino-2-(2-aminoethyl)-2,5,7-trimethylchroman-6-ol – 111:

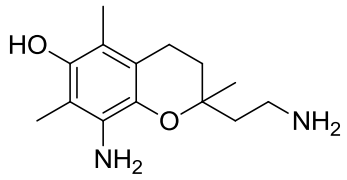

Nitro compound **110** (701 mg, 2.50 mmol) was dissolved in MeOH (15 mL) and 5% Pd/C (140 mg) was added to the solution. The reaction vessel was flushed with N_2, and a H_2 balloon was applied. The reaction mixture was stirred at room temperature for 5 d, during which time the reaction was monitored by mass spectrometry. On completion, the reaction mixture was filtered through celite and the product washed through with MeOH. The mixture was centrifuged, the solution decanted, and MeOH was added to the remaining white insoluble material and centrifuged and decanted a second time. The solutions were combined and concentrated *in vacuo* to yield **111** (510 mg, 81%), as a red-brown oil. The product was used in subsequent reactions without purification.

^{1}H NMR (300 MHz, CDCl$_3$) δ: 2.61, m, 4H, -CH$_2$C*H*$_2$NH$_2$/-C*H*$_2$CH$_2$-; 2.14, s, 6H, Ar-C*H*$_3$; 1.9-1.7, m, 4H, -CH$_2$C*H*$_2$-/-C*H*$_2$CH$_2$NH$_2$; 1.32, s, 3H, -C*H*$_3$. **^{13}C NMR (75 MHz, CDCl$_3$) δ:** 145.3, 139.2, 136.7, 129.7, 128.6, 122.0, 77.4, 39.3, 37.0, 33.8, 21.8, 20.4, 11.0, 9.9. **MS (ESI, +ve):** *m*/*z* 251.2 [M+H]$^+$. **HRMS (ESI, +ve):** *m*/*z* 251.1747 [M+H]$^+$, $C_{14}H_{22}N_2O_2$ required *m*/*z* 251.1754.

Synthesis of diethyl 2,2'-((2-(8-(bis(2-ethoxy-2-oxoethyl)amino)-6-hydroxy-2,5,7-trimethylchroman-2-yl)ethyl)azanediyl)diacetate – 112:

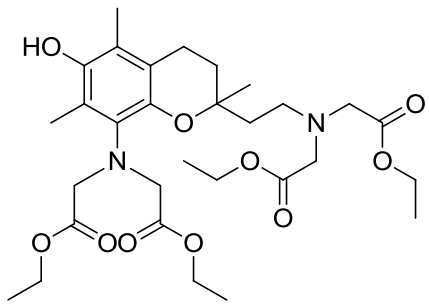

Diamine **111** (500 mg, 2.00 mmol) was stirred in acetonitrile (30 mL), and DIEPA (3.83 mL, 22.0 mmol), ethyl bromoacetate (2.22 mL, 19.9 mmol) and NaI (156 mg, 1.04 mmol) were added. The reaction was heated at reflux and monitored by TLC for 3 d, after which time a further 1.91 mL (11.0 mmol) of DIPEA was added. The reaction was heated at reflux for a further 2 d, after which time low resolution ESI mass spectrometry indicated product formation, with an absence of any peaks corresponding to the starting

material **111** or any mono-, di- or tri-alkylated intermediates. The reaction was cooled to room temperature and filtered to remove insoluble material. The filtrate was concentrated under reduced pressure, H_2O (100 mL) was added and the product was extracted with EtOAc (2 × 100 mL). The organic extracts were washed with H_2O (4 × 100 mL), dried over $NaSO_4$, filtered and concentrated *in vacuo* to give a brown oil (3.50 g). Purification by column chromatography (2% MeOH/CH_2Cl_2 to 20% MeOH/CH_2Cl_2) yielded **112** (124 mg, 10%) as a brown oil.

^{1}H NMR (300 MHz, $CDCl_3$) δ: 4.14, m, 12H, -N-C*H*$_2$-CO$_2$-/-C*H*$_2$CH$_3$; 3.55, s, 4H, -N-C*H*$_2$-CO$_2$-; 2.92, t, ^3J 8.1 Hz, 2H, -CH$_2$C*H*$_2$-N-; 2.57, t, ^3J 6.6 Hz, 2H, -C*H*$_2$CH$_2$-; 2.37, s, 3H, Ar-C*H*$_3$; 2.06, s, 3H, Ar-C*H*$_3$; 1.82, m, 4H, -CH$_2$C*H*$_2$-/-C*H*$_2$CH$_2$-N-; 1.25, m, 15H, -C*H*$_3$/-CH$_2$C*H*$_3$. **^{13}C NMR (100 MHz, $CDCl_3$) δ:** 171.8 (*C*=O), 171.2 (*C*=O), 145.3, 145.2, 135.5, 122.4, 119.8, 118.0, 74.4, 60.7, 60.6, 60.4, 55.2, 49.6, 38.4, 31.2, 23.3, 20.5, 14.4, 14.3, 11.5, 11.3. **MS (ESI, +ve):** *m*/*z* 298.1 $[M+2H]^+$, 595.3 $[M+H]^+$, 617.3 $[M+Na]^+$. **HRMS (ESI, +ve):** *m*/*z* 595.3229 $[M+H]^+$, $C_{30}H_{46}N_2O_{10}$ required *m*/*z* 595.3225; *m*/*z* 617.1046 $[M+Na]^+$, $C_{30}H_{46}N_2O_{10}$ required *m*/*z* 617.3045.

4.8 References

1. Scott, J. W.; Bizzarro, F. T.; Parrish, D. R.; Saucy, G., *Helv. Chim. Acta* **1976**, *59*, 290-306.

2. Grisar, J. M.; Petty, M. A.; Bolkenius, F. N.; Dow, J.; Wagner, J.; Wagner, E. R.; Haegele, K. D.; De Jong, W., *J. Med. Chem.* **1991**, *34*, 257-260.

3. Macfarlane, K. J. Small Molecules & Peptide Nucleic Acids for the Treatment and Prevention of Neurodegeneration. PhD Thesis, Monash University, Melbourne, 2004.

4. Cohen, N.; Schaer, B.; Saucy, G.; Borer, R.; Todaro, L.; Chiu, A.-M., *J. Org. Chem.* **1989**, *54*, 3282-3292.

APPENDIX

CRYSTAL DATA TABLES

Table A.1 Crystal data and structure refinement for **19**$(H_2O)_{1.5}$ (a44_08a).

Identification code	a44_08a
Empirical formula	$C_{30}H_{43}N_2O_{13.5}$
Formula weight	647.66
Temperature	123(2) K
Wavelength	0.71073 Å
Crystal system	Triclinic
Space group	P -1
Unit cell dimensions	a = 10.1025(3) Å, α = 103.639(2)°
	b = 11.8819(4) Å, β = 101.782(2)°
	c = 15.3910(5) Å, γ = 108.034(2)°
Volume	1628.57(9) $Å^3$
Z	2
Density (calculated)	1.321 g/cm^3
Absorption coefficient	0.104 mm^{-1}
F(000)	690
Crystal size	0.25 × 0.10 × 0.10 mm^3
Theta range for data collection	1.90 to 25.00°
Index ranges	-10 ≤ h ≤ 12, -14 ≤ k ≤ 14, -18 ≤ l ≤ 18
Reflections collected	20090
Independent reflections	5598 [R(int) = 0.0304]
Completeness to theta = 25.00°	97.9 %
Absorption correction	Semi-empirical from equivalents
Refinement method	Full-matrix least-squares on F^2
Data / restraints / parameters	5598 / 9 / 487
Goodness-of-fit on F^2	1.070
Final R indices [I>2sigma(I)]	R1 = 0.0566, wR2 = 0.1159
R indices (all data)	R1 = 0.0698, wR2 = 0.1243
Largest diff. peak and hole	0.624 and -0.620 $e.Å^{-3}$

Notes: One of the substituent arms on the amine N(2) atom is disordered over two positions; one component has a H-bonded water molecule associated with it but the other does not – hence the half water molecule in the overall formula.

Table A.2 Crystal data and structure refinement for **39** (a42_07).

Identification code	a42_07
Empirical formula	$C_{10}H_{12}O_3$
Formula weight	180.20
Temperature	123(2) K
Wavelength	0.71073 Å
Crystal system	Orthorhombic
Space group	$P2_12_12_1$
Unit cell dimensions	a = 7.1666(4) Å, α = 90.00°
	b = 11.4345(6) Å, β = 90.00°
	c = 11.6327(6) Å, γ = 90.00°
Volume	953.26(9) $Å^3$
Z	4
Density (calculated)	1.256 g/cm^3
Absorption coefficient	0.092 mm^{-1}
F(000)	384
Crystal size	0.25 × 0.20 × 0.13 mm^3
Theta range for data collection	2.50 to 29.00°
Index ranges	$-9 \le h \le 9$, $-10 \le k \le 15$, $-15 \le l \le 13$
Reflections collected	5270
Independent reflections	1467 [R(int) = 0.0207]
Completeness to theta = 29.00°	99.3%
Absorption correction	Semi-empirical from equivalents
Refinement method	Full-matrix least-squares on F^2
Data / restraints / parameters	1467 / 0 / 125
Goodness-of-fit on F^2	1.076
Final R indices [I>2sigma(I)]	R1 = 0.0330, wR2 = 0.0831
R indices (all data)	R1 = 0.0369, wR2 = 0.0854
Largest diff. peak and hole	0.234 and −0.185 $e.Å^{-3}$

Table A.3 Crystal data and structure refinement for **61** (LOD02M).

Identification code	LOD02M
Empirical formula	$C_{10}H_{11}BrO_3$
Formula weight	259.10
Temperature	123(2) K
Wavelength	0.71073 Å
Crystal system	Monoclinic
Space group	$P2_1/c$
Unit cell dimensions	a = 9.0829(19) Å, α = 90.00°
	b = 8.984(2) Å, β = 99.576(7)°
	c = 13.158(3) Å, γ = 90.00°
Volume	1058.7(4) Å^3
Z	4
Density (calculated)	1.626 g/cm^3
Absorption coefficient	3.861 mm^{-1}
F(000)	520
Crystal size	0.30 × 0.20 × 0.10 mm^3
Theta range for data collection	2.76 to 27.50°
Index ranges	−8 ≤ h ≤ 11, -11 ≤ k ≤ 10, -14 ≤ l ≤17
Reflections collected	6283
Independent reflections	2381 [R(int) = 0.0642]
Completeness to theta = 27.50°	97.9%
Absorption correction	None
Refinement method	Full-matrix least-squares on F^2
Data / restraints / parameters	2381 / 0 / 131
Goodness-of-fit on F^2	0.991
Final R indices [I>2sigma(I)]	R1 = 0.0490, wR2 = 0.1096
R indices (all data)	R1 = 0.0901, wR2 = 0.1249
Largest diff. peak and hole	0.748 and −0.790 e.Å^{-3}